

Drug Adapted Breast Cancer Cell Lines as Models of Acquired Resistance

2019

Joanna. L. Bird

A thesis submitted to the University of Kent for the degree of Doctor of Cell Biology

Supervisors: Martin Michaelis & Mark Wass

University of Kent

Faculty of Sciences

Declaration

I declare that the work in this thesis is my own and has not been submitted to the University of Kent in application of any other degree, or to any other institute of learning.

Name: Joanna Bird

Date: 20.9.19

Signature:

Acknowledgements

I would first and foremost like to thank my principal supervisors, Martin Michaelis and Mark Wass for their guidance and support during the course of this project and for offering me the opportunity to undertake this journey. They have taught me a great deal over the last few years. I would also like to thank all of the PIs and members of the cancer research groups at the University of Kent for their insight in all things research related, from whom I have also learnt a great deal. I would also like to thank the MRC and Eli Lilly for the funding that made this research project possible.

I would like to thank the fellow postgraduate students that I have had the great pleasure of working with, past and present, over the last few years. I believe that you learn something from everyone you meet in life; the course of this PhD project has delivered a great deal of lessons. As such, I would like to thank Helen for her undying energy and enthusiasm for life. Andy for his tenacity and kindness. Lara, Emilie and Hannah for taking me under their wing in the Michaelis laboratory. To everyone who puts up with my sense of humour – you are great sports. Budge, for the laughs. To autocorrect, for stopping me from constantly writing ‘cacner’ in this thesis. To Henry, for teaching me the value of keeping focus on knowing what you want in life. To Tanya, for being everything I need you to be and more without having to ask. You’ve been there at my lowest points and have lifted me up more times than I can count.

I would like to thank the engineer(s) that invented automated multichannel pipettes – you have now had a major impact on my life. Also, to all of the undergraduate, postgraduate and secondary school students that endured my teaching.

To my family; your constant understanding and kindness have not gone unnoticed. Without you, this would not have been possible, nor would either of my other degrees been possible. I know that I work too much, but know that you never leave my thoughts. Finally, to mum. Even though you were sadly taken from us too soon, know that I finished this project by the strength of will that you taught me to have.

Abstract

It is estimated that approximately half a million women are alive today thanks to the use of endocrine therapy in ER+ breast cancer, and even more have benefitted from its life-extending affect and palliation. There are two main forms of endocrine therapy: aromatase inhibition (the enzyme responsible for converting androgens to oestrogen) and direct inhibition of the oestrogen receptor with tamoxifen. A large proportion of ER+ breast cancer patients are treated with endocrine therapy as a first-line therapy or an adjuvant therapy. Several mechanisms have been suggested to explain resistance to tamoxifen, but given the complexity of oestrogen signalling itself, there are a number of mechanisms that could potentially be altered to result in increased tolerance to the drug. Most publications investigate mechanisms of resistance in a single cell line setting, here we have systematically generated two panels of 6 ER+ breast cancer cell lines in tandem (resulting in a total of 46 sublines) one as a potential model for resistance to long-term systemic oestrogen deprivation, like that naturally found in postmenopausal women or patients treated with aromatase inhibitors (24 sublines), the other a model for acquired resistance to long-term tamoxifen exposure (22 sublines). These panels have been characterised for response to tamoxifen, clinically relevant metabolites of tamoxifen and other commonly used anti-cancer agents to treat breast cancer. Oestrogen receptor localisation and expression levels were evaluated for the purpose of gaining an idea of changes found in aromatase inhibitor resistance vs tamoxifen resistance. Over the course of this thesis, drug response data has been presented for a large number of drug-adapted breast cancer cell lines.

Additionally to this, we have investigated cross resistance to DNA damaging agents in the advent of resistance to platinum (Pt) based anti-cancer drugs in triple negative breast cancer cell lines. We have used a range of DNA-damaging agents as preliminary data to gain insight into potential sensitivity or cross-resistance to other modes of DNA damage in triple negative breast cancer cell lines that have acquired resistance to cisplatin, carboplatin and oxaliplatin. We also looked at potential changes to MEK/ERK and AKT signalling as a result of drug resistance in the Pt-drug resistant sublines compared to parental cell lines, along with sensitivity to MEK, AKT and ChK1 inhibitors.

List of Abbreviations

AF	Activation function
AIs	Aromatase inhibitors
AR	Androgen receptor
ATCC	American Type Culture Collection
BCA	bicinchoninic acid
CARBO	Carboplatin
CDDP	Cisplatin
DBD	Drug-binding domain
DSMZ	German Collection of Microorganisms and Cell Culture
E1	Estrone
E2	Estradiol
E3	Estriol
EGFR	Epidermal growth factor receptor
EMT	Epithelial-mesenchymal transition
ER	Oestrogen receptor
ERα	Oestrogen receptor alpha
ERβ	Oestrogen receptor beta
EREs	Oestrogen response elements
HSP90	Heat shock protein 90
IMDM	Iscove's modified Dulbecos Medium
IGF1R	Insulin-like growth factor 1
LBD	Ligand-binding domain
MTT	3-(4,5-di**m**ethyl**t**hiazol-2-yl)-2,5-diphenyl**t**etrazolim bromide
nM	nanomolar
NTD	N-terminal domain
OXALI	Oxaliplatin
PDX	Patient derived xenograft
PR	Progesterone receptor
Pt	Platinum
RCCL	Resistant cancer cell line collection
TNBC	Triple negative breast cancer
TAM	Tamoxifen

SERM	Selective oestrogen receptor modulator
4-OH	(Z)-4-OH-tamoxifen
µl	microlitre
µM	micromolar

Table of Contents

Declaration 2

Acknowledgements 3

Abstract 4

List of Abbreviations 5

Table of Contents 7

List of Figures 12

List of Tables 17

Chapter 1: General Introduction 18

1.1 Introduction to breast cancer in general 18

1.2 Heterogeneity of cell lines 21

1.3 Oestrogen signalling in normal breast tissue – the duality of oestrogen signalling 22

1.4 Oestrogen receptors (alpha and beta) 23

1.5: Mechanisms of Oestrogen Signalling 28

1.5.1 Classical Oestrogen Signalling 28

1.5.2 Non-classical Oestrogen Signalling 30

1.5.3 First Method of Non-Classical Signalling (Forming Complexes With Transcription Factors) 31

1.5.4 Second Method of Non-classical Signalling (Regulating Protein-Kinase Pathways) 32

1.6: What genes are regulated by oestrogen? 33

1.7 GPER1 35

1.8 Cross-talk with other signalling pathways 38

1.9 Oestrogen signalling in cancerous tissue 38

1.10 Phenol red in culture media 39

1.11 Drug resistance in cancer 41

1.12 Endocrine therapy 42

1.13 Tamoxifen (duality of tamoxifen signalling) 42

1.14 Resistance to tamoxifen 46
1.14.1 Changes to the nuclear oestrogen receptors 46
1.15.2 Differential responses of tamoxifen with truncated ER isoforms 48
1.14.3: GPER1 in tamoxifen resistance 48
1.14.4: Androgen receptor in tamoxifen resistance 50
1.14.5: Other potential mechanisms of resistance of interest 51
1.15 Introduction to the work conducted in this thesis 51
Chapter 2: General Methods and Materials 53
2.1 Materials 53
2.1.1 Cell Culture – Cells, Media and Other Solutions 53
2.1.2 Glassware and Plasticware 54
2.2 Methods 55
2.2.1: Cell Culture 55
2.2.2: Cryopreservation of cell lines 55
2.2.3: Adaptation of growth hormone-deprived sub-lines 56
2.2.4: Generation of resistant cell lines 57
2.2.5: Cell Growth Characterisation 57
2.2.6: The MTT Assay 58
2.2.7: Immunostaining 59
2.2.8: Quantification of ER expression from immunostain images 60
2.2.9: Western Blot Analysis 61
2.2.10: Statistical Analysis 62
Chapter 3: Production and characterisation of growth hormone deprived breast cancer cell lines 63
3.1 Introduction 63
3.1.1 Introduction to the Data in This Chapter 63
3.1.2: The use of 2D cell culture methods 64
3.2: Results 66
3.2.1: Images of the Oestrogen/Phenol Red Starved Cell Lines 66
3.2.2: Growth kinetics 71

3.2.3: Response to β-oestradiol 77
3.2.4: Qualitative evaluation of ERα and ERβ expression 81
3.2.5: Quantification of ERα and ERβ expression 90
3.2.6: Response to tamoxifen and its primary metabolites 94
3.2.7: Response to other anti-cancer compounds 104
3.3: Discussion 110
3.3.1: Oestrogen deprivation as a potential mimic for aromatase inhibitor resistance 110
3.3.2: The use of MDA-MB-468 as an additional control cell line 110
3.3.3: Cell line adaptation to growth in conditions in low levels of growth hormones 111
3.3.4: Potential variability of residual growth hormones in foetal bovine serum after charcoal stripping 112
3.3.5: Clinical implications of toxic effects of high dose oestrogen seen in growth hormone deprived breast cancer cell lines 113
3.3.6: Clinical implications of differential responses to tamoxifen, tamoxifen metabolites and other anti-cancer drugs 113
3.3.7: Conclusion and General Summary 115
Chapter 4: Production and characterisation of (Z)-4-OH-tamoxifen resistant breast cancer cell lines 117
4.1: Introduction 117
4.1.1 Tamoxifen resistance in breast cancer 117
4.1.2: Generating drug-resistant cell lines and their significance in cancer research 117
4.1.3: Introduction to the results in this chapter 119
4.2 Results 120
4.2.1: Generation of resistant cell lines 120
4.2.2: Cell line morphology 122
4.2.3: Growth Kinetics 126
4.2.4: Response to tamoxifen and tamoxifen metabolites 129

4.2.5: Qualitative evaluation of ERα and ERβ expression in tamoxifen-resistant sub-lines 138
4.2.6: Quantification of ERα and ERβ expression in the tamoxifen-resistant sub-lines 146
4.2.7: Stability of drug-resistance to (Z)-4-OH-tamoxifen, tamoxifen and tamoxifen metabolites after cryopreservation 152
4.2.8: Response to other commonly used chemotherapeutics used to treat breast cancer 156
4.3: Discussion 164
4.3.1: Generation of resistant sub-lines 164
4.3.2: Response to Tamoxifen and Metabolites 165
4.3.3: Oestrogen receptor expression changes as a result of acquired resistance to tamoxifen 166
4.3.4: Response to other anti-cancer compounds 168
4.4: Conclusion and general summary 169
Chapter 5: Evaluation of Cross-Resistance to DNA Damaging Agents in Platinum Drug-Resistant Triple Negative Breast Cancer 171
5.1: Introduction 172
5.2: Results 175
5.2.1: Images of the cell lines 175
5.2.2: Cell Growth Characterisation 178
5.2.3: Resistance status of the platinum drug resistant-cell lines 179
5.2.4: Cross-resistance evaluation of other DNA damaging agents 182
5.2.5: Western blot analysis of changes to intracellular signalling pathways 187
5.2.6: Sensitivity to MEK, AKT and ChK1 Inhibition 189
5.3: Discussion 193
5.3.1: Resistance status of the cell lines 194
5.3.2: Cross resistance to other DNA-damaging agents 196
5.3.4: Evaluation of changes to intracellular signalling pathways 197
5.3.5: Rationale for Selection of MEK, AKT and ChK1 Inhibitiors for This Study 198
5.4: Conclusions 200
Chapter 6: General Discussion 201
6.1: General research aims of this work 201

6.2 Why MTT assays? 202
6.3: Comparison and summary between cell lines in chapters 3 and 4 203
6.4: Heterogeneity of drug adapted cancer cell lines 205
6.5: Future Work for chapters 3 and 4 205
Appendix 208
References 214

List of Figures

Figure 1.1: Schematic of classification system for breast cancer……19
Figure 1.2: Schematic of the oestrogen metabolic pathway……23
Figure 1.3: Schematic of oestrogen receptors alpha and beta, and their respective splice variant isoforms……24
Figure 1.4: Schematic of the oestrogen signalling pathways……33
Figure 1.5: Map of GPER1 signalling pathways……36
Figure 1.6: The effect of phenol red in culture media……40
Figure 1.7: Tamoxifen and aromatase inhibits interfere with oestrogen signalling ……43
Figure 1.8: Oestrogen receptors dimerise and bind to EREs……44
Figure 1.9: Tamoxifen, tamoxifen metabolites and CYP450s……45
Figure 2.1: Pipetting scheme for the MTT assay……59
Figure 2.2: Screenshots from ER quantification with ImageJ……61
Figure 3.1: Images of MCF-7 hormone deprived sublines……67
Figure 3.2: Images of BT-474 hormone deprived sublines……68
Figure 3.3: Images of EFM-19 hormone deprived sublines……68
Figure 3.4: Images of T47D hormone deprived sublines……69
Figure 3.5: Images of CAMA-1 hormone deprived sublines……69
Figure 3.6: Images of MDA-MB-468 hormone deprived sublines……70
Figure 3.7: Growth curves of preadapted hormone deprived sublines……73
Figure 3.8: Growth curves of adapted hormone deprived sublines……74
Figure 3.9: Doubling times of adapted hormone deprived sublines……75
Figure 3.10: Post hormone deprivation-adapted subline response to β-oestradiol……79
Figure 3.11: β-oestradiol IC_{50} values from adapted hormone deprived sublines……80
Figure 3.12: ERs alpha and beta target validation……81
Figure 3.13: ER alpha and beta immunostain images of MCF7 hormone deprived sublines……84
Figure 3.14: ER alpha and beta immunostain images of BT-474 hormone deprived sublines……85
Figure 3.15: ER alpha and beta immunostain images of EFM-19 hormone deprived sublines……86

Figure 3.16: ER alpha and beta immunostain images of T47D hormone deprived sublines……..87
Figure 3.17: ER alpha and beta immunostain images of CAMA-1 hormone deprived sublines……..88
Figure 3.18: ER alpha and beta immunostain images of MDA-MB-468 hormone deprived sublines……..89
Figure 3.19: ER alpha expression in growth hormone deprived sublines……..91
Figure 3.20: ER beta expression in growth hormone deprived sublines……92
Figure 3.21: Ratio of whole cell:nuclear ER alpha ER beta expression……..93
Figure 3.22: Response to tamoxifen in growth hormone deprived sublines…..96
Figure 3.23: Response to (Z)-4-OH-tamoxifen in growth hormone deprived sublines……98
Figure 3.24: Response to alpha-hydroxytamoxifen in growth hormone deprived sublines……99
Figure 3.25: Response to endoxifen in growth hormone deprived sublines…101
Figure 3.26: Response to n-desmethyltamoxifen in growth hormone deprived sublines……103
Figure 3.27: Response to 2-methoxyoestradiol in growth hormone deprived sublines……105
Figure 3.28: Response to vincristine in growth hormone deprived sublines…107
Figure 3.29: Response to olaparib in growth hormone deprived sublines….109
Figure 4.1: Drug adaptation protocol for (Z)-4-OH-tamoxifen resistant cell lines……121
Figure 4.2: Images of (Z)-4-OH-tamoxifen resistant MCF7 cell line and sublines……122
Figure 4.3: Images of (Z)-4-OH-tamoxifen resistant BT-474 cell line and sublines……123
Figure 4.4: Images of (Z)-4-OH-tamoxifen resistant EFM-19 cell line and sublines……123
Figure 4.5: Images of (Z)-4-OH-tamoxifen resistant T47D cell line and sublines……124
Figure 4.6: Images of (Z)-4-OH-tamoxifen resistant CAMA-1 cell line and sublines……124
Figure 4.7: Images of (Z)-4-OH-tamoxifen resistant MDA-MB-468 cell line and sublines……125

Figure 4.8: (Z)-4-OH-tamoxifen resistant subline growth curves……..……127
Figure 4.9: (Z)-4-OH-tamoxifen resistant subline doubling times……..…..128
Figure 4.10: Response to (Z)-4-OH-tamoxifen in (Z)-4-OH-tamoxifen resistant sublines…….…..131
Figure 4.11: Response to tamoxifen in (Z)-4-OH-tamoxifen resistant sublines…….……133
Figure 4.12: Response to alpha-hydroxytamoxifen in (Z)-4-OH-tamoxifen resistant sublines……..……..134
Figure 4.13: Response to endoxifen in (Z)-4-OH-tamoxifen resistant sublines…….……..…135
Figure 4.14: Response to n-desmethyltamoxifen in (Z)-4-OH-tamoxifen resistant sublines…….……137
Figure 4.15: ER alpha and beta immunostain images of MCF7 (Z)-4-OH-tamoxifen resistant sublines……140
Figure 4.16: ER alpha and beta immunostain images of BT-474 (Z)-4-OH-tamoxifen resistant sublines……141
Figure 4.17: ER alpha and beta immunostain images of EFM-19 (Z)-4-OH-tamoxifen resistant sublines……142
Figure 4.18: ER alpha and beta immunostain images of T47D (Z)-4-OH-tamoxifen resistant sublines…….……143
Figure 4.19: ER alpha and beta immunostain images of CAMA-1 (Z)-4-OH-tamoxifen resistant sublines…….……144
Figure 4.20: ER alpha and beta immunostain images of MDA-MB-468 (Z)-4-OH-tamoxifen resistant sublines……..……..…145
Figure 4.21: ER alpha expression in (Z)-4-OH-tamoxifen resistant sublines..148
Figure 4.22: ER beta expression in (Z)-4-OH-tamoxifen resistant sublines …150
Figure 4.23: Ratio of whole cell:nuclear ER alpha ER beta expression in the 4-OH resistant cell lines……..……..…151
Figure 4.24: Stability of drug resistance after cryopreservation to tamoxifen and metabolites (early 2018)……..……..…154
Figure 4.25: Stability of drug resistance after cryopreservation to tamoxifen and metabolites (early 2019)……..……..……155

Figure 4.26: Response to 2-methoxyoestradiol in (Z)-4-OH-tamoxifen resistant sublines……..157
Figure 4.27: Response to vincristine in (Z)-4-OH-tamoxifen resistant sublines……..159
Figure 4.28: Response to olaparib in (Z)-4-OH-tamoxifen resistant sublines……..161
Figure 4.29: Stability of drug resistance after cryopreservation to 2-methoxyoestradiol, vincristine and olaparib (early 2019)……..163
Figure 5.1: Images of the HCC1806 cell line and platinum-drug resistant sublines……...176
Figure 5.2: Images of the SUM159PT cell line and platinum-drug resistant sublines……..176
Figure 5.3: Images of the CAL51 cell line and platinum-drug resistant sublines……177
Figure 5.4: Images of the HCC38 cell line and platinum-drug resistant sublines……177
Figure 5.5: Growth characterisation of the Pt-adapted TNBC cell line panel……178
Figure 5.6: Drug sensitivity profiles of the TNBC cell lines and their drug resistant sub-lines to cisplatin, carboplatin and oxaliplatin……180
Figure 5.7: Drug sensitivity profiles of the TNBC cell lines and their drug resistant sub-lines to cisplatin, carboplatin and oxaliplatin (grouped by drug resistance status)……181
Figure 5.8: Drug sensitivity profiles of the TNBC cell lines and their drug resistant sub-lines to zeocin, mitomycin C etoposide and bleomycin……184
Figure 5.9: Drug sensitivity profiles of the TNBC cell lines and their drug resistant sub-lines to zeocin, mitomycin C etoposide and bleomycin (grouped by drug resistance status)……186
Figure 5.10: Western blot analysis is MEK and AKT signalling pathways in Pt-resistant TNBC cell panel……188

Figure 5.11: Drug sensitivity profiles of the TNBC cell lines and their drug resistant sub-lines to MEK, AKT and ChK1 inhibition…….……....191
Figure 5.12: Drug sensitivity profiles of the TNBC cell lines and their drug resistant sub-lines to MEK, AKT and ChK1 inhibition (grouped by drug resistance status)…….……...193

List of Tables

Table 2.1: List of antibodies used for immunofluorescence……49
Table 2.2: List of antibodies used for western blotting……..50
Table 3.1: List of ER+ cell lines used for this project……..……...…52
Table 3.2: List of doubling times of ER+ cell lines and growth hormone deprived sublines……..64
Table 3.2: Comments on observations made on oestrogen receptor locality from immunofluorescence images of six breast cancer cell lines and growth hormone deprived sublines……..70
Table 4.1: Concentration of (Z)-4-OH-tamoxifen used to begin establishing drug-resistant sub-lines……..…106
Table 4.2: Doubling times of (Z)-4-OH-tamoxifen resistant sublines……..115
Table 4.3: Comments on observations made on oestrogen receptor locality from immunofluorescence images of the tamoxifen-resistant sub-lines and the effect of growth in oestrogen-deprived conditions on this……..…124
Table 5.1: List of the cell lines used and the concentrations of platinum drug the cell line is maintained in……160
Table 5.2: Description of changes seen to AKT, MEK and ERK signalling in Pt-drug resistant TNBC cell lines……..173

Chapter 1: General Introduction

1.1 Introduction to breast cancer in general

Breast cancer is the most common malignancy seen in women worldwide. It is thought that one in every 8-10 women will develop breast cancer during their lifetime. However, mortality rates from breast cancer have seen a decline in recent years due to better systemic therapies and earlier detection rates in developed parts of the world (Sabaila, Fauconnier and Huchon, 2015). Mortality rates in the EU were projected to decrease by 8% in 2016 (Malvezzi *et al.*, 2016). But, in less developed parts of the world, incidence rates have been increasing, mainly due to changes in lifestyle choices and an increased availability of screening programmes (Harbeck and Gnant, 2016). With regards to available literature on currently accepted dogma for the treatment of breast cancer - it is clear that treatment approaches are divided not only by hormone receptor status, but also menopausal status. Breast cancer under the age of 40 is known to be a more complex disease to manage with fertility having to be taken into consideration (Ribnikar *et al.*, 2015).

Breast cancer is a heterogeneous disease – encompassing a considerable variability in clinical, morphological and molecular attributes. Traditionally, breast cancer has been classified by hormone receptor presenting status by immunohistochemistry techniques, but in recent years progress has been made towards molecular analysis which will ultimately contribute to our understanding of breast cancer classification (Alizart *et al.*, 2012). Around 70% of breast tumours are luminal type (positive for either oestrogen or progesterone receptors) and HER2 negative. Very few breast cancer centres offer determination of molecular subtype by multigene assay, as such, immunohistochemistry from single-area biopsy sections is the most routinely used technique to differentiate luminal subtypes (between A&B). Currently, luminal subtype is classified by Ki-67 score, Ki-67 being a marker of proliferation rate. A score <14% places the tumour in the lower risk luminal A subtype (deemed to be a low rate of proliferation), with a score above that putting it in the higher risk luminal B category (Sun and Kaufman, 2018). The limiting factor for this is that classification by luminal

subtype does not necessarily indicate that one group or the other would be more responsive to systemic chemotherapy – moreover, immunohistochemistry itself has a major flaw in its inability to accurately distinguish intermediates between the two classifications. The technique reportedly struggles to define Ki-67 values within the 10-30% range (Harbeck and Gnant, 2016), which would influence directly false-positives for the groups.

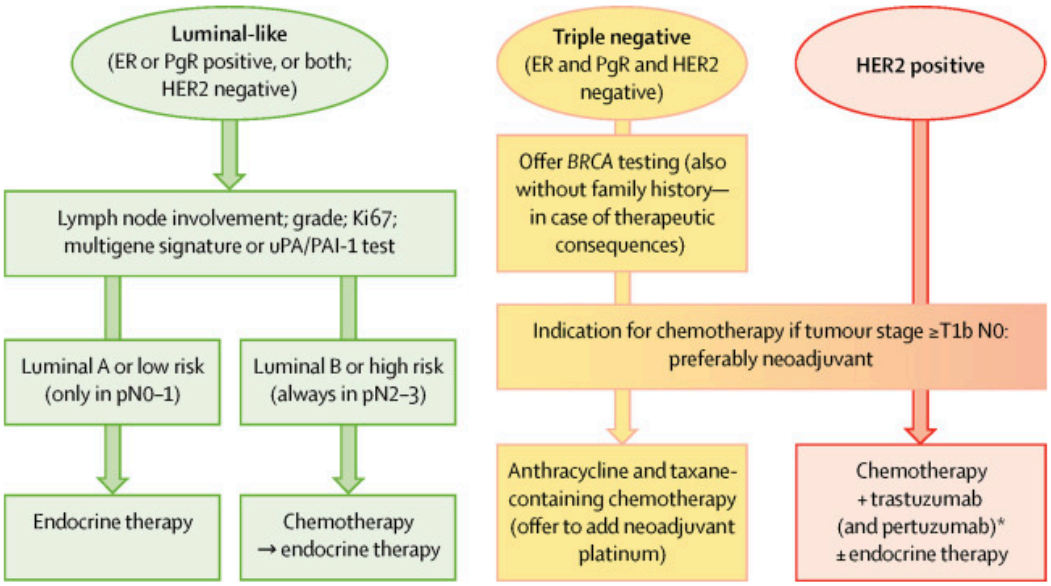


Figure 1.1: Schematic of classification system for breast cancer. Taken from Harbeck and Gnant (2017). Highlights the currently practised principles for systemic therapy in early breast cancer. The source article discusses how individual therapy decisions are highly subjective based on presenting disease characteristics and patient preferences. ER = oestrogen receptor. PgR = Progesterone receptor. Endocrine therapy is always indicated if ER positive, PgR positive or both.

Premenopausal patients are the group that are most at risk from highly aggressive disease and relapse. Women under 40 years of age are statistically more likely to develop breast cancer with worse pathological features that are associated with a worse recurrence-free survival and overall survival for luminal type disease (Ribnikar *et al.*, 2015). Naturally, the generalisation of younger women developing worse disease is not accurate for all cases in younger women, therefore a controversial prognostic marker by itself. The incidence of breast cancer in younger women in general is certainly linked to greater risk of psychosocial instability due to the need to cope with factors linked to younger families, career progression and fertility/sexual function (Freedman and Partridge, 2013).

Adjuvant endocrine therapy over the course of 5-10 years is considered the standard for luminal type breast cancer, meaning that they are hormone-receptor positive (ER or PgR staining >1% positive). Response to endocrine therapy is generally considered to correlate directly to hormone receptor positivity (Early Breast Cancer Trialists' Collaborative Group (EBCTCG), (2011). For luminal-type tumours in post-menopausal patients, tamoxifen and aromatase inhibitors are the standard therapeutic options. A meta-analysis that compared clinical data available for the comparison of aromatase inhibitors vs tamoxifen as an adjuvant therapy in postmenopausal women, both as initial monotherapy (cohort 1, n = 9,856) and as a second-line therapy following 2-3 years of tamoxifen treatment (cohort 2, n = 9,015) concluded that aromatase inhibitors produce a significantly lower recurrence rate compared with tamoxifen - as both a monotherapy and 2nd-line following prior tamoxifen treatment, but there was no significant difference in overall mortality rates. This meta-analysis also includes a very useful breakdown of analyses of patient responses into PgR status, age, nodal state and tumour grade – the vast majority of which place aromatase inhibitors as slightly better than tamoxifen. However, slightly is an apt word in this context as improvements seen, albeit better, are still only marginal (Dowsett *et al.*, 2010).

The idea that oestrogen is implicated as the 'fuel for the fire' of breast cancer has been ingrained in women's psyche. It is, after all, one of the main factors for the classification of breast cancer and the eventual selection of treatment methods – regardless of the undeniably heterogeneous and subjective nature of breast cancer in the clinic (when speaking with regards to the cumulative incidence of all breast cancers). Professional bodies have engrained this ideal with warnings of the dangers of oestrogens for women who have had breast cancer, both pharmaceutically and nutritionally (Jordan, 2015). This is, generally speaking, correct – but the vast array of literature available on cancer teaches us as researchers that in an ideal world, the advancement of treatment of cancer is not something to be approached as 'general'. But looking generally, the success of antioestrogens such as tamoxifen and aromatase inhibitors (AIs) proves the point that oestrogens play a main role in the progression of breast cancer.

1.2 Heterogeneity of cell lines

The emergence of varied responses to therapy is not just seen in the clinic – as researchers we must also be mindful that heterogeneity is also seen in *in vitro* models used to study responses to oestrogen and antioestrogens in breast cancer. Whether that be variability between differing cell lines, or variability seen in the same cell lines but used in different laboratories and research groups. Variability between cells from the same lineage when used in different locations (HeLa in this case) has been documented by Liu *et al.*, (2019). A multi-omics study by this team documents that a marked difference can be seen between cell populations after 50 successive passages. Hence the reason for using a relatively large number of cell lines in this study – cell lines can never perfectly be compared to those from other labs or used decades prior, but can be directly compared when cultured in the same conditions, by the same person, systematically and over time.

Upon searching through available literature, regardless of cancer type, it is evident that there is never simply one suggested marker of disease or mechanism of resistance to any one anti-cancer drug. When reading independent studies and reviews alike, authors often document discrepancies in molecular mechanisms of resistance from cell line to cell line for individual anti-cancer compounds (Dagogo-Jack and Shaw, 2018; Joseph *et al.*, 2018; Panda and Biswal, 2019; Yin *et al.*, 2019) – indirectly supporting the necessity of personalised treatment regimens. It can naturally be argued that this will be due to discrepancies in culture techniques from person to person, human error, difference in media type used, apparatus used etc. But what must also be considered is genetic drift in as many directions as there are people using the cell line around the world, that will be influencing the conclusions taken from each independent study.

1.3 Oestrogen signalling in normal breast tissue – the duality of oestrogen signalling

The majority of the work described in this thesis will surround the action of the anti-oestrogen tamoxifen – but to understand the molecular basis of tamoxifen, we must first understand the molecular basis of what it inhibits. Our understanding of the roles that oestrogens play in the body has changed significantly in recent years. It is well known that oestrogen plays a major role in both female and male reproductive function, but it also has functions beyond the conventional endocrine system. Firstly, as a generalisation of the function of oestrogens, they work by regulating transcriptional processes - mainly those related to cellular growth (Carroll, 2016). Oestrogen does not regulate gene transcription by any one mechanism, however; which makes its direct effect on breast tissue difficult to elucidate completely or describe simply. Rather, the mechanisms of oestrogen signalling are controlled by a combination of activation of three receptors: ERα, ERβ and a G protein-coupled receptor referred to as GPER1 or GPR30 in literature. ERα and ERβ are thought to both directly and indirectly mediate ER-responsive gene transcription (Björnström and Sjöberg, 2005; Vrtačnik *et al.*, 2014; Lipovka and Konhilas, 2016). The structure of these receptors will be described in more detail in section 1.5 of this chapter.

Oestrogen is a generalised term for multiple compounds found in the human body that stimulate oestrogen receptors, which mainly consists of three main oestrogenic compounds: estrone (E1), estradiol (E2) and estriol (E3). Estradiol is the main form found in premenopausal women, and estrone is the predominant form in circulation following the menopause and are synthesised by the aromatisation of androstenedione and testosterone respectively (Thomas and Potter, 2013). Estriol is the main oestrogen synthesised during pregnancy and is synthesised from an intermediate of estrone (Ali, Mangold and Peiris, 2017).

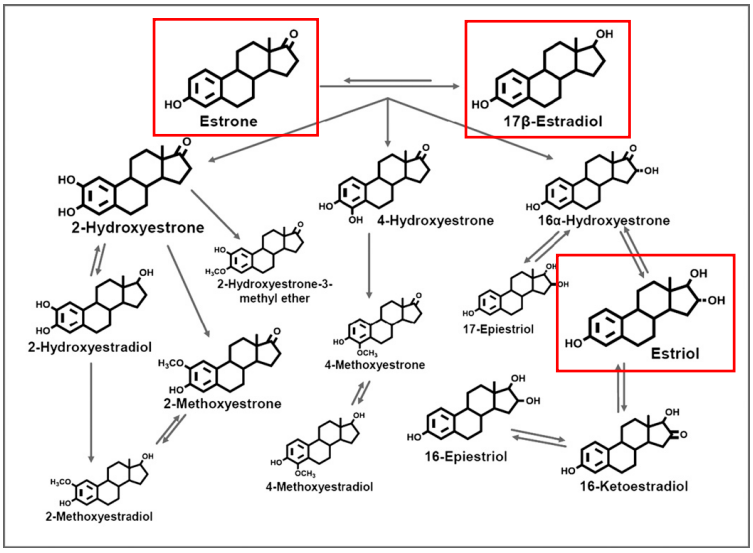


Figure 1.2: Schematic of the oestrogen metabolic pathway. Adapted from (Sampson *et al.*, 2017). Schematic of the oestrogen metabolic pathway. The sizes of the chemical structures shown are representative to their abundance. Red boxes highlight the three main active forms of oestrogen in circulation, mentioned in the body of text for this section.

Oestrogen signalling can be classified into two major categories: classical (genomic) and non-classical (non-genomic). The classical pathway results in direct modulation of transcription with the ER acting as a transcription factor that directly binds to DNA, and the non-classical initiates activation of intra-cellular signalling cascades (mainly PI3K/AKT) that in turn regulate gene transcription via other transcription factors such as NF-κB. Figure 1.4 (page 32), in a later section, shows a simplified diagram of the pathways associated with oestrogen signalling.

1.4 Oestrogen receptors (alpha and beta)

The physiological actions of oestrogen are mainly mediated through oestrogen receptors (ERs) alpha (ERα) and beta (ERβ). Although it is directly stated in literature surprisingly sparsely, it should be noted that it is the presence of ERα alone is the accepted marker of ER positivity in breast cancer (Molina *et al.*, 2017; Girgert, Emons and Gründker, 2019).

The majority of the actions of oestrogen, classical or non-classical, are mediated through ERs α and β. These are both members of the nuclear hormone receptor family and comprise several functional domains. Spanning from N to C terminus, the main functional domains for both isoforms of the receptor are: N-terminal domain (NTD), drug-binding domain (DBD) and ligand-binding domain (LBD). The size of these receptors vary between the isoform (α or β) and variants of the

isoforms themselves, but do not change in order within the structure. These can be seen in the schematics of ERs shown in figure 1.3, below. The LBD contains the position of hormone binding in the structure of the ER, along with the position of binding for co-regulators of ER function and dimerisation interface. The DBD contains the region at which the ER docks with EREs in the genome (which as previously stated reside near promoter or enhancer regions of target genes, at variable distances). There are two activation function (AF) domains present in the structure of ERs – AF-1 and AF-2 which reside in the NTD and LBD respectively. These are responsible for regulating the function of ERs. As can be assumed from the location of these two AFs, AF-1 is not reliant on hormone presence for function, whereas AF-2 is (Tora *et al.*, 1989). The C-terminal portion of the receptor is also thought to regulate gene transcription by affecting dimerisation of the receptors in a ligand-dependent manner (Yang *et al.*, 2008).

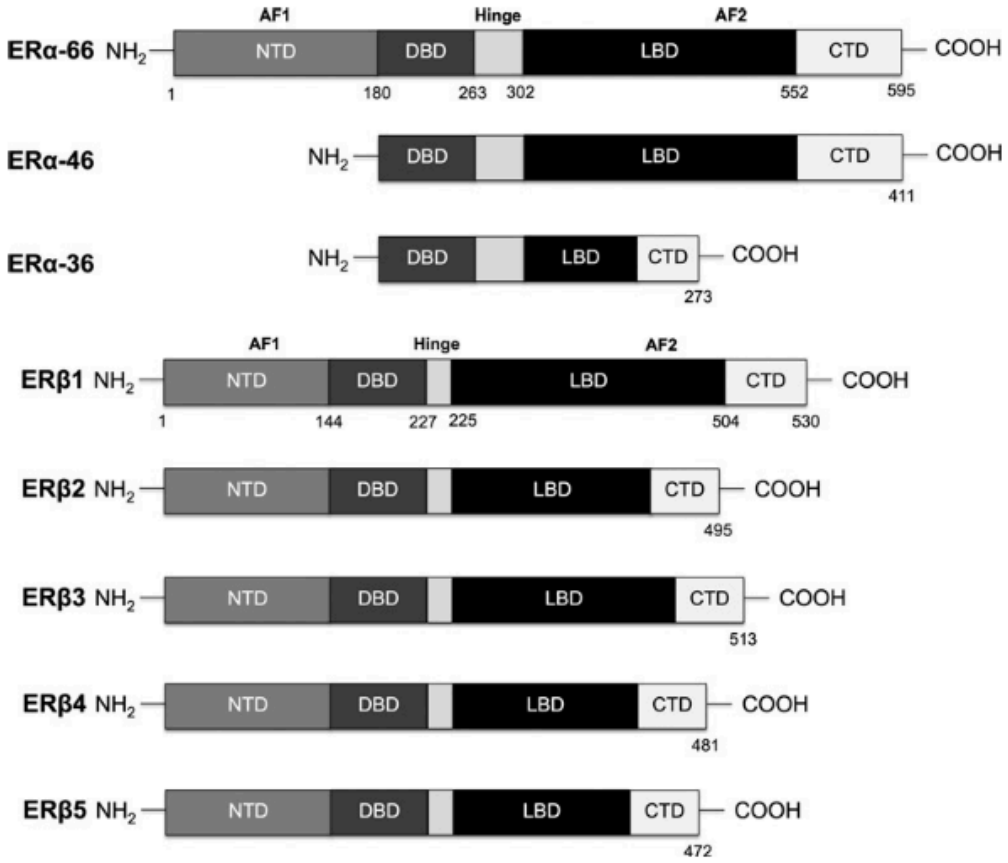


Figure 1.3: Schematic of oestrogen receptors alpha and beta, and their respective splice variant isoforms. Taken from (Lipovka and Konhilas, 2016). Schematic representation of the functional domains that make up wild-type oestrogen receptors (ERα-66, ERβ1), and their most commonly known splice variants. ERs are composed of an N-terminal domain (NTD), DNA-binding domain (DBD), hinge region, ligand-binding domain (LBD) and C-terminal domain (CTD).

ERα and ERβ are coded for by two separate genes, on two separate chromosomes – loci 6q25.1 and 14q23-24.1 respectively (Menasce *et al.*, 1993; Enmark *et al.*, 1997). The 66kDa ERα was discovered first, and thought to be the only nuclear receptor stimulated by oestrogen until Kuiper *et al.*, (1996) discovered a novel 54kDa nuclear receptor (ERβ) that was highly homologous with ERα, particularly in the DBD. The wild-type nuclear receptors for α and β (ERα-66 and ERβ1 in figure 1.3) share a degree of homology, mainly in the DBD (~96% amino acid homology) and LBD (~58% homology), the residues that line the binding cavity are almost completely conserved between the two receptors however with only two amino acid differences. These substitutions are conservative, with them having a similar hydrophobicity and side chains that occupy a similar volume of space (Kenneth S. Korach *et al.*, 2003). The NTD of ERβ is much shorter than that of ERα, and only shares a sequence homology of 15% - the hinge region and CTD are also quite different (Mosselman, Polman and Dijkema, 1996).

Additionally to the wild type ERs, there are multiple variant isoforms of both ERα and β. The most commonly referred to in literature for ERα, is ERα-46. This variant lacks the functional AF-1 domain. Penot *et al.*, (2005) document the expression pattern changes of the wild-type ERα and ERα-46 in MCF7 cells – the truncated version is seen to be expressed in low levels in the nucleus, compared to a relatively large accumulation of the wild type receptor in the same place. However, when confluency is reached, the proportions of the two seem to switch in the same location. The ERα-36 isoform lacks both the AF-1 and AF-2 functional domains, making its theoretical function unclear but is still known to dimerise with other ERs – this isoform is generally thought to be located at the plasma membrane and have the potential to trigger membrane-initiated mitogenic oestrogen signalling (non-classical oestrogen signalling) (Zhao *et al.*, 2005).

Since the discovery of ERβ in 1996, efforts have been made to elucidate its biological function, and how this differs from ERα in particular. Unfortunately, this remains relatively poorly understood today. It is generally thought that ERβ has anti-proliferative function, contrary to the proliferative function of ERα - it regulates apoptosis, the control of antioxidant gene expression and certain

aspects of immune responses (Mosselman, Polman and Dijkema, 1996; Kuiper *et al.*, 2002; Leung *et al.*, 2006). We should assume that all prior information that has been discussed about ERs in this chapter, and its proliferative directionality, is referring to ERα. The question now is, if ERβ and ERα are both stimulated by oestrogen, how does their mechanism of action differ to elicit differential functions? From available literature on the matter, and to follow on from a previously mentioned point - it is evident that the two receptors appear to have an antagonistic relationship. One signals for enhanced proliferation, one inhibits it. Yet both are stimulated by oestrogen – one hormone signal, two opposite effects. As an example to support this: in cell lines, specifically HC11 in this instance that expresses both ERα and ERβ, in the presence of a specific ERα agonist proliferation is seen, but proliferation is inhibited in the presence of an ERβ agonist. These same cells did not seem to proliferate greatly in the presence of E2 (which is not selective to either receptor) with expression of both receptor isoforms – suggesting that growth is regulated by the control of expression of these two antagonistic receptors, and in this case they were close to equally expressed (Ström *et al.*, 2004). This gives an insight to the potential of balances or imbalances in particular with expression of these receptors for the enhancing or inhibitory effects of oestrogen on cancer progression.

ERβ has multiple splice variants (ERβ2, ERβ3, ERβ4, ERβ5) – these all differ in their ligand binding domain. A more recent study showed that only the wild-type ERβ/ERβ1 showed functional activity, whereas the others were only shown to form heterodimers with wild type ERβ with no innate activity on their own. Interestingly, heterodimerisation between wild type β1 and the other variants is much stronger than that of homo-dimers of β1, suggesting that those are the preferred binding partners of β1 under standard oestrogen stimulated conditions. The isoform variants exhibit a distinct tissue distribution which could potentially give an insight into the functionality of ERβ in those tissue types (Saji *et al.*, 2000; Makinen, 2001; Välimaa *et al.*, 2004).

Before 1995, the word oestrogenic was synonymous to uterotropic. When ERα is inactivated in mice, the uterus shows very little response to oestrogen, and when there is no circulating oestrogen (due to treatment with aromatase

inhibitors), the uterus fails to grow – highlighting the significance of ERα with uterine development (Lubahn *et al.*, 1993; Kenneth S Korach *et al.*, 2003). In contrast, when ERβ is inactivated, the uterus has been observed to grow larger, and has a stronger response to E2 stimulation (Weihua *et al.*, 2000). Which, is in-keeping with the logic of ERα having an overall proliferative effect, and ERβ anti-proliferative. In the uterus, ERα is the predominant receptor.

The answer to differences in functionality of the two receptors may lie in the fact that the ligand binding domains, specificity of oestrogen binding, and selective tissue distribution are different for each isoform of the receptor. We know that both ERβ and ERα are highly expressed in a wide range of tissues in the body, in both males and females; such as the prostate, salivary glands, testis, ovary, vascular endothelium and certain cell types in the immune and nervous system (Lindner *et al.*, 1998; Makinen, 2001; Weihua *et al.*, 2002; Mitra *et al.*, 2003; Shim *et al.*, 2003; Välimaa *et al.*, 2004; Cheng *et al.*, 2005). We also know that ERβ and ERα have different transcriptional activities in differing ligand, cell-type and promoter contexts – and that both receptors are co-expressed in these differing tissue types (Matthews and Gustafsson, 2003).

It should also be noted that truncated versions of this receptor isoform have been found in ER negative breast tumours but the wild-type is the only form meant to be functional (Lipovka and Konhilas, 2016). It is estimated that about 60% of tumours that test negative for ERα, tested positive for ERβ - as do 44.4% of all triple negative breast cancers (Skliris *et al.*, 2006; Litwiniuk *et al.*, 2008).

Interestingly, patients that do not express wild type ERβ showed significantly worse overall survival than patients with tumours that did express the receptor. Patients with tumours that test ERα- and progesterone receptor negative also, but expressed ERβ presented with a better prognosis – irrespective of HER-2 expression (Honma *et al.*, 2008).

With regards to the elucidation of any differential responses that the different combinations of heterodimers that can be formed from ERα and β produce – unfortunately not much is known. It is known that the truncated versions of the

receptors have a lower binding affinity to EREs than the wild type receptors, which suggests that the actions of ERs are preferentially executed by the wild type nuclear receptors (Moore *et al.*, 1998). It is suggested in literature that the truncated versions of both ERs, play more of a role in regulating the wild-type receptors. For example, a study by Zhao *et al.*, (2007) showed that heterodimerisation of ERβ2 to ERα causes proteasome-dependent degradation of ERα, leading to the suppression of ERα regulated genes. It is even suggested that heterodimerisation of the wild type receptors is to regulate the activity of ERα - a study by Gruvberger-Saal *et al.*, (2007) as α/β heterodimers have been shown to reduce the transcriptional activity of ERα. It is evident however that the specific palindromic sequence of the ERE dictates what receptor it can bind (a previously mentioned point in this chapter), and perhaps this also regulates the specific dimers that can bind.

1.5: Mechanisms of Oestrogen Signalling

1.5.1 Classical Oestrogen Signalling

The mechanisms of action of nuclear receptors ERα and β is similar. Prior to ligand binding, both receptors are localised to the chaperon heat shock protein 90 (HSP90) in the cytosol. Lipophilic steroid hormones like oestrogen passively diffuse into the cell, and the binding of this ligand to the respective receptors causes a conformational change that leads to their release from HSP90 and into the cytosol (Girgert, Emons and Gründker, 2019).

Following activation by binding to an oestrogenic ligand, receptors dimerise in the cytoplasm of the cell (both homo- and hetero-dimers of ERα and ERβ are possible), and translocate to the nucleus to bind to specific regions of DNA known as oestrogen response elements (EREs) - these are 13-15 base pair palindromic sequences located in or near to promoters close to target genes, activate recruitment of translational machinery and promote gene expression (Klinge, 2001). It is estimated that there are 70,000 EREs in the human genome, of which 17,000 are located close to transcriptional start sites (Bourdeau *et al.*, 2004). The specific sequence of the ERE affects the binding affinity for ERs, which can in

turn affect the extent of activation of particular genes and which particular isoform of ER can bind (Yi *et al.*, 2014).

Once bound to EREs, it is purported that ER can initiate gene transcription, making the complex of receptor and ligand the sole determinant of its activity. It is now understood, after the discovery of several oestrogen receptor associated co-factors, that this process actually requires the co-ordination of dozens of co-factors (Halachmi *et al.*, 1994; Anzick *et al.*, 1997; O ate *et al.*, 2006) to perform a multitude of functions. This includes the opening of chromatin for ERs to bind and the functionality of numerous co-factors that have enzymatic properties required for correct protein assembly and function.

The advent of genome-wide studies have provided the opportunity to access ER function – by purifying ER-associated DNA by chromatin immunoprecipitation (ChIP) and high-throughput DNA sequencing a number of new conclusions have been made. Such as, changes to the way we know that EREs are positioned in the genome – ER was thought to bind to the promoters of target genes, but unbiased mapping approaches showed that ER can associate typically with enhancer elements that can be relatively far away from target genes (Carroll *et al.*, 2005). Following on from this, given that the vast majority of ER binding sites are not at promoter proximal regions, the challenge was to identify whether all binding events of ER to DNA are active or elicit a response. Carroll *et al.* (2006) discusses that a marker of transcriptional activity was the co-presence of ER and other important co-factors that demarcate functionality – and that mapping of these couplings reveals a sub-set of transcriptionally active sites (Carroll *et al.*, 2006). Identifying which genes are specifically controlled (whether that be induced or repressed) by ER target sites that are conventionally far from their target coding region has presented an additional challenge – but, techniques such as identifying chromatin loops that form between enhancer regions of DNA and promoters of target genes can be performed (Dekker *et al.*, 2002). A milestone study by Fullwood *et al.*, (2009) details a global snapshot of the interactome that occurs between ERα binding to EREs and their target genes - this also shows ERα dimers to function by extensive chromatin looping to bring genes together for coordinated regulation of transcription. Showing that the ER complex can reach over significant distances to regulate coding genes.

A number of oestrogen responsive genes that lack EREs do contain ERE half-sites (SFREs) – which, are binding sites for the orphan nuclear hormone receptor SF-1. Which, interestingly, ERα is known to be able to bind to, but not ERβ (Vanacker *et al.*, 1999). To further complicate the story of oestrogen-receptor mediated transcription - around one third of the genes that are known to be regulated by oestrogen do not contain ERE-like sequences, however, which much suggest that they are not regulated by ER complexes binding directly with DNA and instead rely on the non-classical pathways, which will be elaborated on in the next section (O'Lone *et al.*, 2004).

From the perspective of the cumulative methods of oestrogen signalling, both the non-transcriptional and transcriptional activity of oestrogen converge to result in finely tuned regulation of target gene activity (Lipovka and Konhilas, 2016).

1.5.2 Non-classical Oestrogen Signalling

It was originally thought that oestrogen must signal in a non-genomic manner because oestrogens exert some effects that are so rapid, they must not rely on the activation of RNA production and protein synthesis, but rather the activation of various protein-kinase cascades, which is where the non-classical method of oestrogen signalling comes into play (Lösel and Wehling, 2003).

The non-classical method of oestrogen signalling itself can be split further into two parts. The first is through protein-protein interactions with other transcription factors, to form complexes that directly bind to DNA and influence gene transcription – the second is membrane associated ERs leading to activation of protein-kinase signalling pathways. These two non-classical general mechanisms allow for a much broader range of gene regulation than the classical mechanism (Björnström and Sjöberg, 2005). It should be noted that these two methods do not factor in the actions of the oestrogen stimulated G protein-coupled receptor, GPER1.

The receptors involved in non-classical signalling are the previously mentioned G-protein coupled receptor - GPER1 (which, as a reminder, is also referred to as GPR30 in literature but for the sake of simplicity I will continue using GPER1 for

the remainder of this work), and variants of the nuclear receptors ERα and ERβ (Chetana M Revankar *et al.*, 2005; Pedram, Razandi and Levin, 2006). Until recently, the idea of oestrogen regulating cellular processes independent of the classical nuclear receptors was controversial – now, some publications hypothesise that there is a subpopulation of classical ERs that reside near or attached to the cell membrane, and upon activation by ligand binding, form dimers and activate cell signalling cascades (Levin, 2009; Mermelstein, 2009). If this is the case, it does raise the question of how these receptors become membrane localised as, unlike GPER1, nuclear receptors like oestrogen receptors cannot form associations directly with the plasma membrane due to the absence of a trans-membrane domain in their structure. One candidate mechanism discussed by Meitzen *et al.*, (2013) is a direct association with metabotropic glutamate receptors by a post-translational S-palmitoylation of the nuclear receptor, to allow for later organisation of discrete functional microdomains with caveolin proteins. For context, caveolin proteins are expressed ubiquitously in mammalian tissues but expression levels vary considerably between different tissues – they participate in many cellular processes, mostly known for caveolin mediated endocytosis, but also for signal transduction and tumour suppression (Williams and Lisanti, 2004). The team shows this by pharmacologically inhibiting palmitoylation in hippocampal neuronal cells, and observing that this eliminated 17β-estradiol mediated phosphorylation of cAMP response element-binding protein, a process that is known to be dependent on non-classical signalling of oestrogen receptors. It should be noted that it is molecular method of localisation is likely to be subjective to the tissue type in question.

1.5.3 First Method of Non-Classical Signalling (Forming Complexes With Transcription Factors)

A number of studies have shown that oestrogen can regulate genes without ERs directly binding to DNA. This is where the first method of non-classical signalling plays a role. ERs in such cases are tethered through protein-protein interactions with other transcription factors to form complexes that in turn bind to DNA. This is thought to be because of the previously mentioned lack of oestrogen response elements (EREs) for one third of oestrogen regulated genes. In the absence of places to bind in the genome, ERs seemingly hijack other transcription factors for

the same end (Lösel and Wehling, 2003). An example of protein-protein interactions between ERs and other proteins within the cell that regulate gene transcription would be the interaction between ERs and an activator protein called AP-1 which is known to control a number of cellular processes including differentiation, proliferation and apoptosis (Hess, 2004). Whether there are differences between the two isoforms of ERs (α and β) and their ability to form these interactions is not clear.

To complicate things further, the functions of many transcription factors, including AP-1, are regulated through protein-kinase mediated phosphorylation – so the signalling pathway can in fact be referred to as a hybrid between non-genomic and genomic. It provides a mechanism distinct from classical signalling where the oestrogen receptors need to enter the nucleus to control transcription (Björnström and Sjöberg, 2005).

1.5.4 Second Method of Non-classical Signalling (Regulating Protein-Kinase Pathways)

For the second method of non-classical signalling; oestrogen receptors can form direct associations with target protein-kinases following stimulation with oestrogen. The receptors are thought to be membrane-associated at this point. This leads to activation of kinases, phosphatases and increases the flux of ions across membranes – examples of this include stimulation of cAMP production, increased signalling via the PI3K and AMPK signalling pathways and mobilisation of intracellular calcium (Björnström and Sjöberg, 2005).

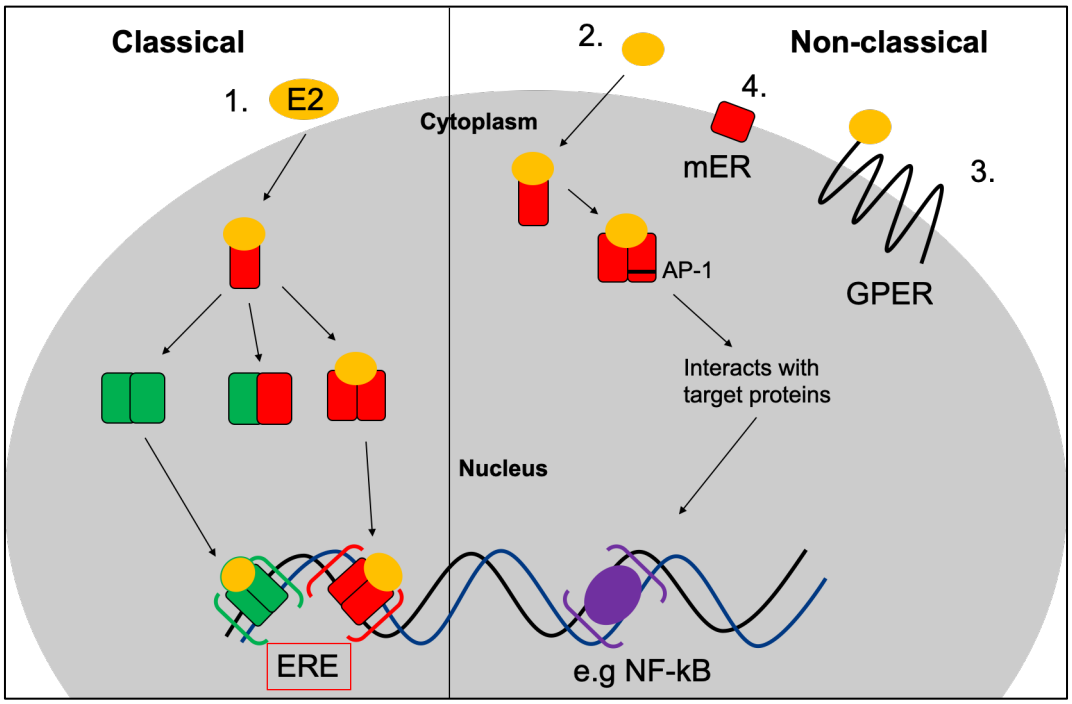


Figure 1.4. Simplified schematic of classical and non-classical oestrogen receptor signalling. Classical: (1) Oestrogen passively diffuses into the cell, and binds to either ERα or ERβ nuclear receptors. These then either homo- or hetero-dimerise and translocate to the nucleus, where they then act as transcription factors, forming complexes bound to oestrogen response elements (EREs). Non-classical: (2) oestrogen passively diffuses into the cell, binds to cytoplasmic/membrane localised ERs, directly interacts with target proteins, which in turn regulate gene transcription via other transcription factors such as NF-κB. (3) Non-classical oestrogen signalling can be regulated through GPER1. (4) Non-classical oestrogen signalling can be regulated by truncated or wild-type membrane localised ERs, by interaction with other growth factor receptors and stimulation of PI3K/AMPK signalling pathways.

From the perspective of the cumulative methods of oestrogen signalling, both the non-transcriptional and transcriptional activity of oestrogen converge to result in finely tuned regulation of target gene activity (Lipovka and Konhilas, 2016).

1.6: What genes are regulated by oestrogen?

Oestrogen regulates a large number of different genes in humans, via a variation of mechanisms as has been previously discussed. The role of oestrogen in general is to initiate timely cell division, which ultimately contributes to the development of mammary tissue, psychological function in adults, and naturally, plays a big role in the reproductive system in humans. It is a co-ordinated process that also involves other hormones and nuclear receptors including progesterone (Brisken and Ataca, 2015).

Speaking generally, and with the points raised in previous sections of this introduction in mind – when considering what genes are regulated by oestrogen,

there will naturally be a divide between genes regulated by the actions of each of the two oestrogen receptors. With regards to genes regulated by ERα, a recent study by Wang *et al.* (2018) highlighted a total of 267 differentially expressed genes using RNA-seq with ER+ breast cancer cell lines, further filtering this with a combination of bioinformatics analyses on the same cell lines, and microarray data from other oestrogen stimulated MCF7 cells to document 126 genes of interest. The expression of ERα was described to be negatively associated with metastasis and epithelial-mesenchymal transition (EMT) by the regulation of JUNB and ID3. This same study also identified the leading five genes involved in cellular proliferation and invasion by ERα activity as *FOS, SP1, CDKN1A* and *CALCR* (S. Wang *et al.*, 2018).

With regards to ERβ, previous studies have found genes involved in cell cycle regulation to be specifically downregulated by this receptor. Expression profiles of *CDC2, CDC6, CKS2* and *DNA2L* were significantly inversely correlated with ERβ transcript levels in patients and *in vitro* studies (Lin *et al.*, 2007).

A surprisingly large proportion of the genome of a breast cancer cell line is transcribed in response to oestrogen stimulation. Studies on gene regulation in breast cancer cell lines (MCF7 in this instance) have shown that oestrogen related gene activation is time dependent, the genome study documents 628 differentially expressed genes showing a robust pattern of regulation 12hrs after E2 stimulation, with a set of 880 different genes differentially regulated after 48hrs of E2 stimulation – this highlights the complexity and variability of E2 signalling in breast cancer and potential for combinatorial factors (Huan *et al.*, 2014).

Analysis of thousands of ER-DNA interaction sites identified novel ER-associated proteins, which contribute to stabilise ER interaction with chromatin, including a number of transcription factors that have the potential to assist with the tethering of ER to DNA: FOXA1, GATA3, PBX1 and AP2γ. The weighting of their specific involvement in oestrogen signalling is unclear, but it is known that inhibition of these individual factors in breast cancer cell lines perturbs ER-DNA interactions (Carroll *et al.*, 2005; Eeckhoute *et al.*, 2007; Magnani *et al.*, 2011; Tan *et al.*, 2011).

Furthermore, a review from Carroll, (2016) discusses the importance of *FOXA1,* and *GATA3* specifically for their importance in ER signalling, and for their consistent observation in ER+ breast cancer, and requirement for the formation of oestrogen-responsive ER complexes.

1.7 GPER1

In an earlier section, the subject of the oestrogen-responsive G protein-coupled receptor, GPER1, was touched upon. Here, it will be described how this fits into the mechanics of oestrogen signalling.

To elaborate on previous points made in this chapter – ERs α & β were discovered more than 20 years apart (Jensen and DeSombre, 1973; Kuiper *et al.*, 1996), and these were thought to be solely responsible for the responses elicited by oestrogens. Until six separate laboratories, employing independent cloning strategies reported the isolation and characterisation of a GPCR homologue that was presumed to have cognate ligand that was a peptide hormone, that scientists later identified as oestrogen (Filardo and Thomas, 2012). Oestrogen induces observable responses in cells in time frames that are too fast for the genomic mechanism induced by the classic signalling mechanism of the wild-type nuclear receptors. Bearing in mind the previously mentioned ability of membrane-localised truncated versions of ERα (ERα-36) to initiate intracellular signalling cascades that could also be responsible for these fast observable responses, this does not explain all cases. The study referred to in this instance is one pertaining to the transfection of and subsequent expression of GPER1 into Cos-7 cells (that are known to not express nuclear ERs). With these cells, an intracellular calcium mobilisation was observed in as little as 20 seconds when stimulated with 17β-oestradiol (Chetana M. Revankar *et al.*, 2005). GPER1 does not only affect intracellular calcium mobilisation however – in rat myometrium cells, GPER specific agonists induced membrane depolarisation by opening certain calcium channels in the cell membrane that allowed influx of extracellular calcium (Tica *et al.*, 2011).

The localisation of GPER1 has been a controversial topic in literature since its discovery. The fact that GPER1 is a 7-transmembrane receptor implies that is characteristically membrane bound, however previous studies have shown that it is also intracellularly located, specifically to the endoplasmic reticulum. There are conflicting statements in literature however about whether or not intracellularly located GPER1 is responsive to oestrogen (Chetana M. Revankar *et al.*, 2005; Broselid *et al.*, 2014).

A study by Filardo *et al.*, (2000) that focussed on elucidating the specific signalling events triggered by stimulation of GPER1 observed that the activation of MAPK/ERK pathways after exposure to 17β-oestradiol in a number of breast cancer cell lines, with differing expression levels of ERα. Even in a cell lines that expressed neither ERα or ERβ, they noticed a marked increase in ERK phosphorylation. Whereas, in a cell line that did not express GPER1, there was no notable increase in ERK phosphorylation. A comprehensive review on GPER1 signalling in the context of ERα negative breast cancer by Girgert, Emons and Gründker (2019) discusses six different pathways being activated by GPER1 stimulation: EGFR pathway (indirectly), calcium-signalling, cAMP-pathway, IχB-pathway, Hippo-pathway and the HOTAIR-pathway. Figure 1.5, below, shows a diagrammatical representation of this.

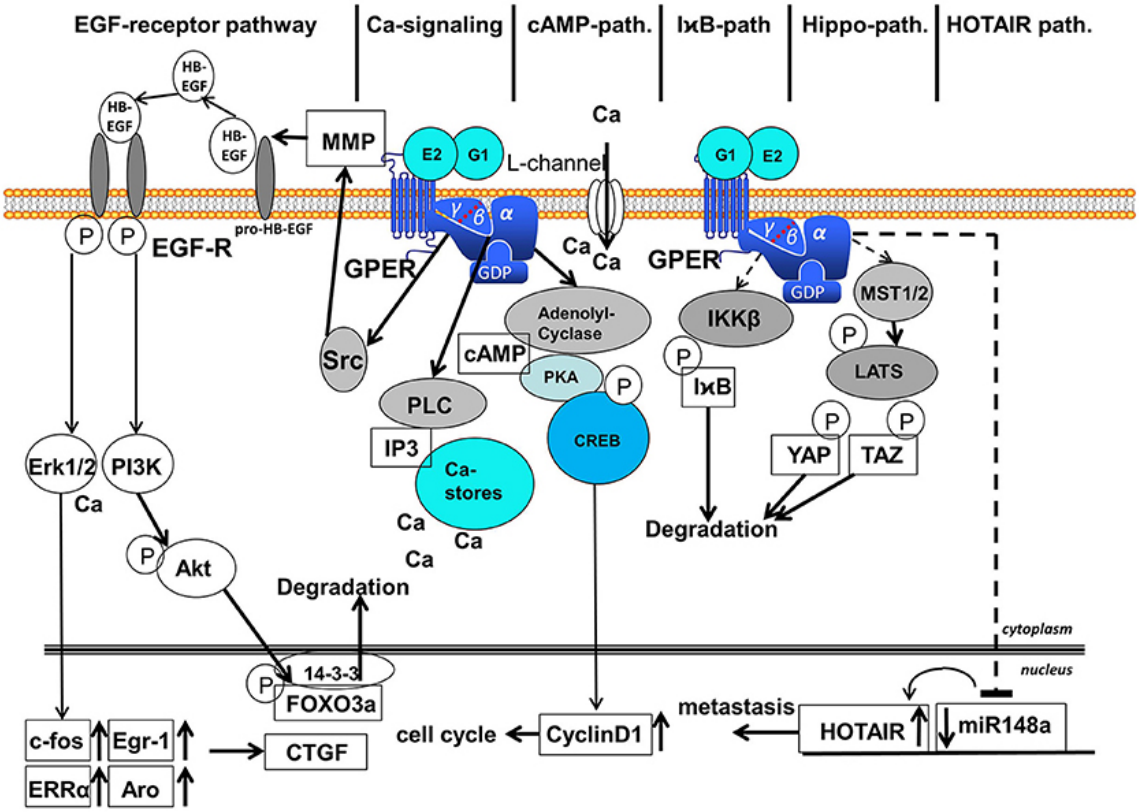


Figure 1.5. Taken from Girgert, Emons and Gründker (2019). A comprehensive map of the signalling pathways involved in GPER1 signalling. Six different pathways are distinguished in this review article.

GPER1 is especially interesting to consider in the context of triple negative breast cancer (TNBC). Dogma surrounding the treatment of breast cancer, if not just the classification of it, depends on the expression of growth hormone receptors. Put simply for the majority of cases, if a tumour is ER+, it will be considered for endocrine therapy. But, it is not commonplace to also consider GPER1 expression (neither is it commonplace to consider ERβ expression, as a side note) – this is especially relevant as GPER1 is known to be expressed in TNBC, making something thought to be non-responsive to oestrogen, ultimately responsive to oestrogen (Yang *et al.*, 2013; Girgert, Emons and Gründker, 2019). In fact, TNBC patients with low GPER1 expression have been found to correlate with decreased tumour recurrence. After a 36-month follow up, 90.5% of TNBC patients with low GPER1 expression were still alive, whereas the cohort with high expression were at 77.8% after this time period (Perez *et al.*, 2012).

1.8 Cross-talk with other signalling pathways

The mechanisms of oestrogen signalling discussed so far have been exclusive to receptors stimulated by oestrogen, but this does not allow for the potential of crosstalk between other nuclear receptors – which has been shown to occur to a substantial degree with both the progesterone receptor (PR) and the androgen receptor (AR) converging on the ER pathway. When considering on a cellular level, under physiological conditions, ER+ breast tissue (cancerous or not) is exposed to a complexity of different hormones and growth factors. AR and PR can alter ER signalling in a number of ways, through sequestering rate-limiting co-factors, direct regulation of ER levels or even direct alteration of ER-DNA interactions by AR or PR (Zheng *et al.*, 2008; Peters *et al.*, 2009). The ability of nuclear receptors to interact within the same cellular environment highlights the potential for them to be substituted for one another – for example, in a rare subtype of breast cancer called apocrine (where gene signatures are similar to that of ER+ cancers, but are actually ER-), it is believed that AR can substitute in the absence of ER as the driving transcription-factor. It is thought that AR continues to regulate ER through ER specific transcription factors such as FOXA1 (that has been previously mentioned in section 1.6.5). There is also evidence to suggest that the downregulation of ER and subsequent mobilisation of AR as a response may be a mechanism of resistance to endocrine therapies (Robinson *et al.*, 2012).

Another consideration is the known rapid activation of classical second messengers such as cAMP and calcium, and stimulation of MAPK and PI3K signalling pathways – it has been touched upon that GPER1 and truncated version of ERs may be responsible for this, but another explanation may be cross-talk with membrane receptors that possess intrinsic tyrosine kinase activity. A study by Filardo, (2002) shows that oestrogen transactivates the epidermal growth factor receptor (EGFR) via GPER1.

1.9 Oestrogen signalling in cancerous tissue

The nature of oestrogen signalling in normal tissue is complex, as we have seen, and involves the modulation of many different targets, ultimately either favouring or counteracting cellular propagation, dependent on a number of different factors. Of course, cancer cells (that are ER+) rely on oestrogen signalling for growth in

the same way that physiologically normal cells grow, but like any tightly controlled growth mechanism, dysregulation is a marker of disease and an oestrogen-induced tumour (Hanahan and Weinberg, 2011). The question is how is signalling in cancerous tissue different from that of physiologically normal tissue?

Essentially, ER continues to operate in its normal role, but ER-mediated cell division occurs in an uncontrolled manner, resulting in tumour initiation and cancer progression. When we consider the generally opposing roles of ERα or ERβ, any preference for the activation of genes associated with the pro-proliferative function of ERα would prove to be a positive influence on cancer progression.

1.10 Phenol red in culture media

In addition to oestrogen, phenol red is a cell culture medium ingredient, which has been shown to exert oestrogenic activity. Oestrogen itself has a high efficacy, inducing responses with concentrations as low as nM ranges (Berthois, Katzenellenbogen and Katzenellenbogen, 1986), whereas phenol red alone has nowhere near this effect. Berthois *et al* (1986), Rajendran *et al* (1987) Glover *et al* (1988) and Welshons *et al* (1988) were some of the first to investigate the effect of phenol red in oestrogen-responsive cell lines – MCF7 and T47D in particular, which are cell lines used in this work along with being among the most common cell lines used to investigate breast cancer *in vitro* (Penot *et al.*, 2005; Zhao *et al.*, 2007; Cochrane *et al.*, 2014). They discuss (amongst many other things that are relevant to this work) how in low concentrations, phenol red does not elicit a response from oestrogen-responsive cells, but the vast majority of culture media harbours phenol red in concentrations somewhere in the range of 15-45μM, within which has been known to exert oestrogenic affects. Notably, they show that phenol red has about 0.001% binding affinity to oestrogen receptors when compared to oestrogen, but at high enough concentrations, like that of culture media, phenol red can independently enhance cell growth rates (Berthois, Katzenellenbogen and Katzenellenbogen, 1986; Rajendran, Lopez and Parikh, 1987; Glover, Irwin and Darbre, 1988; Welshons *et al.*, 1988). Upon inspection of the culture media used for the entirety of this study, the company specifies on the provided product formulation specifications that phenol red is included at a

concentration of 39.9μM. Figure 1.6 below shows the most generally notable figures taken from Berthois *et al* (1986) that display the above points. Looking specifically at **B,** this figure shows that phenol red can independently influence MCF7 cell growth when exposed to cells that have been otherwise deprived of oestrogens, at a concentration representative of that in phenol-red containing culture media.

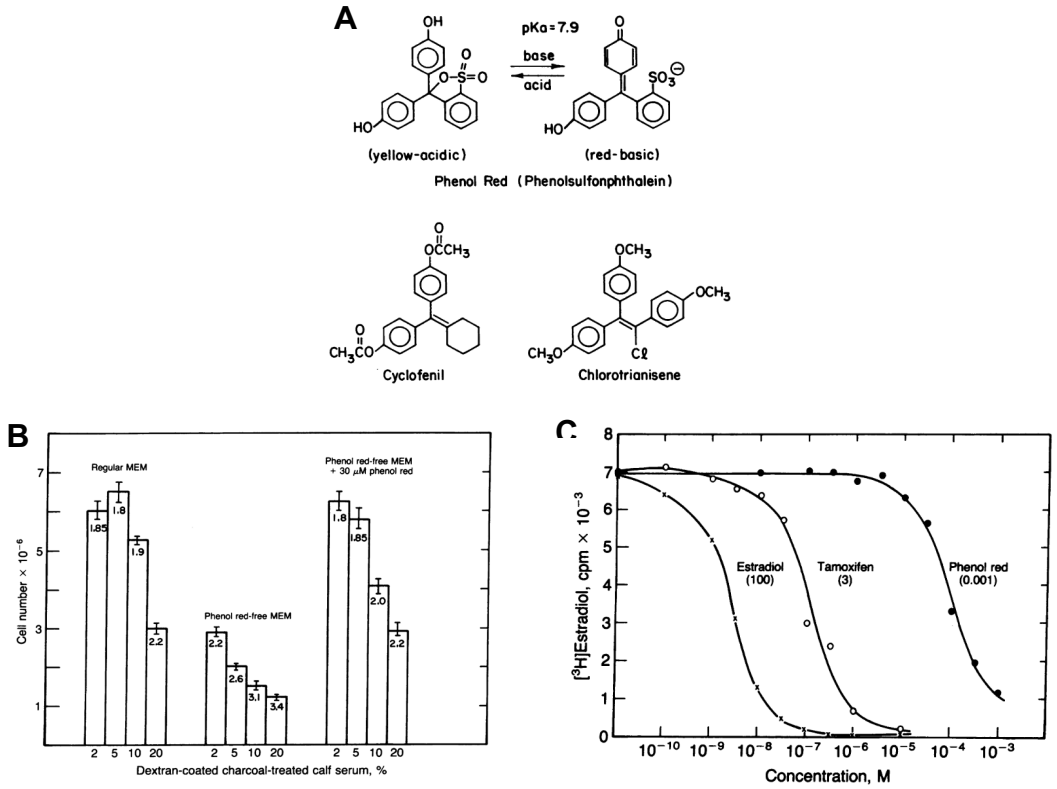


Figure 1.6: The effect of phenol red in culture media. taken from Berthois *et al,* (1986) **A**: shows the structure of phenol red, in both acidic and basic forms, and two structurally related non-steroidal oestrogens. **B:** shows the effect of phenol red, and differing proportions of charcoal stripped serum in the culture media on the growth of MCF7 cells. **'regular MEM'** = MCF7 cells grown with phenol red present. **'phenol red-free MEM'** = MCF7 cells grown with phenol red absent. '**phenol red-free MEM +30μM phenol red'** = MCF7 cells grown with phenol-red absent from the base culture media, but with 30μM phenol red added. **C:** shows a competitive binding assay of phenol red and tamoxifen compared to estradiol in MCF7 cells. Binding of a radioactive competitor, [^{3}H]estradiol, was determined to establish concentrations of estradiol, phenol red or tamoxifen needed to displace bound [^{3}H]estradiol. Parenteses under each compound indicate relative affinities of each compound to oestrogen receptors (estradiol set to 100) – which isoform of oestrogen receptor was not specified.

Liu *et al.*, (2013) looked at the effect of phenol red on primary neuronal cultures. They documented that phenol red had the capability of suppressing abnormal bursts of epileptiform activity in neurones – that culture of hippocampal pyramidal neurones cultured in neurobasal culture medium without the presence of phenol

red had large amounts of depolarisation-associated bursts of epileptiform activity, that is not seen in mirrored conditions in the presence of phenol red. They hypothesise that this is due to the oestrogen receptor activation as the effect of phenol red is mimicked when exposed to the oestrogen receptor agonist, 17-β-estradiol, and inhibited by an oestrogen receptor antagonist.

1.11 Drug resistance in cancer

Our knowledge, as a scientific community, of the biological characteristics of cancer is updating every day – an ever-expanding picture of dynamicity and subjectivity. In an ideal world, cancer treatments would be highly personalised to account for this, but that is not commonly possible, yet. As such, clinicians and scientists alike must be mindful that as no tumour is identical, neither is the mechanism at which cells develop acquired resistance, or passively maintain intrinsic resistance to anti-cancer drugs. But, patterns can be observed from resistance to specific drugs in specific cancers.

Despite advancing technologies with gene therapy and immunotherapies, systemic chemotherapy remains a promising and well-established option for cancer treatment. But, drug-resistance is a major issue for this type of cancer therapy. Resistance can either be intrinsic (meaning present before treatment begins) or acquired over time by various exposure-induced adaptive responses to an anti-cancer drug. Tumours are heterogenous by nature, and the systemic treatment selected by the clinician will naturally select for subpopulations of cells that are more drug tolerant, shaping the tumour landscape over time (Holohan *et al.*, 2013). Increasingly, high-throughput and systems biology screening techniques are being employed to identify novel, and more importantly personalised, mechanisms of resistance to anti-cancer drugs; meaning that biomarkers of resistance are increasingly being used to guide and stratify patients to receive certain therapies (Williams and McDermott, 2017).

Acquired resistance to a drug is first and foremost dependent on the anti-cancer drug in question and its mechanism of action. At the tumour level, various resistance mechanisms can operate such as increased drug efflux, mutations of the drug target, intrinsic alterations to DNA damage repair mechanisms and

activation of alternative signalling pathways (Holohan *et al.*, 2013). In this work, endocrine therapy is the focus, specifically of tamoxifen and its active metabolites, so mutation of target sites and activation of alternate pathways is the focus.

1.12 Endocrine therapy

Endocrine therapy represents an important and commonly used anti-cancer strategy in the management of ER+ metastatic breast cancer. There are two main forms of endocrine therapy: aromatase inhibition (the enzyme responsible for converting androgens to oestrogen) and direct inhibition of the oestrogen receptor with tamoxifen or fulvestrant for example. The former is generally the go-to treatment for post-menopausal women, as their primary source of oestrogen is by the release of androgens from the adrenal gland and adipose tissue and subsequent conversion to oestrogen by aromatase; the latter is generally the go-to for premenopausal women. It should be noted however, that it is also possible to reduce endogenous oestrogen levels in premenopausal women by both surgical (ovariectomy) and pharmacological (luteinizing hormone-releasing hormone agonists) means. Therefore, endocrine therapy in general works by blocking the effects of oestrogen - either at the receptor level or by inhibiting its production (Chang, 2012; Reinbolt *et al.*, 2015).

1.13 Tamoxifen (duality of tamoxifen signalling)

It is estimated that approximately half a million women are alive today thanks to the use of tamoxifen in ER+ breast cancer, and even more have benefitted from its life-extending affect and palliation (Jordan, 2003). Tamoxifen is known as a selective oestrogen receptor modulator (SERM) because of its tissue specific activity. To summarise loosely what is meant by tissue specific, tamoxifen is thought to be an ER antagonist in the breast, but an agonist in uterine/endometrial tissues - hence, why uterine cancers are linked to long-term tamoxifen treatment (Pearce and Jordan, 2004). Naturally, the relationship between tamoxifen and the two distinct areas of human physiology is more complex than this face value summary however.

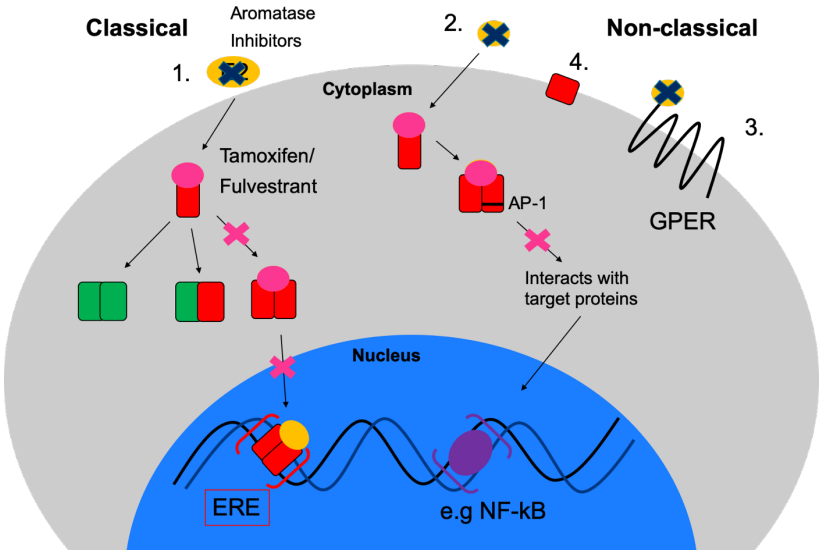


Figure 1.7: Tamoxifen and aromatase inhibits interfere with oestrogen signalling. Simplified schematic of classical and non-classical oestrogen receptor signalling, and how endocrine therapy affects this. Aromatase inhibitors are represented by navy blue crosses. ER antagonists, tamoxifen and fulvestrant are represented by pink crosses and circles.

Tamoxifen (TAM) exerts anti-oestrogenic activity in the breast through partial inhibition of ER dimerisation by competitive binding. As has been discussed before, ERs are required to either homo- or heterodimerise in order to make contact with the palindromic sequences of EREs in the genome. In contrast, fulvestrant, another commonly used endocrine therapy completely inhibits ER dimerisation. Tamoxifen binds to ERs with a lower affinity than that of oestradiol. A complex of tamoxifen and ER forms and dimerises with another TAM-ER complex, this inactivates the ligand-dependent AF-2 domain of the ER, and activates the ligand-independent AF-1 region (see section 1.8 for more on AF domains). The TAM-ER complex binds to the EREs in the genome, in promoter regions of oestrogen responsive genes. Transcription of these genes is attenuated because of the inactivation of the AF-2 region. ER co-activator binding is also reduced by the TAM-ER complex. Partial agonist activity results from the AF-1 domain remaining active (Rondon-Lagos *et al.*, 2016). See figure 1.8 below for a diagrammatical representation of this.

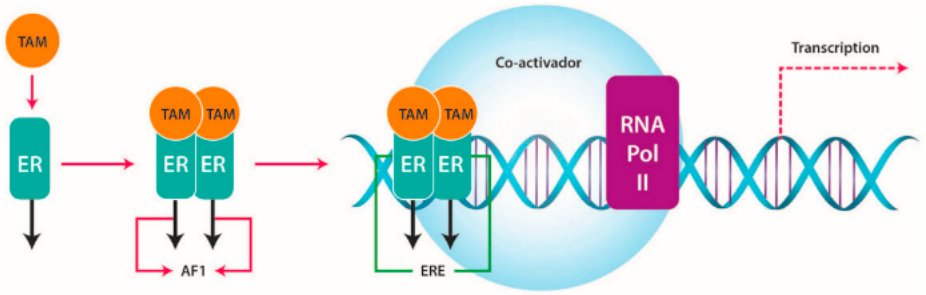


Figure 1.8: Oestrogen receptors dimerise and bind to EREs. Taken from Rondon-Lagos *et al.*, (2016). Tamoxifen competitively binds to ERs and inactivates the ligand-dependent AF-2 domain of ERs – maintaining activation of the ligand independent AF-1 domain. TAM-ER complexes bind to EREs and attenuate gene transcription of oestrogen controlled genes.

Tamoxifen itself is metabolised extensively in the liver by cytochrome P450 enzymes, and to a lesser extent in the breast also. These enzymes mediate the transformation of tamoxifen into a several primary and secondary metabolites, mainly through hydroxylation and demethylation – these are known to have high potencies than the parent drug, and therefore thought to exert the anti-tumour effects of tamoxifen *in vivo* (see figure 1.9 below). The major metabolic pathway involves initial conversion of tamoxifen to n-desmethyltamoxifen, then to endoxifen. This is the conversion with the highest throughput. The second-most preferred conversion is tamoxifen to 4-hydroxytamoxifen, which is in turn also converted to endoxifen (Cronin-Fenton, Damkier and Lash, 2014). Polymorphisms in several CYP enzymes involved in the metabolism of tamoxifen impact on the relative abundance of the metabolites in systemic circulation; which, adds to the already existing patient-to-patient subjectivity you would expect as these enzymes will be differentially expressed naturally from person to person (Rondon-Lagos *et al.*, 2016).

Endoxifen, the major metabolite responsible for the actions of tamoxifen, appears to have differential effects on the two nuclear oestrogen receptors – it stabilises ERβ, promoting hetero-dimerisation and has an increased inhibitory effect on oestrogen-responsive genes whilst simultaneously targeting ERα for proteasomal degradation (Wu *et al.*, 2011).

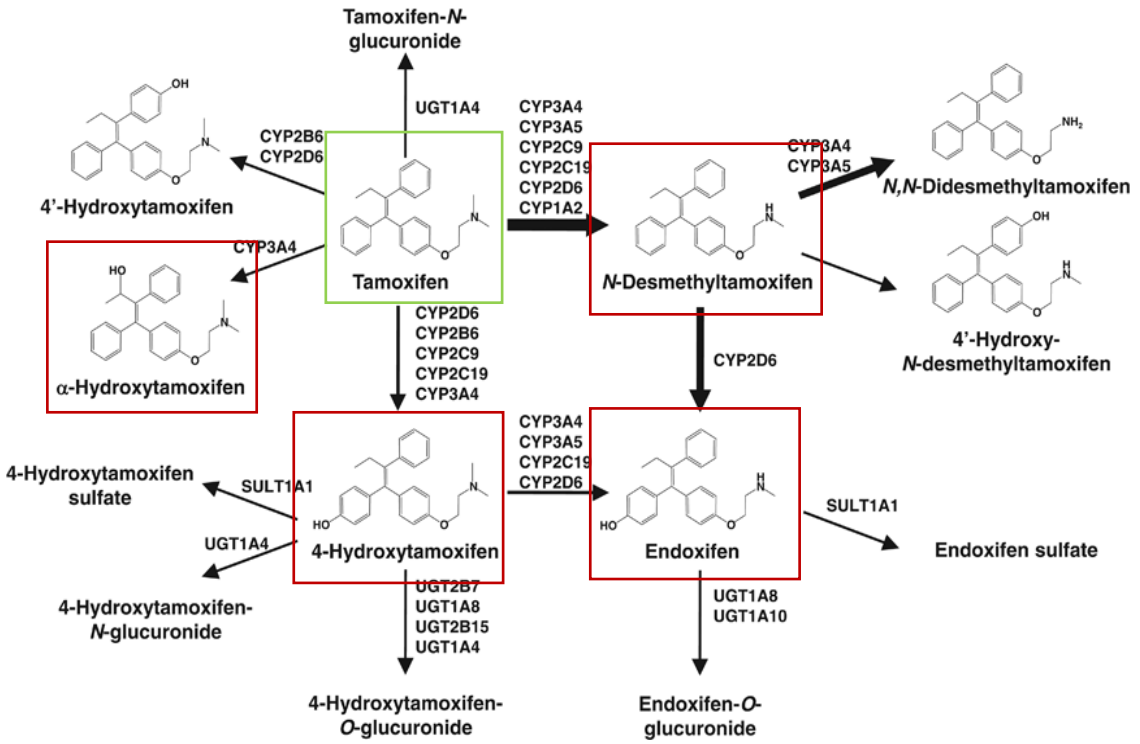


Figure 1.9: Tamoxifen, tamoxifen metabolites and CYP450s. Shows the primary metabolites of tamoxifen that were used in this study. Tamoxifen (green box) and the four primary metabolites (red boxes): Endoxifen, (Z)-4-OH tamoxifen, N-desmethyltamoxifen and α-hydroxytamoxifen that were used in this study. The size of the arrow is representative of the relative abundance of the metabolite.

In premenopausal patients, which are the most commonly treated group with this drug; 20mg of tamoxifen per day is the standard endocrine therapy. A meta-analysis of a breadth of clinical data published in the Lancet by the Early Breast Cancer Trialists' Collaborative Group in 2011 states that five years of adjuvant tamoxifen therapy robustly showed a reduced recurrence of disease. But not just in the first five years, but also for 5-9 years following the termination of a continuous treatment regimen for patients with ER-positive disease. Mortality was also documented to be down by a third throughout the first 15 years of follow-up care. This effect was documented to be also independent of PR status, chemotherapy use and age.

In the case of type B luminal tumours (to recap; those are high Ki-67 expressing hormone receptor positive tumours, high risk), chemotherapy is often indicated for concurrent use with anti-oestrogen therapy. Naturally, care is taken when prescribing any pharmaceutical, regardless of its purpose, for patient susceptibility to off-target effects, contraindications and moreover antagonistic properties to other pharmaceuticals that the patient is taking. This, naturally, is

also the case with the combination of cytotoxic chemotherapy with anti-oestrogen therapies. Cytotoxics are known to have certain non-specific effects on the endocrine system, which in the case of breast cancers that are potentially influenced by fluctuations in steroid hormones, is a very important consideration. In assessing the potential for combinations of chemotherapy and anti-oestrogens, it is important to note that an increased response rate is not necessarily the most important end point. Ideally, the desired combination would harbour an increased response rate and an increased response duration compared with the rates provided by the same agents used as monotherapies or used sequentially - considering that two anti-cancer agents administered together will almost certainly increase overall toxicity (Pritchard, 2008).

1.14 Resistance to tamoxifen

Despite the obvious benefits of tamoxifen – a large proportion of patients at all stages of ERα+ breast cancer treatment with tamoxifen as a first-line therapy or an adjuvant therapy eventually relapse. Furthermore, patients with early-stage disease that initially respond well to tamoxifen treatment develop recurrent tumours not only in the breast, but also in the endometrium (Pearce and Jordan, 2004).

Several mechanisms have been suggested to explain resistance to tamoxifen, but given the complexity of oestrogen signalling itself, there are a number of mechanisms that could potentially be altered to result in increased tolerance to the drug. The main mechanisms accepted today are alterations to bioavailabilty of tamoxifen, changes to both the nuclear receptors and GPER1, alterations to oestrogen controlled intracellular signalling pathways (from ERα-36, GPER1 and GPER1-EGFR crosstalk) or switching to signalling through other nuclear receptors like androgen receptor (which has been previously discussed in section 1.8). Clinical evidence suggests that patients that over-express HER2 are more likely to develop resistance to tamoxifen, which may suggest a switch in preference for signalling with certain hormones (Massarweh *et al.*, 2008).

1.14.1 Changes to the nuclear oestrogen receptors

The most obvious change to the nuclear receptors that could result in increased tolerance to tamoxifen would be a downregulation of its target ERs. As ERα out

of the two isoforms (ERα and ERβ) is the one known to encourage tumour growth – that is the one that has always been of the most interest for targeted cancer treatments. ERα expression has always been a good predictor of a beneficial response to tamoxifen treatment, and patients with higher levels show increased beneficial responses compared to those that express it at low levels (Droog *et al.*, 2013). Loss of ERα expression has mainly been linked with adherent methylation of CpG islands and increased deacetylation of histones – this is thought to result in more compact nucleosomes structure, and limit transcription (Yang *et al.*, 2001).

Another logical alteration to ERs, that results in resistance to tamoxifen, would be mutations that cause functional differences. In hyperplastic breast lesions, a single amino acid substitution (K303R), has been observed to increase the sensitivity of ERα to oestrogen and alter cross-talk with other signalling pathways that usually negatively control oestrogen signalling (Fuqua *et al.*, 2000). The significance of this mutation is unclear however as it has not been detected in large publicly available genomic data sets, like the TCGA, nor does it have a high frequency in clinical samples (~10%) (Abbasi *et al.*, 2013). Recently, more studies have reported mutations to the ligand binding domain of ERα, that promote agonist confirmation of ERα, in the absence of oestrogen, leading to hormone-independent tumour growth and resistance to endocrine therapy (Merenbakh-Lamin *et al.*, 2013; Toy *et al.*, 2013; Jeselsohn *et al.*, 2014). Interestingly, the reported incidence of these mutations were low in primary tumour samples, but high in samples taken of metastases – and, appear more frequently in patients that had previously received hormonal therapy (Niu *et al.*, 2015).

The modulation of ER activity is another factor to consider when thinking of its interaction with both oestrogen and tamoxifen. As we already know, it is the modulation of ER activity that is the basis for functionality of tamoxifen. However, another consideration is our understanding of the functionality of the ER by post-translational modifications, such as phosphorylation, and how this affects the interaction of ERs with tamoxifen and oestrogen – also in the context of ligand independent ER activity. Previous studies have identified that changes to post translational modifications, especially phosphorylation, like that of position S305

has been shown to have an effect on tamoxifen resistance. As well as observed changes to the conformation, dimerisation and DNA binding of ERs. Studies have suggested that observed increased phosphorylation to certain sites of ERs predict a poor outcome to tamoxifen therapy, as well as an increase in observed ligand-independent cell growth and gene regulation. It is therefore an important consideration when assessing possible mechanisms of tamoxifen resistance (Kastrati *et al.*, 2019).

1.15.2 Differential responses of tamoxifen with truncated ER isoforms

Resistance to tamoxifen has also been linked with high expression of the membrane-localised, truncated version of ERα (ERα-36) that is known to be able to stimulate non-genomic intracellular signalling pathways (Wang *et al.*, 2006). To support this, clinical data shows that tumours that highly express ERα-36 appear to benefit less from tamoxifen treatment (Teymourzadeh *et al.*, 2017). Upon the commencement of tamoxifen use as an anti-oestrogen, it was specifically intended to antagonise ERα. Due to a lack of information about the complexity of oestrogen signalling, specifically that pertaining to the discovery of the non-genomic signalling capacity of oestrogen mediated by ERα-36 and GPER1; the idea that tamoxifen could also have additional effects to the antagonism of ERα was not adequately explored. As a delve into available literature on this subject, with the intention of finding an explanation for tamoxifen's ability to both antagonise and agonise in *in vivo* environments - a large cohort study by Wang *et al.*, (2018) demonstrates that tamoxifen can directly bind to and activate ERα-36 to enhance stemness and metastasis of breast cancer cells via transcriptional stimulation of aldehyde dehydrogenase 1A1. Essentially acting as an agonist in this truncated from of ERα but not in the wild-type form. This raise the question of what other effects tamoxifen has on all of the other nuclear receptor isoforms, and how this changes if the nuclear receptors were mutated.

1.14.3: GPER1 in tamoxifen resistance

GPER1 is expressed in approximately 50-60% of all breast carcinomas, along with endometrial and ovarian cancer cells. Importantly GPER1 is expressed in a large proportion of triple negative, and generally ERα- breast cancers, as

discussed in section 1.7. It was also mentioned in section 1.7 that GPER1 has been found to be both membrane localised (as expected for a G-protein coupled receptor) and internally localised. It is this subcellular localisation that is thought to contribute to tamoxifen resistance. The exacts of this subcellular localisation is a topic of debate in literature and as such has not been clarified. But, studies have suggested that GPER1 can be located in the nucleus and in the cytoplasm. Perhaps this can be explained by a transport mechanism from the membrane to the nucleus. GPER1 localisation has been correlated with differing clinicopathological characteristics – for instance, cytoplasmic localisation has been associated with low grade tumour stage and high levels of nuclear localised GPER1 is associated with poorly differentiated carcinomas and TNBC subtypes (Samartzis *et al.*, 2014).

In addition to estradiol, tamoxifen and its metabolite 4-OH-tamoxifen also have a high affinity for direct binding to GPER1 - causing rapid activation of intracellular signalling cascades including ERK, PI3K, calcium mobilisation and cAMP production (Girgert, Emons and Gründker, 2012). This regards tamoxifen as a GPER1 agonist – meaning that the balance between the expression and activation of the nuclear receptors and GPER1, together, is important when visualising the role that oestrogen, and by extension tamoxifen, plays in breast cancer. As already discussed in section 1.10, this not only highlights in role GPER1 may play in tamoxifen resistance, but also on in breast cancer progression on a larger scale when considering its significance in TNBC.

As tamoxifen acts as a GPER1 agonist – signalling incurred by direct activation of GPER1 is not the only thing to consider. Cross-talk with other signalling pathways must also be considered. It has been reported thatGPER1-positive breast cancer patients, tamoxifen activates cross-talk between GPER1 and EGFR. This cross-talk is thought to contribute to an increased cellular growth that is associated with tamoxifen resistance, but also with enhanced ability to metastasise. It is also thought that in GPER1-positive breast cancer patients, treatment with tamoxifen will increase GPER1 expression – in such cases, the effects of estradiol will also be enhanced. As such, GPER1 expression should be taken into careful consideration by clinicians when contemplating any courses of tamoxifen treatment (Rakha, El-Sayed, Green, Andrew H.S. Lee, *et al.*, 2007).

1.14.4: Androgen receptor in tamoxifen resistance

The role of the androgen receptor (AR) in breast cancer remains controversial as it is not yet completely clear whether it has an overall proliferative or anti-proliferative affect. Literature predominantly suggests that the affect is proliferative, with the main mechanism being a dysregulation of PI3K/AKT/mTOR signalling pathways (Costa, Han and Gradishar, 2018). This would support the idea surrounding enhanced tumour propagation and ARs involvement in tamoxifen resistance in ER+ breast cancer, considering a switch of predominant use between the two is a potential mechanism of resistance.

It has been reported that tamoxifen resistant tumours express high levels of AR, while tamoxifen-sensitive tumours show the opposite pattern of expression. This observation suggests that high AR expression may be a good prognostic marker for intrinsic resistance to tamoxifen – potentially suggesting that high AR expression may play a role in enhancing the agonistic properties of tamoxifen (De Amicis *et al.*, 2010). A study by Cochrane *et al.*, (2014) postulates that the ratio of AR:ER is a better marker of response to tamoxifen in ER+ breast cancer, as opposed to expression levels of AR alone. The study states that women expressing a high AR:ER ratio (>2.0) had over four times higher risk for failure in tamoxifen treatment compared to women with a lower ratio (<2.0). It was also postulated in this study that a high ratio would be a marker of *de novo* or acquired resistance to tamoxifen. This accompanies a switch from oestrogen dependence to androgen dependence.

It is coming to light, that ARs play a role in the progression of TNBC in particular. As (previously discussed) one potential mechanism for tamoxifen resistance is a ‘switching over’ from the use of ERs to ARs in ER+ breast cancer, this could also be an intrinsic mechanism for TNBC that does not express ERs to begin with (Rakha, El-Sayed, Green, Andrew H. S. Lee, *et al.*, 2007; Anestis *et al.*, 2019).

Approximately 90% of ER+ tumours are also AR+, and this is associated with a favourable prognosis and lower tumour grade and size (Park *et al.*, 2010).

1.14.5: Other potential mechanisms of resistance of interest

The first additional pathway of interest is the hedgehog pathway. This pathway is most commonly associated with cell proliferation, embryonic development and tissue repair – dysregulation of this pathway is commonly seen with various types of cancer, including tumours of the breast, prostate and basal cell carcinoma (Bhateja *et al.*, 2019). This naturally raises the question of whether dysregulation of the hedgehog signalling pathway is anything to do with tamoxifen-resistance in breast cancer, or simply just to do with breast cancer. However, a study by Matevossian and Resh, (2015) has shown that in tamoxifen-resistant cell lines (MCF7 in this instance; ERα+, HER2+), an enzyme that catalyses the palmitoylation (HH acetyltrasferase) of Sonic HH, the major ligand in the pathway, is required for proliferation in breast cancer. Pharmacological inhibition of this decreased growth in ERα+ tamoxifen-resistant cell lines, but not in TNBC cell lines. Hedgehog signalling has not only been implicated with endocrine therapy resistance, but also to chemotherapy resistance in TNBC (Bhateja *et al.*, 2019).

Recent studies have found that the mRNA-editing enzyme APOBEC3B may have a role to play in the emergence of endocrine therapy resistance. The insightfully written works, by Law *et al.*, (2016) comments on the development of drug resistance in the context of anti-cancer therapy as testament to the fundamentally evolutionary nature of cancer. They suggest that APOBECs (traditionally associated with the immune system) play a role in this evolution towards a higher tolerance of tamoxifen in ER+ breast cancer. They state that APOBEC3B levels inversely correlate with the clinical benefit of tamoxifen, and that APOBEC3B overexpression also correlates with an accelerated development of endocrine resistance. Moreover, the team also states that APOBEC3B depletion in ER+ breast cancer cell lines results in prolonged tamoxifen responses in *in vivo* models, and that overexpression results in an accelerated development of resistance in the same models, by a mechanism that is known to require the enzymes catalytic activity.

1.15 Introduction to the work conducted in this thesis

The original aims of this project, as determined by our collaborators at Eli Lilly, were to produce tamoxifen resistant breast cancer cell lines from a pre-determined collection of cell lines and have them transferred to the Eli Lilly

Corporate Headquarters in Indianapolis, along with myself as the researcher, for further investigation using their equipment. This was to include metabolomics and proteomics studies on the cell lines in question. Unfortunately Eli Lilly had a change in interest in tamoxifen shortly after starting this project, so this was not followed up. The work in this thesis therefore pertains solely to investigations carried out at the University of Kent.

The use of cell line models has permitted the ability to study adaptation to growth in the presence of reduced growth hormones, including oestrogen, from culture in order to study the effect that growth hormones have on response to endocrine therapy, and their downstream consequences. In this work, we have not studied these in-depth mechanisms, but we have created two panels of cell lines to allow for this in future works. The ‘workhorse’ in the field of breast cancer research is the MCF-7 cell line – which has helped to elucidate a substantial amount about ER structure and functionality, but it is only one model and does not allow for heterogeneity, which is essentially the pillar issue with cancer research. As such, the MCF-7 cell line has been used in this works, along with a number of other breast cancer cell lines to directly compare any potential differences. Details of these other cell lines are documented in chapter 2 of this thesis.

Chapter 2: General Methods and Materials

2.1 Materials

2.1.1 Cell Culture – Cells, Media and Other Solutions

MCF-7, BT-474, EFM-19 and T47D lines were purchased from the German Collection of Microorganisms and Cell Cultures (DSMZ). CAMA-1 and MDA-MB-468 cell lines were purchased from the American Type Culture Collection (ATCC). SUM159PT (ATCC), CAL51 (DSMZ), HCC1806 (ATCC) and HCC38 (ATCC) cell lines, The platinum drug-adapted sub-lines of SUM159PT (carboplatin-resistant, SUM159PT^{r}CARBO^{4000}; cisplatin-resistant, SUM159PT^{r}CDDP^{1000}; oxaliplatin-resistant, SUM159PT^{r}OXALI^{5000}), CAL51 (CAL51^{r}CARBO^{5000}, CAL51^{r}CDDP^{1000}, CAL51^{r}OXALI^{5000}), HCC1806 (HCC1806^{r}CARBO^{2500}, HCC1806^{r}CDDP^{1000}, HCC1806^{r}OXALI^{2500}), HCC38 (HCC38^{r}CARBO^{3000}, HCC38^{r}CDDP^{3000}, HCC38^{r}OXALI^{5000}), were established as previously described (Kotchetkov *et al.*, 2005; Michaelis, Rothweiler, Barth, Cinat, M Van Rikxoort, *et al.*, 2011) and obtained from the Resistant Cancer Cell Line (RCCL) collection (https://research.kent.ac.uk/industrial-biotechnology-centre/the-resistant-cancer-cell-line-rccl-collection/; (Michaelis, Wass and Cinatl, 2016).

Word on the nomenclature of drug-resistant cell lines: The cell line that the resistant sub-line originates from is listed first, followed by the letter 'r' denoting it as a resistant sub-line, and the media condition that it was grown in (if a cell line from chapters 3 or 4, the sub-lines from chapter 5 do not have this). Then follows the shortening of the drug that it is resistant to, which will either be '4-OH' meaning (Z)-4-OH-tamoxifen for chapters 3 and 4, or 'OXALI', 'CDDP' or 'CARBO' meaning oxaliplatin, cisplatin and carboplatin respectively for chapter 5. Finally, the number stated at the end refers to the concentration of drug that the cell line is maintained in during routine cell culture. For results chapters 3 and 4, this in in μM, but for results chapter 5, it is stated in nM. This is because the cell lines in chapters 3 and 4 were produced during the course of this PhD project and were named later than the cell lines for chapter 5, which remains consistent with the nomenclature they possess in the RCCL collection.

Iscove's Modified Dulbecco's Medium (IMDM) was purchased from Thermo Fisher Scientific, along with the anhydrous SDS powder, dimethylformamide, absolute ethanol, penicillin/streptomycin solution (10,000 units/ml penicillin, 10,000μg/ml streptomycin) and 0.12% trypsin solution (devoid of phenol red). MTT powder was obtained from Universal Biologicals, Cambridge. Foetal bovine serum (ref: F7524, lot:BCBV8017) and charcoal stripped foetal bovine serum (ref: F6765, lot: 16C075) were obtained from Sigma Aldrich (Shaftesbury, UK).

Tamoxifen, (Z)-4-OH-tamoxifen, alpha-hydroxytamoxifen and endoxifen were all purchased from Cambridge Biosciences (UK), N-desmethyltamoxifen was purchased from Sigma Aldrich (Shaftesbury, UK). All were dissolved in absolute ethanol (Thermo Fisher Scientific, Ashford, UK). All drugs were aliquoted, stored at -80°C and thawed immediately before use.

2-methoxyoestradiol (Selleckchem, UK), olaparib (Selleckchem, UK) and vincristine (Cambridge Biosciences, Cambridge, UK) were all dissolved in DMSO. All were aliquoted, stored at -20°C and thawed immediately before use.

Oxaliplatin and carboplatin were purchased from Stone Healthcare (Derby, UK) dissolved 5% (w/v) aqueous glucose solution. Cisplatin was obtained from Sigma Aldrich (Shaftesbury, UK) as solution in 0.9% (w/v) aqueous NaCl solution. PD0325901 (Selleck Chemicals, Munich, Germany), MK8776 (AdooQ Bioscience via Bioquote, York, UK), MK2206 (Selleck Chemicals), mitomycin C (Cayman Chemical via Cambridge Bioscience, Cambridge, UK), etoposide (Cayman Chemical), and bleomycin (Cayman Chemical) were dissolved in DMSO. Zeocin (Thermo Fisher Scientific, Ashford, UK) was dissolved in PBS. All drugs were aliquoted, stored at -20°C, and thawed immediately before use.

2.1.2 Glassware and Plasticware

All plasticware for routine cell culture were purchased from Sarstedt: T25, 75 and 175cm^3 sterile vented cap culture flasks, sterile plastic stripettes of variable sizes and sterile falcons tubes (15/50ml). 24- and 96-well plates were purchased from Greiner. Glass slides and coverslips were obtained from Thermo Fisher Scientific, Ashford, UK).

2.2 Methods

2.2.1: Cell Culture

All cell lines were initially cultivated in Iscove's Modified Dulbecco's Medium (IMDM) with phenol red as standard, supplemented with 10% foetal bovine serum (FBS), 100IU/ml of penicillin, and 100μg/ml of streptomycin. The cells were regularly checked and passaged when they reach a confluency of ~70%. To passage, culture medium was aspirated off, cells were washed with PBS and detached from the flask using 0.12% trypsin solution (which, importantly for this work, does not contain phenol red) at 37°C, 5% CO_2 and 95% relative humidity. When detached, the indicated cell culture medium was added. The cell culture media used included IMDM supplemented with 10% FBS and antibiotics (IMDM/+FBS), IMDM supplemented with 10% charcoal-stripped (to remove oestrogen) FBS and antibiotics (IMDM/+CS), phenol red-free (phenol red exerts oestrogenic effects) IMDM supplemented with 10% FBS and antibiotics (IMDM/-FBS), and phenol red-free IMDM supplemented with 10% charcoal-stripped FBS and antibiotics (IMDM/-CS). Colour coding has also been used consistently in this thesis to ease understanding of bar graphs containing large amounts of data. Blue = charcoal stripped FBS. Red = Standard FBS.

Each parental cell line is cultured in each of the listed conditions. There are six parental cell lines – totalling in 24 individually cultured flasks. No experiments were conducted on the cell lines growing in their variable media conditions unless they had been growing in it for at least six months to allow for time to adapt to their new growth conditions – in the majority of cases, the cell lines had been growing in their new media condition for at least one year.

For chapter 5 of this thesis, both parental cell-lines and platinum drug resistant sub-lines were used. For that, the parental lines were cultured in IMDM, with 10% FBS and pen/strep as described above, with the addition of the amount of platinum drug that they are resistant to, as denoted in the nomenclature of the cell line itself.

2.2.2: Cryopreservation of cell lines

The parental panel of cells were banked down periodically (once per year) during culture, and the resistant cell lines were banked down once per year following confirmation of resistance. An attempt was made to bank down the drug-resistant

cell lines during development, but they proved to be too frail to revive successfully afterwards. Cells were banked down using a modification of standard culture media, to contain a greater percentage of FBS (20%), 10% DMSO and a greater percentage of antibiotics. Recipe below:

Cryoprotectant (to make 50ml): **34.5ml IMDM** (containing phenol red for those cell lines maintained in culture media containing phenol red, devoid of phenol red for those that were not), **10ml FBS** (FBS for the cell lines grown in FBS, charcoal stripped for those grown in charcoal stripped serum), **5ml DMSO**, **0.5ml pen/strep solution**. These were all the same consumables as those used to make up standard culture media, documented in section 2.2.1. All reagents were sterile and were prepared in a tissue culture hood.

T75 flasks were grown to 80% confluency, trypsinised, and the cell suspension was then centrifuged for five minutes at 1000g to produce cell pellets. Pellets were then resuspended in 4.5ml of appropriate cryoprotectant and aliquoted into 1.5ml fractions in 3 cryovials. The vials (after being appropriately labelled) were then frozen down at -20°C in a 'Mr Frosty' cell culture cryopreservation aid (which ensures freezing at a rate of 1°C per minute to avoid additional cell stress from fast freezing due to the addition of isopropanol) for 30 minutes before being transferred to a -80°C freezer, after 24 hours they were further transferred to storage in liquid nitrogen.

Resuscitation when required, involved transport on dry ice to a (previously prepared set-up of culture materials within a tissue culture hood), thawing the vials quickly in a water bath and transfer into an excess of complete culture media - 10ml sufficed. The solution was then centrifuged for 5 minutes at 1000g, and the resulting cell pellet was resuspended in a further 10ml of complete culture media, transferred to a T25 culture flask and left to incubate. This process ensured removal of residual DMSO. Speed and diligence was key for this process, especially with the more temperamental drug-resistant cell lines.

2.2.3: Adaptation of growth hormone-deprived sub-lines

Oestrogen/phenol red sub-lines were adapted to growth in their new media by constant culture in new media conditions for at least 6 months. Cell lines grown

in oestrogen deprived conditions (+CS/-CS) showed very notable decreases in cell growth, and complete loss of viability if passaged any lower than 3/10. As such, cell lines were passaged 3/10-5/10 (this was determined subjectively after visual inspection) for at six months or until cell growth improved to a rate that was similar to that of the parental cell line.

2.2.4: Generation of resistant cell lines

Resistant sub-lines were produced using a dose-escalation method. IC50 concentrations for the metabolite of tamoxifen selected for this process, (Z)-4-OH-tamoxifen (as it was the most potent of the metabolites used in this work and also the most commonly reported for this purpose in literature), were experimentally obtained from respective parental cell lines by MTT assay. The parental cell lines were then routinely cultured in the presence of their IC50 concentration for this drug, being escalated by 0.5μM at a time for around two years. Determining when the cell lines were ready for dose-escalation was done qualitatively based on the apparent health of the cell line after visual inspection, but generally done bi-weekly. Concentrations were also reduced at times when necessary. The cell lines were considered resistant when the IC50 against this metabolite of tamoxifen was twice that of the parental cell line. Tamoxifen-resistant sub-lines were generated in the four different media types, from parental cell lines that were already adapted to growth in these individual media conditions – meaning that the resistant cell lines were generated with differing amounts of oestrogenic stimulation.

The drug-resistant sub-lines used on chapter 5 of this thesis were received already resistant to platinum drugs. They were obtained from the resistant cancer cell line (RCCL) collection, where they would have been developed slightly differently to this.

2.2.5: Cell Growth Characterisation

Cell growth characteristics were evaluated in real-time by the xCelligence system (ACEA biosciences) that uses electrical impedance across interdigitated microelectrodes, which are embedded in the base of special assay plates, using a 96 well plate format according to the manufacturer's instructions. Cells were seeded at a density of 5,000 cells per well (n=4) and growth was tracked over

144hrs (6 days), with readings being taken every 30 minutes. Parental cell lines MCF7, T47D, CAMA-1, MDA-MB-468 and SUM159PT cell lines were all seeded at 5,000 cells per well. BT-474, EFM-19 were seeded at 10,000 cells per well. (Z)-4-OH-tamoxifen resistant cell lines were all seeded at this same density for respective tamoxifen resistant sublines. Parental and platinum-drug resistant cell lines HCC1806, CAL51 and SUM159PT cell lines were all seeded at 5,000 cells per well. Parental and platinum-drug resistant HCC38 cells were seeded at 10,000 cells per well. Cell seeding density was selected by one where the respective parental cell lines, or control +FBS cell line remained in log phase of growth, and did not enter stationary, up 120 hours of growth. Sublines derived from this were standardised to this same seeding density to observe the effects of changes in media/adaptation to growth in the presence of drug had on its growth rate. Doubling times were calculated by plotting the data obtained from the xCelligence system (impedence readings every 30 minutes for 6 days) in Microsoft Excel, and using the line equation (y=mx+c) to extrapolate the number of hours taken for the reading to double, using only data from the log phase of growth.

2.2.6: The MTT Assay

Cell viability was determined by 3-(4,5-dimethylthiazol-2-yl)-2,5-diphenyltetrazolium bromide (MTT) dye reduction assay (Mosman et al., 1983), modified as previously described (Michaelis et al., 2000) in 96-well plates using 100µL of medium according to the pipetting scheme below (Figure 2.1). Viable cells metabolise yellow MTT into an insoluble purple formazan. After 120h of incubation at 37°C, 5% CO_2 and 95% relative humidity, 25µL of 2% (w/v) MTT solution were added per well followed by a further 4h incubation period at 37°C, 5% CO_2 and 95% relative humidity. Then, 100µL 20% (w/v) sodium dodecyl sulfate (SDS) solution in 50% 400ml dimethylformamide (DMF) and 50% water adjusted to pH 4 to solubilise the formazan. The formazan content was quantified using a standard spectrophotometric microplate reader at a wavelength of 600nm. After subtracting of the background absorption, the results are expressed as percentage viability relative to control cultures which received no drug. Drug concentrations that inhibited cell viability by 50% (IC50) were determined using CalcuSyn (Biosoft, Cambridge, UK).

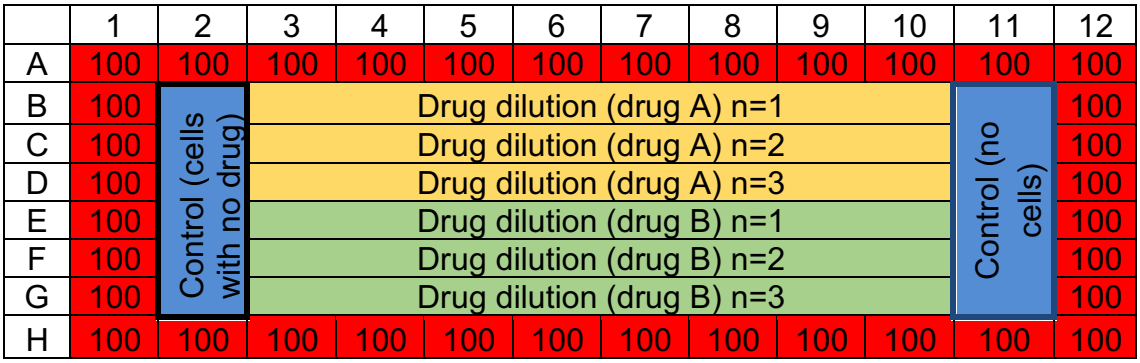


Figure 2.1: Pipetting scheme of the MTT assay.

2.2.7: Immunostaining

Cells were grown to a confluency of 70% in standard culture, as stated in 2.2.1. Cells are then seeded into 24 well plates, containing sterile glass coverslips at the base of the well, at a density of $1x10^4$ and cultured for 48hrs. Then, culture media was aspirated and cells were washed 3x with sterile phosphate buffered saline (PBS) and fixed for 20 minutes in 0.5mL/well of 4% (w/v) paraformaldehyde in PBS at room temperature. Next, cells were washed 3x with PBS and incubated for 20 minutes at room temperature with a permeabilisation solution containing 0.1% (w/v) Triton-X 100 in 3% (w/v) bovine serum albumin (BSA) in PBS. After washing 3x with PBS, the coverslips were transferred to a labelled section of parafilm and (cell-covered side down) placed onto a 30µL drop of a 3% BSA/PBS solution containing two primary antibodies (see section 2.2.1 for more details) directed against human oestrogen receptor alpha and beta at a 1:250 dilution. This section of parafilm was incubated on a raised platform in a humidity chamber overnight at 4°C. Then, the coverslips were washed 4x with PBS and placed onto a drop of secondary antibody conjugated to AlexaFluor 647 (red colour) at a 1:500 dilution in the dark. The coverslips atop the parafilm sheet were placed back into the humidity chamber and left to incubate for further three hours at 4°C. The secondary antibody corresponding to oestrogen receptor alpha is conjugated to AlexaFluor 647 (red colour, oestrogen receptor beta) or AlexaFluor 488 (green colour, oestrogen receptor beta), more information about these antibodies can be found in table 1.1. The coverslips were then washed 4x with PBS and mounted onto glass slides with an anti-fade agent (ProLong™ Diamond from Invitrogen) with integrated DAPI nucleic acid stain. The samples were imaged using a Zeiss LSM 880/Elyra/Axio Observer ZI confocal microscope. UV, 488 and 655 argon lasers were used to excite DAPI, green (AlexaFluor 488) and red (AlexaFluor

647) colours seen respectively. Laser power (gain) was kept as standard as per manufacturer's instructions. Black (B) and white (W) settings were set to B-10/W-7000 for DAPI, B-22/W-30,000 for green and B-10/W-25 for red. This remained consistent for all images.

Antibody	Manufacturer	Dilution	Product Number
ERα (rabbit)	Sigma Aldrich	1:250	MA3-310
ERβ (mouse)	Life Technologies	1:250	SAB4500814
Alexafluor™ 488 anti-mouse	Invitrogen – Thermo Fisher Scientific	1:500	A21206
Alexafluor™ 647 anti-rabbit	Invitrogen – Thermo Fisher Scientific	1:500	A21235

Table 2.1: List of antibodies used, manufacturer obtained from and working dilutions used for western blot analysis. Antibodies were diluted in 3% BSA/PBS.

2.2.8: Quantification of ER expression from immunostain images

Once the images had been taken using the method described above (2.2.7), and importantly saved as split channel images (each fluorophore being individually displayed, not as just an overlay of all dyes imaged) as you can see below, they were individually analysed using Image J software for the overall fluorescence intensity of each target. An n=6 images was acquired for each cell line - this was to compensate for the fact that not every image would have exactly the same number of cells captured in it as the positions of the images were selected randomly. An n=3 was captured for the negative controls. Each cell in the image was evaluated manually (by hand drawing the boundaries of the cell membrane – this allows for cells being different shapes), an average intensity was taken for the cell lines and normalised by the subtracting background/autofluorescence elucidated from appropriate negative controls.

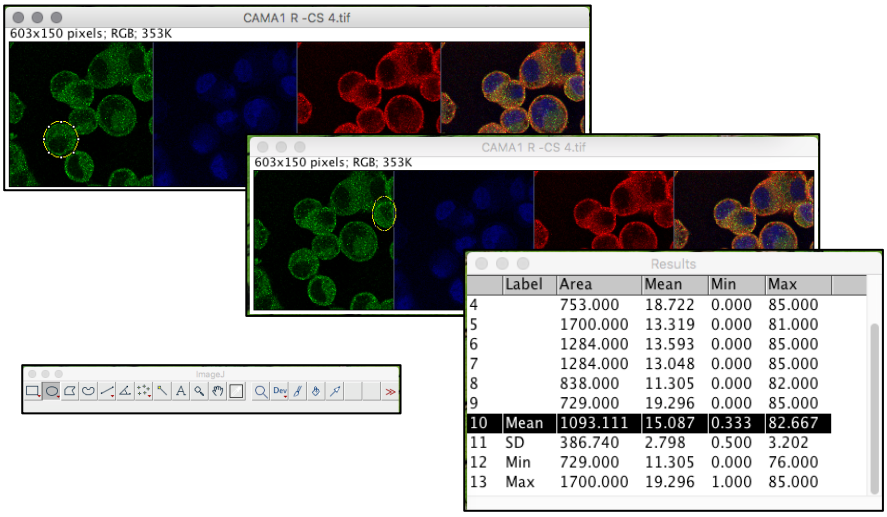


Figure 2.2: screen shots of the process of quantifying florescence intensity using ImageJ.

2.2.9: Western Blot Analysis

Cellular proteins were extracted using a cell lysis buffer (containing: 50mM HEPES pH7.4, 250mM NaCl, 0.1% v/v NP40, cOmplete™ protease inhibitor as per manufacturer's instructions (Roche), 1mM DTT, 1mM EDTA, 1mM NaF, 10mM ß-glycerophosphate and 0.1mM Sodium orthovanadate) and quantified by BCA (bicinchoninic acid) assay (Sigma Aldrich). 30-40µg/well (dependent on cell line) of protein was separated by running on a 12% Bis-Tris polyacrylamide gel. Proteins were transferred to a PVDF membrane (Sigma Aldrich), and subsequently blocked in 5% (w/v) skimmed milk in TBS-T (Tween-20, 0.1% v/v) for one hour at room temperature, prior to incubation with primary antibody. The membranes were incubated overnight at 4°C with primary antibody (see table 1.2) diluted in 5% milk in TBS-T. Membranes were washed for 4x 10 minutes in TBS-T, followed by an incubation with HRP-conjugated secondary antibody (see table 1 for manufacturer, also diluted in 5% milk) for one hour at room temperature. Antibody complexes were detected using ECL reagent (Thermo-Fisher Scientific) and Amersham Hyperfilm™ chemiluminescence detection film (GE Healthcare).

Antibody	Manufacturer	Dilution	Product Number
pAKT	Cell Signalling	1:1000	4060S
AKT	Cell Signalling	1:1000	4691S
pERK	Cell Signalling	1:1000	4370S
ERK	Cell Signalling	1:1000	4695S
pGSK3β	Cell Signalling	1:1000	5558S
GSK3β	Cell Signalling	1:1000	9315S
pS6RP	Cell Signalling	1:2000	2211S
S6RP	Cell Signalling	1:2000	2217S
pMEK	Cell Signalling	1:1000	9154S
MEK	Cell Signalling	1:1000	9122S
β-actin	Santa Cruz Biotechnology	1:1000	H1914

GAPDH	Santa Cruz Biotechnology	1:100,000	-
Anti-mouse HRP	Sigma-Aldrich	1:10,000	A9044
Anti-rabbit HRP	Sigma-Aldrich	1:10,000	A0545

Table 2.2: List of antibodies used, manufacturer obtained from and working dilutions used for western blot analysis. Antibodies were diluted in 5% milk/TBS-T.

2.2.10: Statistical Analysis

Statistical analysis for comparison between IC_{50} values and fold change values in this work conducted using two-way ANOVA with tukeys or bonferonnis correction dependent on the data set (**** - $p<0.0001$)(*** - $p<0.001$)(** - $p<0.01$)(* - $p<0.05$). Simpler comparisons between single data values were conducted by students t-test (* - $p<0.05$). Which statistical tests were used is stated in the figure legends of the appropriate figures. GraphPad 6.0 software package was used to conduct statistical analyses.

Chapter 3: Production and characterisation of growth hormone deprived breast cancer cell lines

3.1 Introduction

3.1.1 Introduction to the Data in This Chapter

This chapter uses five oestrogen-receptor (ER) positive, and one triple negative breast cancer cell line as a control (see table 3.1 below). Each has been separated to grow in four media conditions with different levels of oestrogenic activity. Oestrogenic activity was reduced by replacing FBS with charcoal stripped FBS and eliminating phenol red from culture, which is known to be oestrogenic (Welshons *et al.*, 1988).

Cell Line	Hormone Receptor Expression	Brief Description of the Cell Line	Origin of Tumour
MCF7	ER+, PR+, HER2-	Luminal A epithelial phenotype	Pleural effusion of metastatic disease, 69yr female
BT-474	ER+, PR+, HER2+	Luminal B epithelial phenotype	Ductal carcinoma, 60yr female
EFM-19	ER+, PR+, HER2-	Luminal B epithelial phenotype	Pleural effusion of ductal type carcinoma, 50yr female
T47D	ER+, PR+, HER2-	Luminal A epithelial phenotype	Pleural effusion of metastatic disease, 54yr female
CAMA-1	ER+, (expression of other receptors is ambiguous in literature)	Epithelial	Pleural effusion of metastatic disease, 51yr female
MDA-MDA-468	ER-, PR-, HER2-	Basal (triple negative)	Pleural effusion of metastatic disease, 51 yr female

Table 3.1: list of parental cell lines utilised for this project, descriptions of hormone receptor expression and phenotypes of these selected cell lines. Information taken from (Kao *et al.*, 2009). All information on the cell lines documented in the table was obtained from their respective provider (ATCC or DSMZ) as documented in section 2.1.1.

The cell lines stated above were grown in the absence of phenol red and in charcoal stripped serum for a period of at least 6 months and characterised for cell growth before and after adaptation. Cells were grown in the presence of charcoal stripped serum to characterise adaptation of the cell lines due to the absence/reduced levels of growth hormones, including estradiol. The oestrogen-deprived cell lines were then analysed for response to tamoxifen and a range of its primary metabolites to evaluate the effect of oestrogen-deprivation on this, as well as other anti-cancer compounds. The cell lines were also evaluated for oestrogen receptor expression as a result of oestrogen deprivation. The purpose of this study was to investigate these factors on a comparatively larger number of cell lines to most studies of its kind, evaluate comparisons between individual cell lines, and to also evaluate the effect that the presence of phenol red has on oestrogen deprivation.

Cell lines were grown in four different media conditions as stated below. To reiterate what is stated about the nomenclature of the culture media throughout this chapter (see section 2.2.1):

+FBS = IMDM with added phenol red and 10% FBS
-FBS = IMDM with no added phenol red and 10% FBS
+CS = IMDM with added phenol red and 10% charcoal stripped FBS
-CS = IMDM with no added phenol red and 10% charcoal stripped FBS

3.1.2: The use of 2D cell culture methods

2D cell culture is a widely used *in vitro* cell culture method that has a long history of helping us, as researchers, understand the mechanisms of cancer propagation, drug action and cell biology in general. However, it should not be overlooked that 2D culture methods also have many limitations, namely the discrepancy between mimicking the extracellular environment that *in vivo* models provide, and the observable changes in morphology tumour cells that can be observed in transferring isolated tissues to 2D culture. This led to the creation of *in vitro* models that are able to more closely mimic these *in vivo* systems, as a potentially better approach to study the processes associated with exposure to chemotherapeutics – namely, 3D culture (Kapałczyńska *et al.*, 2018). The work

displayed in this chapter, and all chapters henceforth is based on *in vitro* experiments carried out in 2D culture models – and although this method may not be the most closely related to the aforementioned 3D culture models, they are still a well trusted and practiced method routine research in cell biology as pre-clinical models. The advantage of 2D culture models is its simplicity and low cost maintenance of the cell lines. All data points and presented experiments in this thesis have been carried out in a reproducible and standardised manner, but the fact that they have been carried out using 2D culture methods should be taken into account when considering the potential clinical implications of this work.

3.2: Results

3.2.1: Images of the Oestrogen/Phenol Red Starved Cell Lines

Figures 3.1-3.7 show images taken of all of the cell lines, that have been adapted to growth in the presence of 10% charcoal stripped serum and/or the absence of phenol red as elaborated upon in section 2.2.1. Images were taken using an Olympus CKX52 light microscope with image capture capabilities.

In a clinical setting, histologists use qualitative measures of cell morphology to roughly scale with severity of malignancy. Observing morphological changes of cancer cells *in vitro* can also be a useful tool for hinting at changes to things like migration potential and cytoskeleton structure (Pasqualato *et al.*, 2012). There are plenty of resources available in literature that report changes in cellular response to oestrogen or other anti-cancer compounds, or changes to the genomic landscape as a result of oestrogen deprivation, but very little to suggest morphological changes as a result of this. Figures 3.1-3.7 of this chapter systematically catalogue representative images of each of the oestrogen/phenol red deprived cell lines in this chapter at both low and high confluences, along with low and high magnifications. These images show how the cell lines selected for this study cover a wide range of morphologies as standard, from island-forming cell lines like BT-474 and EFM-19, to grape-like spherical cells like CAMA-1. It is clear from the images which of the cell lines form uniform monolayers during culture (MCF-7, T47D, MDA-MB-468), and which prefer to grow in more 3D-like structures or mounds of cells (BT-474, EFM-19). Generally speaking, an observation that applies to the cell lines that grew in the -CS media condition, a number of the cell lines began to grow in this much more clustered fashion, neglecting to spread out into even monolayers like that of the respective parental cell lines. Other than this, the cell lines did not appear to change morphology greatly as a result of oestrogen deprivation, nor from phenol red deprivation. The only exception to this rule are the MCF-7 and BT-474 cell lines. For MCF7, during the initial stages of adaptation to growth in oestrogen deprived media, it consisted of much larger (increased diameter), flatter cells that looked similar to that you would expect from senescent cells (like the tamoxifen-resistant sub-lines generated from MCF-7 that can be seen in a later chapter of this thesis, in figure 4.2). These cells reverted to a more similar morphology to that of the +FBS

parental cell line after around 6 months of adaptation which is what can be seen in Fig. 3.1.

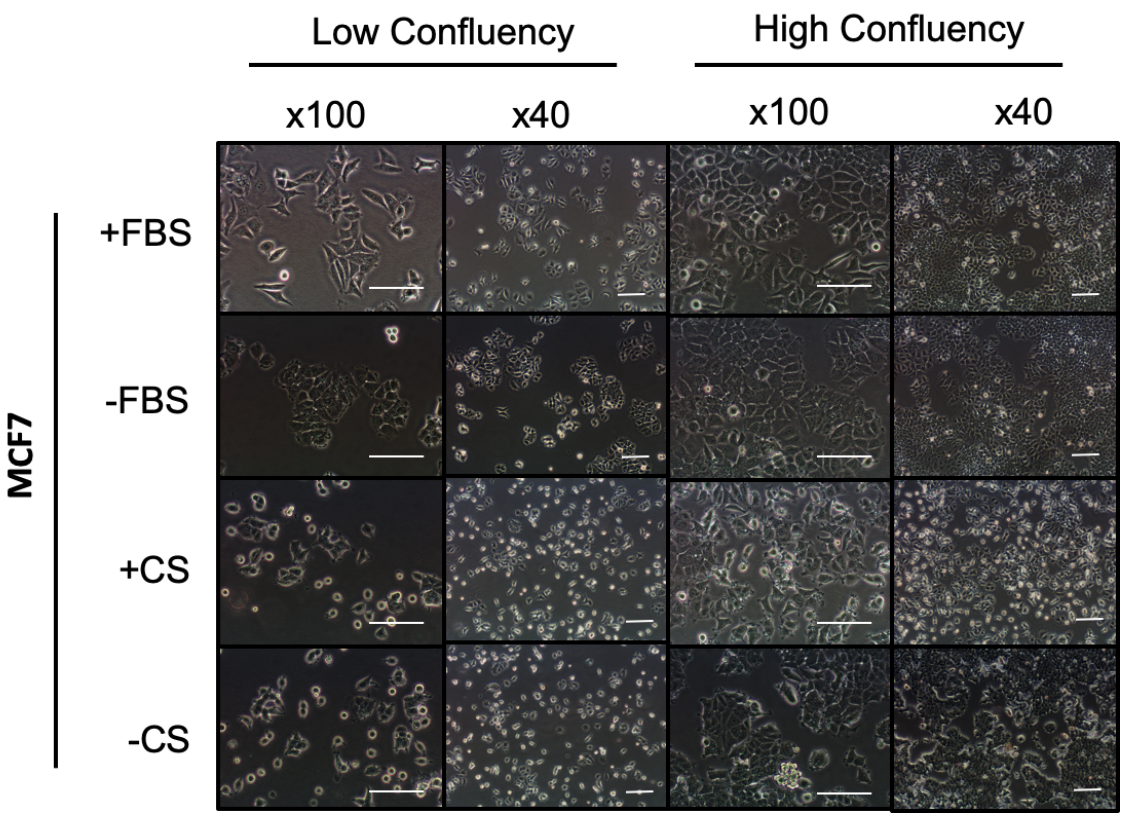


Figure 3.1: Images of MCF-7 cell line and derived oestrogen/phenol red deprived sub-lines. Images were taken at both a low and high confluency to show differences in cell morphology when given a greater amount of space to grow at a lower confluency, and when more tightly packed at a higher confluency. There are also images at a lower magnification (x40) and a higher one (x100). **Scale bars are representative of 50 microns.**

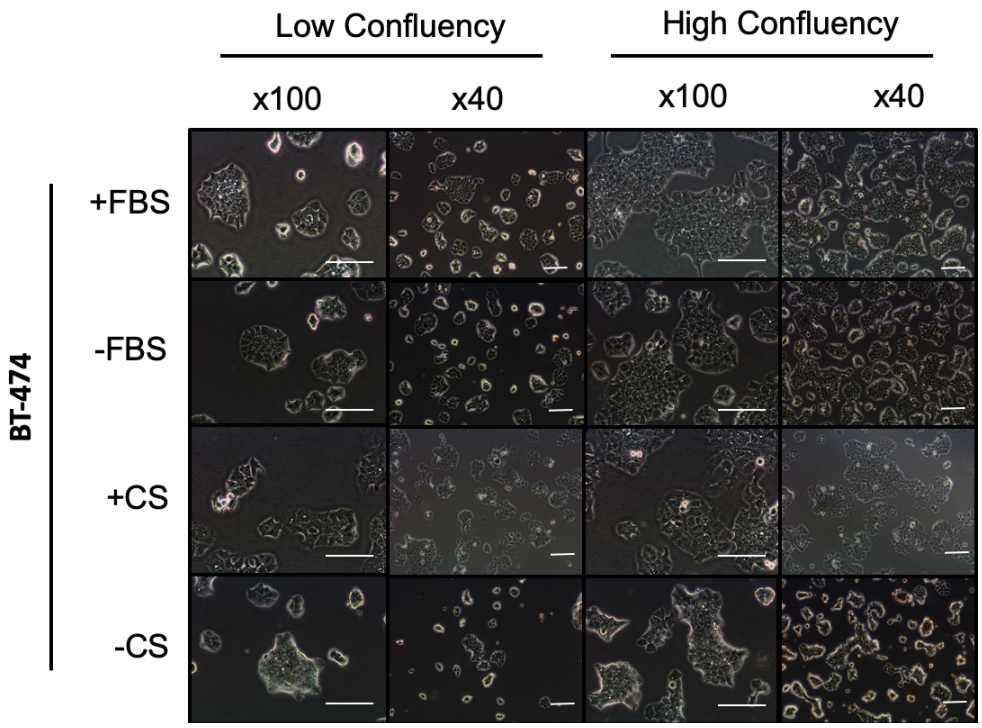


Figure 3.2: Images of BT-474 cell line and derived oestrogen/phenol red deprived sub-lines. Images were taken at both a low and high confluency to show differences in cell morphology when given a greater amount of space to grow at a lower confluency, and when more tightly packed at a higher confluency. There are also images at a lower magnification (x40) and a higher one (x100). **Scale bars are representative of 50 microns.**

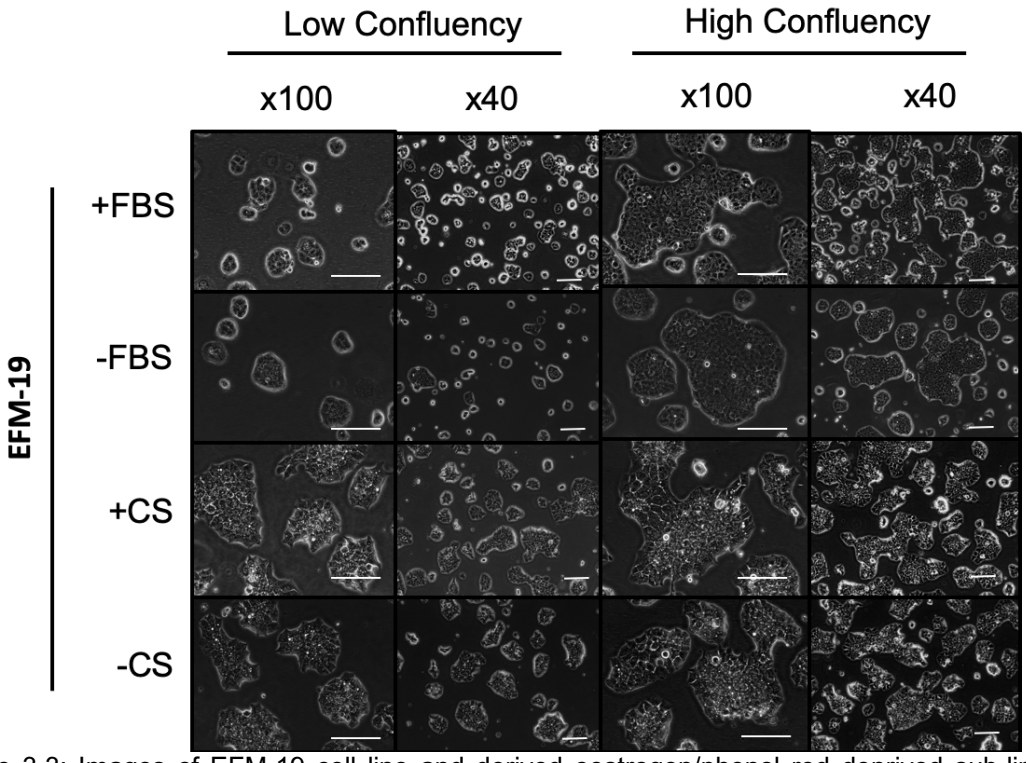


Figure 3.3: Images of EFM-19 cell line and derived oestrogen/phenol red deprived sub-lines. Images were taken at both a low and high confluency to show differences in cell morphology when given a greater amount of space to grow at a lower confluency, and when more tightly packed at a higher confluency. There are also images at a lower magnification (x40) and a higher one (x100). **Scale bars are representative of 50 microns.**

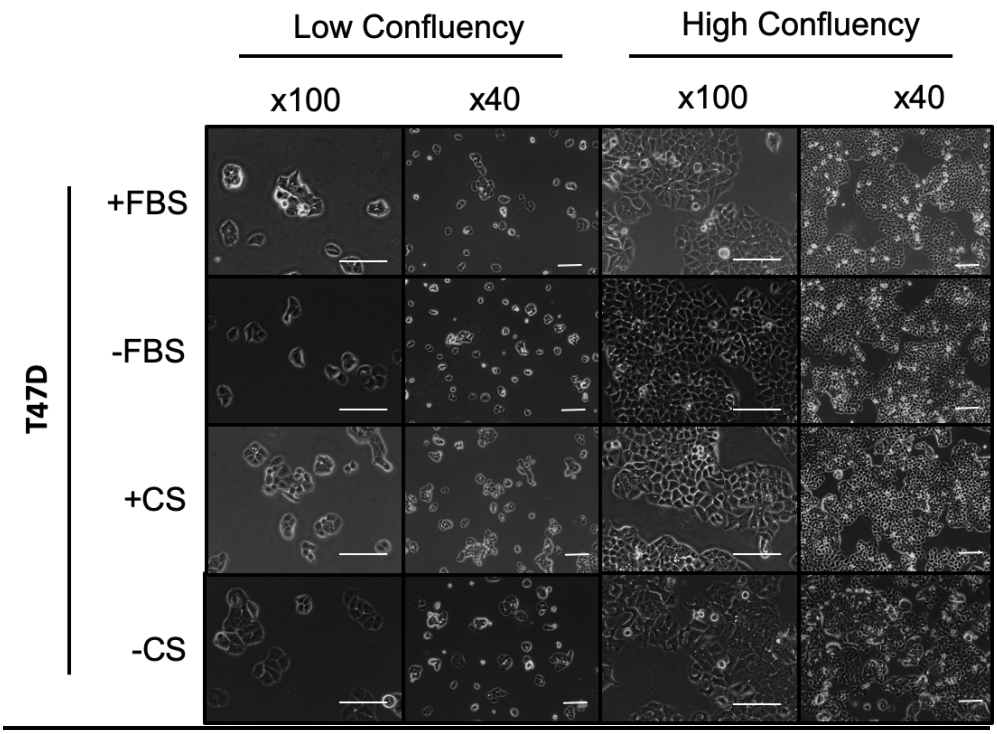


Figure 3.4: Images of T47D cell line and derived oestrogen/phenol red deprived sub-lines. Images were taken at both a low and high confluency to show differences in cell morphology when given a greater amount of space to grow at a lower confluency, and when more tightly packed at a higher confluency. There are also images at a lower magnification (x40) and a higher one (x100). **Scale bars are representative of 50 microns.**

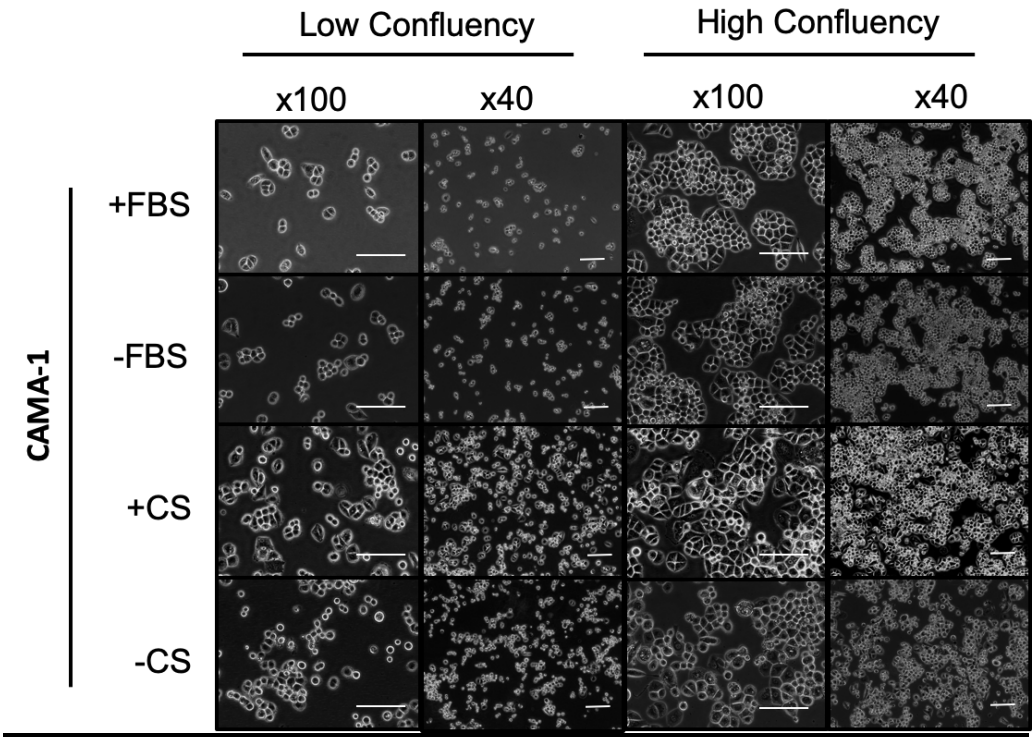


Figure 3.5: Images of CAMA-1 cell line and derived oestrogen/phenol red deprived sub-lines. Images were taken at both a low and high confluency to show differences in cell morphology when given a greater amount of space to grow at a lower confluency, and when more tightly packed at a higher confluency. There are also images at a lower magnification (x40) and a higher one (x100). **Scale bars are representative of 50 microns.**

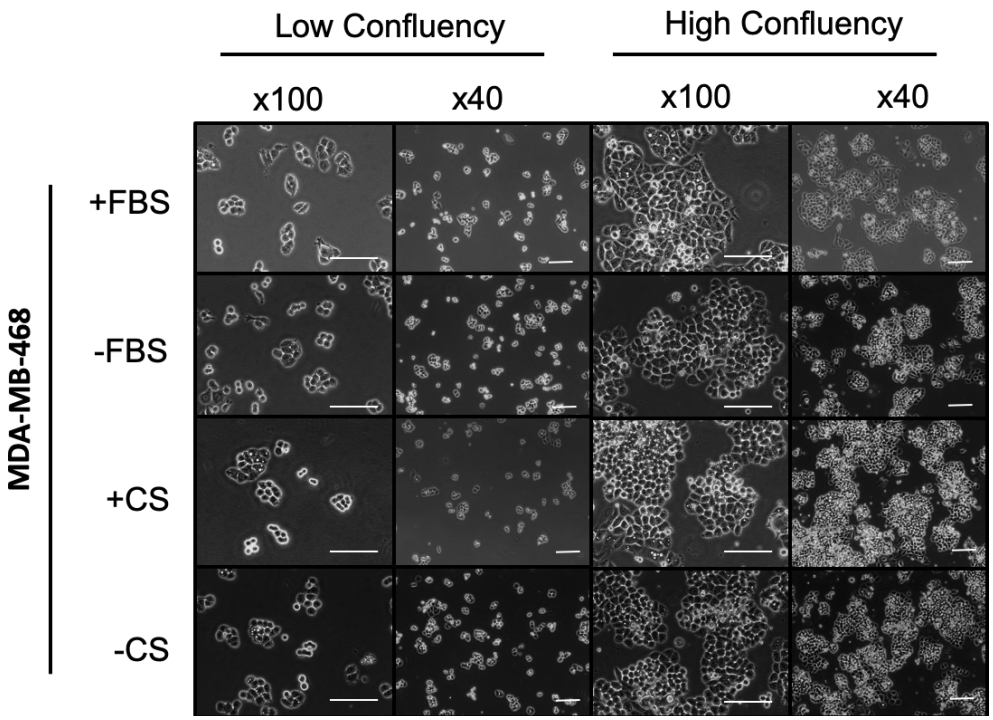


Figure 3.6: Images of MDA-MB-468 cell line and derived oestrogen/phenol red deprived sub-lines. Images were taken at both a low and high confluency to show differences in cell morphology when given a greater amount of space to grow at a lower confluency, and when more tightly packed at a higher confluency. There are also images at a lower magnification (x40) and a higher one (x100). **Scale bars are representative of 50 microns.**

3.2.2: Growth kinetics

The cell lines were adapted to growth in medias with differing levels of oestrogen and phenol red content, as described in section 2.2.3. Cell growth was then characterised as stated in section 2.2.5. Growth of the cell lines before adaptation was completed was evaluated and is displayed in figure 3.7 – this is where the cells have only been in their respective new medias for around one month and are most are struggling to grow in +CS/-CS conditions. Once the cell lines had begun to comfortably grow in their new culture medias, which was determined visually, their growth was characterised as is shown in Fig. 3.8. The adaptation process took around 6 months to complete, particularly with the cell lines grown in -CS conditions. Cells were seeded as stated in section 2.2.5. The cells were grown over a period of 6 days (one day longer than the five-day time-course used for the viability assays in this chapter). A measure of cell growth was taken by electrical impedance at 30-minute intervals. Figure 3.8 (a-f) below shows growth curves generated from the cell lines before the adaptation process was completed.

Most oestrogen deprived sub-lines (+CS/-CS) show a marked reduction in cell growth compared to their oestrogen containing counterparts before adaptation was completed. The MDA-MB-468 cell line was selected as a control cell line for this work – as a triple negative breast cancer cell line, this was the only one expected to show little to no response to being transferred to oestrogen deprived conditions. It should be noted that charcoal stripped calf serum is not only devoid of oestrogen, but also of other growth hormones so the assumption that this would not affect the cell line at all could not be made. However, the MDA-MB-468^{-CS} subline still showed reduced growth compared to the other growth conditions (this is also reflected in the calculated doubling time shown in Fig 3.10). All other +CS/-CS sublines show little to no cellular growth during this period. These cell lines were still observed to grow, yet slowly, during routine culture - the purpose of this experiment was to compare the growth rate to that of the respective control +FBS cell lines so the seeding density was kept the same. It is possible that the reason for the failure to grow may be due to the seeding density being too low for the establishment of autocrine signalling which breast cancer cells are thought to do (Tan, Zhong and Pan, 2009).

Figure 3.9 (a-f) below shows a comparison from the growth of the non-adapted oestrogen deprived sublines shown in Fig. 3.8. The growth curves for the cell lines after the adaptation process (Fig 3.9) show that although growth rates are ubiquitously still slower than those of the +FBS control sublines (which is reflected in the doubling times shown in Fig 3.10), they do now all show increased cellular growth compared to their non-adapted counterparts. The MDA-MB-468 set of sub-lines showed comparatively little change during the adaptation process.

The subtraction of phenol red alone from culture media affects the growth of a number of the cell lines when comparing sublines cultivated in -FBS conditions compared to those in +FBS conditions in (figures 3.7). -FBS counterparts of MCF-7, BT-474 and CAMA-1 groups all show reduced growth compared to their +FBS subline. Slight changes are also evident in the adapted sub-lines (Fig. 3.8), but this does not appear to have a marked effect on their doubling times after adaptation (Fig. 3.10). Suggesting that phenol red affects growth during routine culture enough to require adaptation to its absence. This cannot be attributed to other changes in base culture media as they are identical, excluding phenol red content.

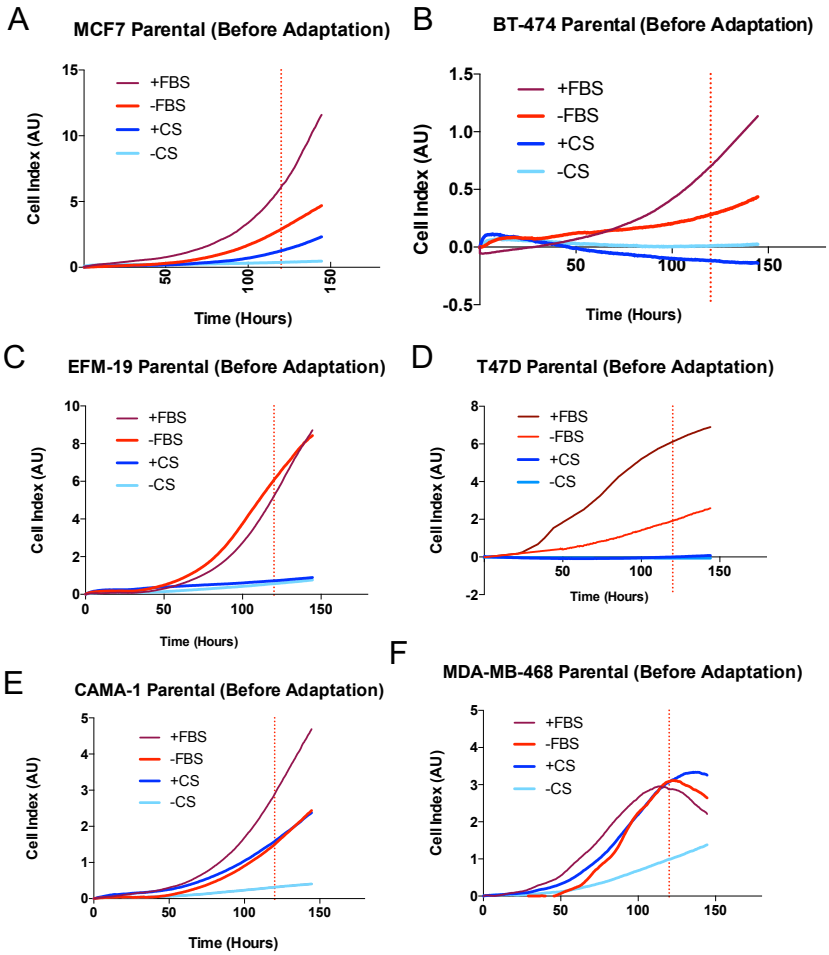


Figure 3.7: Growth curves of all of the oestrogen/phenol red deprived cell lines generated, and their respective control cell lines that are grown in conventional, FBS containing media. Each cell line was grown for 6 days, and cell density was measured using electrical impedance every 30 minutes for that length of time. Graphs are colour coded for the type of culture media they were grown in as noted in the key. A) MCF-7, B) BT-474, C) EFM-19, D) T47D, E), CAMA-1, F) MDA-MB-468. Each individual graph title includes the word 'parental' to differentiate these growth curves/cell lines from the drug-resistant cell lines that were generated from these in chapter 4.

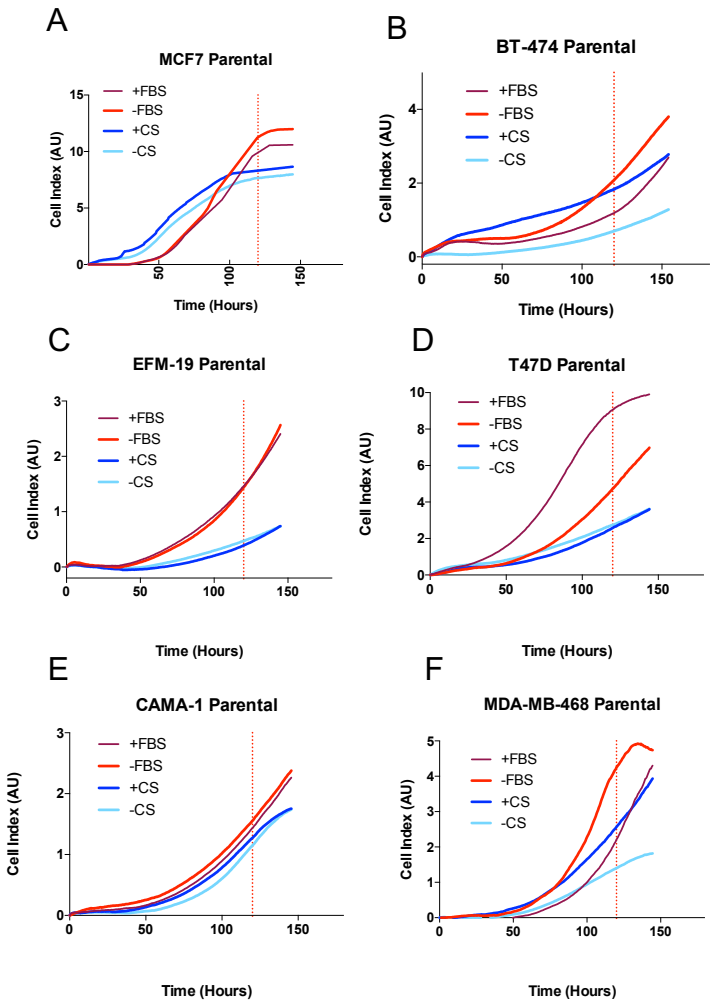


Figure 3.8: Growth curves of all of the oestrogen/phenol red deprived cell lines generated after adaptation to growth in their respective media conditions, and their respective control cell lines that are grown in conventional, FBS containing media. Each cell line was grown for 6 days, and cell density was measured using electrical impedance every 30 minutes for that length of time. Graphs are colour coded for the type of culture media they were grown in as noted in the key. A) MCF-7, B) BT-474, C)EFM-19, D) T47D, E), CAMA-1, F) MDA-MB-468. Each individual graph title includes the word 'parental' to differentiate these growth curves/cell lines from the drug-resistant cell lines that were generated from these in chapter 4.

Figure 3.9, below, accompanied by table 3.2, depict and state the doubling times of these growth-hormone/phenol red deprived sub-lines as calculated from the growth curves in figure 3.8. Doubling times for the oestrogen deprived sublines have generally higher doubling times than those in oestrogen containing conditions.

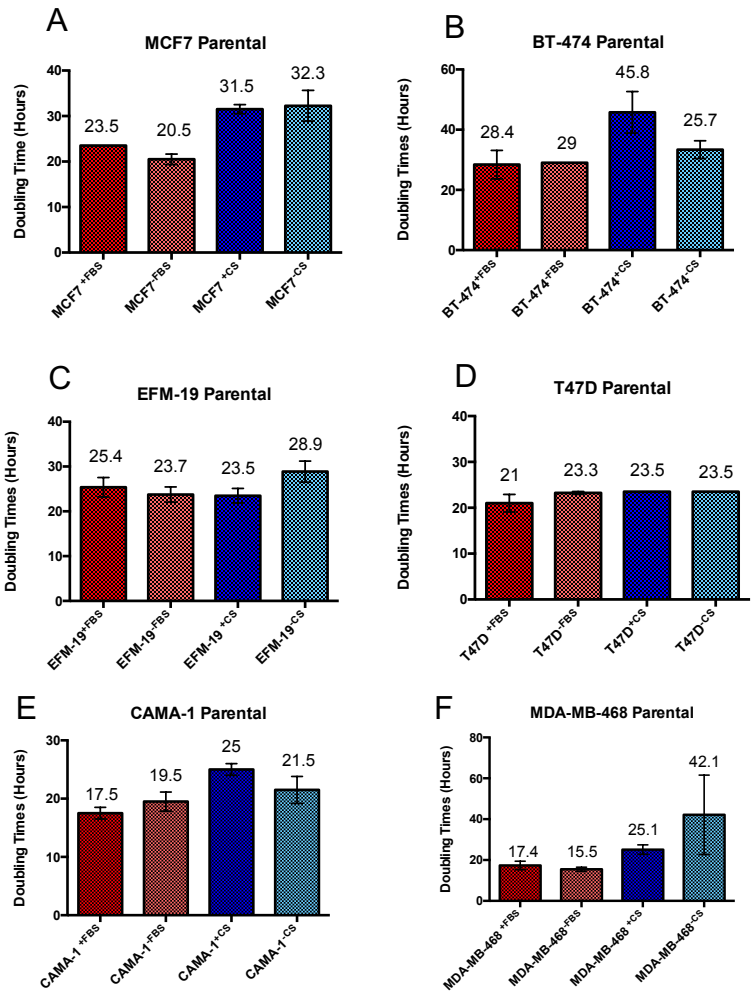


Figure 3.9: Doubling times for all of the growth-hormone/phenol red deprived cell and sub-lines. The graph is colour-coded to represent the media type that each cell line was grown in. Data points are representative of n=4 repeats. Error bars are representative of +/-SD. Doubling times were calculated as per section 2.2.5.

	Doubling time in hours (+/- SD)			
Cell Line	**+FBS**	**-FBS**	**+CS**	**-CS**
MCF7	23.5 (+/-0.00)	20.5 (+/-1.16)	31.5 (+/-1.00)	32.3 (+/-3.38)
BT-474	28.4 (+/-4.73)	29.0 (+/-0.00)	47.8 (+/-6.9)	33.4 (+/-2.96)
EFM-19	25.4 (+/-2.17)	23.7 (+/-1.7)	23.5 (+/-1.63)	28.9 (+/-2.36)
T47D	21.0 (+/-1.91)	23.3 (+/-0.29)	23.5 (+/-0.00)	23.5 (+/-0.00)
CAMA-1	17.5 (+/-1.00)	19.5 (+/-1.63)	25.00 (+/-1.00)	21.5 (+/-2.31)
MDA-MB-468	17.38 (+/-2.06)	15.5 (+/-1.00)	25.1 (+/-2.29)	42.1 (+/-19.43)

Table 3.2: Doubling times of each growth hormone/phenol red deprived cell and sub-line, organised by the originating control/parental cell line and the media condition in which it has been adapted to. Each value is the average of n=4, that standard deviation of which accompanies the value in brackets.

3.2.3: Response to β-oestradiol

Figure 3.10 looks at the response of the oestrogen/phenol red deprived sub-lines to the addition of β-oestradiol, compared to those of the control, non-oestrogen deprived sub-lines. The rationale behind this being to evaluate whether the oestrogen-deprived cell lines show a marked increase in growth to reintroduction of β-oestradiol, despite long-term adaptation to the absence of it. A study by Darbre, (2014) states that long-term oestrogen deprivation results is eventual hypersensitivity to oestrogen, meaning enhanced cellular growth compared to controls (MCF7 cells were used in this particular study). Looking at figure 3.10, this did not appear to be the case for the group of MCF-7 cells used in this study - cell growth was not increased for the oestrogen deprived sublines compared to the other conditions. This may suggest that adaptation to growth in the absence of oestrogen, if not just in lower levels of oestrogen, makes this cell line unresponsive to growth stimulation by oestrogen. Increased cell growth was observed in all of the sublines compared to the vehicle control apart from MDA-MB-468. T47D, EFM-19 and CAMA-1 cell lines had oestrogen deprived sub-lines that showed enhanced growth compared to the +FBS parental lines, these cell lines show hypersensitivity to oestrogen as a result of long-term deprivation. Whereas this is not seen with the MCF7 or BT-474 cell lines. As there were differential responses to the re-introduction of oestrogen to the culture media between the cell lines, this suggests that the acquisition of unresponsiveness to oestrogen due to complete deprivation is a subjective observation. This could be applied to a clinical setting by suggesting the importance of identifying responsiveness to oestrogen prior to treatment using aromatase inhibitors – if cells are unresponsive to high concentrations of oestrogen (like the MCF7 and BT-474 cell lines in Fig. 3.11), this could mean a aggregatory effect of aromatase inhibitor action, as the cell population may prefer growth in lower levels of oestrogen. As some of the cell lines become hypersensitive to β-oestradiol compared to control cell lines, this shows that response to oestrogen deprivation has the potential to work to two extremes and is subjective to the cell line in question.

Phenol red inclusion in the +CS media does not appear to affect growth differently to -CS sublines in any other cell line than T47D (-CS subline shows enhanced growth with the reintroduction of β-oestradiol, but the +CS subline doesn't),

perhaps suggesting that oestrogenic activity elicited by phenol red is enough to mimic maximum oestrogenic requirements in routine culture, and stop any adaptation to become hypersensitive to oestrogen that its -CS counterpart may have undergone.

Cell viability begins to decrease, until an eventual large decrease in viability for all of the cell line groups towards the higher concentrations of β-oestradiol, showing that high doses of oestrogen show a similar level of anti-cancer effects to some of the metabolites of tamoxifen that will be discussed later in this chapter – high doses of oestrogen are seen to have anti-cancer effects and has been shown to be successful option for the treatment of breast cancer (Jordan, 2015).

This data gives insight into the potential for high dose oestrogens to be used as a treatment option in the event of resistance to aromatase inhibitors. Fig. 3.11 shows the IC_{50} values calculated from the growth curves presented in Fig. 3.10 – here three of the six -CS cell lines are significantly less sensitive to beta-oestradiol than their corresponding +FBS counterpart, with the MCF7 cell line standing as the least sensitive. This could suggest the contraindication of high-dose oestrogens in the instance of resistance to aromatase inhibition, but would need to be coupled with clinically relevant serum concentrations taken from patients treated with high-dose oestrogens to make that inference. Unfortunately, although there is a wealth of information available about treatment regimes, there is little information about serum concentrations of oestrogens following treatment (Coelingh Bennink *et al.*, 2017).

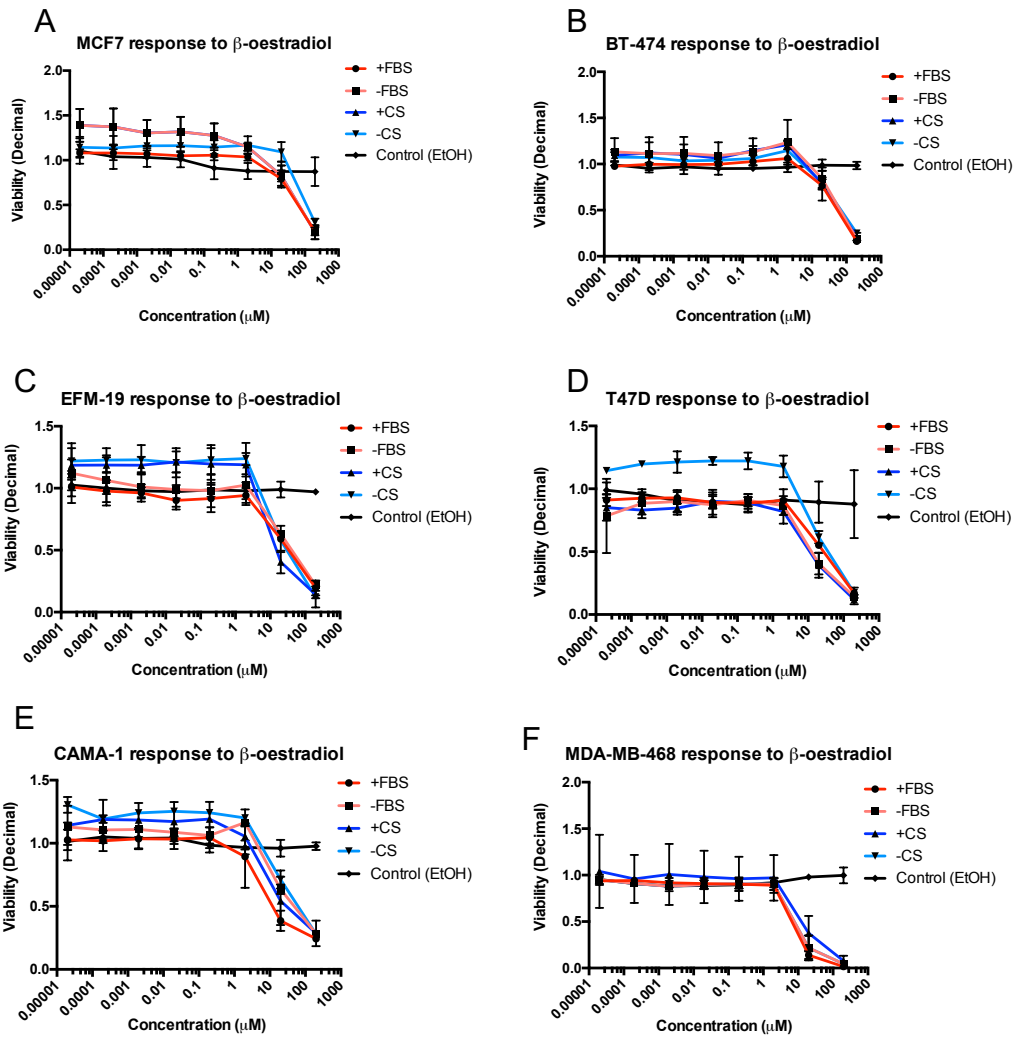


Figure 3.10: Growth curves for oestrogen deprived adapted breast cancer cell lines MCF-7 (A), BT-474 (B), EFM-19 (C), T47D (D), CAMA-1 (E), MDA-MB-468 (F) when grown in the presence of additional β-oestradiol over a range of concentrations. Each subline was cultivated in their respective media type, but with additional β-oestradiol. Each data point represents the average of three biological repeats – error bars are representative of +/-SD. Viability is relative to control cells that were grown in the absence of β-oestradiol. Vehicle control is ethanol. The graphs are colour coded to be representative of the media that the cell lines and growth oestrogen-deprived sub-lines were cultivated in for this experiment.

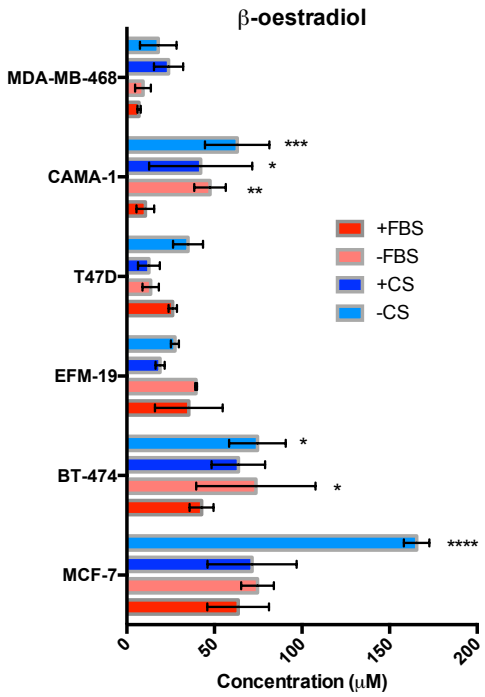


Figure 3.11**: (A)** β-oestradiol IC_{50} values experimentally obtained from originating control cell lines and the oestrogen-deprived sub-line, indicated on the y-axis of the graphs. The graph is colour coded for the cell line that the data is related to. Data is representative of n=3 biological repeats, error bars are representative of +/- SD. Statistical analysis was conducted using two-way ANOVA with tukeys correction. (**** - p<0.0001)(*** - p<0.005)(** - p<0.01)(* - p<0.05).

3.2.4: Qualitative evaluation of ERα and ERβ expression

The physiological actions of oestrogen are mainly mediated through oestrogen receptors (ERs) alpha (ERα) and beta (ERβ). Although it is directly stated in literature surprisingly sparsely, it should be noted that it is the presence of ERα alone is the accepted marker of ER positivity in breast cancer (Molina *et al.*, 2017; Girgert, Emons and Gründker, 2019). The locality and expression levels of the two wild-type ER isoforms (α and β) were qualitatively assessed by immunofluorescence (figures 3.13-18). The primary antibodies used for this purpose were monoclonal.

Figure 3.12 shows whole unedited western blots using the same antibodies utilised for the immunostaining protocol and both show specific binding to the sizes expected of the wild-type nuclear receptors. Western blots were performed as per section 2.2.9. The antibody for ERβ shows another faint band just below the expected size of ERβ, which is likely a smaller splice variant of ERβ due to the size.

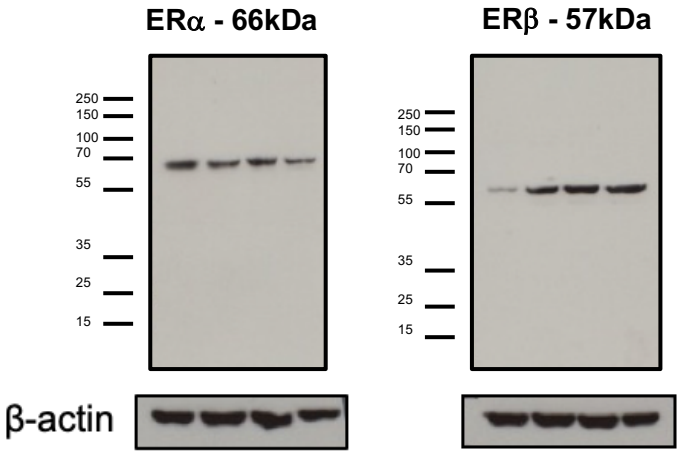


Figure 3.12: Uneditted scans whole developed western blots of cell lysates from CAMA-1 cell line to show specificity of the antibodies used for immunofluorescence. Samples were loaded from left to right in each of the blots: CAMA-1^{+FBS}4-OH^{10}, CAMA-1^{-FBS}4-OH^{10}, CAMA-1^{+CS}4-OH^{10}, CAMA-1^{-CS}4-OH^{10}. CAMA-1 that is known to be ER+, hence selection for this experiment. Left – antibody for ERα. Right – antibody for ERβ. β-actin loading control is included to show correct loading. A single band can be seen for ERα. A single main band can be seen for ERβ, but also a very faint second band can be seen just below this – this is likely specific to a smaller splice variant of ERβ due to the size of the band.

Distribution of oestrogen receptors is known to differ in normal and cancerous breast tissue. Oestrogen receptors alpha and beta are expressed in a manner that warrants a balance of pro- and anti-proliferative properties (Saji *et al.*, 2000; Makinen, 2001; Penot *et al.*, 2005; Mermelstein, 2009). This balance may be altered in cancer.

ER expression is used as a clinical marker to ascertain cancer malignancy (Shoker *et al.*, 1999). Previous studies showed that breast cancer cells can adapt to growth in oestrogen-deprived conditions by upregulation of oestrogen receptors and their signalling (Jeng *et al.*, 1998). However, little has been published to describe how the location of these receptors changes as a result of oestrogen deprivation. Table 3.2 below documents observations that can be made from the representative immunofluorescence images in figures 3.13-18 on the locations of the two oestrogen receptors in the four media conditions investigated.

Figure	Cell Line	Observation
3.13	MCF7	Nuclear localisation for oestrogen deprived conditions only for both ERα and ERβ, in defined punctate regions. ERs are cytoplasm localised in +FBS/-FBS conditions
3.14	BT-474	No apparent nuclear localisation – all cytoplasmic for both receptor isoforms and sub-lines. Observed phenomenon of ERβ lining up in a similar position to the spindle fibres in dividing cells. ERα does not localise in the same place
3.15	EFM-19	Cytoplasmic localisation for both receptor isoforms – no apparent difference elicited from oestrogen deprivation
3.16	T47D	Nuclear localisation observed in +CS/-CS conditions only for ERα, nuclear localisation is seen in all conditions for ERβ. Cytoplasmic localisation observed for all.
3.17	CAMA-1	Mainly nuclear localisation for all sub-lines and both receptors. Some membrane localisation, limited cytoplasmic localisation.
3.18	MDA-MB-468	No nuclear localisation observed for either receptor or any condition. Mostly cytoplasmic localisation. Very minimal staining for ERα which is in-keeping with TNBC status of the cell line, but ERα expression is observed in other media conditions.

Table 3.2: Comments on observations made on oestrogen receptor locality from immunofluorescence images of six breast cancer cell lines: MCF-7, BT-474, EFM-19, T47D, CAMA-1, MB-MB-468, and the effect of growth in oestrogen-deprived conditions on this.

Although all parameters of the confocal microscope used to capture the immunofluorescence images were kept constant, such as laser power, post-imaging processing, expression of ERα and ERβ intensity shouldn't be compared directly. The antibodies used for the experimental procedure are not equal in single molecule florescence intensity when stimulated by the lasers of the confocal microscope. The changes between individual ER isoform expression however, can be commented on.

Although the main controls for this study were the parental cell lines (+FBS), the MDA-MB-468 cell line was selected for this study with the intention of serving as an additional triple negative breast cancer control cell line. The cell line positively stained for ERα, which is the oestrogen receptor that determines oestrogen receptor positivity or negativity in a clinical setting (Molina *et al.*, 2017; Girgert, Emons and Gründker, 2019). As the antibodies used for this procedure had been previously confirmed for specific binding, this confirms positive staining is not due to non-specific binding (Fig 3.12). This negates the use of the MDA-MB-468 cell line henceforth for comparison as a true triple negative breast cancer cell line for comparison, and will be considered as an additional ER+ cell line.

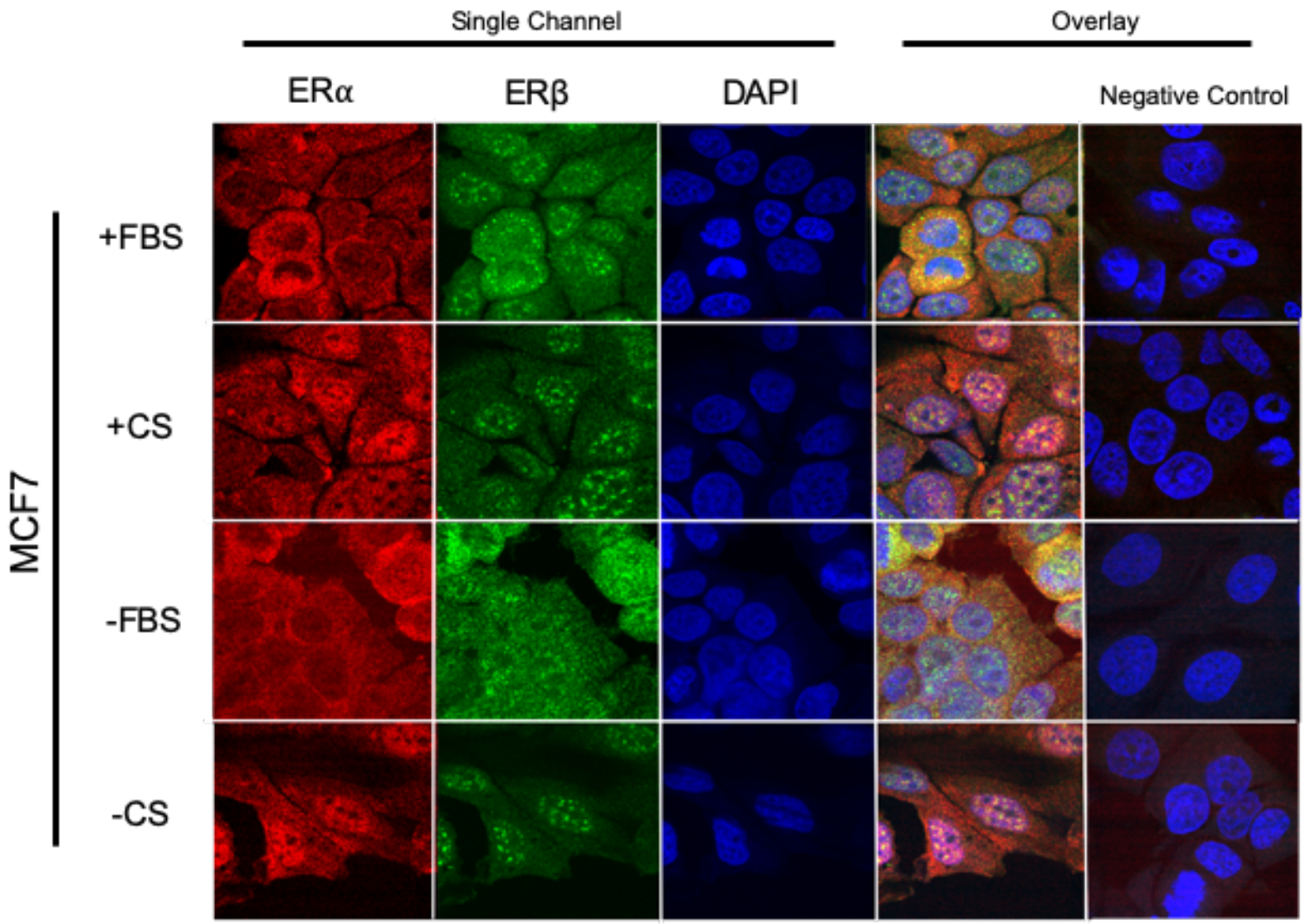


Figure 3.13: Representative immunofluorescence images of an N=6 images of the MCF-7 cell line and all phenol red/growth hormone deprived sub-lines as indicated by the labelling on the left hand side of the figure. Lanes are divided into single channels and labelled appropriately. **RED - ERα, GREEN - ERβ, BLUE – DAPI/nucleic acids.**

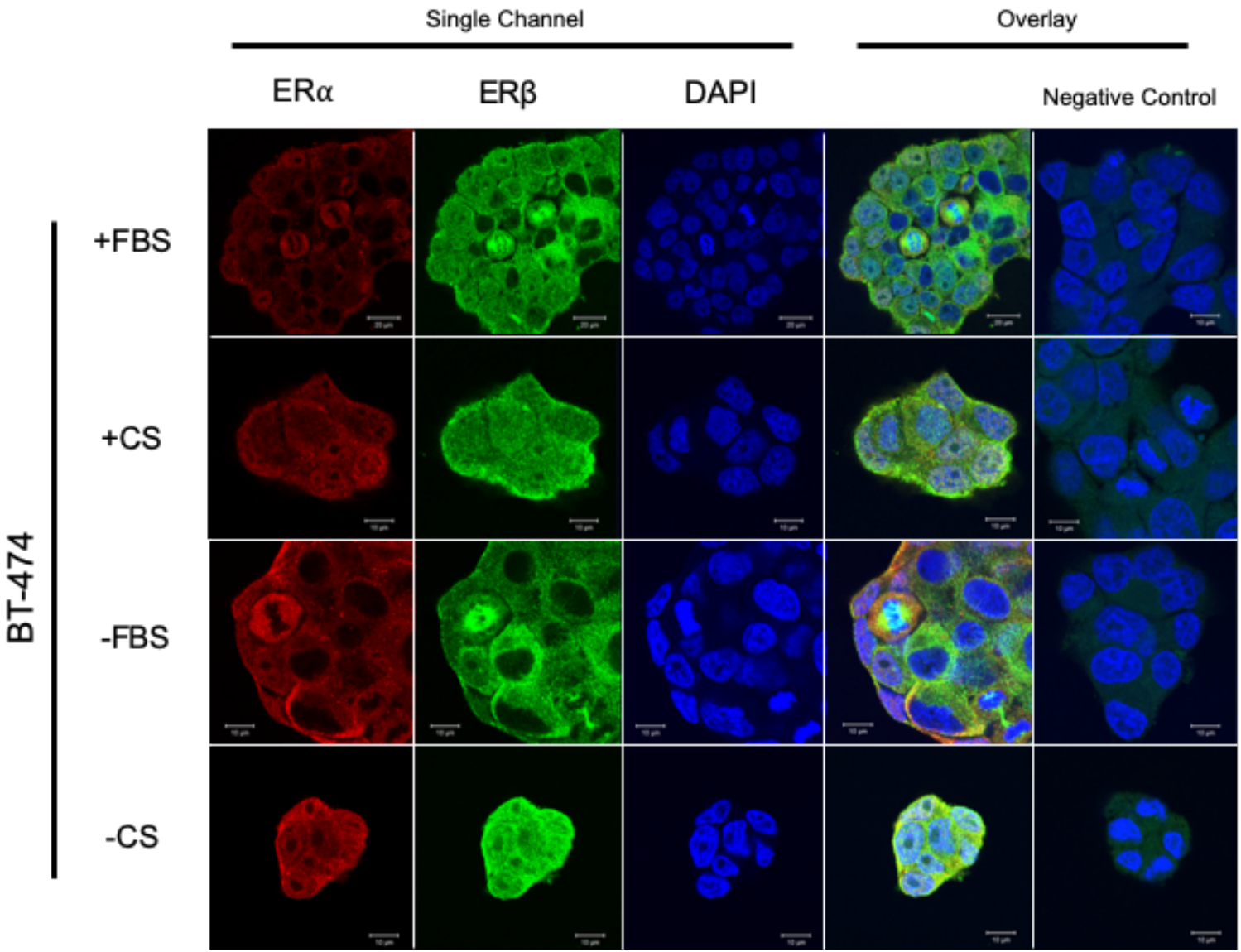


Figure 3.14: Representative immunofluorescence images of an N=6 images of the BT-474 cell line and all phenol red/growth hormone deprived sub-lines as indicated by the labelling on the left hand side of the figure. Lanes are divided into single channels and labelled appropriately. **RED - ERα, GREEN - ERβ, BLUE – DAPI/nucleic acids. Scale bar is reprehensive of 10 microns. Note: +FBS cell-line in this figure is less magnified than the others – this is represented by the scale bar of 20 microns.**

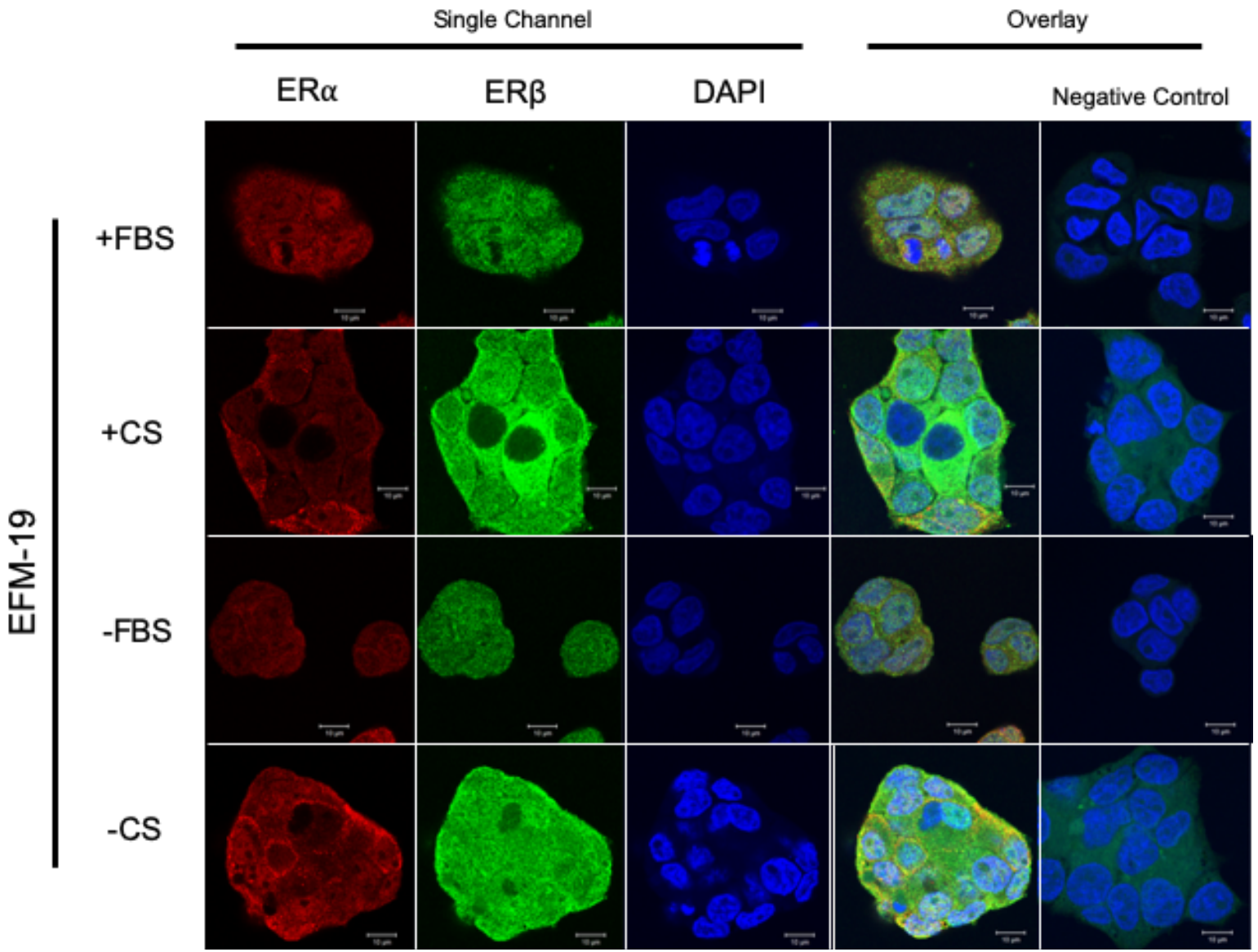


Figure 3.15: Representative immunofluorescence images of an N=6 images of the EFM-19 cell line and all phenol red/growth hormone deprived sub-lines as indicated by the labelling on the left hand side of the figure. Lanes are divided into single channels and labelled appropriately. **RED - ERα, GREEN - ERβ, BLUE – DAPI/nucleic acids. Scale bar is representative of 10 microns.**

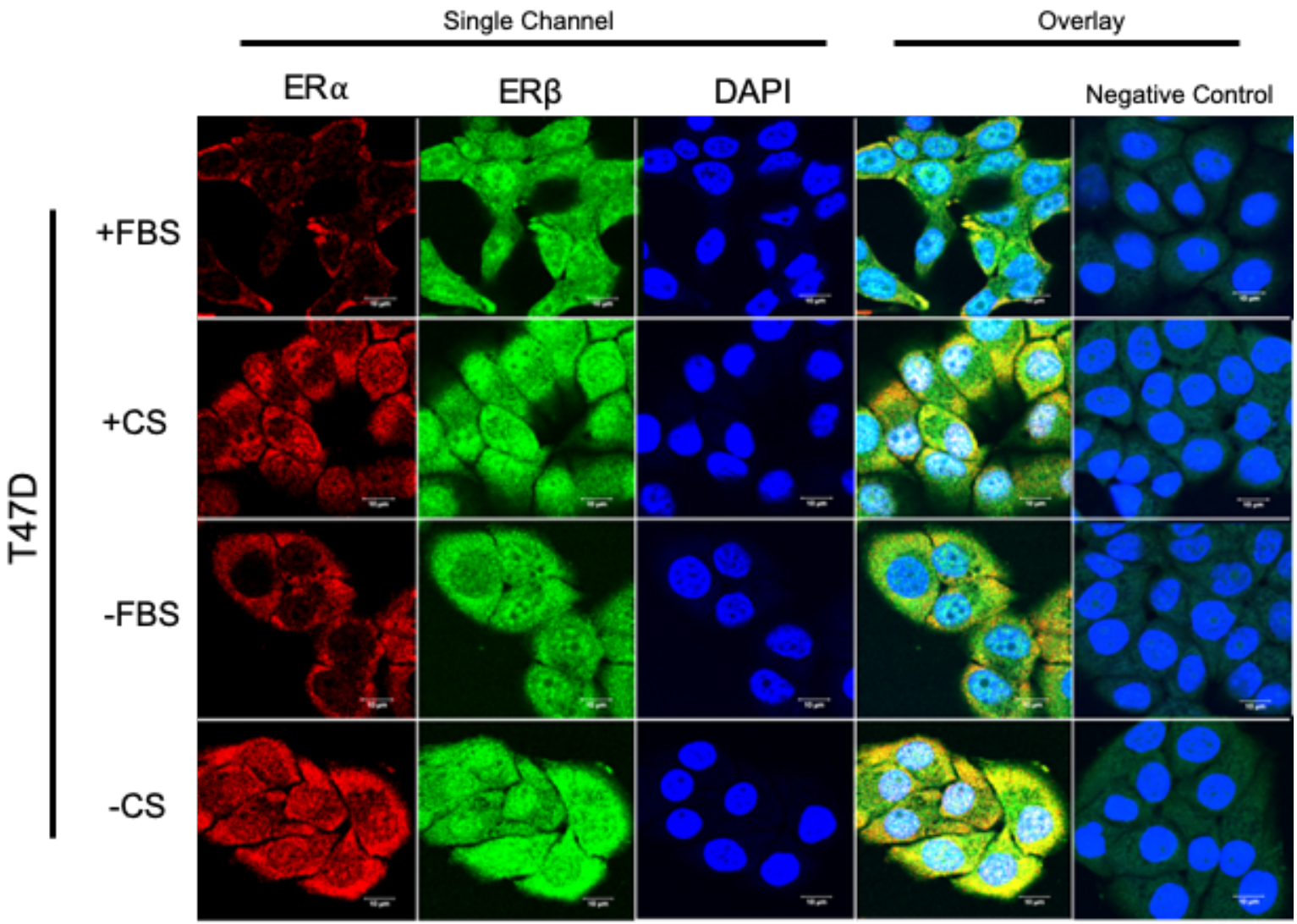


Figure 3.16: Representative immunofluorescence images of an N=6 images of the T47D cell line and all phenol red/growth hormone deprived sub-lines as indicated by the labelling on the left hand side of the figure. Lanes are divided into single channels and labelled appropriately. **RED - ERα, GREEN - ERβ, BLUE – DAPI/nucleic acids. Scale bar is representative of 10 microns.**

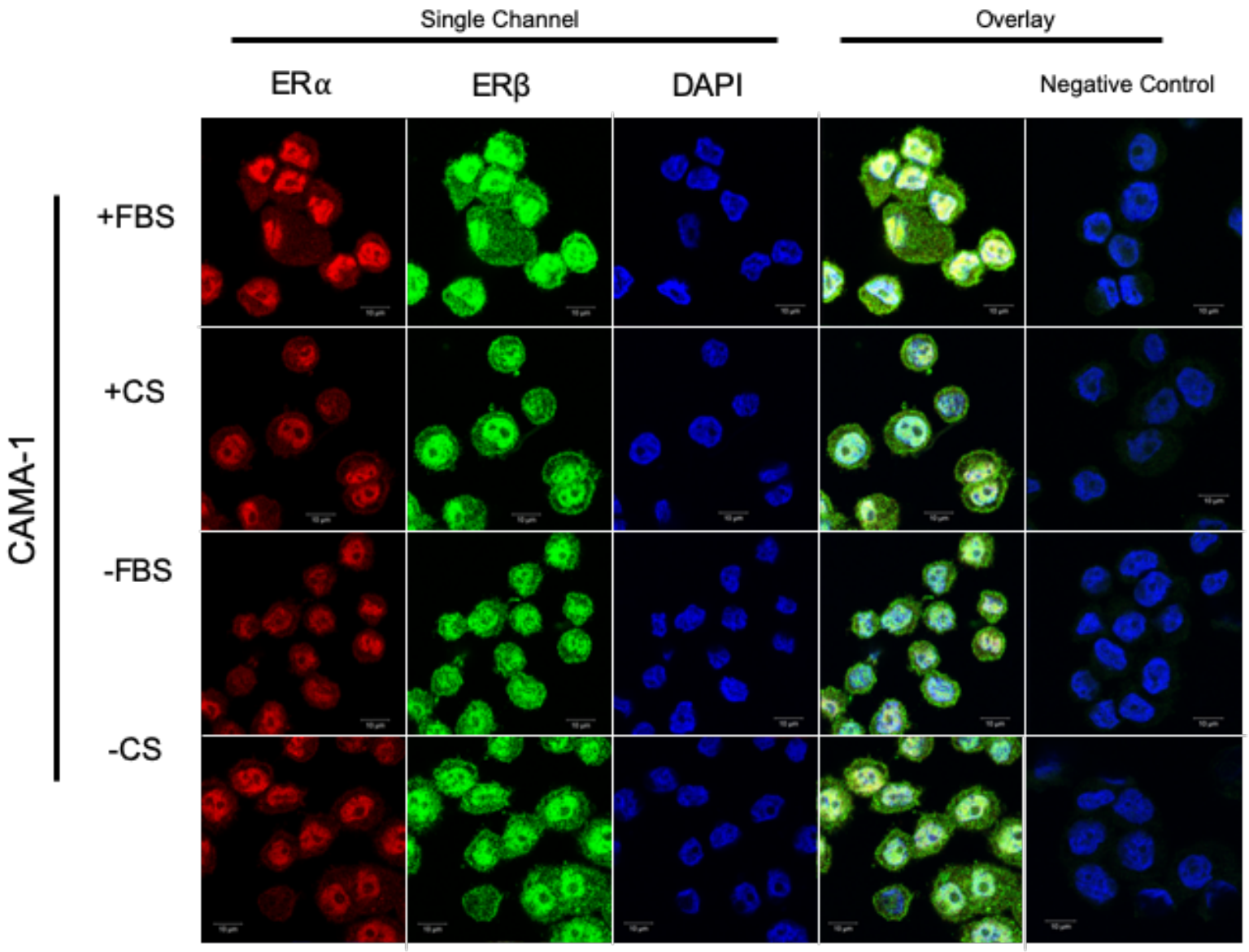


Figure 3.17: Representative immunofluorescence images of an N=6 images of the CAMA-1 cell line and all phenol red/growth hormone deprived sub-lines as indicated by the labelling on the left hand side of the figure. Lanes are divided into single channels and labelled appropriately. **RED - ERα, GREEN - ERβ, BLUE – DAPI/nucleic acids. Scale bar is representative of 10 microns.**

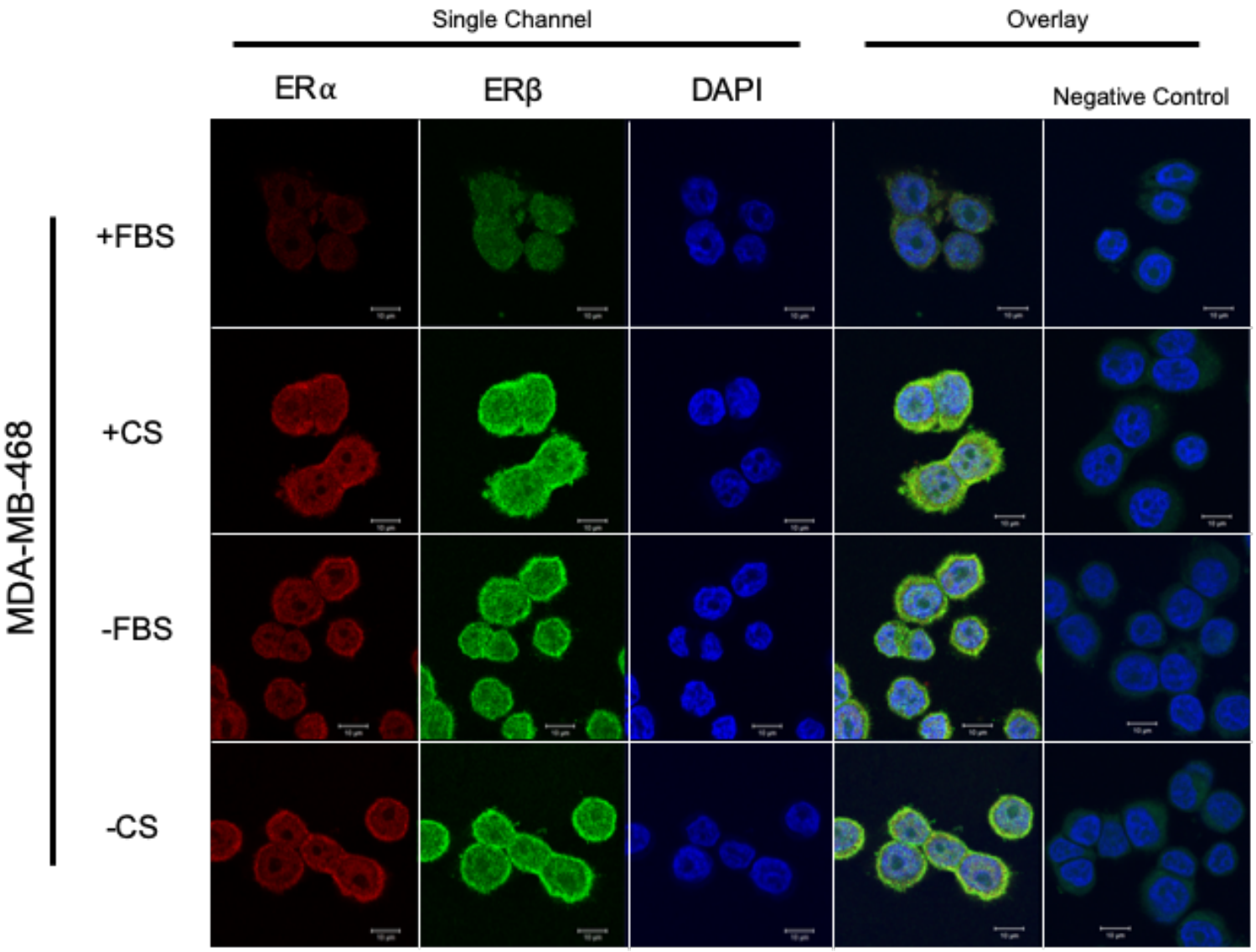


Figure 3.18: Representative immunofluorescence images of an N=6 images of the MDA-MB-468 cell line and all phenol red/growth hormone deprived sub-lines as indicated by the labelling on the left hand side of the figure. Lanes are divided into single channels and labelled appropriately. **RED - ERα, GREEN - ERβ, BLUE – DAPI/nucleic acids. Scale bar is representative of 10 microns.**

3.2.5: Quantification of ERα and ERβ expression

Oestrogen receptor expression was quantified using ImageJ software and is representative of the average expression of each receptor per cell, calculated from n=6 images of each sub-line of similar confluency. Part B to both figures 3.19 and 3.20 show the fold changes of ERα and ERβ expression, both whole cell (i) and nuclear only (ii) fluorescence respectively, compared to that of the originating parental cell line. These have been normalised for autofluorescence and non-specific antibody binding by subtracting the fluorescence intensity of appropriate negative controls. This should act as preliminary data in the absence of other quantifying techniques such as western blotting.

Although all parameters of the confocal microscope used to capture the immunofluorescence images were kept constant, such as laser power and magnification (as this would affect the area of the cell used to calculate the intensity of it relative to its size), expression of ERα and ERβ shouldn't be compared directly. The antibodies used for the experimental procedure are not equal in single molecule florescence intensity when stimulated by the lasers of the confocal microscope. The changes between individual ER isoform expression from cell-line to cell-line however, can be commented on.

Changes in ER expression levels appear to be cell line specific. Looking at figure 3.19, ERα expression is significantly changed in 15/18 of the sublines compared to their parental cell line. Literature suggests an upregulation of ERα as a response to long-term oestrogen deprivation (Darbre, 2014), which was not necessarily the case here. Significantly increased expression of ERα was seen in the BT-474, EFM-19, T47D and MDA-MB-468 cell lines, as can be seen in (B) of Fig. 3.19. However, this was not just seen in oestrogen-deprived conditions, this was also seen in -FBS conditions that had only been modified by phenol red content compared to the parental cell lines. There is no literature that documents the effect of phenol red on oestrogen receptor expression, but this may suggest that removing phenol red from culture media is enough of a change in oestrogenic stimulation to warrant a change in oestrogen receptor expression, or the change in receptor expression is due to adaptation to a new culture media in general. No change was seen in the MCF7 cell line as a result of oestrogen deprivation, but

downregulation of ERα was seen in the CAMA-1 cell line. Oestrogen deprivation resulted in a significant decrease of ERα in this case. Receptor expression profiles for the data pertaining to whole cell fluorescence are all consistent with the data for nuclear only, suggesting that expression is fairly ubiquitous for these cell lines, and is relatively unaffected by media conditions. The CAMA-1 cell line has a comparatively higher intensity for the nuclear readings compared to whole cell, which is consistent with the images in figure 3.17, placing this cell line as the only one of the cohort that displays a preference for nuclear localisation for ERα.

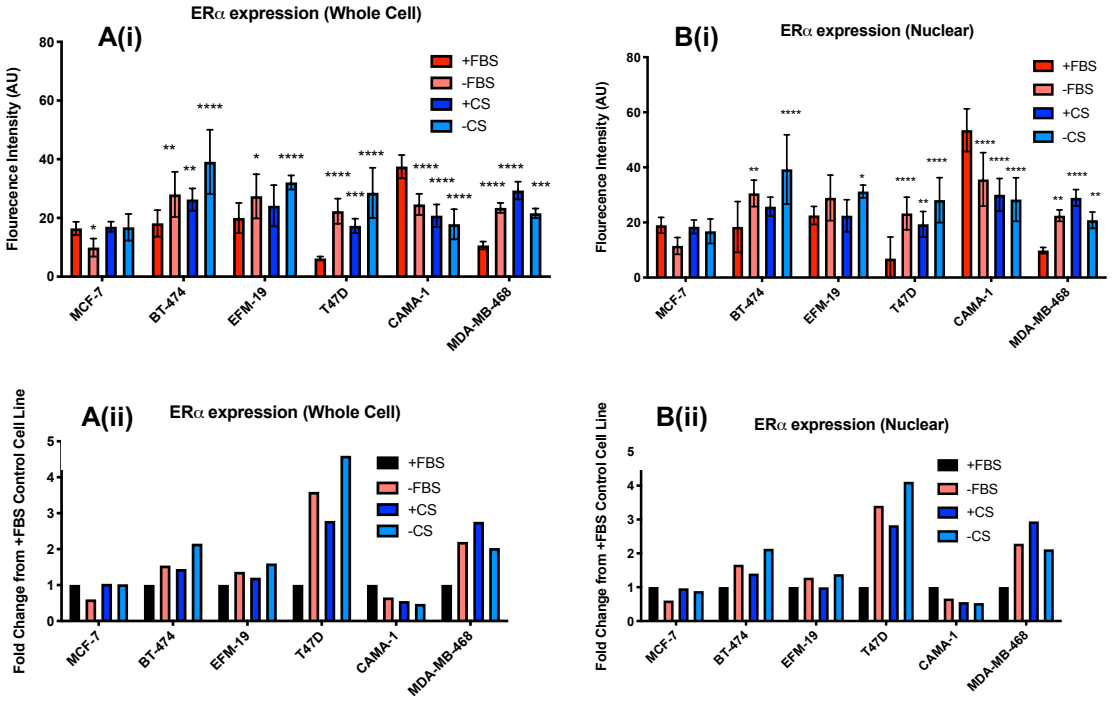


Figure 3.19: (A) Fluorescence intensity of ERα in each of the originating breast cancer cell lines and all of the oestrogen/phenol red deprived sub-lines generated from those. A) Whole cell fluorescence, B) Nuclear only expression, i) fluorescence intensity values, ii) fold change in fluorescence intensity values respectively. Data points are representative of the average of n=6 images per cell line, and of the average intensity of a single cell. Each data point is therefore roughly representative of the intensity of 50 individual cells. Error bars are representative of +/- SD. Statistical analysis was conducted using two-way ANOVA with bonferroni correction (**** - p<0.0001)(*** - p<0.001)(** - p<0.01)(* - p<0.05**) –** data points were compared to originating +FBS cell line for statistical analysis. (B) Plotted fold changes from fluorescence intensity of originating +FBS control cell line., calculated from (A)

Changes to ERβ expression were seen in in 12/18 of the sublines compared to their parental counterparts (Fig. 3.20). No significant difference was seen in the MCF7 or EFM-19 cell lines. Significant increases in ERβ expression was seen in the BT-474, T47D and MDA-MB-468 cell lines. However, fold change values in (B) of Fig 3.20, show only moderate changes in ERβ expression in the BT-474 and T47D cell lines, a notable increase is seen in the MDA-MB-468 cell line. When comparing expression levels between whole cell and nuclear positions, like that of ERα, expression patterns appear to be relatively consistent for the majority of the cell lines – suggesting that receptor expression is fairly ubiquitous in the cell also for ERβ. However, when comparing the fold changes for whole cell vs nuclear expression for the T47D cell line, there does appear to be a higher levels of nuclear expression, which is consistent with the images in figure 3.16.

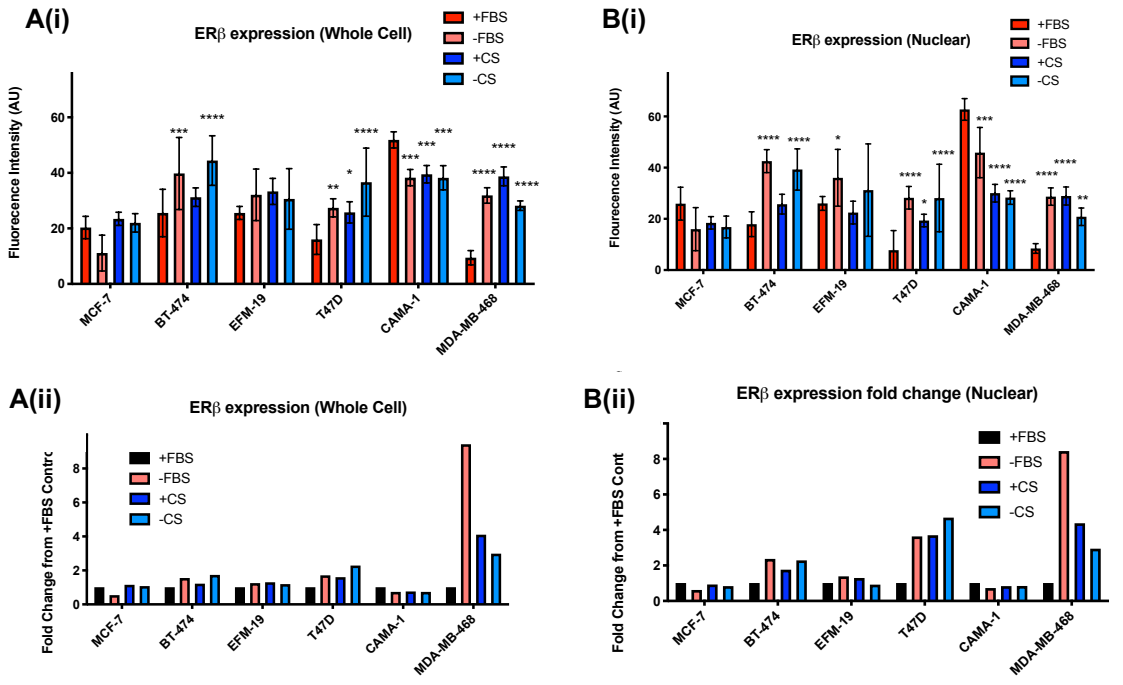


Figure 3.20: Fluorescence intensity of ERβ in each of the originating breast cancer cell lines and all of the oestrogen/phenol red deprived sub-lines generated from those. Data points are representative of the average of n=6 images per cell line, and of the average intensity of a single cell. A) Whole cell fluorescence, B) Nuclear only expression, i) fluorescence intensity values, ii) fold change in fluorescence intensity values respectively. Each data point is therefore roughly representative of the intensity of 50 individual cells. Error bars are representative of +/-SD. Statistical analysis was conducted using two-way ANOVA with bonferroni correction (**** - p<0.0001)(*** - p<0.001)(** - p<0.01)(* - p<0.05**) –** data points were compared to originating +FBS cell line for statistical analysis. **(B)** Plotted fold changes from fluorescence intensity of originating +FBS control cell line, calculated from (A).

Furthermore, the fluorescence intensity data plotted in figures 3.19, and 3.20 (above) were used to calculate the ratio of expression between whole cell and nuclear only. A value below 1 is indicative of a preference for nuclear localisation within the cell. Looking at the data displayed in figure 3.21, below, it is evident that the only cell line to display a preference for nuclear localisation is the CAMA-1 cell line in all media conditions for both receptors ERα and ERβ. However, for the rest of the cell lines and their differing media conditions, the values all appear to remain around a value of 1, suggesting again, the receptor expression is fairly ubiquitous throughout the panel of cell lines, with the exception of the T47D^{+FBS} cell line, that shows a greater amount of cytoplasmic localisation compared to the other cell lines.

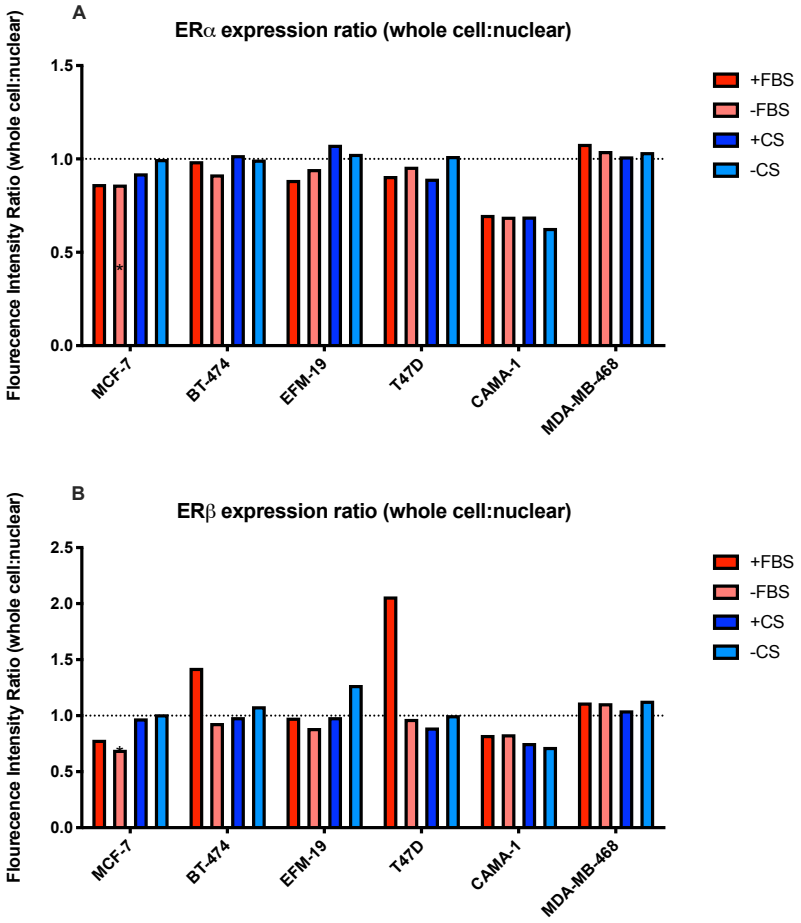


Figure 3.21: **(A)** Fluorescence intensity ratios of ERα (A) and ERβ (B) in each of the originating breast cancer cell lines and all of the oestrogen/phenol red deprived sub-lines generated from those. Data points are representative of the average of the data obtained from n=6 images per cell line, and of the average intensity of the whole cell divided by the average intensity of the nuclear only reading. Values below one are indicative of a preference for nuclear localisation. Colour coding is consistent with the media condition in which the cell line was cultivated in.

3.2.6: Response to tamoxifen and its primary metabolites

The majority of anti-cancer effects in response to tamoxifen treatment are thought to be elicited through primary tamoxifen metabolites which have a greater potency than tamoxifen itself (Helland *et al.*, 2017). The oestrogen-deprived sub-lines established in this chapter have been characterised for their response to the most clinically relevant tamoxifen metabolites – (Z)-4-OH-tamoxifen, alpha-hydroxytamoxifen, endoxifen and N-desmethyltamoxifen (Kisanga *et al.*, 2004a; Madlensky *et al.*, 2011; Helland *et al.*, 2017), and in each of the four media types described in section 2.2.1. This was to assess the effect of differing levels of oestrogenic stimulation on the breast cancer cells, and on their response to tamoxifen and these primary metabolites. The metabolites of tamoxifen used for this study have differing potencies as can be seen in figures 3.22-26.

Long term oestrogen-deprivation of breast cancer cells *in vitro* may be a method of mimicking resistance to aromatase inhibitors as these share a commonality of growth in the absence of oestrogen. Therefore, we can here look at the effect of tamoxifen and its active metabolites on a sub-set of oestrogen-deprived sublines (modelled as potentially aromatase inhibitor resistant ER+ breast cancer cell lines), and compare them to their counterpart parental cell lines as controls.

There is a physiological bias, from patient to patient, as to the proportions of these metabolites that are synthesised after administration of bolus and continuous doses of tamoxifen – a number of CYP450 enzymes facilitate this synthesis, which are notoriously polymorphic and differentially expressed (Kisanga *et al.*, 2004b; Ahmad *et al.*, 2010; Madlensky *et al.*, 2011). This makes the anti-cancer activity of each individual metabolite an important experimental question as preference for lesser potent metabolites could carry negative implications in the clinic.

It is clear from figures 3.22-3.26, that the metabolites all have differing potencies, but none more so than that of alpha-hydroxytamoxifen, showing the highest IC_{50} values. Figures 3.22-3.26 show IC_{50} values for each of tamoxifen, (Z)-4-OH-tamoxifen, alpha-hydroxytamoxifen, endoxifen and N-desmethyltamoxifen. These figures are also accompanied by calculated fold changes relative to their respective originating parental cell line (+FBS). This makes trends in either

reduced or increased sensitivity to these compounds as a direct result of oestrogen deprivation easier to interpret.

Tamoxifen is thought to be metabolically converted to form pharmacologically active metabolites that mediate the majority of anti-cancer effects that can be seen from the drug (Chang, 2012). This would suggest that tamoxifen itself is not as potent as its 'active' metabolites. Most tamoxifen IC_{50} values, regardless of oestrogen deprivation, fall below 4μm (displayed in fig. 3.22), which is most similar to those of (Z)-4-OH-tamoxifen (Fig. 3.22), which presents the lowest IC_{50} values of all metabolites investigated in this section. This may suggest that either tamoxifen is just as potent as (Z)-4-OH-tamoxifen, or that there is an intracellular metabolic activity and preference for this metabolite as breast cancer cell lines are known to express low levels of the CYP450 enzymes that facilitate the transformation of tamoxifen to its active metabolites (Mitra *et al.*, 2011). Other than the EFM-19^{-FBS} subline, the set of CAMA-1 cell lines appears to be the only cell line to show a consistent change in response to tamoxifen compared to its control +FBS subline. Comparing the response of these cell lines to the other metabolites, the CAMA-1 (+CS/-CS) sublines also show sensitivity to n-desmethyltamoxifen (Fig. 3.26B) which could suggest similarities in the mechanisms of actions of these two compounds and dissimilarities with the others, however, the EFM^{-FBS} and CAMA-1^{-FBS} sublines do not share sensitivity to n-desmethyltamoxifen also. This may be explained by sensitivity to tamoxifen/n-desmethyltamoxifen being caused by differing factors in oestrogen deprived conditions compared to in the presence of oestrogen.

When all six cell lines are grouped into media conditions, the average tamoxifen IC_{50} values are as follows (in μM): +FBS: 3.6 ± 2.22, -FBS: 2.7 ± 2.20, +CS: 3.3 ± 1.86, -CS: 2.9 ± 2.02. The average fold changes are as follows: +FBS 1 ± 0, -FBS: 0.97 ± 0.06, +CS: 1.12 ± 0.11, -CS: 0.91 ± 0.11.

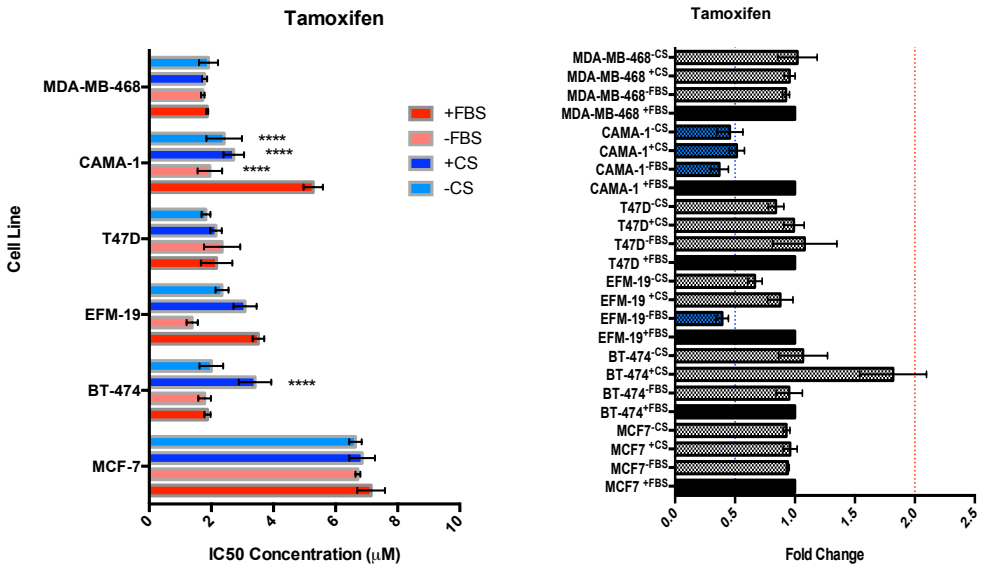


Figure 3.22**: (A)** Tamoxifen IC_{50} values experimentally obtained from the originating control cell lines and the oestrogen-deprived sub-lines in this chapter, indicated on the y-axis of the graphs. The graph is colour coded for the cell line that the data is related to. Data is representative of n=3 biological repeats, error bars are representative of +/- SD. Statistical analysis was conducted using two-way ANOVA with tukeys correction. (**** - p<0.0001)(*** - p<0.005)(** - p<0.01)(* - p<0.05**). (B)** Fold change values obtained from (A) that have been calculated relative to the control originator from that particular cell line (coloured in black). Horizontal blue line marks when x=0.5, whilst horizontal red line marks where x=2. A value below 0.5 indicates increased sensitivity to the compound relative to the respective parental cell line, whereas a value above 2 indicates cross-resistance relative to the respective parental cell line. Bars are coloured to reflect this – blue = sensitive.

Figures 3.23-3.26 display data in the same way to figure 3.22 above, with the same statistical analysis carried out - they show data obtained from the tamoxifen metabolites considered to be most clinically relevant: (Z)-4-OH-tamoxifen, alpha-hydroxytamoxifen, endoxifen, and n-desmethyltamoxifen (Madlensky *et al.*, 2011). (Z)-4-OH-tamoxifen, endoxifen and n-desmethyltamoxifen in particular have focus placed on them as candidates for eliciting the majority of 'beneficial' anti-cancer effects of tamoxifen. N-desmethyltamoxifen has previously been found to be the most abundant metabolite found in serum from clinical data (Robinson *et al.*, 1991; Kisanga *et al.*, 2004).

For (Z)-4-OH-tamoxifen (figure 3.23), only the BT-474 cell line (in both +CS and -CS conditions) becomes markedly more resistant to this metabolite – this is the only cell line to show this trend. It does not appear to be resistant to any of the other metabolites (Fig. 3.22-26), however it is sensitive to n-desmethyltamoxifen, suggesting that the two compounds have opposing effects on oestrogen deprived BT-474. The presence of phenol red does not affect the trends seen. It should be noted that the BT-474^{+FBS} cell line is particularly sensitive to (Z)-4-OH-tamoxifen, as is its phenol red deprived counterpart. Again, suggesting that phenol red does not have an effect on this.

When all six cell lines are grouped into media conditions, the average (Z)-4-OH-tamoxifen IC_{50} values are as follows (in μM): +FBS: 2.99 ±1.79, -FBS: 2.53 ± 1.50, +CS: 3.83 ± 1.00, -CS: 3.42 ± 3.42. The average fold changes are as follows: +FBS 1 ± 0, -FBS: 0.83 ± 0.09, +CS: 4.84 ± 0.95, -CS: 2.74 ± 1.16.

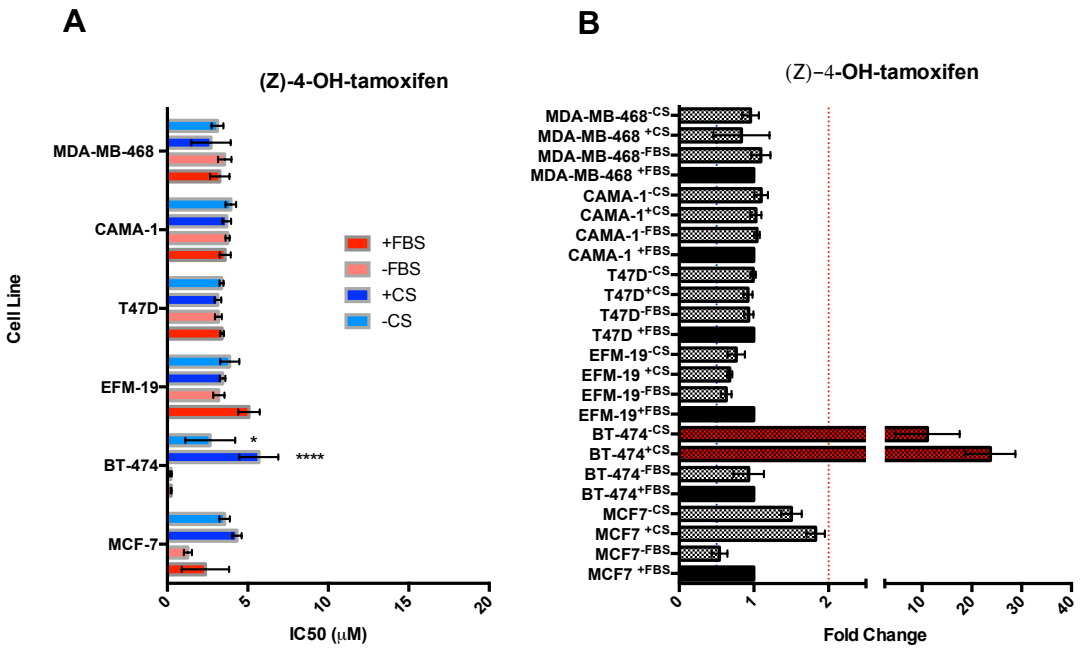


Figure 3.23**: (A)** (Z)-4-OH-tamoxifen IC_{50} values experimentally obtained from the originating control cell lines and the oestrogen-deprived sub-lines in this chapter, indicated on the y-axis of the graphs. The graph is colour coded for the cell line that the data is related to. Data is representative of n=3 biological repeats, error bars are representative of +/- SD. Statistical analysis was conducted using two-way ANOVA with tukeys correction. (**** - p<0.0001)(*** - p<0.005)(** - p<0.01)(* - p<0.05**). (B)** Fold change values obtained from (A) that have been calculated relative to the control originator from that particular cell line (coloured in black). Horizontal blue line marks when x=0.5, whilst horizontal red line marks where x=2. A value below 0.5 indicates sensitivity to the compound, whereas a value above 2 indicates resistance. Bars are coloured to reflect this – blue = sensitive, red = resistant.

Alpha-hydroxytamoxifen (figure 3.24) has the highest IC_{50} values against the cell lines, with most data points ranging from 30-40μM. This is considerably higher considering all other metabolites display IC_{50} values of below 10μM (Fig 3.22-26). Oestrogen deprivation does not appear to affect cellular response to this metabolite generally, however the MDA-MB-468^{-FBS} cell line does show increased sensitivity to this metabolite – this is the only significant difference seen here. The higher IC_{50} values here suggest that alpha-hydroxytamoxifen is an unfavourable metabolite when considering clinical response. Oestrogen deprivation or the presence of phenol red do not have an effect on response to alpha-hydroxytamoxifen.

When all six cell lines are grouped into media conditions, the average alphahydroxytamoxifen IC_{50} values are as follows (in μM): +FBS: 38.35 ±3.18, -FBS: 38.25 ± 3.5, +CS: 35.36 ±1.45, -CS: 33.27 ± 3.77. The average fold changes are as follows: +FBS 1 ± 0, -FBS: 0.98 ± 0.04, +CS: 0.92 ± 0.04, -CS: 0.87 ± 0.05.

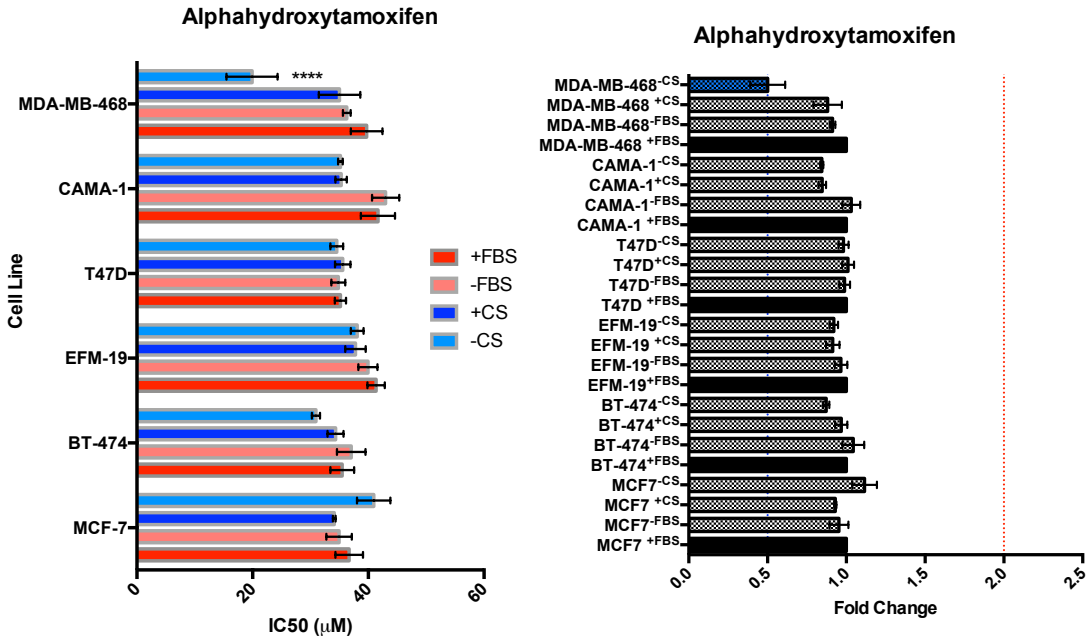


Figure 3.24**: (A)** Alpha-hydroxytamoxifen IC_{50} values experimentally obtained from the originating control cell lines and the oestrogen-deprived sub-lines in this chapter, indicated on the y-axis of the graphs. The graph is colour coded for the cell line that the data is related to. Data is representative of n=3 biological repeats, error bars are representative of +/- SD. Statistical analysis was conducted using two-way ANOVA with tukeys correction. (**** - p<0.0001)(*** - p<0.005)(** - p<0.01)(* - p<0.05**). (B)** Fold change values obtained from (A) that have been calculated relative to the control originator from that particular cell line (coloured in black). Horizontal blue line marks when x=0.5, whilst horizontal red line marks where x=2. A value below 0.5 indicates sensitivity to the compound, whereas a value above 2 indicates resistance. Bars are coloured to reflect this – blue = sensitive

From the endoxifen fold changes in Fig. 3.25B, no ubiquitous trend can be seen between the oestrogen deprived sublines and their parental cell lines apart from the T47D cell line. $T47D^{-FBS}$ and $T47D^{-CS}$ qualify as resistant compared to their parental cell line, and although the fold change value for $T47D^{+CS}$ is below 2, it still shows an increase from the parental cell line.

Looking at the endoxifen IC_{50} values in figure 3.25A, no significant difference is seen between the culture medias for MCF-7 and EFM-19. A significant difference can be seen in the -CS conditions for CAMA-1 and BT-474 only, marking a decrease in IC_{50} value relative to the parental +FBS condition. The T47D cell line shows a significant increase in IC_{50} value for all of the adapted sublines – with the greatest increase seen in the -CS counterpart. The opposite trend to the T47D cell line is seen in the MDA-MB-468 cell line, that shows a significant decrease in IC_{50} value in the oestrogen deprived sub-lines. Therefore, over the panel of cell lines used in this study, we have seen a range of responses to endoxifen as a result of oestrogen deprivation – no response, an increase in IC_{50} and a decrease in IC_{50}. As no steps have been taken to evaluate the mechanisms of action of this metabolite, it cannot be commented on as to why this is, but it can be assumed that there are individual adaptation processes that are specific to each cell line and have caused differences in response to this metabolite. The trend seen with this metabolite is individual to all of the other metabolites looked at in this study.

When all six cell lines are grouped into media conditions, the average endoxifen IC_{50} values are as follows (in μM): +FBS: 7.15 ± 3.28, -FBS: 8.10 ± 2.22, +CS: 7.40 ± 2.1, -CS: 7.16 ± 0.93. The average fold changes are as follows: +FBS 1 ± 0, -FBS: 1.1 ± 0.08, +CS: 0.99 ± 0.07, -CS: 1.37 ± 0.09.

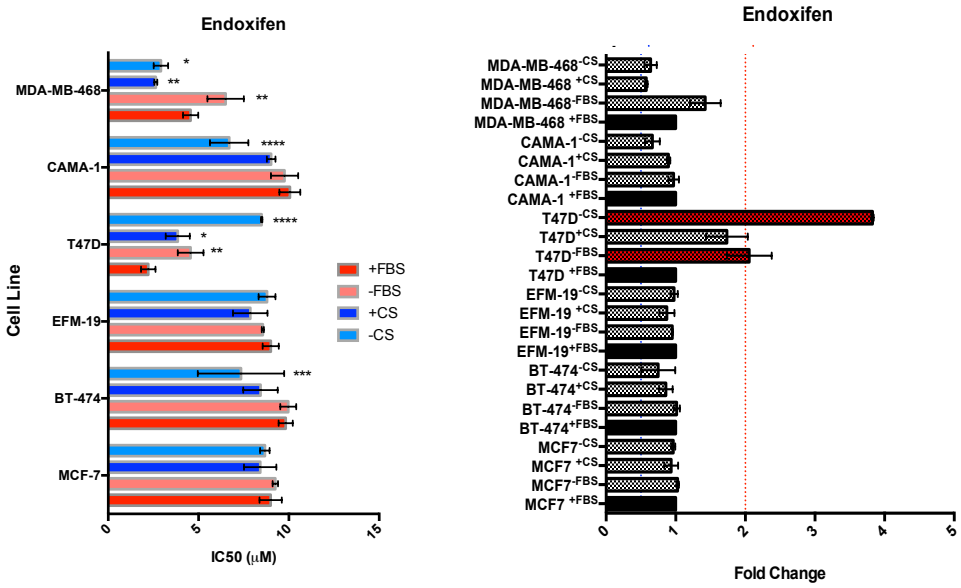


Figure 3.25**: (A)** (Z)-Endoxifen IC_{50} values experimentally obtained from the originating control cell lines and the oestrogen-deprived sub-lines in this chapter, indicated on the y-axis of the graphs. The graph is colour coded for the cell line that the data is related to. Data is representative of n=3 biological repeats, error bars are representative of +/- SD. Statistical analysis was conducted using two-way ANOVA with tukeys correction. (**** - p<0.0001)(*** - p<0.005)(** - p<0.01)(* - p<0.05**). (B)** Fold change values obtained from (A) that have been calculated relative to the control originator from that particular cell line (coloured in black). Horizontal blue line marks when x=0.5, whilst horizontal red line marks where x=2. A value below 0.5 indicates sensitivity to the compound, whereas a value above 2 indicates resistance. Bars are coloured to reflect this – blue = sensitive.

From literature, endoxifen and (Z)-4-OH-tamoxifen are thought to have the most comparable anti-oestrogenic activity, and have 30-100 times the affinity for ERs compared to n-desmethyltamoxifen (Jager *et al.*, 2014). Fig 3.26 shows that this is not the case in the context of the cell lines used for this study. All n-desmethyltamoxifen data points range from 2.26-9.69μM which displays a very similar range in IC_{50} values to endoxifen (2.22-10.4 μM). IC_{50} values for (Z)-4-OH-tamoxifen range from 0.21-6.75μM.

Fold change values in (B) of figure 3.26 (below), show this metabolite to be the only one of those tested in this chapter to have cell response affected by growth in growth hormone reduced conditions – with four of the cell lines having both hormone-deprived sub-lines under the threshold for 'increased sensitivity' (fold change below 0.5) to the drug when compared to the control cell line (CAMA-$1^{+cs/-cs}$, T47D$^{+cs/-cs}$, EFM-$19^{+cs/-cs}$ and BT-$474^{+cs/-cs}$). The MCF7 and MDA-MB-468 cell lines do not have fold changes lower that 0.5 to qualify as sensitive to this metabolite compared to parental controls, however a reduction in IC_{50} value is apparent (Fig 3.26A) in the MDA-MB-468 cell line. No difference is seen in the MCF7 sublines.

These is currently no report of this finding in literature with regards to its effect on growth hormone deprivation – phenol red does not appear to have an effect on this apart from the T47D^{-FBS} cell line that shows a significant reduction in n-desmethyltamoxifen IC_{50} when compared to its parental cell line.

When all six cell lines are grouped into media conditions, the average n-desmethyltamoxifen IC_{50} values are as follows (in μM): +FBS: 7.65 ± 0.96, -FBS: 7.02 ± 2.05, +CS: 6.71 ± 2.22, -CS: 3.99 ± 2.67. The average fold changes are as follows: +FBS 1 ± 0, -FBS: 0.9 ± 0.1, +CS: 0.52 ± 0.06, -CS: 0.55 ± 0.05.

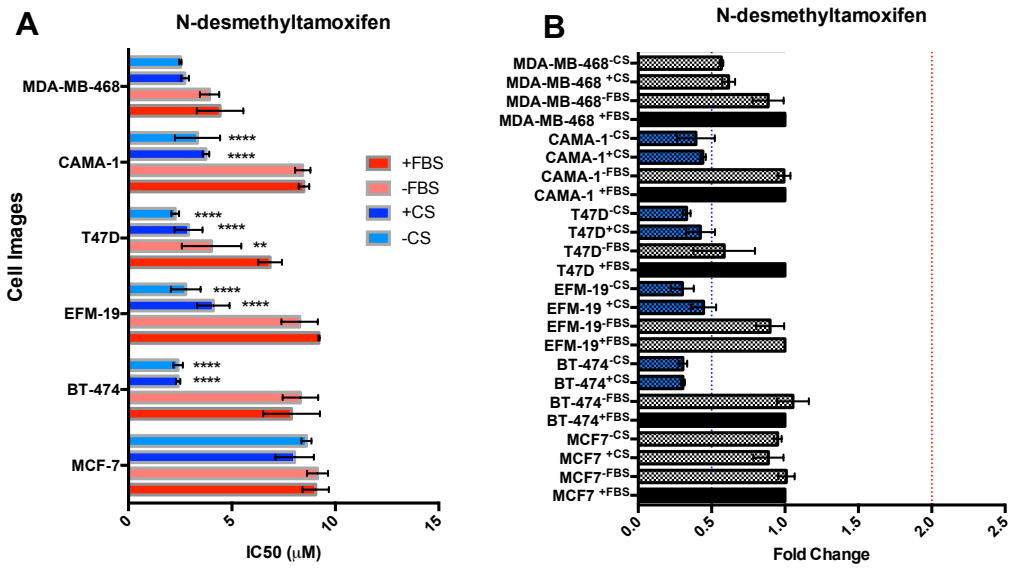


Figure 3.26**: (A)** N-desmethyltamoxifen IC_{50} values experimentally obtained from the originating control cell lines and the oestrogen-deprived sub-lines in this chapter, indicated on the y-axis of the graphs. The graph is colour coded for the cell line that the data is related to. Data is representative of n=3 biological repeats, error bars are representative of +/- SD. Statistical analysis was conducted using two-way ANOVA with tukeys correction. (**** - p<0.0001)(*** - p<0.005)(** - p<0.01)(* - p<0.05**). (B)** Fold change values obtained from (A) that have been calculated relative to the control originator from that particular cell line (coloured in black). Horizontal blue line marks when x=0.5, whilst horizontal red line marks where x=2. A value below 0.5 indicates sensitivity to the compound, whereas a value above 2 indicates resistance. Bars are coloured to reflect this – blue = sensitive.

3.2.7: Response to other anti-cancer compounds

The oestrogen deprived sublines were then evaluated for response to 2-methoxyoestradiol (Fig 3.27), vincristine (Fig. 3.28) and olaparib (Fig. 3.29).

2-methoxyoestradiol is an endogenous metabolite of oestrogen, that lacks oestrogenic activity, but has been shown to bind to GPER1 with a high affinity (Thekkumkara, Snyder and Karamyan, 2016), and acts as a tubulin binding agent (Dumontet and Jordan, 2010). The mechanism of action of 2-methoxyoestradiol is largely unknown (quantifying binding affinities of steroid hormones is notoriously difficult because they are lipophilic, and prone to non-specific binding in lipid-rich membrane preparations), but has been seen to exhibit antiproliferative, antiangiogenic and anti-tumour properties in an *in vivo* setting. (Bansal and Acharya, 2014; Thekkumkara, Snyder and Karamyan, 2016; Tao, Mei and Tang, 2019).

Figure 3.27A shows 2-methoxyoestrodiol IC_{50} values for the oestrogen-deprived sub-lines. No significant difference in response is observed between sublines BT-474, CAMA-1 and MDA-MB-468. A significant increase in IC_{50} is seen in the MCF7 cell line - the presence of phenol red did not have an effect on this. IC_{50} values were generally higher for this particular cell line, perhaps showing intrinsic resistance to 2-methoxyoestradiol. Fig 3.27B shows sublines EFM-19^{+CS}, EFM-19^{-CS}, T47D^{-FBS} and T47D^{-CS}. 5/6 of the sublines found to be resistant are adapted to growth in the presence of reduced levels of oestrogen – suggesting that in these cell lines, an increase in tolerance to 2-methoxyoestradiol could be a result of oestrogen deprivation. As this compound is a known tubulin-binding agent also, it should be compared to another known tubulin binding agent to elucidate whether the response seen is due to tubulin interference of another mechanism of action.

When all six cell lines are grouped into media conditions, the average 2-methyoxyoestradiol IC_{50} values are as follows (in μM): +FBS: 2.51 ± 4.3 -FBS: 2.03 ± 3.6, +CS: 18.05 ± 42.77, -CS: 15.07 ± 34.26. The large standard deviation for +CS and -CS conditions show a great deal of variability is hormone deprived subline response to this compound. The average fold changes are as follows: +FBS 1 ± 0, -FBS: 1.17 ± 0.17, +CS: 0.49 ± 0.09, -CS: 0.59 ± 0.15.

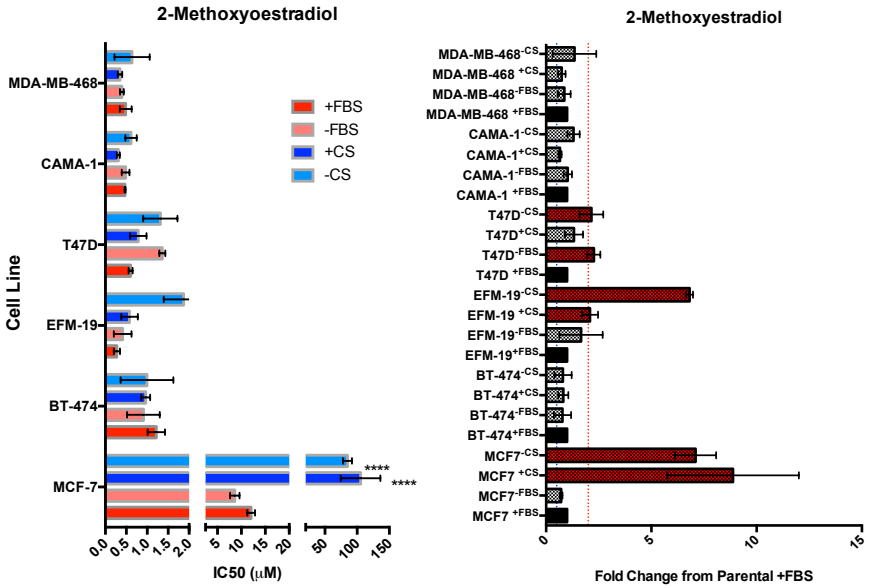


Figure 3.27**: (A)** 2-methoxyoestradiol IC_{50} values experimentally obtained from the originating control cell lines and the oestrogen-deprived sub-lines in this chapter, indicated on the y-axis of the graphs. The graph is colour coded for the cell line that the data is related to. Data is representative of n=3 biological repeats, error bars are representative of +/- SD. Statistical analysis was conducted using two-way ANOVA with tukeys correction (**** - p<0.0001)(*** - p<0.001)(** - p<0.01)(* - p<0.05**). (B)** Fold change values obtained from (A) that have been calculated relative to the control originator from that particular cell line (coloured in black). Horizontal blue line marks when x=0.5, whilst horizontal red line marks where x=2. A value below 0.5 indicates sensitivity to the compound, whereas a value above 2 indicates resistance. Bars are coloured to reflect this – blue = sensitive.

The sublines were then investigated for response to another known tubulin binding agent – the vinca alkaloid, vincristine. Vinca alkaloids are a group of anti-mitotic and anti-microtubule alkaloid compounds that block beta-tubulin polymerisation and therefore cell division. Microtubule-interfering drugs, like vincristine, are used as part of treatment regimens for advanced stage metastatic breast cancer. Vincristine itself is a microtubule-destabilising agent and an example of a vinca alkaloid that is most commonly used to treat leukaemia and lymphomas (Avramis, Kwock and Avramis, 2001; Escuin, Kline and Giannakakou, 2005; Park *et al.*, 2016). Here, we looked at the effect of vincristine on the panel of oestrogen-deprived sublines.

From Fig 3.28, the growth hormone deprived MCF7 cell lines showed the same pattern of response to vincristine as to 2-methoxyoestradiol (Fig 3.27) – exhibiting higher IC_{50} values for both of the hormone deprived sublines. This suggests that the effects of 2-methoxyoestroadiol on this cell line are caused by tubulin binding. This is interesting considering that 2-methoxyoestradiol and vincristine interact with tubulin at two different sites - colchicine site and the vinca site respectively (D'Amato *et al.*, 1994; Dumontet and Jordan, 2010). A number of other cell lines are also resistant to vincristine: BT-474^{-CS}, EFM-19^{-FBS}, EFM^{-CS}, T47D^{+CS}, T47D^{-CS}, MDA-MB-468^{+CS} and MDA-MB-468^{-CS}. 8/9 sublines resistant to vincristine are also oestrogen deprived, suggesting that oestrogen deprivation may have an effect on tubulin structure or function.

When all six cell lines are grouped into media conditions, the average vincristine IC_{50} values are as follows (in μM): +FBS: 0.45 ± 0.35, -FBS: 0.66 ± 0.64, +CS: 1.09 ± 1.49, -CS: 1.8 ± 2.40. The average fold changes are as follows: +FBS 1 ± 0, -FBS: 1.17 ± 0.26, +CS: 2.39 ± 0.65, -CS: 3.2 ± 0.78.

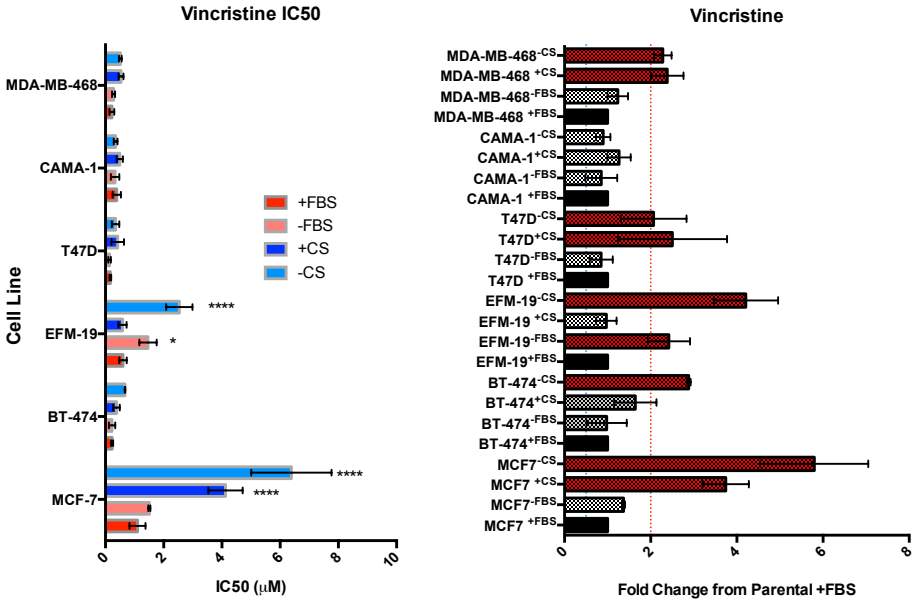


Figure 3.27**: (A)** Vincristine IC_{50} values experimentally obtained from the originating control cell lines and the oestrogen-deprived sub-lines in this chapter, indicated on the y-axis of the graphs. The graph is colour coded for the cell line that the data is related to. Data is representative of n=3 biological repeats, error bars are representative of +/- SD. Statistical analysis was conducted using two-way ANOVA with tukeys correction (**** - p<0.0001)(*** - p<0.001)(** - p<0.01)(* - p<0.05**). (B)** Fold change values obtained from (A) that have been calculated relative to the control originator from that particular cell line (coloured in black). Horizontal blue line marks when x=0.5, whilst horizontal red line marks where x=2. A value below 0.5 indicates sensitivity to the compound, whereas a value above 2 indicates resistance. Bars are coloured to reflect this – blue = sensitive.

Olaparib is one of the most widely investigated PARP inhibitors for the treatment of triple negative breast cancer (TNBC), as BRCA1/BRCA2 mutations are found in a relatively large percentage of patients with TNBC tumours (Lord and Ashworth, 2016; Robert *et al.*, 2017). Olaparib has proven to be a successful treatment option for ovarian, prostate and pancreatic cancers (Kamel *et al.*, 2018), following the dogma of synthetic lethality when coupled with inherent deficiencies in DNA repair that accompany BRCA mutations. However, relatively little is reported in literature as to its effect on ER+ tumours, or its effect on breast cancers that are BRCA wild-type.

The MDA-MB-468 cell lines show the most sensitivity to olaparib of all of the cell lines investigated. A significant reduction in IC_{50} values are seen in sublines of EFM-19, BT-474 and CAMA-1 (Fig. 3.29A). Fold changes (Fig 3.29B) shows the cell lines MDA-MB-468, CAMA-1, T47D and EFM-19 to contain sub-lines that show increased sensitivity to olaparib as a result of oestrogen deprivation, showing that this may bring about increases in homologous recombination DNA damage repair faults. The MDA-MB-468 cell line appears to be the most sensitive to olaparib of all of the cell lines tested, regardless of growth media.

When all six cell lines are grouped into media conditions, the average olaparib IC_{50} values are as follows (in μM): +FBS: 31.47 ± 31.1, -FBS: 30.46 ± 23.81, +CS: 18.05 ± 17.2, -CS: 19.4 ± 17.11. High standard deviations highlight a great deal of variability that can be observed between the individual cell lines, average values for hormone deprived sublines are on average higher than those grown in the presence of growth hormone. The average fold changes are as follows: +FBS 1 ± 0, -FBS: 1.29 ± 0.3, +CS: 2.1 ± 0.53, -CS: 3.02 ± 0.52.

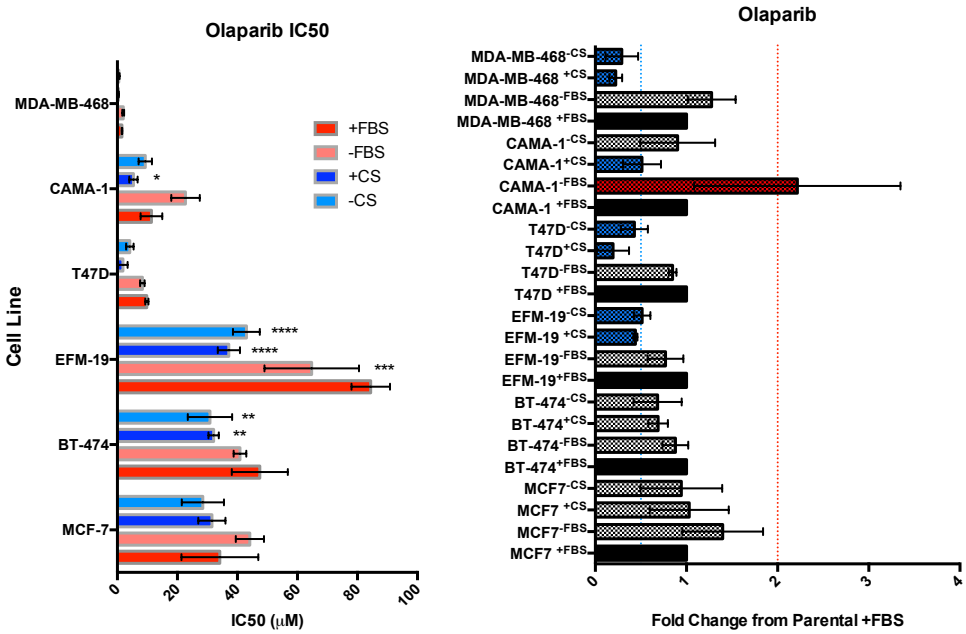


Figure 3.29**: (A)** Olaparib IC_{50} values experimentally obtained from the originating control cell lines and the oestrogen-deprived sub-lines in this chapter, indicated on the y-axis of the graphs. The graph is colour coded for the cell line that the data is related to. Data is representative of n=3 biological repeats, error bars are representative of +/- SD. Statistical analysis was conducted using two-way ANOVA with tukeys correction (**** - p<0.0001)(*** - p<0.001)(** - p<0.01)(* - p<0.05**). (B)** Fold change values obtained from (A) that have been calculated relative to the control originator from that particular cell line (coloured in black). Horizontal blue line marks when x=0.5, whilst horizontal red line marks where x=2. A value below 0.5 indicates sensitivity to the compound, whereas a value above 2 indicates resistance. Bars are coloured to reflect this – blue = sensitive.

3.3: Discussion

3.3.1: Oestrogen deprivation as a potential mimic for aromatase inhibitor resistance

The treatment of ER+ breast tumours with aromatase inhibitors (AIs) seeks to deprive oestrogen dependent tumour cells of this hormone by blocking the conversion of androgens to oestrogen in a physiological system (Dowsett and Howell, 2002). AIs have improved the treatment of ER+ breast cancer since their introduction to use in the clinic, but like other endocrine therapies, the biggest hurdle in clinical management of hormone receptor positive breast cancer is the emergence of endocrine resistance (Martin *et al.*, 2011). In an *in vivo* system, the majority of aromatase is produced in the ovaries of females (Stocco, 2012), making *in vitro* systems that model physiological conditions tricky to produce. Studies have been conducted that focus on the identification of molecular mechanisms associated with relapse to endocrine therapy by means of adaptation to growth in the presence of charcoal stripped serum – these can be seen to model relapse to treatment with AIs (Coutts and Murphy, 1998; Chan *et al.*, 2002; Martin *et al.*, 2011). The long term oestrogen-deprivation of breast cancer cells *in vitro,* and their adaptation to become oestrogen independent may therefore be a model method of mimicking resistance to AIs as these share a commonality of preference to growth in reduced levels or the absence of oestrogen.

3.3.2: The use of MDA-MB-468 as an additional control cell line

The MDA-MB-468 cell line was included in this work with the intention of serving as an additional control to the parental cell lines used in this study, to allow comparisons between ER+ breast cancer cell lines and a triple negative breast cancer cell line. Qualitative assessment of oestrogen receptor expression showed that both oestrogen receptors were expressed in this cell line (Fig. 3.19), negating their ability to be a true triple negative breast cancer control. The antibodies used to assess this were confirmed for specific target binding (Fig 3.13). This cell line should therefore be considered as an additional ER+ cell line when the data in this chapter. However, initial growth of this cell line in hormone deprived conditions (Fig. 3.7) showed similarly comparable growth patterns to those of the adapted counterparts (Fig. 3.8), which was the only cell line observed to not show cell line quiescence upon exposure to growth hormone deprived

conditions, showing characteristics separate from the other cell lines. It was also the only cell line for none of its sublines to show any response to additional β-oestradiol (Fig. 3.11F) – showing that although the cell line stains positively for oestrogen receptor alpha, it is still unresponsive to β-oestradiol compared to control cell lines.

3.3.3: Cell line adaptation to growth in conditions in low levels of growth hormones

The effect of hormone deprivation on breast cancer cells *in vitro* was first examined by Katzenellenbogen *et al* (1987), both short-term and long-term, where FBS was replaced for dextran treated charcoal-stripped foetal calf serum and growth was observed. This study was conducted using only MCF7 cells. The team reported that for periods of up to one month in the absence of oestrogens for growth (and in the absence of phenol red), estradiol stimulated growth and the anti-oestrogen, tamoxifen, inhibited proliferation. Following deprivation for a period of 5-6 months, the team noticed a marked increase in the basal rate of cell proliferation that is unaffected by the reintroduction of oestrogen or tamoxifen to culture media – showing that time frames of longer than one month of oestrogen deprivation are needed for the adaptation of breast cancer cell lines to grow in the absence of oestrogen.

This effect was found in the MCF7 and BT-474 cells used in this study when re-introduced to oestradiol after at least 6 months in oestrogen deprived conditions (Fig. 3.11) as they display similar cellular growth to control cell lines that have not been growth hormone deprived. However, three of the other cell lines that were cultivated in reduced oestrogen remain responsive to the re-addition of oestradiol (EFM-19, T47D and CAMA-1) and show increased cellular growth compared to the vehicle control and counterpart cell lines that have been cultivated in FBS. This shows potential variance in time needed for the adaptation process, or perhaps even the possibility that some cells lines do not become completely independent of oestrogen stimulation following long-term oestrogen deprivation, and instead become hypersensitive to oestrogen stimulation. Hypersensitivity to oestrogen is also a documented phenomenon in literature as a result of long term oestrogen deprivation (Darbre, 2014).

The observed quiescence of the all cell lines, apart from MDA-MB-468, after initial cultivation in growth hormone deprived media (Fig 3.7), compared to 6 months later (Fig. 3.8) shows that adaptation has occurred.

3.3.4: Potential variability of residual growth hormones in foetal bovine serum after charcoal stripping

Charcoal-stripped bovine serum is a critical reagent for the study of steroid hormones. However, charcoal stripped serum will have moderate lot-to-lot variabilities in residual growth factor and steroid hormone content. The charcoal stripped serum used in this study originated from a single batch to ensure hormone content consistency throughout. The non-charcoal stripped FBS used in this study was also batch tested and used consistently. Batch and lot references are provided in section 2.2.1. A study by Sikora *et al.*, (2016) discusses the implication of this with regards to studies on endocrine resistance and differential phenotypes that can arise from this, which should be kept in mind when comparing data between different models of endocrine resistance. The study uses the observed response on the growth of breast cancer cell lines to differentiate between partial and complete reduction in growth hormone content of several batches of charcoal stripped serum. The study states that if only partial reduction of growth hormones is identified in charcoal stripped media, cells are observed to continue to grow, just at a reduced rate compared to control cell lines. Fig 3.7 shows that all cells but MDA-MB-468 showed almost complete quiescence when introduced to growth in the presence of charcoal stripped serum, suggesting near-complete reduction in growth hormone content. The presence of phenol red for the CAMA-1^{+CS} and MCF7^{+CS} sublines (Fig. 3.7) appeared to stimulate growth enough to show enhanced growth compared to -CS counterparts. Upon inspection of the culture media used for the entirety of this study, the company specifies on the provided product formulation specifications that phenol red is included at a concentration of 39.9μM. Welshons *et al.*, (1988) discusses how in low concentrations, phenol red does not elicit a response from oestrogen-responsive cells, but the vast majority of culture media harbours phenol red in concentrations somewhere in the range of 15-45μM, within which it has been known to exert oestrogenic affects.

3.3.5: Clinical implications of toxic effects of high dose oestrogen seen in growth hormone deprived breast cancer cell lines

The use of endocrine therapy, such as tamoxifen for the treatment of ER+ breast cancer is the gold standard for treatment of ER+ breast cancer (Nass and Kalinski, 2015) via inhibition of oestrogen receptors. However - the use of synthetic high-dose oestrogens used to be the standard treatment for breast cancer before the introduction of tamoxifen in the 70s - and has become a successful therapy option for post-menopausal women with metastatic breast cancer due to oestrogen-induced apoptosis in more recent years (Jordan, 2015).

A quandary, aptly referred to as the 'estrogen paradox' in literature, with regards to the use of high dose oestrogens, has existed in the clinic since the end of the 20th century. Breast cancer has always thought to be relatively dependent on oestrogen for growth, yet in high doses it causes regression of tumours. It also refers to there being a clear, and mostly unexplained, divide in responses to oestrogen replacement therapy observed in post-menopausal women resulting in either cancer cell growth or regression. This appears to be dependent on time since initiation of the menopause for response rates for breast cancer patients, and successful attainment of sufficient oestrogen induced apoptosis is now thought to be reliant on prior selection of cell populations that are resistant to long-term oestrogen deprivation (Jordan, 2015). The differential responses seen to the reintroduction of growth-hormone deprived cell lines in this study (Fig 3.11) show a similar trend. Some of the oestrogen-deprived cell lines showed no difference in growth compared to control cell lines (MCF7, BT-474). The naturally low levels of circulating oestrogen in post-menopausal women can be compared to the low levels of oestrogen in the growth-hormone deprived conditions in this study, and comparison between the cell lines, and how we see subjectivity between development of oestrogen independence in some of the cell lines (MCF7 and BT-474), and continue to see enhanced response to oestrogen stimulation following long term deprivation with others (EFM-19, CAMA-1 and T47D).

3.3.6: Clinical implications of differential responses to tamoxifen, tamoxifen metabolites and other anti-cancer drugs

Tamoxifen is metabolised extensively in the liver by cytochrome P450 enzymes, and to a lesser extent in the breast also. These enzymes mediate the transformation of tamoxifen into a several primary and secondary metabolites,

mainly through hydroxylation and demethylation – these are known to have higher potencies than the parent drug, and therefore thought to exert the anti-tumour effects of tamoxifen *in vivo.* The major metabolic pathway involves initial conversion of tamoxifen to n-desmethyltamoxifen, then to endoxifen. This is the conversion with the highest throughput. The second-most preferred conversion is tamoxifen to 4-hydroxytamoxifen, which is in turn also converted to endoxifen (Cronin-Fenton, Damkier and Lash, 2014). Polymorphisms in several CYP enzymes involved in the metabolism of tamoxifen impact on the relative abundance of the metabolites in systemic circulation; which, adds to the already existing patient-to-patient subjectivity you would expect as these enzymes will be differentially expressed naturally from person to person (Rondon-Lagos *et al.*, 2016).

From literature, endoxifen and (Z)-4-OH-tamoxifen are thought to have the most comparable anti-oestrogenic activity, and have 30-100 times the affinity for ERs to that of N-desmethyltamoxifen (Jager *et al.*, 2014). Literature suggests that endoxifen is an important metabolite with regards to eliciting the majority of beneficial antagonist effects as it is thought to be the most pharmacologically available and is the most correlated with patient outcome - low levels in serum = poor outcome (Madlensky *et al.*, 2011; Jager *et al.*, 2014). This metabolite is thought to remain in a steady state in patient serum longer that of (Z)-OH-tamoxifen (Teunissen *et al.*, 2011). CYP2D6 and CYP3A4 are thought to play the biggest role in the production of these metabolites, highlighting the importance of individual genotyping (Madlensky *et al.*, 2011; Mitra *et al.*, 2011). When evaluating the active concentration ranges of tamoxifen and the metabolites used in this study, it is evident that they differ, which should be considered in a clinical setting. On the other hand, the administration of individual metabolites as a first line therapy could also be considered to overcome any unfavourable metabolic bias.

2-methoxyoestradiol and vincristine, which are both known tubulin binding agents (D'Amato *et al.*, 1994; Dumontet and Jordan, 2010) were also tested against the growth hormone deprived sublines to evaluate therapeutic potential. There is no literature currently to expand on our understanding on the use of tubulin binding agents in the advent of adaptation to growth in the absence of growth hormones,

that may mimic its use in endocrine therapy resistance, or post-menopausal women. 5/6 of the sublines found to be resistant to vincristine were growth hormone deprived. This is preliminary data, but it suggests that changes to tubulin structure and organisation should be investigated to explain this. As 2-methoxyoestradiol is both a known tubulin binding agent and a substrate for GPER1, we are unable to draw conclusions from the mechanism of action on these subline, however 8/9 of the sublines found to be resistant to this compound were growth hormone deprived – showing that growth hormone deprivation has an effect on response. GPER1 expression should be evaluated to allow more conclusions to be drawn between any differential responses seen between these two compounds.

No notable trend was observed in response to olaparib due to growth hormone deprivation. The only conclusion that can be drawn from this data is that more differences were observed between individual cell lines than there is between growth hormone deprived lines. Response is likely due to individual capacity for DNA repair than for growth hormone deprivation.

3.3.7: Conclusion and General Summary

This chapter documents the adaptation of six oestrogen-receptor (ER) positive cell lines to cultivation in the absence of growth hormones by supplementation with charcoal stripped bovine serum. The cell lines were observed to become quiescent upon initial exposure to growth hormone reduced conditions, confirming growth hormone reduced status of the culture media. Adaptation to growth took around six months. The cells were evaluated for response to β-oestradiol after long-term oestrogen deprivation – response was seen to be cell line specific, with some cell lines exhibiting growth independence from oestrogen, with others exhibiting hypersensitivity. The cell lines were then characterised for oestrogen receptor expression and found to either upregulate or down regulate receptors in a cell line specific manner. This may carry clinical significance if tumours have the ability to either upregulate or downregulate oestrogen receptors as a response to oestrogen deprivation – this should be evaluated before treatment regimens are decided in the advent of resistance to endocrine therapy. The effects of tamoxifen and four of its clinically relevant metabolites were investigated on the growth hormone deprived sublines – the only notable trend

between oestrogen deprivation and response to tamoxifen was seen with the metabolite n-desmethyltamoxifen. A trend was seen between growth hormone deprivation and a reduction in IC_{50} value to n-desmethyltamoxifen. No trend was observed in cellular response to olaparib, but a decrease in sensitivity was seen to vincristine and 2-methoxyoestroadiol in growth hormone deprived sublines.

Chapter 4: Production and characterisation of (Z)-4-OH-tamoxifen resistant breast cancer cell lines

4.1: Introduction

4.1.1 Tamoxifen resistance in breast cancer

The main mechanisms underlying intrinsic resistance to tamoxifen are a lack of ERα expression and a failure to convert tamoxifen into its active metabolites, while acquired resistance is thought to be associated with a plethora of mechanisms (Rondon-Lagos *et al.*, 2016). Several mechanisms have been suggested to explain resistance to tamoxifen, but given the complexity of oestrogen signalling itself, there are a number of mechanisms that could potentially be altered to result in increased tolerance to the drug. The main mechanisms accepted today are alterations to bioavailabilty of tamoxifen, changes to both the nuclear receptors and GPER1, alterations to oestrogen controlled intracellular signalling pathways (from ERα-36, GPER1 and GPER1-EGFR crosstalk) or switching to signalling through other nuclear receptors like the androgen receptor. Though many studies have been conducted using *in vitro* models of endocrine resistance, no definitive consensus has yet been reached as to the main underlying mechanisms of resistance (Poulard *et al.*, 2019).

4.1.2: Generating drug-resistant cell lines and their significance in cancer research

Acquired resistance to anti-cancer drugs is a serious impediment to successful treatment of patients suffering from a variety of cancer-types – hence, an understanding of the development of resistance is needed to improve therapy in the clinic (Salgia and Kulkarni, 2018). Drug-adapted cancer cell lines are a preclinical model of drug-resistance that have been shown to reflect mechanisms of acquired resistance in the clinic (Crystal *et al.*, 2014). Studying the acquisition of resistance over time is essential to obtaining a complete understanding of the difference between innate and acquired resistance to anti-cancer drugs, and to evaluate how these drugs play a role in tumour recurrence and progression (Steding, 2016).

There are several commonly employed methods of establishing anti-cancer drug resistant cell lines, and is generally thought to take from 3 to 18 months. However, relatively little has been published on comparing methodologies in doing so. The first acknowledged published strategy came in 1970 (Biedler and Riehm, 1970),

and involved the stepwise increase of exposure to a drug continuous manner (meaning that the cells were never without exposure to the drug for any length of time). Then, with the advent of consideration of what would be more clinically relevant as a way to adapt cells to exposure of chemotherapeutics, pulsing methods were also practiced in laboratories – where cell lines are exposed to drug for a short length of time, and then released from this to recover until the next dosing stage. This was considered to be more closely related to the way that cancer cells in patients are exposed to chemotherapeutics in dosing regimens (McDermott *et al.*, 2014). Ultimately, when considering data obtained from drug resistant cell lines, it should be taken into consideration how the cell line was initially adapted to the drug, as should be with the data in the upcoming chapters results.

For the data in this chapter, it was experimentally obtained, the concentration at which the viability of the cells was decreased by 50%, and dose-escalated, in a continuous culture, until a fold change greater than twice that of the originating cell line was reached. The important aspect of this, is that this was standardised for all of the cell lines, from which data is presented in this chapter. But as previously mentioned, this is not the only method in which to establish drug-resistant cancer cell lines. First, the researcher needs to decide whether their model of resistance is to be one that is just clinically relevant (when resistance generation only spans so far as to encompass drug concentrations that are seen in the clinic, in patient serum samples), or a high-level laboratory model (where the sky is the limit, and dose-escalation is taken past this point). Either way, drug naïve cells are to exposed to increasing concentrations of anti-cancer drugs, in either a continuous of pulsed fashion (McDermott *et al.*, 2014).

Another factor to consider is whether this method selects for cells that have either acquired or innate immunity to the anti-cancer drug in question. Dose escalation methods will be selecting cell populations over a long span of time, and will allow for time-dependent adaptation and alterations to the phenotype of the cell population, whereas selecting cells via exposure to a high concentration of the drug, followed by clonal selection (cells that are immediately intrinsically resistant to an anticancer drug) will allow for models of intrinsic resistance as opposed to

acquired resistance, like the cell lines discussed and displayed in this chapter (Franken *et al.*, 2006).

4.1.3: Introduction to the results in this chapter

In this part of the work, the cell lines established in chapter 3 were adapted to grow in the presence of increasing concentrations of (Z)-4-OH-tamoxifen, the tamoxifen metabolite generally considered to be the most potent against ER^+ breast cancer cells and the most commonly used to generate tamoxifen-resistant sub-lines with (Gao *et al.*, 2018; Wu *et al.*, 2018). We found this metabolite to be the most active in this study (Fig. 3.22). (Z)-4-OH-tamoxifen-resistant cell lines were established by cultivating them in increasing drug concentrations starting an appropriately selected concentration of (Z)-4-OH-tamoxifen for each cell line and applying 0.5μM increments. Unlike most other studies into acquired tamoxifen resistance in breast cancer cell lines, resistant sub-lines were cultivated in the absence of endogenous oestrogen and phenol red to assess their impact on the generation of resistance. The cell lines were assessed for stability of resistance, oestrogen receptor expression, response to tamoxifen metabolites and a set of anti-cancer agents.

4.2 Results

4.2.1: Generation of resistant cell lines

Figure 4.1 shows the (Z)-4-OH-tamoxifen concentrations that the cell lines were cultured in, starting with the IC_{50} concentration rounded to the nearest 0.5μM (Table 4.1) and applying 0.5μM dose increments over 52 weeks. Concentrations were increased when the cells looked healthy and were growing well. The splitting rate was 3/10, this remained consistent for the entirety of the project. Cells were passaged when they reached ~80% confluency. Cultivation of the MCF-7 sublines grown in media containing charcoal stripped serum did not result in readily growing cell lines, over multiple attempts, which enabled to increase the (Z)-4-OH-tamoxifen concentration. Dose escalation was continued until subsequent increases resulted in loss of viability – at that point, provided resistance was confirmed, the concentration was lowered or maintained until the cells grew happily. Figure 4.1C plots the IC_{50} values obtained at select intervals (as shown in figure 4.1A&B) throughout cell line development.

Cell Line	Initial (Z)-4-OH-tamoxifen concentration used to begin resistant sub-line development (μM)			
	Media Condition			
	+FBS	-FBS	+CS	-CS
MCF7	2.5	1	4.5	3.5
BT-474	0.5	0.5	5.5	3.5
EFM-19	6	3	3.5	4
T47D	3.5	3	3	3
CAMA-1	3.5	4	4	4
MDA-MB-468	3	3.5	3	3

Table 4.1: Concentration of (Z)-4-OH-tamoxifen used to begin establishing drug-resistant sub-lines

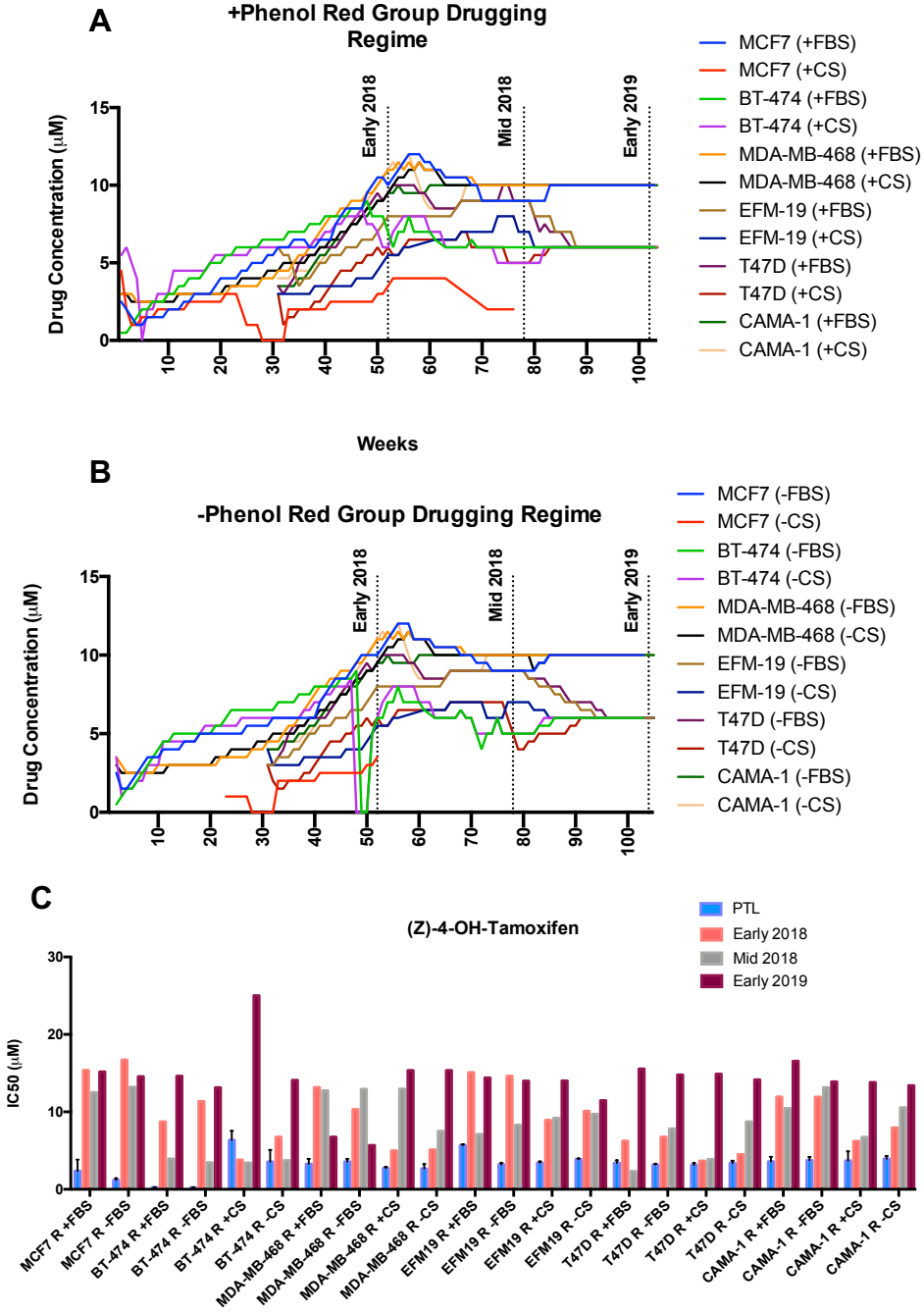


Figure 4.1: Shows the dose-escalation of (Z)-4-OH-tamoxifen used to produce the tamoxifen resistant cell lines used in this works. **A)** dose-escalation regime used for the cell lines grown in the presence of phenol red, including both +FBS and +CS culture medias. Vertical lines indicate the stage of cell-line production that resistance status was determined, and shown in C) **B)** dose-escalation regime for the cell lines grown in conditions devoid of phenol red, also including both -FBS and -CS conditions. Vertical lines indicate the stage of cell-line production that resistance status was determined, and shown in C). **C)** (Z)-4-OH-tamoxifen IC_{50} values of the (Z)-4-OH-tamoxifen resistant sub-lines during different stages of cell-line production compared to their respective parental sub-lines (PTL)

4.2.2: Cell line morphology

Figures 4.2-4.7 show images taken of all resistant sub-lines in the panel of cell lines used in this works. Images were taken using an Olympus CKX52 light microscope with image capture capabilities.

Section 3.2.1 discussed observed changes in morphology in the panel of parental oestrogen-deprived sub-lines – no changes in morphology were seen in the tamoxifen-resistant sub-lines in this chapter compared to these despite cultivation in growth hormone deprived conditions also; the parental BT-474 and EFM-19 cell lines from chapter 3 grew in a more tightly packed 'island like' manner when exposed to growth hormone deprived conditions, forming mounds of cells of greater height that that seen from the other cell lines. This was not seen in the tamoxifen-resistant cell lines generated for this chapter – suggesting that exposure to tamoxifen inhibits the morphological changes that the cell lines exhibit in response to growth hormone inhibition alone. The most notable changes in morphology were observed in the 4-OH-tamoxifen-adapted MCF7 sublines. 4-OH-adapted MCF-7 cells displayed a reduction in cellular height and an increase in cellular diameter, compared to parental MCF-7 cells. 4-OH-tamoxifen adaptation of CAMA-1, T47D, and MDA-MB-468 cells did not substantially change cell morphology.

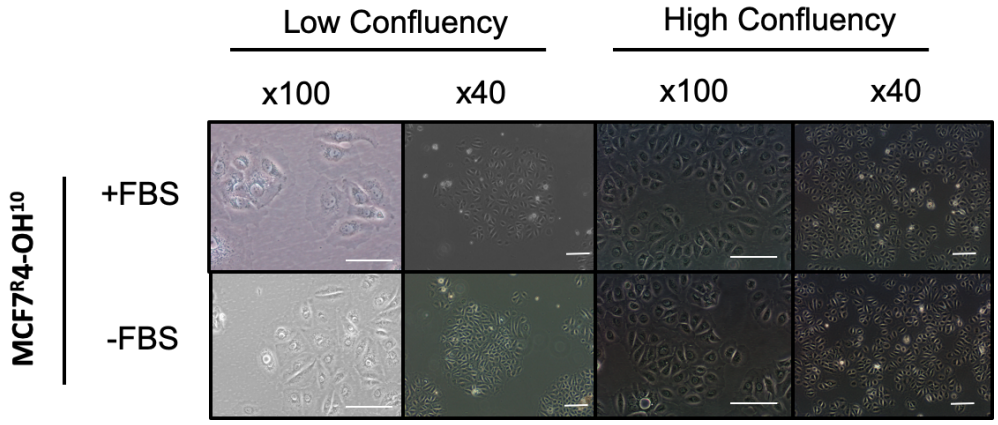


Figure 4.2: Images of the tamoxifen resistant MCF-7 sub-lines. Images were taken at both a low and high confluency to show differences in morphology when spread vastly across the base of culture flasks, and more tightly packed at higher confluences. There are also images at both a lower magnification (x40) and a higher one (x100). **Scale bars are representative of 50 microns.**

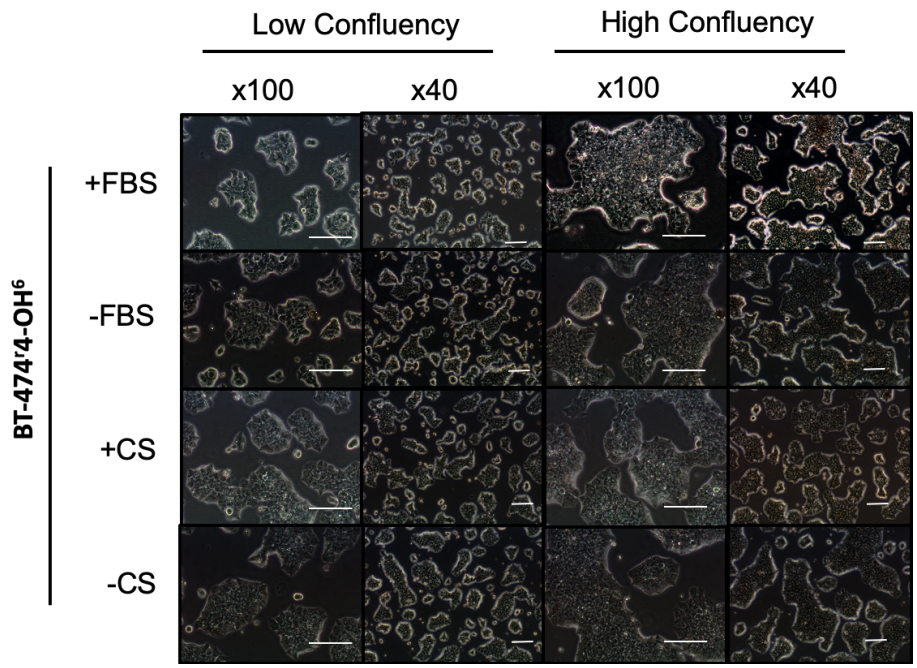


Figure 4.3: Images of the BT-474 (Z)-4-OH-tamoxifen resistant sub-lines. Images were taken at both a low and high confluency to show differences in morphology when spread vastly across the base of culture flasks, and more tightly packed at higher confluences. There are also images at both a lower magnification (x40) and a higher one (x100). **Scale bars are representative of 50 microns.**

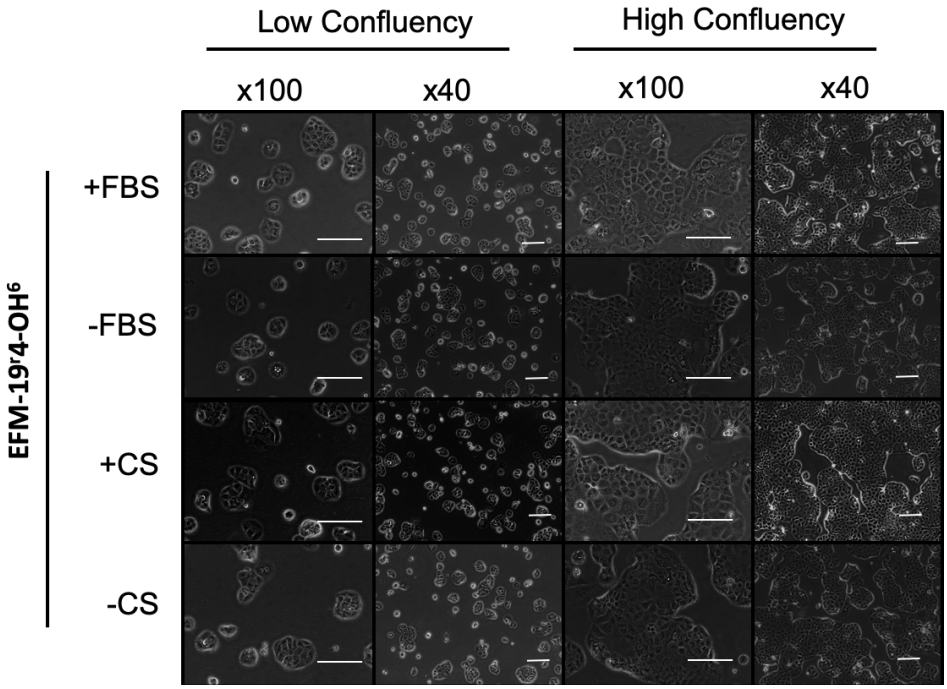


Figure 4.4: Images of the EFM-19 (Z)-4-OH-tamoxifen resistant sub-lines. Images were taken at both a low and high confluency to show differences in morphology when spread vastly across the base of culture flasks, and more tightly packed at higher confluences. There are also images at both a lower magnification (x40) and a higher one (x100). **Scale bars are representative of 50 microns.**

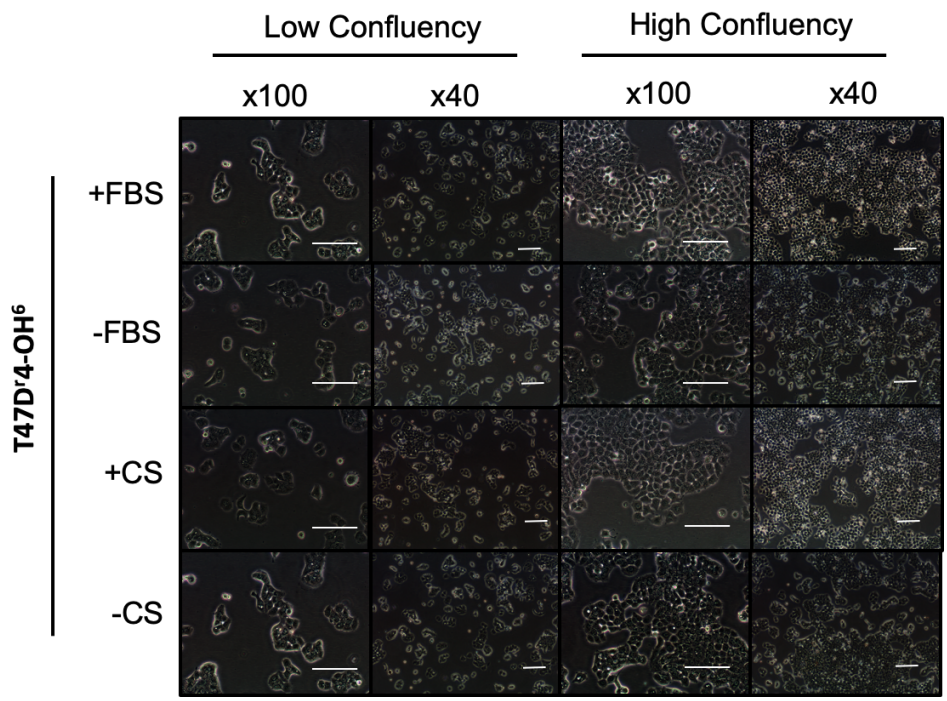


Figure 4.5: Images of T47D (Z)-4-OH-tamoxifen resistant sub-lines. Images were taken at both a low and high confluency to show differences in morphology when spread vastly across the base of culture flasks, and more tightly packed at higher confluences. There are also images at both a lower magnification (x40) and a higher one (x100). **Scale bars are representative of 50 microns.**

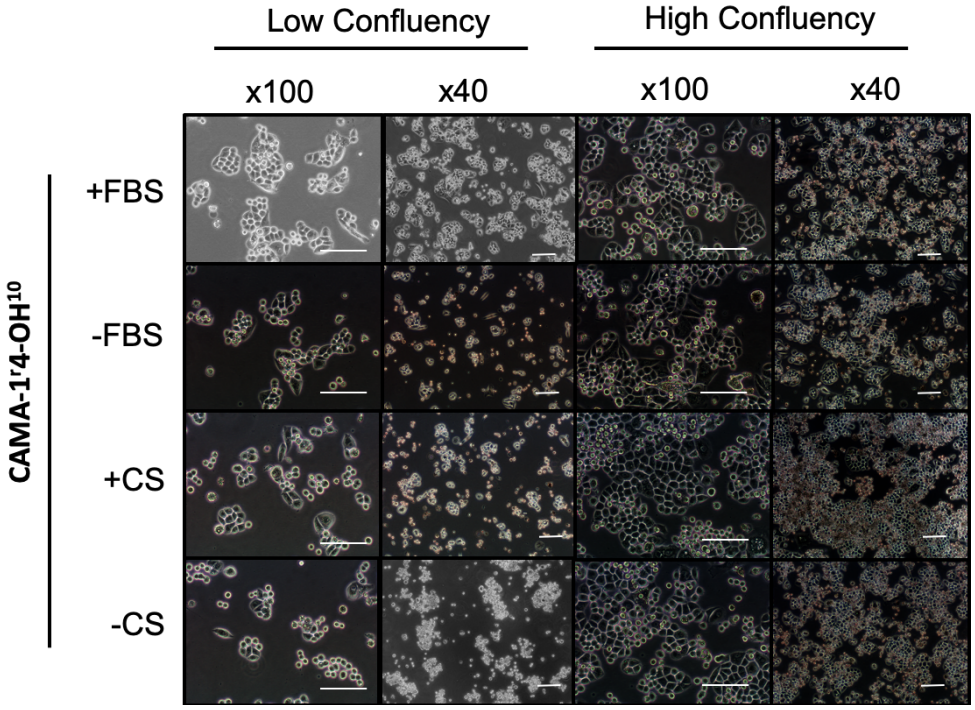


Figure 4.6: Images of CAMA-1 (Z)-4-OH-tamoxifen resistant sub-lines. Images were taken at both a low and high confluency to show differences in morphology when spread vastly across the base of culture flasks, and more tightly packed at higher confluences. There are also images at both a lower magnification (x40) and a higher one (x100). **Scale bars are representative of 50 microns.**

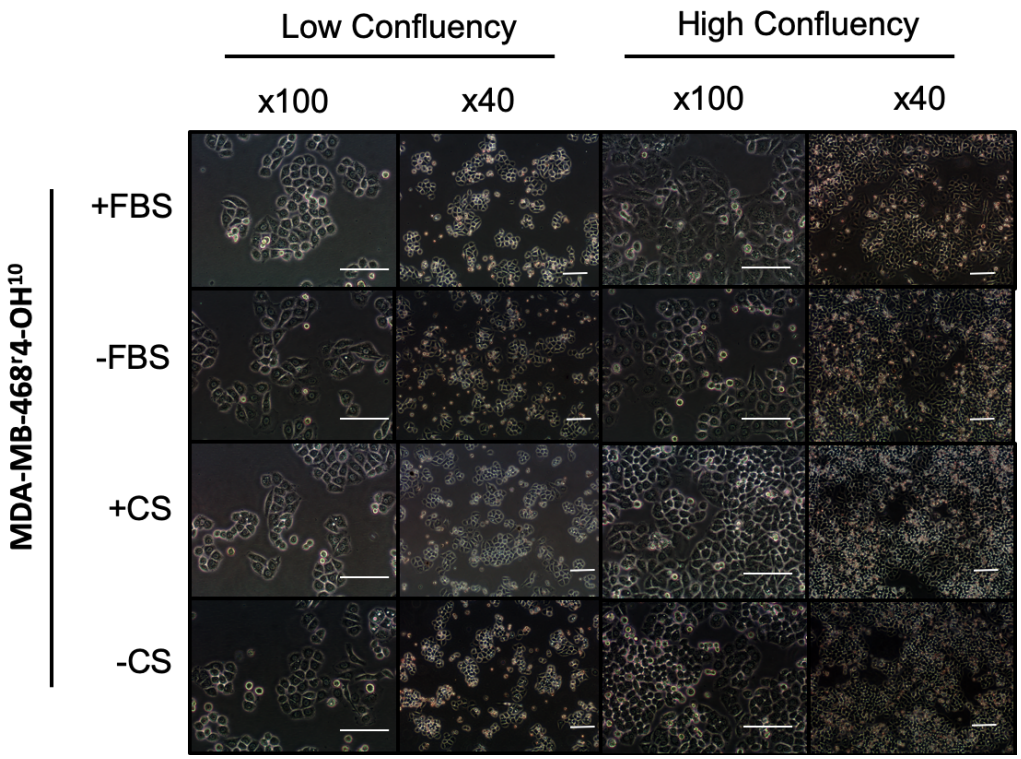


Figure 4.7: Images of MDA-MB-468 (Z)-4-OH-tamoxifen resistant cell lines. Images were taken at both a low and high confluency to show differences in morphology when spread vastly across the base of culture flasks, and more tightly packed at higher confluences. There are also images at both a lower magnification (x40) and a higher one (x100). **Scale bars are representative of 50 microns.**

4.2.3: Growth Kinetics

Once the resistant sub-lines were determined to be resistant to (Z)-4-OH-tamoxifen, their growth was characterised as is described in section 2.2.5. The cells were grown over a period of 6 days, in the presence of (Z)-4-OH-tamoxifen (concentration stated in the sub-line name), with a measure of cell count taken (by electrical impedance) taken every 30 minutes of culture. Cells were seeded as per section 2.2.5, at the same cell density as their parental counterparts in chapter 3. Care was taken to ensure that the cells were not disturbed at all during this time. Figure 4.8 below shows the growth curves generated from this data.

As a comparison between the drug-resistant sub-lines and their respective parental sub-lines in chapter 3; parental sub-lines in the presence of phenol red, and oestrogen (in FBS) grew faster than those deprived of oestrogen – even after adaptation to growth in growth hormone-deprived media over time (Fig 3.7 & 3.8). When looking at the drug-resistant cell lines in this chapter, a number of the oestrogen-deprived sub-lines grow faster than those in the presence of oestrogen – which is the opposite trend to that seen in their parental counterpart cell lines). This can be seen by the growth curves and doubling times in figures of 3.8 and 4.8, and 3.9 and 4.9 respectively. In a clinical setting, this *in vitro* finding may highlight differences between treatment with tamoxifen and aromatase inhibitors as cell lines that have been adapted to growth in the presence of reduced levels of growth hormone exhibit a slower rate of proliferation compared to those that are both growth hormone deprived and tamoxifen resistant. Serum starvation has been previously shown to reduce cellular proliferation in breast cancer cell lines, but nothing thus far has been reported on the affect that serum starvation has on cellular proliferation when coupled with resistance to tamoxifen (Nakhjavani, Stewart and Shirazi, 2017). Phenol red only appears to make a notable difference to the BT-474^{R+CS}4-OH^{6} sub-line, perhaps suggesting that the reduced oestrogenic stimulation that phenol red only provides is beneficial for this cell line.

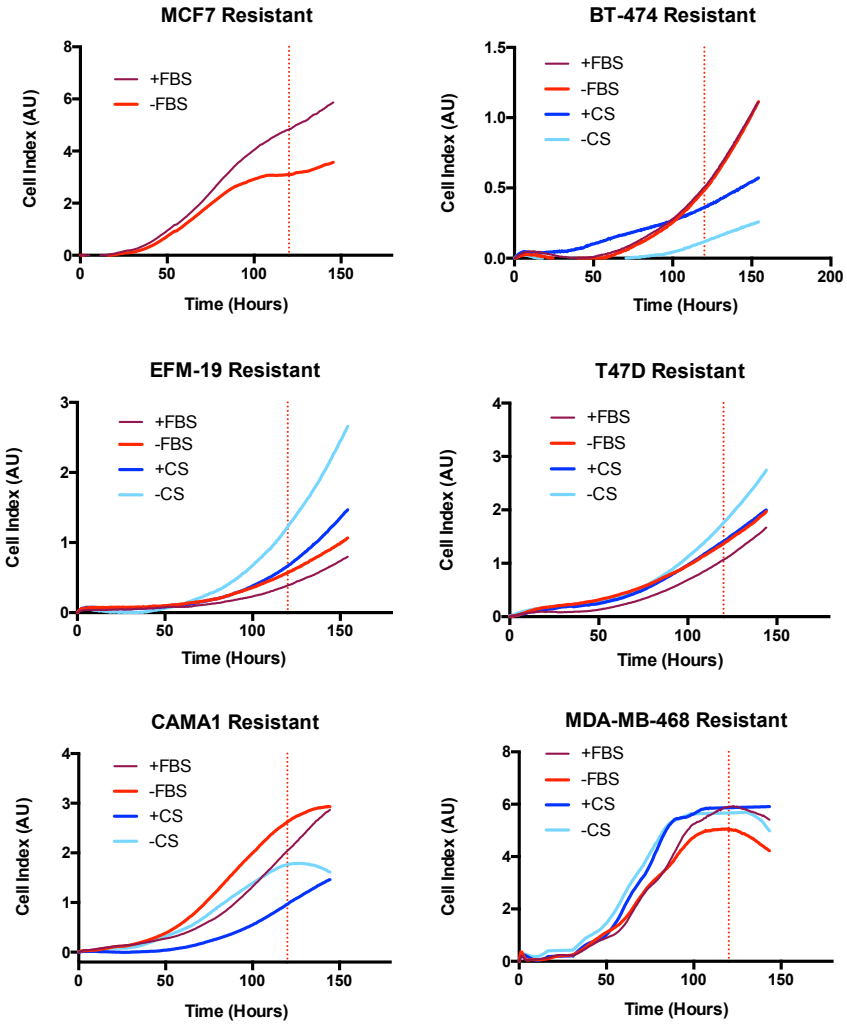


Figure 4.8: Growth curves of all of the (Z)-4-OH-tamoxifen resistant cell lines generated. Each cell line was grown for 6 days, and cell density was measured using electrical impedance every 30 minutes for that length of time. Cells were grown in the presence of (Z)-4-OH-tamoxifen (MCF7, CAMA-1 and MDA-MB-468 in 10μM, BT-474, EFM-19 and T47D in 6 μM. These concentrations are equal to standard culture conditions). Graphs are colour coded for the type of culture media they were grown in as noted in the key. All cell lines were seeded as per section 2.2.5).

Figure 4.9 below, accompanied by table 4.2, depict and state the doubling times of these resistant sub-lines as calculated from linear growth phase of the growth curves in figure 4.8.

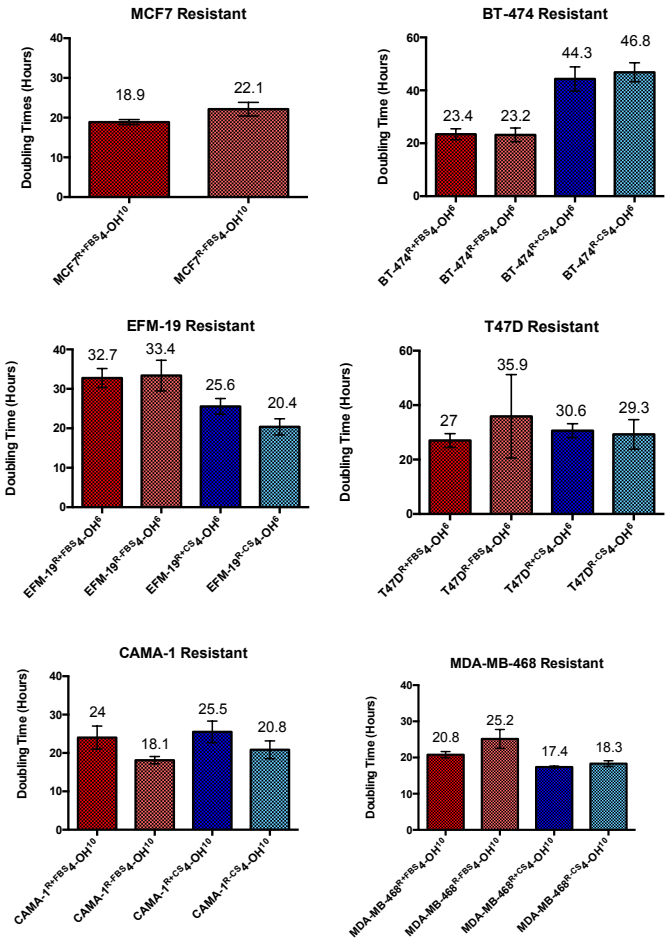


Figure 4.9: Doubling times for all of the (Z)-4-OH-tamoxifen resistant sub-lines. The graph is colour-coded to represent the media type that each cell line was grown in. Data points are representative of n=4 repeats. Error bars are representative of +/-SD. Doubling times were calculated as per section 2.2.5.

	Doubling time in hours (+/- SD)			
Cell Line	**+FBS**	**-FBS**	**+CS**	**-CS**
MCF7^{R}	18.9 (+/- 0.63)	22.1 (+/- 1.7)	N/A	N/A
BT-474^{R}	23.4 (+/- 2.04)	23.2 (+/- 2.60)	44.3 (+/- 4.58)	46.8 (+/- 3.57)
EFM-19^{R}	32.7 (+/-2.39)	33.4 (+/-3.88)	25.56 (+/-1.98)	20.37 (+/-2.06)
T47D^{R}	27.01 (+/- 2.52)	35.9 (+/-15.32)	30.6 (+/-2.56)	29.3 (+/-5.43)
CAMA-1^{R}	24.0 (+/- 3.00)	18.1 (+/-0.95)	25.5 (+/-2.82)	20.8 (+/-2.31)
MDA-MB-468^{R}	20.8 (+/-0.87)	25.2 (+/-2.60)	17.4 (+/-0.25)	18.3 (+/-0.80)

Table 4.2: Doubling times of each resistant sub-line, organised by originating parental cell line, and the media condition in which it was developed in. Each value is the average of n=4, the standard deviation of which accompanies the value in brackets.

4.2.4: Response to tamoxifen and tamoxifen metabolites

In chapter 3, the effect of oestrogen deprivation was examined on the counterpart parental cell lines of the tamoxifen resistant sub-lines in this chapter. There, it was explained that the majority of anti-cancer effects in response to tamoxifen treatment are thought to be elicited through primary tamoxifen metabolites which have a greater potency than unmetabolised tamoxifen (Helland *et al.*, 2017); these same metabolites have been used to assess cellular response in the advent of acquired tamoxifen resistance in order to compare responses to our model of aromatase inhibitor resistance. This also allows us to speculate on the use of tamoxifen as a second-line therapy after potential aromatase inhibitor failure in the clinic – as has been discussed in literature previously (Dowsett *et al.*, 2010). MTT viability assays were used to assess response to tamoxifen, (Z)-4-OH-tamoxifen, alpha-hydroxytamoxifen, endoxifen and n-desmethyltamoxifen. This was also to provide data to elucidate whether acquired resistance to (Z)-4-OH-tamoxifen (the previously identified most potent metabolite from chapter 3; see figure 3.23), also conferred resistance to the other metabolites, or perhaps if they became more susceptible to reductions in cell viability from these other metabolites as a result of this. Changes in response to acquired tamoxifen resistance as a result of hormone deprivation could also carry clinical significance for the use of tamoxifen as a second-line therapy in the advent of endocrine resistance.

IC_{50} values for tamoxifen and the four most abundant tamoxifen metabolites were compared to the IC_{50} values of the respective parental cell lines. In the appendix, (appendix I-VII) the IC_{50} values for other points in time during the development of the resistant cell lines can be found.

Figures 4.1 and 4.10 show us that all cell lines and sub-lines, apart from EFM-19^{R+FBS}4-OH^{6} and EFM-19^{R-FBS}4-OH^{6} became resistant to (Z)-4-OH-tamoxifen over the time-course of cell line production. There were no notable differences between the cell lines generated in the presence of growth hormone, and those generated in the absence of oestrogen, apart from those of BT-474^{-CS} (figure 4.10). It was shown in fig 3.23, in the aromatase inhibitor resistance model, that response to (Z)-OH-tamoxifen is not affected by growth hormone deprivation in the majority of cases. Here, in figure 4.10 (below), we see the same effect, just with reduced sensitivity to (Z)-4-OH-tamoxifen across the panel of 22 sublines.

When looking at figures 4.11-4.15 (tamoxifen and all of the four metabolites analysed), with regards to response to the other metabolites, resistance to (Z)-4-OH-tamoxifen also instigates cross-resistance to tamoxifen, and slightly less so to n-desmethyltamoxifen. The effects of these metabolites will be discussed individually. Which highlights that resistance to one metabolite of tamoxifen does not necessarily confirm resistance to the others as this is not seen with response to endoxifen. Cross-resistance to endoxifen and alpha-hydroxytamoxifen was not as common in the panel of cell lines as to n-desmethyltamoxifen (only present in one cell line, MDA-MB-468^{R+FBS}4-OH^{10}, for alpha-hydroxytamoxifen). Cross-resistance to n-desmethyltamoxifen was the only metabolite that seemed to show preference to cell lines that had been grown in the absence of oestrogen (those in either +CS or -CS media).

When all six 4-OH resistant cell lines are grouped into media conditions, the average (Z)-4-OH-tamoxifen IC_{50} values are as follows (in μM): +FBS: 6.22 ± 1.38, -FBS: 6.12 ± 1.26, +CS: 5.59 ± 1.20, -CS: 6.43 ± 0.92. The parental counterparts: +FBS: 2.99 ±1.79, -FBS: 2.53 ± 1.50, +CS: 3.83 ± 1.00, -CS: 3.42 ± 3.42. The average fold changes are as follows: +FBS 2.1 ± 0.79 , -FBS: 3.1 ± 1.1 , +CS: 2.23 ± 0.46 , -CS: 3.1 ± 0.47 .

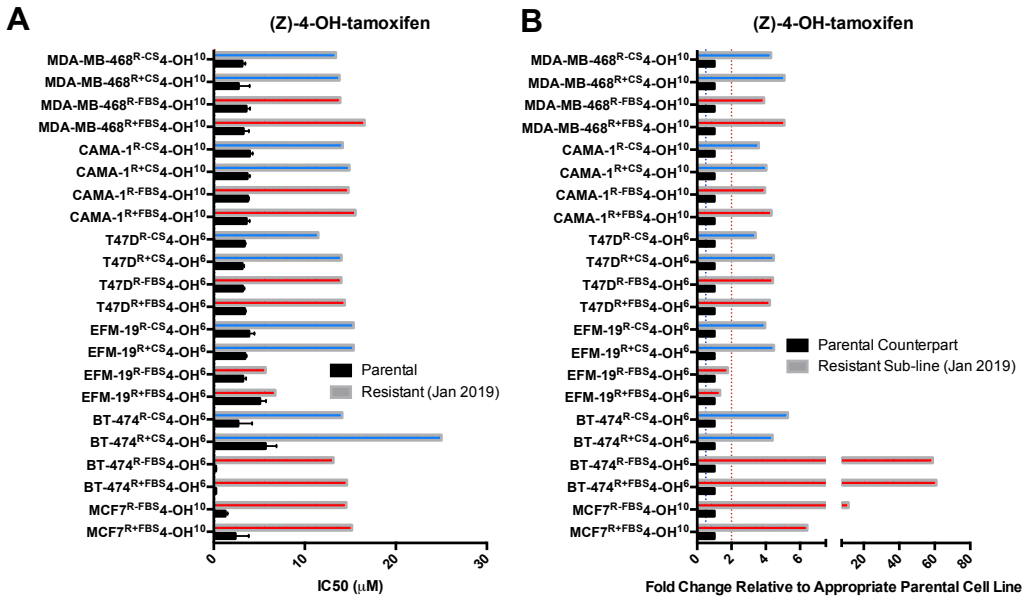


Figure 4.10**: (A)** (Z)-4-OH-tamoxifen IC_{50} values experimentally obtained from the originating parental cell lines (n=3, mean +/-SD) and the tamoxifen-resistant sub-lines generated in this chapter (n=1, as this is reprehensive of the most recent IC_{50} data only), indicated on the y-axis of the graphs. The graph is colour coded for the cell line that the data is related to. Blue coloured bar = resistant sub-line generated in conditions containing charcoal-stripped FBS, Red coloured bar = resistant sub-line generated in conditions containing FBS. **(B)** Fold change values obtained from (A) that have been calculated relative to the control parental from that particular cell line (coloured in black, and equal to 1). Horizontal blue line marks when x=0.5, whilst horizontal red line marks where x=2. A value below 0.5 indicates sensitivity to the compound, whereas a value above 2 indicates resistance. Bars are coloured to reflect this – blue = sensitive.

18/20 of the (Z)-4-OH-tamoxifen resistant cell lines showed cross resistance to tamoxifen (fig. 4.11). Here we evaluate cross-resistance by a fold change value greater than 2. This is the compound that has the greatest number of (Z)-4-OH-tamoxifen-resistant sublines to show cross-resistance to. This is the strongest trend that can be taken from the data in this section. In section 3, it was shown that although tamoxifen is thought to have a vastly reduced potency compared to its 'active' metabolites (Chang, 2012), cell viability data shows that it has an active concentration range relatively similar to these metabolites that are thought to be more active. This is also likely either explained by underestimated similarities in binding efficacies or due to metabolic conversion of tamoxifen within the breast cancer cells themselves. They are known to express low levels of the CYP450s that are responsible for these conversions (Mitra *et al.*, 2011). This same trend can be seen between cellular responses to tamoxifen and (Z)-4-OH-tamoxifen in the 4-OH resistant sublines, indicating that although the 4-OH resistant sublines show reduced sensitivity to (Z)-OH-tamoxifen compared to the parental lines, it does not affect the trend in relationship between response to tamoxifen and (Z)-

4-OH-tamoxifen. As a large degree of cross-resistance is seen between these two compounds, and not with the other tamoxifen metabolites (fig 4.12, 13 &14). Figure 1.8, and Cronin-Fenton, Damkier and Lash, (2014) describes the CYP450 enzymes involved in metabolism of tamoxifen. Tamoxifen can be metabolised to either N-desmethyltamoxifen (largely by CYP3A4) or 4-OH-tamoxifen (largely by CYP2D6) first. Then, both of these compounds are converted into endoxifen. Perhaps this relationship between cellular response to tamoxifen and (Z)-OH-tamoxifen may be due to naturally higher levels of CYP2D6 in the cell lines.

Fig 3.22 (tamoxifen IC50s) from the previous chapter chow all IC_{50} values for the MCF7 cell line to be comparatively higher than the other cell line groups (perhaps showing some intrinsic resistance – oestrogen deprivation had no effect on this). Both MCF7 (Z)-4-OH-tamoxifen resistant sublines do not have a fold change >2 compared to their parental cell lines, therefore are not considered cross-resistant by adaptation to growth in the presence of (Z)-4-OH-tamoxifen. Fig 3.22 also shows the CAMA-1^{-FBS}, CAMA-1^{+CS} and CAMA-1^{-cs} sublines to show sensitivity to tamoxifen (FC<0.5), but in the 4-OH adapted sublines they are the only subline in the group to show cross-resistance to tamoxifen (FC>2) – showing a reversal in response due to drug resistance.

When all six 4-OH resistant cell lines are grouped into media conditions, the average tamoxifen IC_{50} values are as follows (in μM): +FBS: 6.22 ± 1.38, -FBS: 6.12 ± 1.25, +CS: 5.59 ± 1.20, -CS: 6.44 ± 0.92. Parental counterparts: +FBS: 3.6 ± 2.22, -FBS: 2.7 ± 2.20, +CS: 3.3 ± 1.86, -CS: 2.9 ± 2.02. The average fold changes are as follows: +FBS 1.2 ± 0.5, -FBS: 1.36 ± 0.23 , +CS: 1.2 ± 0.26 , -CS: 1.3 ± 0.2.

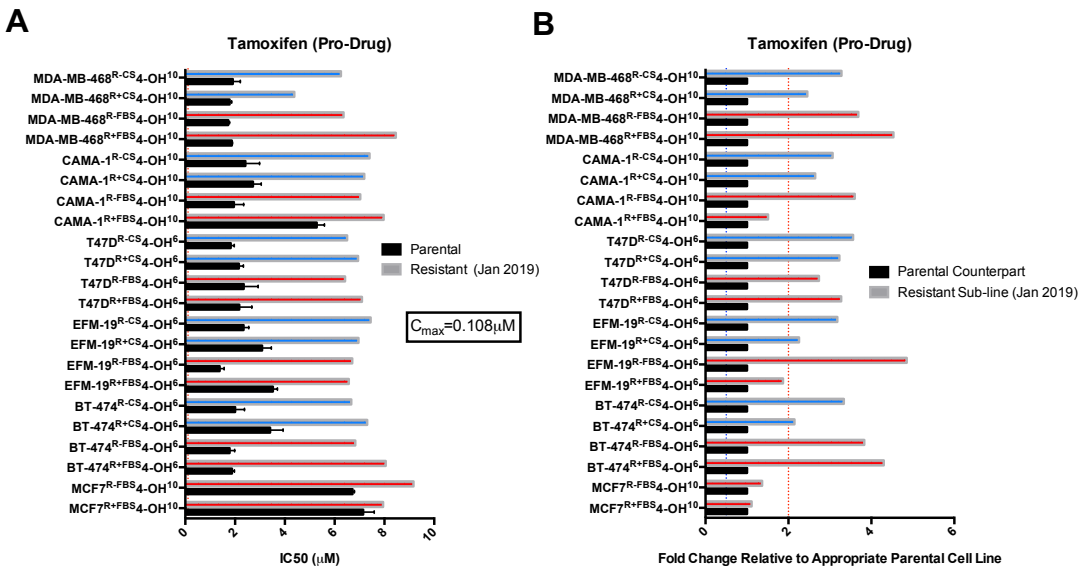


Figure 4.11**: (A)** Tamoxifen IC_{50} values experimentally obtained from the originating parental cell lines (n=3 +/-SD) and the tamoxifen-resistant sub-lines generated in this chapter (n=1, as this is reprehensive of the most recent IC_{50} data only), indicated on the y-axis of the graphs. The graph is colour coded for the cell line that the data is related to. Blue coloured bar = resistant sub-line generated in conditions containing charcoal-stripped FBS, Red coloured bar = resistant sub-line generated in conditions containing FBS. **(B)** Fold change values obtained from (A) that have been calculated relative to the control parental from that particular cell line (coloured in black, and equal to 1). Horizontal blue line marks when x=0.5, whilst horizontal red line marks where x=2. A value below 0.5 indicates sensitivity to the compound, whereas a value above 2 indicates resistance. Bars are coloured to reflect this – blue = sensitive.

Only 3/22 sublines showed cross-resistance to alpha-hydroxytamoxifen (MDA-MB-468^{R+FBS}4-OH^{10,} MCF7^{R+FBS}4-OH^{10} and MCF7^{R-FBS}4-OH^{10}; fig. 4.12). The MCF7^{R-FBS}4-OH^{10} subline also shares this increased IC_{50} value over the time course of resistance development (see appendix II), so this result is not an anomaly. As discussed in chapter 3, this metabolite presents the highest IC_{50} values of all the metabolites assessed.

When all six 4-OH resistant cell lines are grouped into media conditions, the average tamoxifen IC_{50} values are as follows (in μM): +FBS: 39.75 ± 7.96, -FBS: 45.33 ± 14.9, +CS: 42.7 ± 6.7, -CS: 33.02 ± 4.28. Parental values are as follows: +FBS: 38.35 ±3.18, -FBS: 38.25 ± 3.5, +CS: 35.36 ±1.45, -CS: 33.27 ± 3.77. This shows little difference in response to alpha-hydroxytamoxifen, regardless of resistance to (Z)-4-OH-tamoxifen. Slight differences in fold change that can be seen in fig 4.12B are cell line specific (BT-474 and T47D), media conditions do not seem to affect this. The average fold changes are as follows: +FBS 1.6 ± 0.32, -FBS: 1.31 ± 0.19 , +CS: 1.76 ± 0.4, -CS: 1.41 ± 0.29.

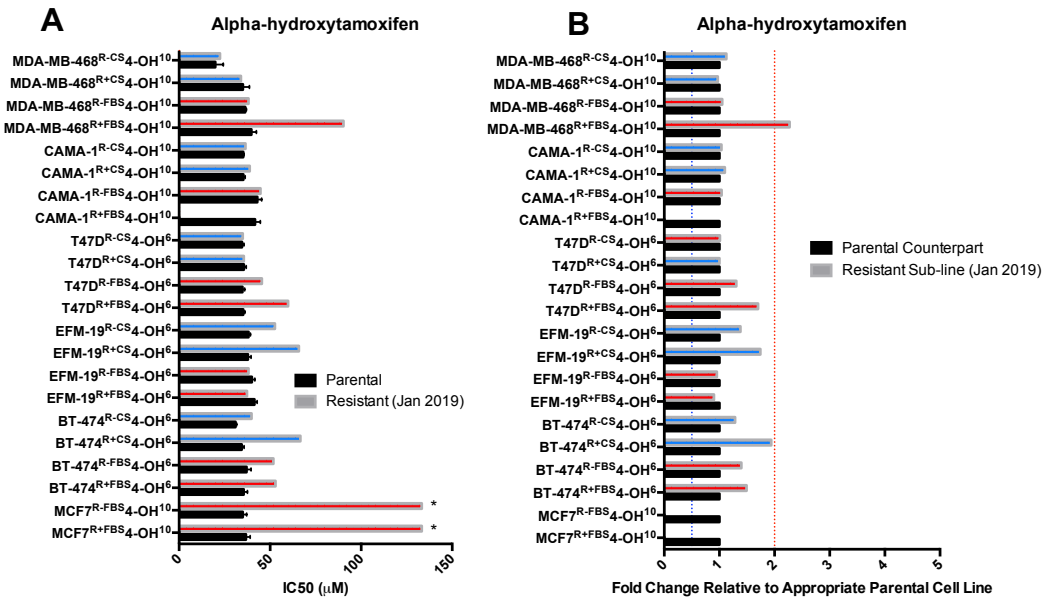


Figure 4.12**: (A)** Alpha-hydroxytamoxifen IC_{50} values experimentally obtained from the originating parental cell lines (black; n=3 +/-SD) and the tamoxifen-resistant sub-lines generated in this chapter (n=1, as this is reprehensive of the most recent IC_{50} data only), indicated on the y-axis of the graphs. The graph is colour coded for the cell line that the data is related to. Blue coloured bar = resistant sub-line generated in conditions containing charcoal-stripped FBS, Red coloured bar = resistant sub-line generated in conditions containing FBS. Asterix* marks data points that went above the maximum drug dilution of the viability assay **(B)** Fold change values obtained from (A) that have been calculated relative to the control parental from that particular cell line (coloured in black, and equal to 1). Horizontal blue line marks when x=0.5, whilst horizontal red line marks where x=2. A value below 0.5 indicates sensitivity to the compound, whereas a value above 2 indicates resistance. Bars are coloured to reflect this – blue = sensitive.

The comparable data for endoxifen in chapter 3 (Fig. 3.25) displays only two cell lines to show decreased sensitivity to endoxifen T47D^{-CS} and T47D^{-FBS}. These two cell lines also show decreased sensitivity to endoxifen in their tamoxifen-resistant counterparts (FC>2) – given this was seen as a result of the change in growth conditions in the previous chapter, it is likely also due to media condition adapted to, rather than drug exposure, in the context of tamoxifen-resistance. In light of this, 3/22 4-OH sublines were cross-resistant to endoxifen (MDA-MB-468R^{-CS}4-OH^{10}, MDA-MB-468^{R+CS}4-OH^{10}, MDA-MB-468^{R+FBS}4-OH^{10}).

When all six 4-OH resistant cell lines are grouped into media conditions, the average endoxifen IC_{50} values are as follows (in μM): +FBS: 7.42 ± 0.72, -FBS: 9.95 ± 0.56, +CS: 9.17 ± 1.71, -CS: 8.61 ± 1.42. Parental lines are: 7.15 ± 3.28, -FBS: 8.10 ± 2.22, +CS: 7.40 ± 2.1, -CS: 7.16 ± 0.93. The average fold changes are as follows: +FBS 1.26 ± 0.14 , -FBS: 1.48 ± 0.32, +CS: 2.5 ± 0.66, -CS: 2.7 ± 0.61.

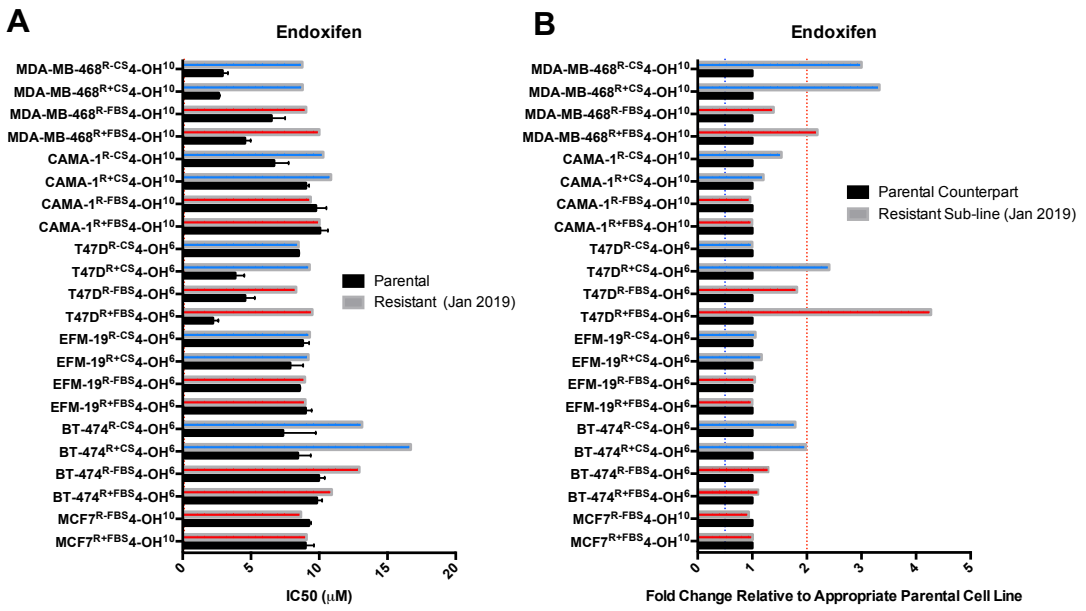


Figure 4.13: **(A)** Endoxifen IC_{50} values experimentally obtained from the originating parental cell lines (n=3 +/-SD) and the tamoxifen-resistant sub-lines generated in this chapter (n=1, as this is reprehensive of the most recent IC_{50} data only), indicated on the y-axis of the graphs. The graph is colour coded for the cell line that the data is related to. Blue coloured bar = resistant sub-line generated in conditions containing charcoal-stripped FBS, Red coloured bar = resistant sub-line generated in conditions containing FBS. **(B)** Fold change values obtained from (A) that have been calculated relative to the control parental from that particular cell line (coloured in black, and equal to 1). Horizontal blue line marks when x=0.5, whilst horizontal red line marks where x=2. A value below 0.5 indicates sensitivity to the compound, whereas a value above 2 indicates resistance. Bars are coloured to reflect this – blue = sensitive.

Before response to the final metabolite is discussed, the directionality or order of metabolism to form these compounds from the parental drug should be reiterated; dependent on the most prevalent CYP450 to facilitate transformation, n-desmethyltamoxifen and (Z)-4-OH-tamoxifen are separately produced, which are both later converted to endoxifen by second pass metabolism (Cronin-Fenton, Damkier and Lash, 2014). It is interesting to consider the effects of these two former compounds compared to the later for this reason. It is not clear from literature how long these individual compounds are bioavailable for, but much emphasis is placed on serum concentrations of endoxifen for treatment success (Ahmad *et al.*, 2010; Helland *et al.*, 2017). Fig 4.14 shows us that far more cell lines are cross-resistant to n-desmethyltamoxifen (10/22) than to endoxifen (3/22) in the advent of resistance to (Z)-4-OH-tamoxifen. Furthermore, in chapter 3 we saw that n-desmethyltamoxifen was the only metabolite to show trend in difference in response across many of the sublines used (that was influenced by growth hormone deprivation) – compared to the rather more heterogeneous

response seen with the other compounds. This is an interesting observation as this trend appears to be reversed by the addition of adaptation to growth in the presence of (Z)-4-OH-tamoxifen as the same hormone deprived parental sublines that showed increased sensitivity to n-desmethyltamoxifen in chapter 3 (fig 3.26B, can also be seen in fig 4.14B), present with a decreased sensitivity to this compound in these conditions here (fig 4.14). This presents the question, would n-desmethyltamoxifen be a successful treatment option in postmenopausal women that would mimic the same conditions that our AI adapted model does initially?

When all six 4-OH resistant cell lines are grouped into media conditions, the average n-desmethyltamoxifen IC_{50} values are as follows (in μM): +FBS: 8.61 ± 0.96, -FBS: 8.39 ± 1.38, +CS: 7.92 ± 1.76, -CS: 8.2 ± 1.46. Parental lines are: +FBS: 7.65 ± 0.96, -FBS: 7.02 ± 2.05, +CS: 6.71 ± 2.22, -CS: 3.99 ± 2.67. The only apparent difference with these figures is the switch from increased sensitivity of the parental cell lines to n-desmethyltamoxifen in our model for resistance to AIs, to a more consistent response across all levels of oestrogenic stimulation in our model for tamoxifen resistance. The average fold changes are as follows: +FBS 0.84 ± 0.34 , -FBS: 0.66 ± 0.38 , +CS: 3.4 ± 2.66 , -CS: 2.43 ± 1.59 .

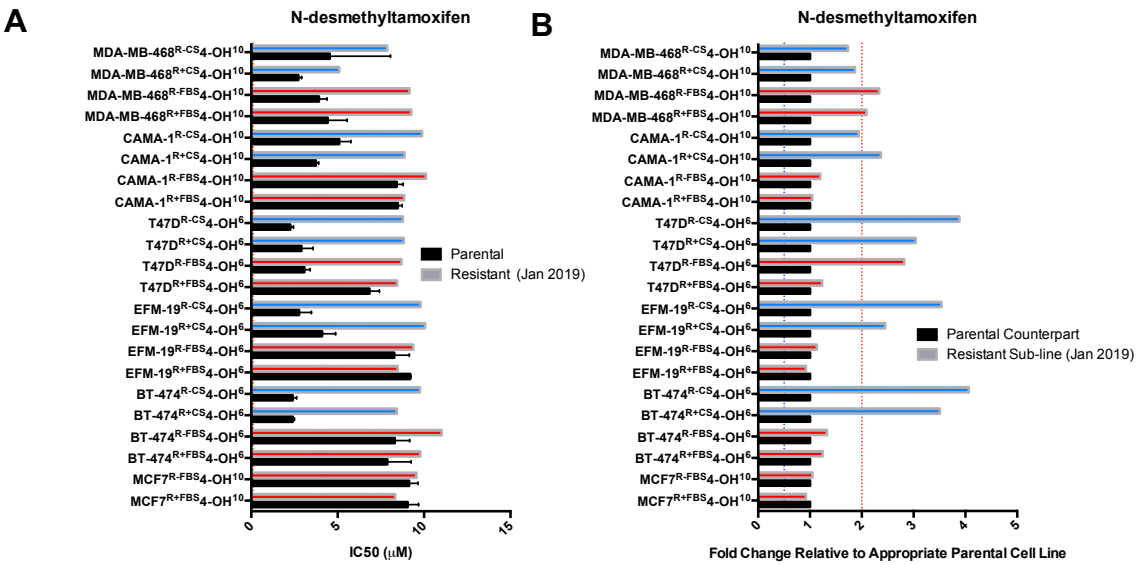


Figure 4.14**: (A)** N-desmethyltamoxifen IC_{50} values experimentally obtained from the originating parental cell lines (n=3 +/-SD) and the tamoxifen-resistant sub-lines generated in this chapter (n=1, as this is reprehensive of the most recent IC_{50} data only), indicated on the y-axis of the graphs. The graph is colour coded for the cell line that the data is related to. Blue coloured bar = resistant sub-line generated in conditions containing charcoal-stripped FBS, Red coloured bar = resistant sub-line generated in conditions containing FBS. **(B)** Fold change values obtained from (A) that have been calculated relative to the control parental from that particular cell line (coloured in black, and equal to 1). Horizontal blue line marks when x=0.5, whilst horizontal red line marks where x=2. A value below 0.5 indicates sensitivity to the compound, whereas a value above 2 indicates resistance. Bars are coloured to reflect this – blue = sensitive.

4.2.5: Qualitative evaluation of ERα and ERβ expression in tamoxifen-resistant sub-lines

The immunofluorescence images in figures 4.15-4.20 show varying localities of both oestrogen receptor isoforms across the 6 originating cell lines. As a generalisation, there does not appear to be any obvious trend between media type cultivated in and locality of the two receptors – the locality of the receptors appears to be cell-line specific, but trends can be seen within the individual sets of cell lines. The table below contains a summary of the conclusions that can be made from the observed locations of the oestrogen receptors.

Table 4.3 summarises the observations that can be made from figure 4.15-4.20.

Figure	Cell Line	Observation
4.15	MCF7^{R}4-OH^{10}	ERβ in punctate spots within the nucleus in -FBS only, generally clustered around the nucleus in both media conditions otherwise in similar location to endoplasmic reticulum within the cell. No nuclear localisation for ERα in either. Overlay looks generally red for predominant ERα expression.
4.16	BT-474 ^{R}4-OH^{6}	+FBS/-FBS look very similar for ERα, no nuclear localisation, generally clustered on the cell membrane. All sub-lines have no obvious nuclear localisation for ERβ, mostly cytoplasmic localisation. Overlay looks generally green, for predominant ERβ expression.
4.17	EFM-19 ^{R}4-OH^{6}	Only nuclear localisation for -CS condition for both ERα and ERβ. +FBS image is a good example of how the population of cells is polyclonal, two of the cells have lower expression than a neighbouring two for both ERs. Mainly cytoplasmic localisation for all cell lines, not obvious membrane localisation.
4.18	T47D ^{R}4-OH^{6}	Nuclear localisation for both ERs in +CS/-CS conditions only. Mainly cytoplasmic locality for all conditions. Overlay is generally red for predominant ERα expression.

4.19	CAMA-1^{R}4-OH^{10}	Mainly nuclear localisation for all cell lines, some membrane localisation. This cell line showed relatively little cytoplasmic localisation compared to the other cell line groups. Overlay is predominantly green for ERβ expression preference.
4.20	MDA-MB-468^{R}4-OH^{10}	More nuclear localisation in +FBS/-FBS conditions. Localisation is mainly cytoplasmic. Overlay images are predominantly red for ERα expression.

Table 4.3: Comments on observations made on oestrogen receptor locality from immunofluorescence images of the tamoxifen-resistant sub-lines and the effect of growth in oestrogen-deprived conditions on this.

Although all parameters of the confocal microscope used to capture the immunofluorescence images were kept constant, such as laser power, magnification (as this would affect the area of the cell used to calculate the intensity of it relative to its size) and post-imaging processing, expression of ERα and ERβ shouldn't be compared directly. The antibodies used for the experimental procedure are not equal in single molecule florescence intensity when stimulated by the lasers of the confocal microscope. This was unfortunately unavoidable. The changes between individual ER isoform expression however, can be commented on.

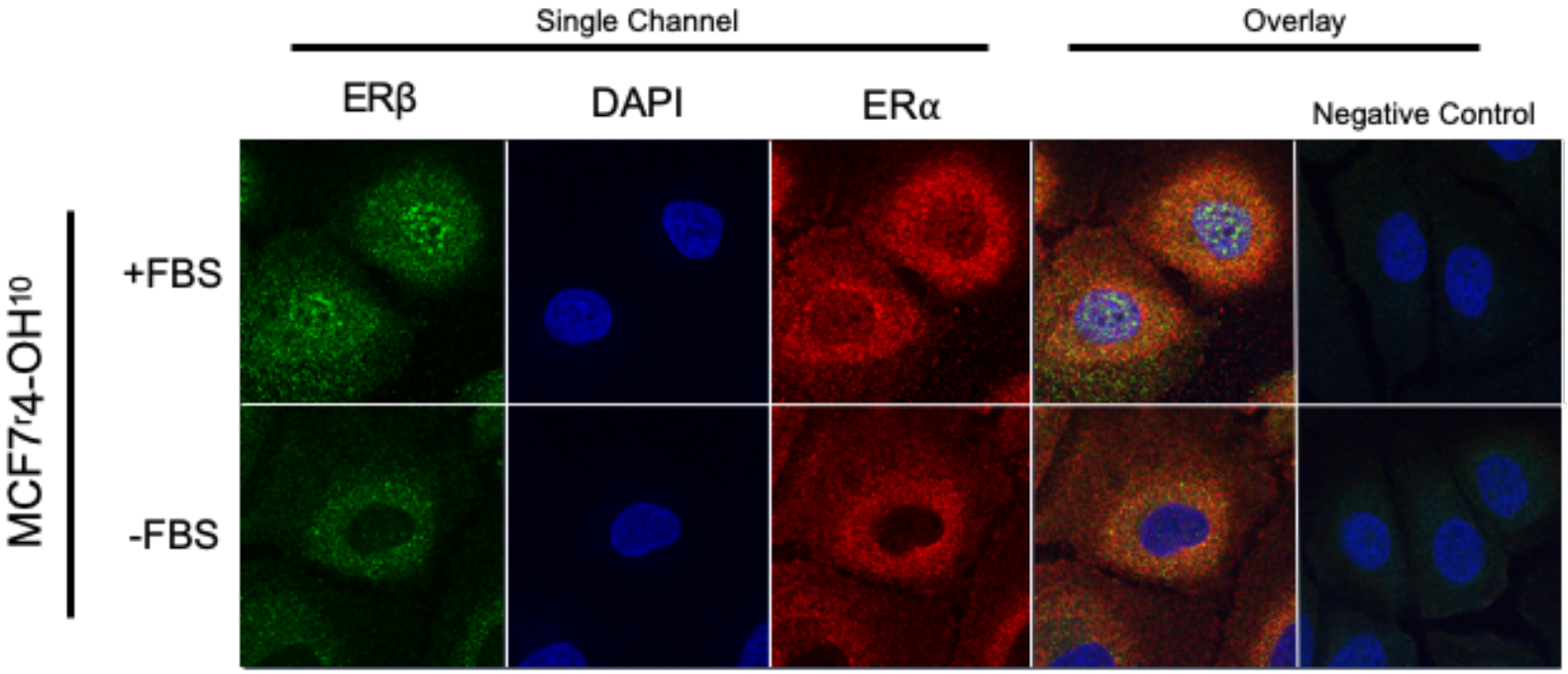


Figure 4.15: Representative immunofluorescence images of an N=6 images of the MCF-7r4-OH tamoxifen-resistant cell line and all phenol red/growth hormone deprived sub-lines as indicated by the labelling on the left hand side of the figure. Lanes are divided into single channels and labelled appropriately. **RED - ERα, GREEN - ERβ, BLUE – DAPI/nucleic acids.**

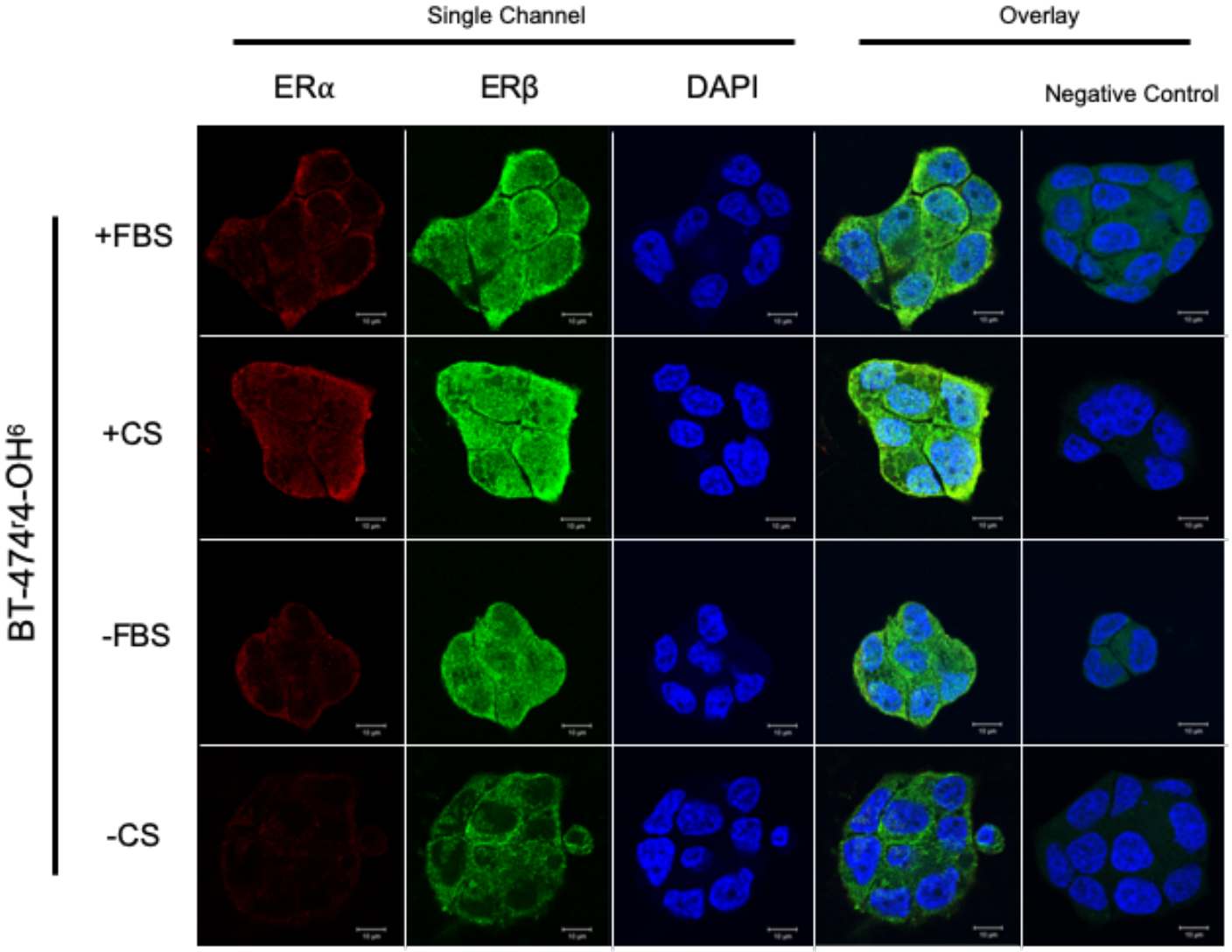


Figure 4.16: Representative immunofluorescence images of an N=6 images of the BT-474r4-OH tamoxifen-resistant cell line and all phenol red/growth hormone deprived sub-lines as indicated by the labelling on the left hand side of the figure. Lanes are divided into single channels and labelled appropriately. **RED - ERα, GREEN - ERβ, BLUE – DAPI/nucleic acids.**

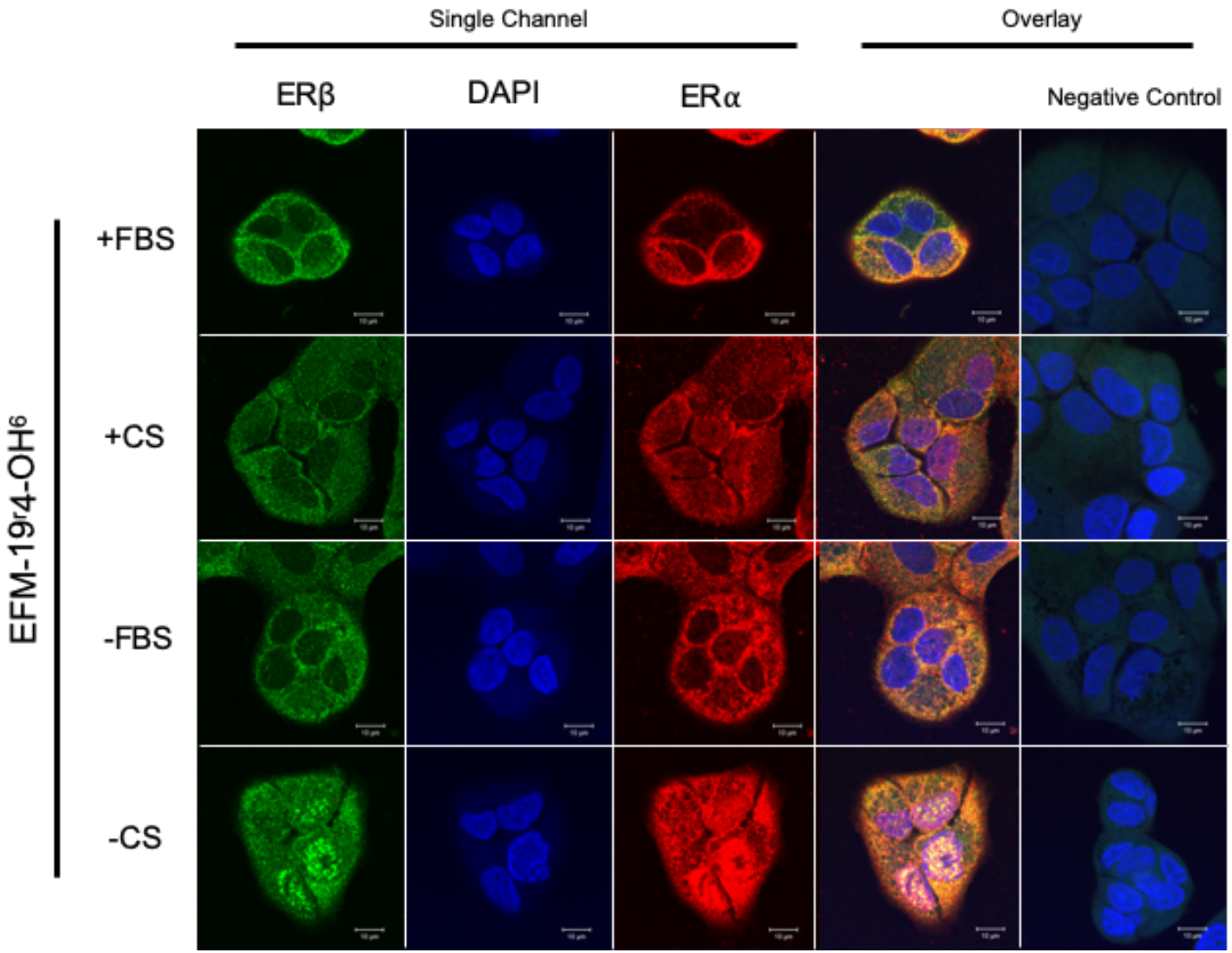


Figure 4.17: Representative immunofluorescence images of an N=6 images of the EFM-19^{r}4-OH tamoxifen-resistant cell line and all phenol red/growth hormone deprived sub-lines as indicated by the labelling on the left hand side of the figure. Lanes are divided into single channels and labelled appropriately. **RED - ERα, GREEN - ERβ, BLUE – DAPI/nucleic acids. Scale bar is representative of 10 microns.**

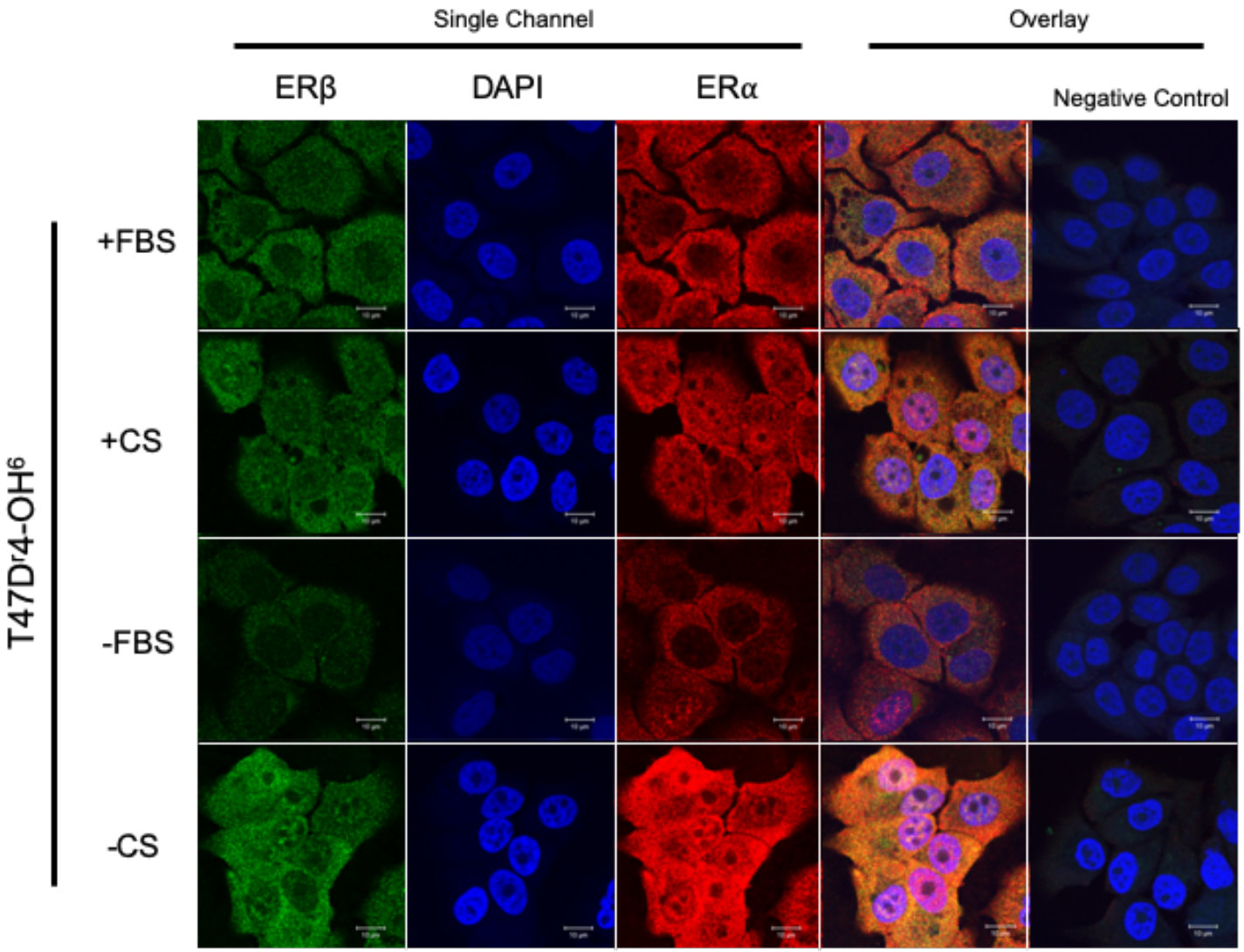


Figure 4.18: Representative immunofluorescence images of an N=6 images of the T47D^{r}4-OH tamoxifen-resistant cell line and all phenol red/growth hormone deprived sub-lines as indicated by the labelling on the left hand side of the figure. Lanes are divided into single channels and labelled appropriately. **RED - ERα, GREEN - ERβ, BLUE – DAPI/nucleic acids. Scale bar is representative of 10 microns.**

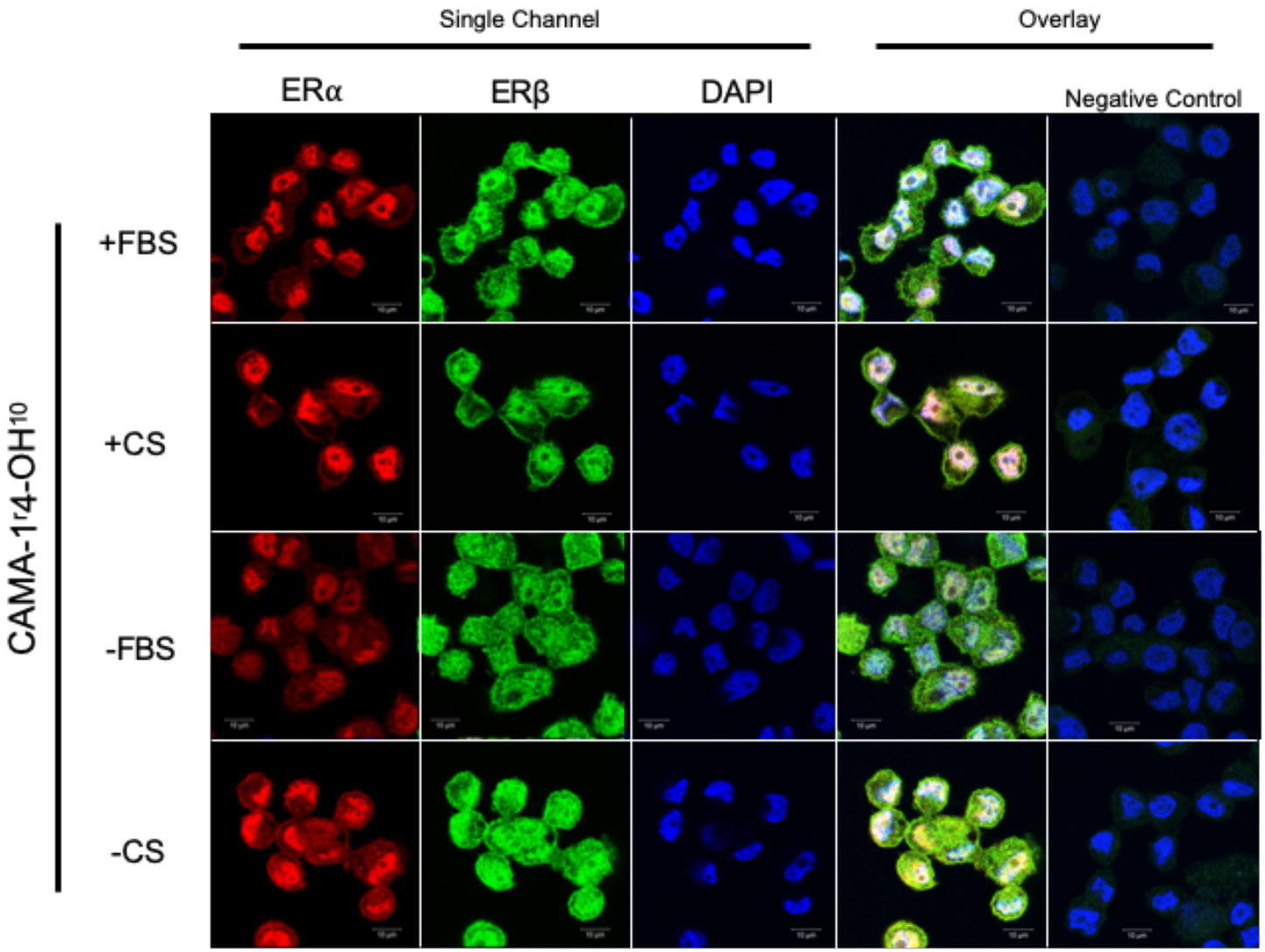


Figure 4.19: Representative immunofluorescence images of an N=6 images of the CAMA-1^{r}4-OH tamoxifen-resistant cell line and all phenol red/growth hormone deprived sub-lines as indicated by the labelling on the left hand side of the figure. Lanes are divided into single channels and labelled appropriately. **RED - ERα, GREEN - ERβ, BLUE – DAPI/nucleic acids. Scale bar is representative of 10 microns.**

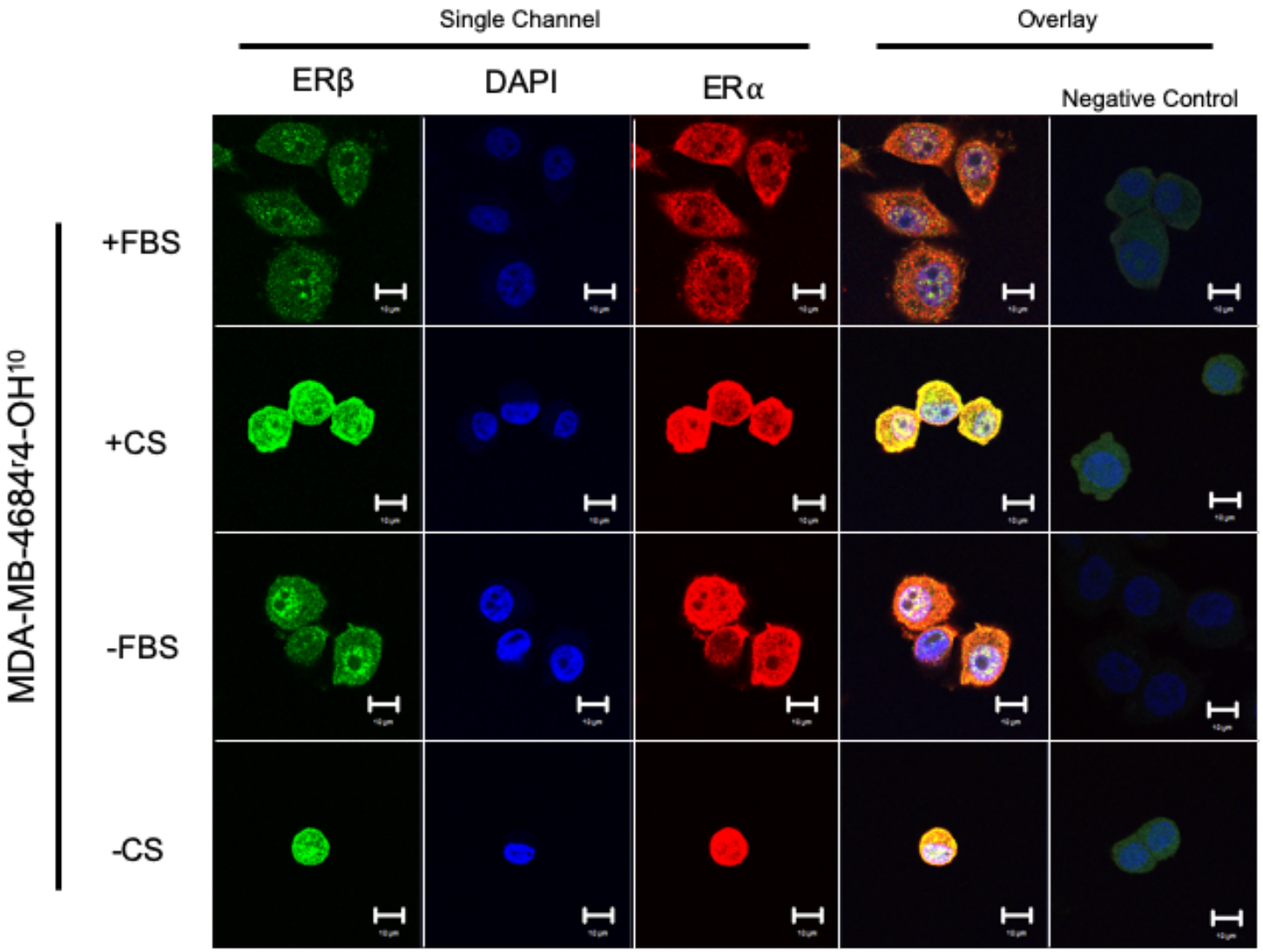


Figure 4.20: Representative immunofluorescence images of an N=6 images of the BT-474r4-OH tamoxifen-resistant cell line and all phenol red/growth hormone deprived sub-lines as indicated by the labelling on the left hand side of the figure. Lanes are divided into single channels and labelled appropriately. **RED - ERα, GREEN - ERβ, BLUE – DAPI/nucleic acids. Scale bar is representative of 10 microns.**

4.2.6: Quantification of ERα and ERβ expression in the tamoxifen-resistant sub-lines

In parallel to the evaluation of our AI resistant model in chapter 3, figures 4.15-4.20, above, show a representative image from n=6 images taken of each tamoxifen-resistant cell line, of ER expression in our cell lines. These are separated into appropriately labelled differentially phenol red/hormone deprived sub-lines. The figures contain a breakdown of the individual fluorophore channels (from the confocal microscope imaging software) that rendered images of ERα and ERβ, along with an overlay of the two and a separate channel for nucleic acid staining with DAPI. Further elaboration of the immunofluorescence and imaging protocols can be found in section 2.2.5. Figures 4.21 and 4.22, below, show the quantification of average cellular fluorescence intensity that have been ascertained using ImageJ software from these images. These have been normalised for autofluorescence and non-specific antibody binding by subtracting the fluorescence intensity of appropriate negative controls. Furthermore, these figures also contain graphs representing the fold changes in intensity seen compared to the appropriate control originator parental cell line – for example, the CAMA-1^{r}4-OH^{+FBS} cell line has been compared to the CAMA-1^{+FBS} parental cell line and the CAMA-1^{r}4-OH^{+CS} resistant sub-line has also been compared to the parental CAMA-1^{+FBS} cell line, as well as being compared to its same media parental counterpart, CAMA-1^{+CS}.

Although all parameters of the confocal microscope used to capture the immunofluorescence images were kept constant, such as laser power, magnification (as this would affect the area of the cell used to calculate the intensity of it relative to its size) and post-imaging processing, expression of ERα and ERβ shouldn't be compared directly. The antibodies used for the experimental procedure are not equal in single molecule florescence intensity when stimulated by the lasers of the confocal microscope. This was unfortunately unavoidable. The changes between individual ER isoform expression however, can be commented on.

When visually inspecting both figures 4.21Bi)and ii) (ERα) and 4.22Bi) and ii) (ERβ) the changes in levels of expression ER appear to be cell-line specific and

vary from general upregulation or downregulation of the receptors as a response to drug adaptation. These figures show changes relative to their parental cell lines that are grown in +FBS conditions. Fig 4.21B shows upregulation of ERα in MCF7, T47D and MDA-MB-468, downregulation in the BT-474 and CAMA-1 cell lines, and no change in the EFM-19 cell line. This is based on fold changes of receptor expression deviating from 1, to either fall below 0.5 or increase above 2.

There is a switch in this trend for expression of ERβ. The MCF7, EFM-19, T47D and CAMA-1 cell lines all show a decrease in ERβ expression compared to the +FBS parental cell line, which is not seen in oestrogen deprivation alone from the previous chapter (fig 3.21B). No notable change in ERβ expression was seen in cell lines from oestrogen deprivation alone. This may highlight an important difference between resistance to aromatase inhibitors and resistance to tamoxifen.

As well as looking at general trends in receptor expression changes for the cell lines, the figures in question below (4.21 and 4.22) are also divided into receptor expression for the whole cell and for the nucleus alone, in an attempt to quantify receptor localisation. We saw in the previous chapter, and in the parental cell lines counterparts to those in this chapter, that receptor expression was generally ubiquitous throughout the cell, with the exception of the CAMA-1 cell line that showed some preference for nuclear localisation. Comparing the fold changes for the cell lines, with regards to nuclear localisation for ERα, the cell lines do not appear to display any shift in trend in preference for either cytoplasmic or nuclear localisation, aside from the T47D and the MDA-MB-468 set of cell lines that show a decrease in nuclear localisation, compared to whole cell. Particularly all media conditions aside from +FBS for T47D.

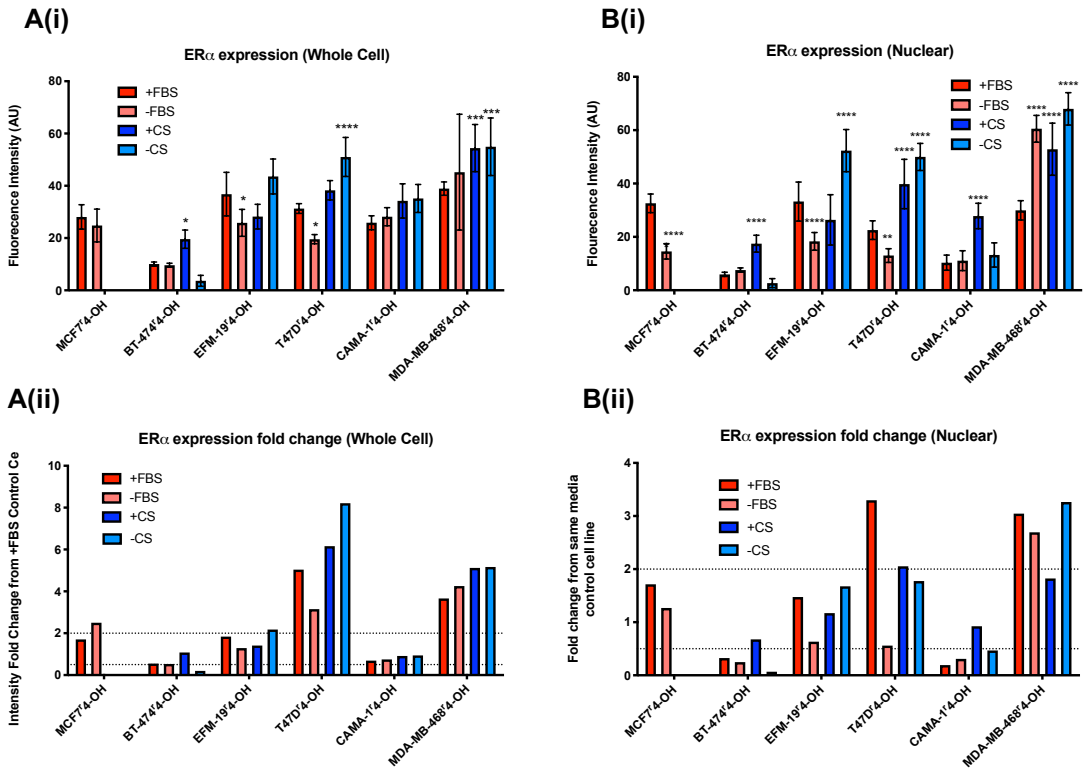


Figure 4.21: Fluorescence intensity of ERα in each of the tamoxifen-resistant breast cancer cell lines and all of the oestrogen/phenol red deprived tamoxifen-resistant sub-lines generated also. A) Whole cell fluorescence, B) Nuclear only expression, i) fluorescence intensity values, ii) fold change in fluorescence intensity values respectively. Data points are representative of the average of n=6 images per cell line, and of the average intensity of a single cell. Each data point is therefore roughly representative of the intensity of 50 individual cells. Error bars are representative of +/-SD. Statistical analysis was conducted using two-way ANOVA with bonferroni correction (**** - p<0.0001)(*** - p<0.001)(** - p<0.01)(* - p<0.05**)** – data points were compared to originating +FBS cell line for statistical analysis. (B) Plotted fold changes from fluorescence intensity of originating +FBS parental control cell line. Horizontal lines indicate 0.5 on the y-axis.

Figure 4.22 below shows fluorescence intensity and fold change values for this for ERβ. In the previous chapter, we saw that ERβ expression, like that of ERα remained generally ubiquitously localised throughout the cell. Comparing Ai) and Bi) shows us that there are some notable differences in localisation with regards to this isoform of the receptor. Decreases in nuclear localisation can be seen in various media conditions in the BT-474^{r}4-OH and CAMA-1^{r}4-OH cell line groups, and increases can be seen , specifically in the growth hormone deprived conditions of the EFM-19^{r}4-OH and T47D^{r}4-OH cell lines. These points pertain specifically to the raw fluorescence intensity values. However , when addressing the fold change values in Aii) and Bii) (which compares to the originating +FBS control cell line), marked decreases in expression can be seen across the cell line groups when compared to the whole cell fluorescence fold changes. This

may suggest that a decrease in nuclear localisation of ERβ may be a factor in tamoxifen resistance.

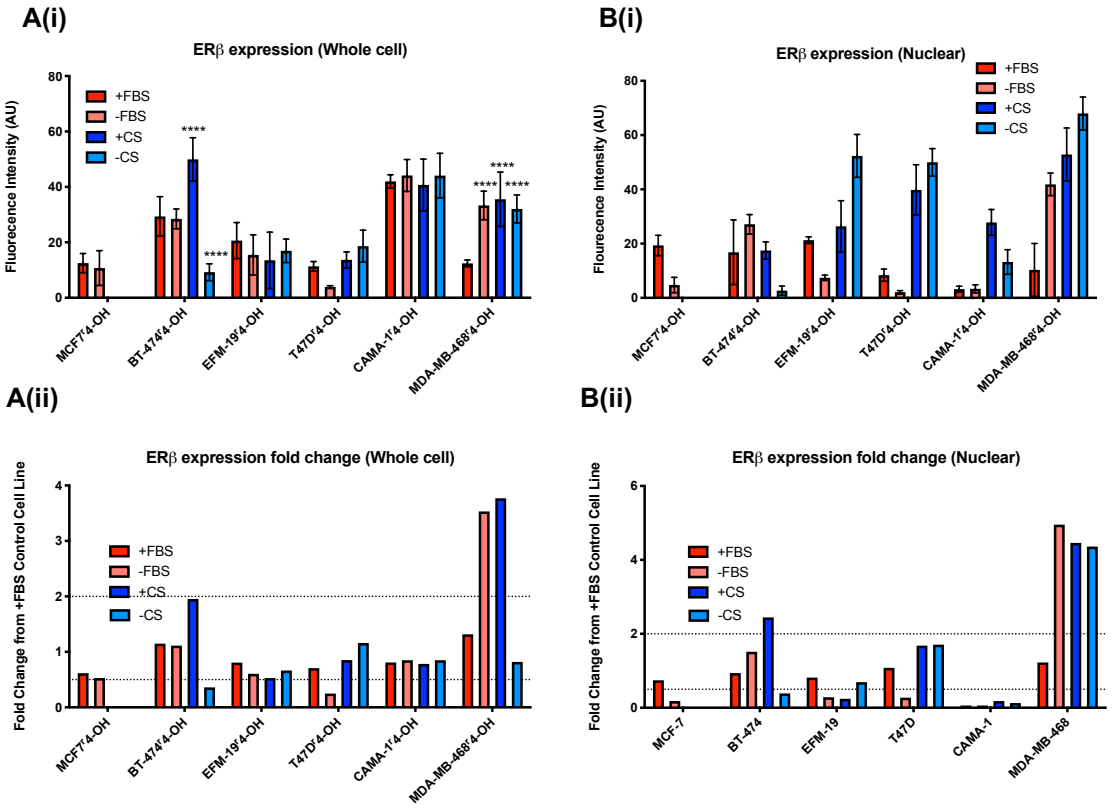


Figure 4.22: Fluorescence intensity of ERβ in each of the tamoxifen-resistant breast cancer cell lines and all of the oestrogen/phenol red deprived tamoxifen-resistant sub-lines generated also. A) Whole cell fluorescence, B) Nuclear only expression, i) fluorescence intensity values, ii) fold change in fluorescence intensity values respectively. Data points are representative of the average of n=6 images per cell line, and of the average intensity of a single cell. Each data point is therefore roughly representative of the intensity of 50 individual cells. Error bars are representative of +/-SD. Statistical analysis was conducted using two-way ANOVA with bonferroni correction (**** - p<0.0001)(*** - p<0.001)(** - p<0.01)(* - p<0.05**)** – data points were compared to originating +FBS cell line for statistical analysis. (B) Plotted fold changes from fluorescence intensity of originating +FBS parental control cell line. Horizontal lines indicate 0.5 and 2 on the y-axis.

Furthermore, the fluorescence intensity data plotted in figures 3.21, and 4.22 (above) were used to calculate the ratio of expression between whole cell and nuclear only. A value below 1 is indicative of a preference for nuclear localisation within the cell. Looking at the data displayed in figure 4.23, below, it is evident that a number of the drug resistant cell lines have values above 1 for the ratio of ERα, yet not greatly above a value of 1 - suggesting that cytoplasmic localisation may show a preference, but not greatly if this is the case. This description would also fit when looking at the ratios of ERβ. The most notable point to be observed from this figure, is an increased ratio of the CAMA-1 cell lines, for both expression of ERα and ERβ. Suggesting that nuclear localisation is not preferred in the drug-resistant lines, like it is in the parental counterparts.

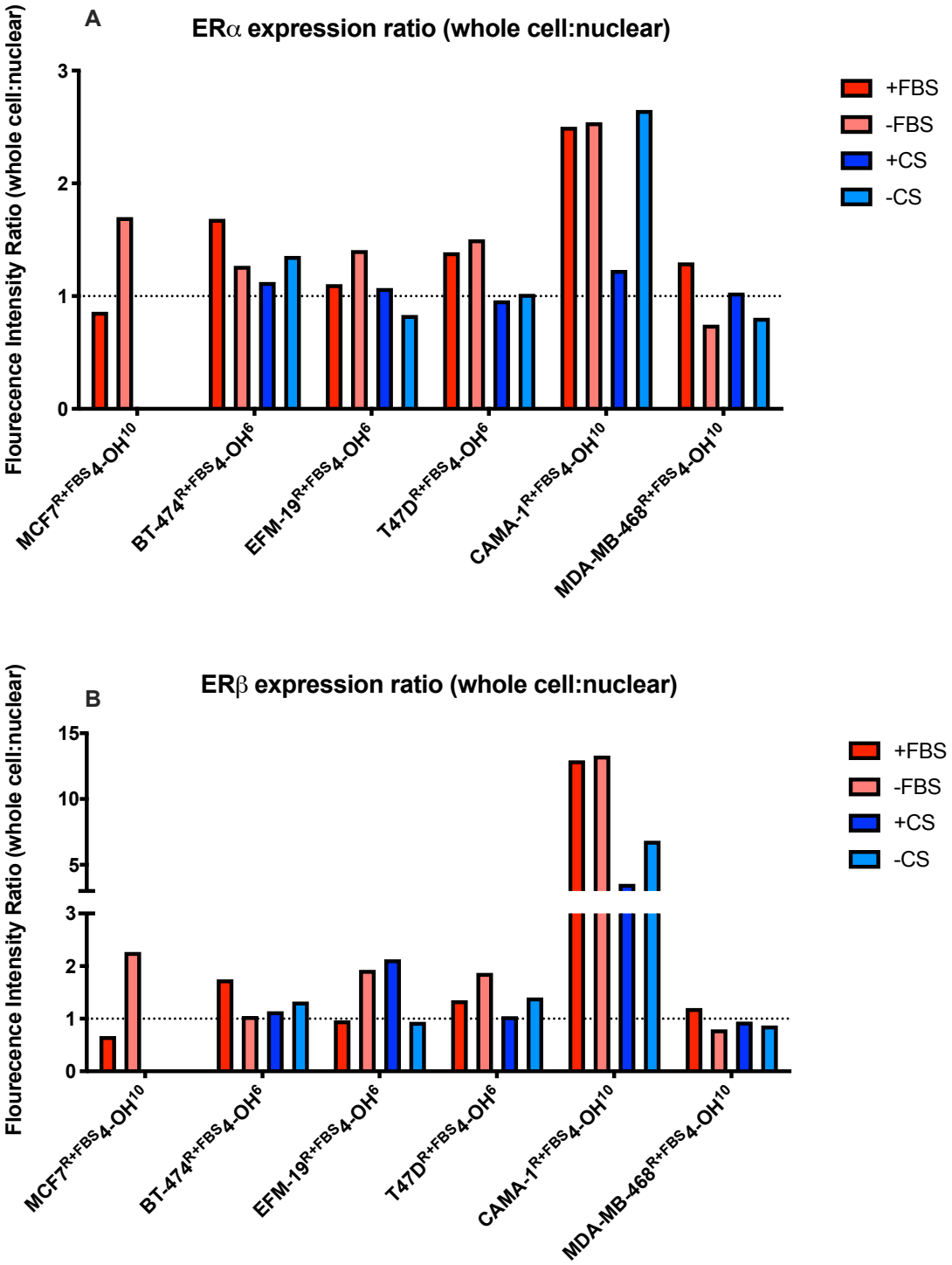


Figure 4.23: **(A)** Fluorescence intensity ratios of ERα (A) and ERβ (B) in each of the tamoxifen-resistant breast cancer cell lines and all of the oestrogen/phenol red deprived tamoxifen-resistant sub-lines generated also. Data points are representative of the average of the data obtained from n=6 images per cell line, and of the average intensity of the whole cell divided by the average intensity of the nuclear only reading. Values below one are indicative of a preference for nuclear localisation. Colour coding is consistent with the media condition in which the cell line was cultivated in.

4.2.7: Stability of drug-resistance to (Z)-4-OH-tamoxifen, tamoxifen and tamoxifen metabolites after cryopreservation

There is a wealth of information in literature surrounding the effect that cryopreservation has on cells, particularly on clinical samples used for characterisation and preservation of other biological components used for industrial purposes (Schumacher, Westphal and Heine-Dobbernack, 2015; Westfalewicz, Dietrich and Ciereszko, 2015; Conde *et al.*, 2016). Slight negative effects have been reported with regards to the use of previously cryopreserved clinical samples for diagnostics or characterisation compared to fresh samples, but these generally pertain to losses of cell viability with samples that contain small amounts of target cells (like circulating tumour cells in blood samples for example) (Nejlund *et al.*, 2016), but very little information is available on the effect that cryopreservation has on drug-resistance status of mammalian cell lines. Figures 4.24 and 4.25, below, show IC_{50} fold change values from their respective parental cell lines for all tamoxifen resistant sub-lines generated, after undergoing cryopreservation on two separate occasions and lengths of time into the adaptation process. MTT viability assays were performed one month after resuscitation, after culture in the presence of drug had been reintroduced. Figures 4.24 and 4.25 show data for tamoxifen, and the clinically relevant metabolites from January 2018 (one year after beginning to generate the resistant sub-lines) and January 2019 (two years after beginning to generate the resistant sub-lines) respectively.

In order for resistance to be deemed ‘stable’, meaning that the cell lines can endure the process of cryopreservation without losing resistance to the drug, the fold change difference between the cryopreserved cells and non-cryopreserved cells must remain at value of 1. There is nothing in currently existing literature that documents any evaluation of resistance retainment to tamoxifen after cryopreservation. Far more cell lines retained cryopreservation naïve cell response values to tamoxifen, alpha-hydroxytamoxifen, endoxifen and n-desmethyltamoxifen in 2019 compared to 2018. If there is no data point for a cell line – it means that the sub-line did not recover from the resuscitation process at all and was discarded. Fewer sub-lines retained the same level of response to (Z)-4-OH-tamoxifen compared to cryopreservation naïve cells, however than to

the other metabolites – further investigation into the cause of this would be needed to suggest why.

Commenting on the most recent cryopreservation data (figure 4.24; from early 2019), cell lines that retained resistance to (Z)-4-OH-tamoxifen after cryopreservation, also retained the same level of response to the other metabolites, none gained resistance compared to cryopreservation naïve sub-lines. The BT-474 and T47D cell lines appeared to be more susceptible to a reduction fold change in response to all metabolites relative to naïve cells.

This experiment was performed to highlight the necessity of confirming drug resistance before any experimentation on drug-resistant cell lines, as these are often shared between research labs, and therefore cryopreserved for transportation. Here we have shown that this process has the potential to drastically alter drug-resistance status.

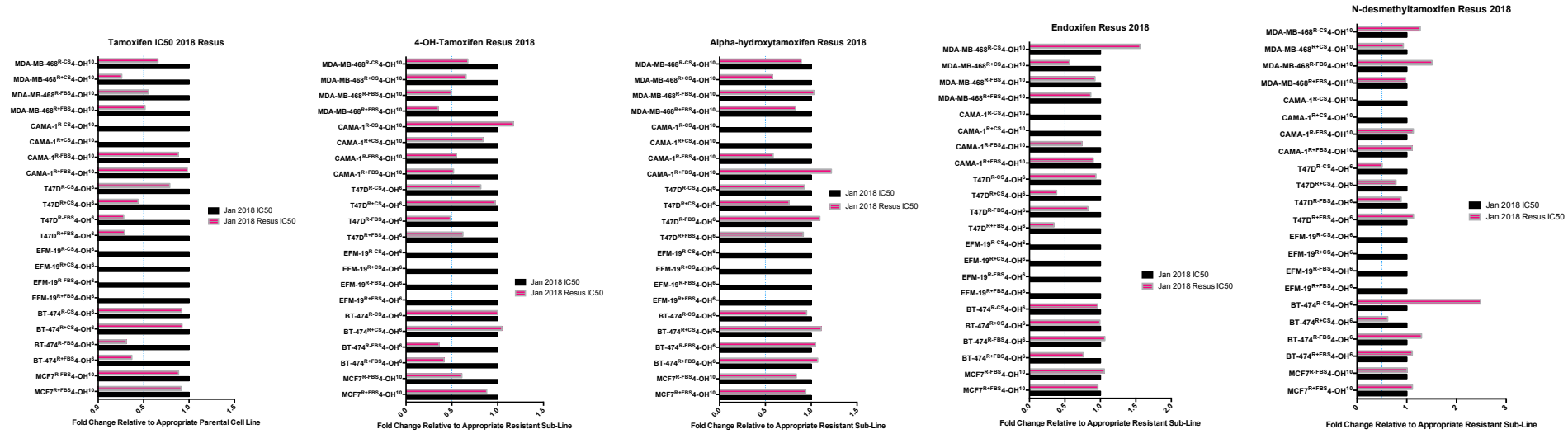


Figure 4.24: This set of data was obtained from cell lines that were banked down during the 'early 2018' stage of cell line development. Fold changes calculated from experimentally obtained tamoxifen/tamoxifen metabolite IC_{50} values for each of the tamoxifen-resistant cell lines. Red = resistant sub-line IC_{50} fold change from the resistant cell line that had previously been cryopreserved. Black =resistant cell line that has not previously been cryopreserved, this will always be equal to 1. Control IC_{50} values (those that were not previously cryopreserved, coloured in black) were obtained simultaneously to the drug-resistant sub-lines. Horizontal blue line marks when x=0.5, whilst horizontal red line marks where x=2. A value below 0.5 indicates sensitivity to the compound, whereas a value above 2 indicates resistance.

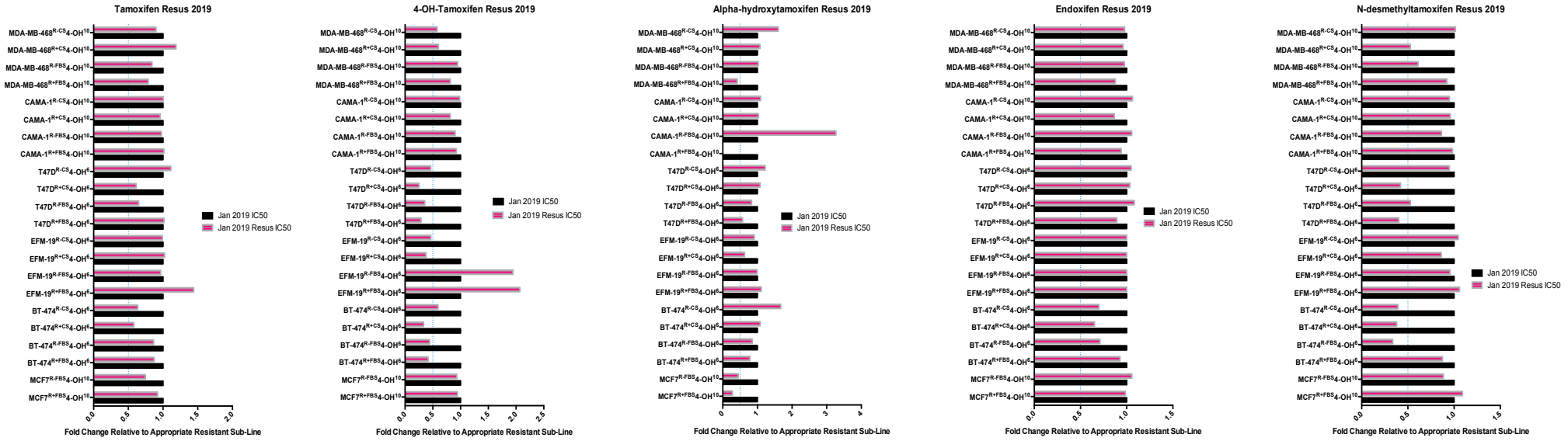


Figure 4.25: This set of data was obtained from cell lines that were banked down during the 'early 2019' stage of cell line development Fold changes calculated from experimentally obtained tamoxifen/tamoxifen metabolite IC_{50} values for each of the tamoxifen-resistant cell lines. Red = resistant sub-line IC_{50} fold change from the resistant cell line that had previously been cryopreserved. Black =resistant cell line that has not previously been cryopreserved, this will always be equal to 1. Control IC_{50} values (those that were not previously cryopreserved, coloured in black) were obtained simultaneously to the drug-resistant sub-lines. Horizontal blue line marks when x=0.5, whilst horizontal red line marks where x=2. A value below 0.5 indicates sensitivity to the compound, whereas a value above 2 indicates resistance.

4.2.8: Response to other commonly used chemotherapeutics used to treat breast cancer

Here, like in the previous chapter, we investigated the response of the cell lines to 2-methoxyoestroadiol (a drug that is a known agonist of GPER1 and a known tubulin-binding agent), olaparib (PARP inhibitor) and vincristine (tubulin binding agent) (D'Amato *et al.*, 1994; Dumontet and Jordan, 2010; Kamel *et al.*, 2018).

Cross-resistance to 2-methoxyoestradiol is seen in 14 of the 20 confirmed tamoxifen-resistant cell lines – suggesting that the causative factors for tamoxifen resistance in these cells may be directly or indirectly inferring cross-resistance to 2-methoxyoestradiol - further investigation would be required to confirm or deny this. A suggestion for future work on this topic would be quantitative evaluation of GPER1 function and expression, and how these change in response to tamoxifen-resistance. Response to 2-methoxyoestradiol was evaluated in the oestrogen-deprived parental cell lines in chapter 3 (figure 3.27) and fewer cell lines were resistant to 2-methoxyoestradiol than seen here in figure 4.26 that refers to tamoxifen-resistant sub-lines. For the cell lines that were seen to be resistant in figure 3.27, 4/5 of them were generated in the absence of endogenous oestrogens in culture media - suggesting that resistance to aromatase inhibitors may also have an effect of reduced sensitivity to 2-methoxyoestradiol. The MCF7 cell lines presented a much higher IC_{50} value compared to the other cell lines in the previous chapter, perhaps suggesting it possesses intrinsic mechanisms of resistance to 2-methoxyoestradiol (as can be seen in fig. 4.26A). This cell line is the only one to show increased sensitivity here, suggesting that adapted growth to (Z)-4-OH-tamoxifen induces sensitivity. There is no obvious trend throughout the cell lines presented by the presence of phenol red.

When all six 4-OH resistant cell lines are grouped into media conditions, the average 2-methoxyoestradiol IC_{50} values are as follows (in μM): +FBS: 13.47 ± 26.03, -FBS: 17.7 ± 26.03, +CS: 24.48 ± 35.12, -CS: 19.73 ± 40.94. The parental counterparts: +FBS: 2.51 ± 4.3 -FBS: 2.03 ± 3.6, +CS: 18.05 ± 42.77, -CS: 15.07 ± 34.26. High standard deviations highlight a great deal of variability of response between the cell lines, but average IC_{50} values of the parental cell lines are lower than those of their tamoxifen resistant counterparts. The average fold changes

are as follows: +FBS 0.84 ± 6.1, -FBS: 5.73 ± 5.84, +CS: 31.94 ± 19.94, -CS: 20.13 ± 1.57.

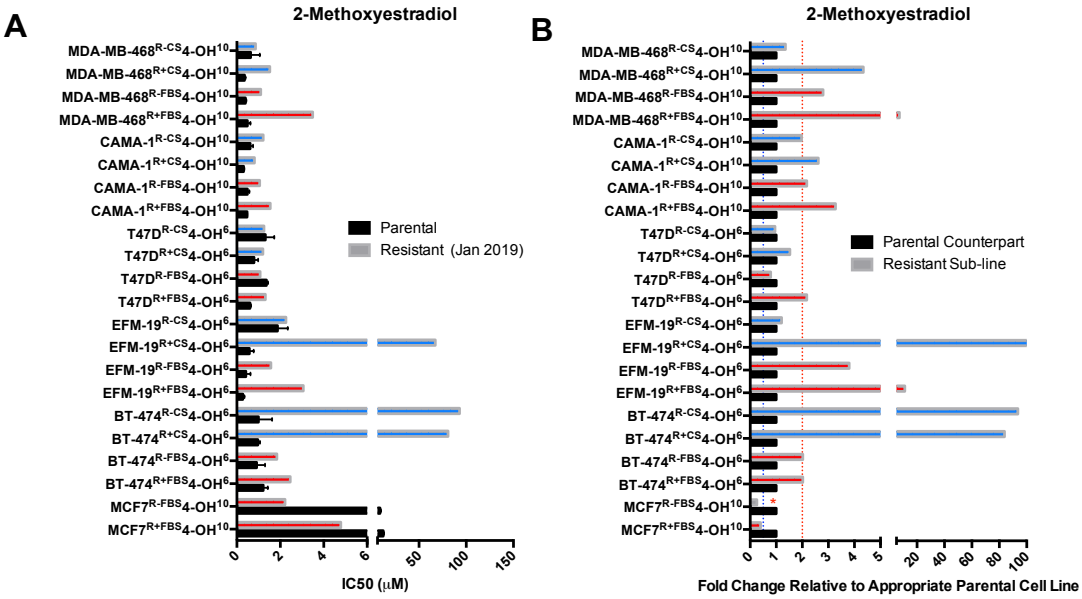


Figure 4.26**: (A)** 2-Methoxyoestradiol IC_{50} values experimentally obtained from the originating parental cell lines (n=3 +/-SD) and the tamoxifen-resistant sub-lines generated in this chapter (n=1, as this is reprehensive of the most recent IC_{50} data only), indicated on the y-axis of the graphs. The graph is colour coded for the cell line that the data is related to. Blue coloured bar = resistant sub-line generated in conditions containing charcoal-stripped FBS, Red coloured bar = resistant sub-line generated in conditions containing FBS. **(B)** Fold change values obtained from (A) that have been calculated relative to the control parental from that particular cell line (coloured in black, and equal to 1). Horizontal blue line marks when x=0.5, whilst horizontal red line marks where x=2. A value below 0.5 indicates sensitivity to the compound, whereas a value above 2 indicates resistance. Bars are coloured to reflect this – blue = sensitive. Asterisks mark the colour of the bar if data point was too small to be made interpretable by eye.

As previously discussed in section 3.2.7 microtubule-interfering drugs, such as vincristine, are commonly used in the treatment of many cancers, including leukaemia/lymphoma, non-small cell lung cancer and metastatic breast cancer (Park *et al.*, 2016). Microtubule-binding agents are one of the oldest and most diverse families of compounds in the context of anti-cancer therapeutics. Vincristine, which binds to the vinca site of microtubules, is an example of this (Dumontet and Jordan, 2010).

Looking at the data in figure 4.27, below there is no obvious trend in response from the media condition that the sub-line was cultivated in, nor are there a large number of tamoxifen-resistant sub-lines that are cross-resistant to vincristine (6/22). Aside from this trend, the MCF-7 cell line in particular does show cross-resistance to vincristine in both of the tamoxifen-resistant sub-lines. The oestrogen-deprived parental counterparts of these cell lines from chapter 3, are also resistant to vincristine, suggesting that there may be a common cellular adaptation of a change to tubulin organisation/mechanism of resistance to vincristine between oestrogen starvation and resistance to inhibition of oestrogen receptors. It may be a commonality between transport of the drug into/out of the cell, and therefore a question of access to the drug to its target. Its effect on cell lines with acquired tamoxifen-resistance has not been reported in literature.

In chapter 3, the $MCF7^{+FBS}$ and $MCF7^{-FBS}$ cell lines did not show cross-resistance between 2-methoxyoestroadiol and vincristine compared to its parental cell line (fig. 3.27 and 3.28). The (Z)-4-OH-tamoxifen resistant subline counterparts show increased response to both of these compounds, in opposing fashions. They show sensitivity to 2-methoxyoestradiol, but resistance to vincristine. Therefore this cell line presents as an interesting model to study the effect of 2-methoxyoestradiol and the proportion of its actions that are elicited through tubulin binding vs GPER1 interaction.

When all six 4-OH resistant cell lines are grouped into media conditions, the average vincristine IC_{50} values are as follows (in μM): +FBS: 0.5 ± 0.41, -FBS: 1.83 ± 2.36, +CS: 1.15 ± 0.79, -CS: 0.97 ± 1.03. The parental counterparts: 0.45 ± 0.35, -FBS: 0.66 ± 0.64, +CS: 1.09 ± 1.49, -CS: 1.8 ± 2.40. No significant difference can be drawn from this. The average fold changes are as follows: +FBS 0.85 ± 0.66 , -FBS: 2.25 ± 2.1, +CS: 1.9 ± 1.7, -CS: 1.2 ± 0.7 .

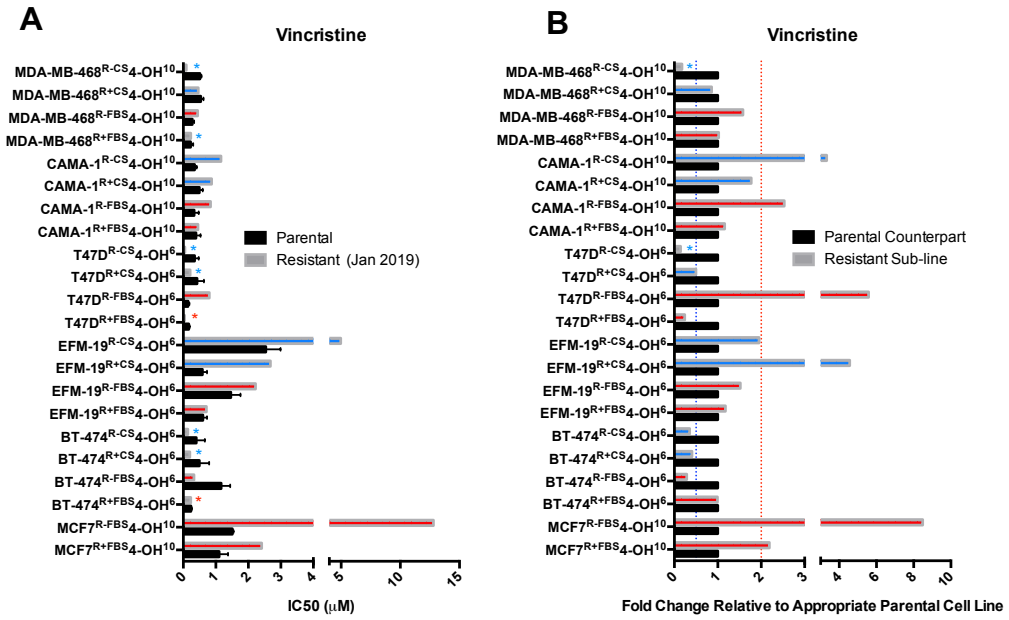


Figure 4.27**: (A)** Vincristine IC_{50} values experimentally obtained from the originating parental cell lines (n=3 +/-SD) and the tamoxifen-resistant sub-lines generated in this chapter (n=1, as this is reprehensive of the most recent IC_{50} data only), indicated on the y-axis of the graphs. The graph is colour coded for the cell line that the data is related to. Blue coloured bar = resistant sub-line generated in conditions containing charcoal-stripped FBS, Red coloured bar = resistant sub-line generated in conditions containing FBS. **(B)** Fold change values obtained from (A) that have been calculated relative to the control parental from that particular cell line (coloured in black, and equal to 1). Horizontal blue line marks when x=0.5, whilst horizontal red line marks where x=2. A value below 0.5 indicates sensitivity to the compound, whereas a value above 2 indicates resistance. Bars are coloured to reflect this – blue = sensitive. Asterisks mark the colour of the bar if data point was too small to be made interpretable by eye.

Figure 4.28 shows olaparib IC_{50} values across the panel of tamoxifen-resistant cell lines. The fold changes of this relative to the originating parental cell line (fig 4.28B) suggests that growth in the absence of endogenous oestrogen does affect this – as only sub-lines generated in +CS/-CS conditions are cross-resistant to olaparib (MDA-MB-468, CAMA-1, T47D, EFM-19 and BT-474 all either have +CS, -CS or both, sub-lines that qualify as resistant). Our results suggest that growth in the absence of oestrogen may therefore affect DNA repair in tamoxifen-resistance. The MDA-MB-468 cell line group appears to be particularly sensitive to olaparib. An interesting observation can be made when comparing the fold changes of the cell lines that were considered sensitive to olaparib in the model for aromatase inhibitor resistance in the previous model – 7/12 sublines that were hormone deprived showed sensitivity (FC<0.5), this effect is reversed in the context of resistance to tamoxifen. The same sublines that were previously considered sensitive, are considered resistant (FC<2) in the context of (Z)-4-OH-tamoxifen resistance.

There is nothing in literature at present to report the affect PARP inhibition has on tamoxifen-resistant breast cancer sub-lines, nor is there anything to report the effect that growth hormone-depletion has. Here we show that growth-hormone depletion does have an effect on response to olaparib, as does direct inhibition of ERs.

When all six 4-OH resistant cell lines are grouped into media conditions, the average olaparib IC_{50} values are as follows (in μM): +FBS: 22.10 ± 22.83, -FBS: 18.96 ± 16.88, +CS: 32.91 ± 33.11, -CS: 35.71 ± 50.33. The parental counterparts: +FBS: 31.47 ± 31.1, -FBS: 30.46 ± 23.81, +CS: 18.05 ± 17.2, -CS: 19.4 ± 17.11. High standard deviations highlight a great deal of variability that can be observed between the individual cell lines, average values for hormone deprived sublines are on average higher than those grown in the presence of growth hormone. The average fold changes are as follows: +FBS 0.84 ± 0.34 , -FBS: 0.67 ± 0.39, +CS: 3.4 ± 2.66 , -CS: 2.4 ± 1.6.

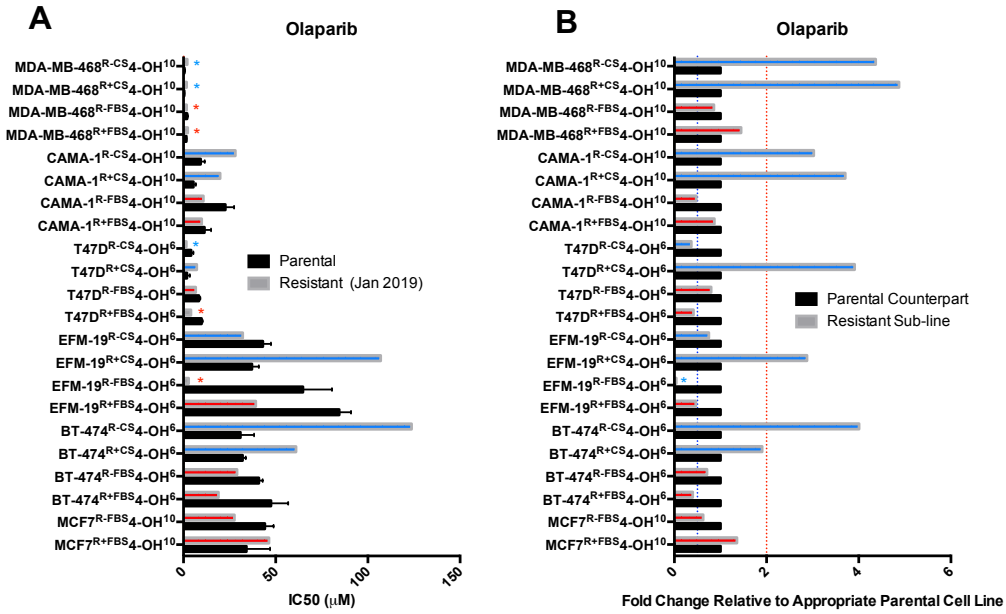


Figure 4.28: **(A)** Olaparib IC_{50} values experimentally obtained from the originating parental cell lines (n=3 +/-SD) and the tamoxifen-resistant sub-lines generated in this chapter (n=1, as this is reprehensive of the most recent IC_{50} data only), indicated on the y-axis of the graphs. The graph is colour coded for the cell line that the data is related to. Blue coloured bar = resistant sub-line generated in conditions containing charcoal-stripped FBS, Red coloured bar = resistant sub-line generated in conditions containing FBS. **(B)** Fold change values obtained from (A) that have been calculated relative to the control parental from that particular cell line (coloured in black, and equal to 1). Horizontal blue line marks when x=0.5, whilst horizontal red line marks where x=2. A value below 0.5 indicates sensitivity to the compound, whereas a value above 2 indicates resistance. Bars are coloured to reflect this – blue = sensitive. Asterisks mark the colour of the bar if data point was too small to be made interpretable by eye.

Similarly to the tamoxifen metabolites, the response of the sub-lines to these other chemotherapeutics was investigated after cryopreservation (Fig. 4.29). This applies to the cell lines cryopreserved during the ‘early 2019’ stage of cell line development. Response to olaparib did not appear to be drastically altered, but the majority cell lines appeared to have a decreased sensitivity to both 2-methoxyoestradiol and vincristine. Since the response to tamoxifen metabolites was not markedly altered after resuscitation, this may indicate that cell line storage in liquid nitrogen and resuscitation may impact on cellular cross-resistance profiles beyond the drug of adaptation.

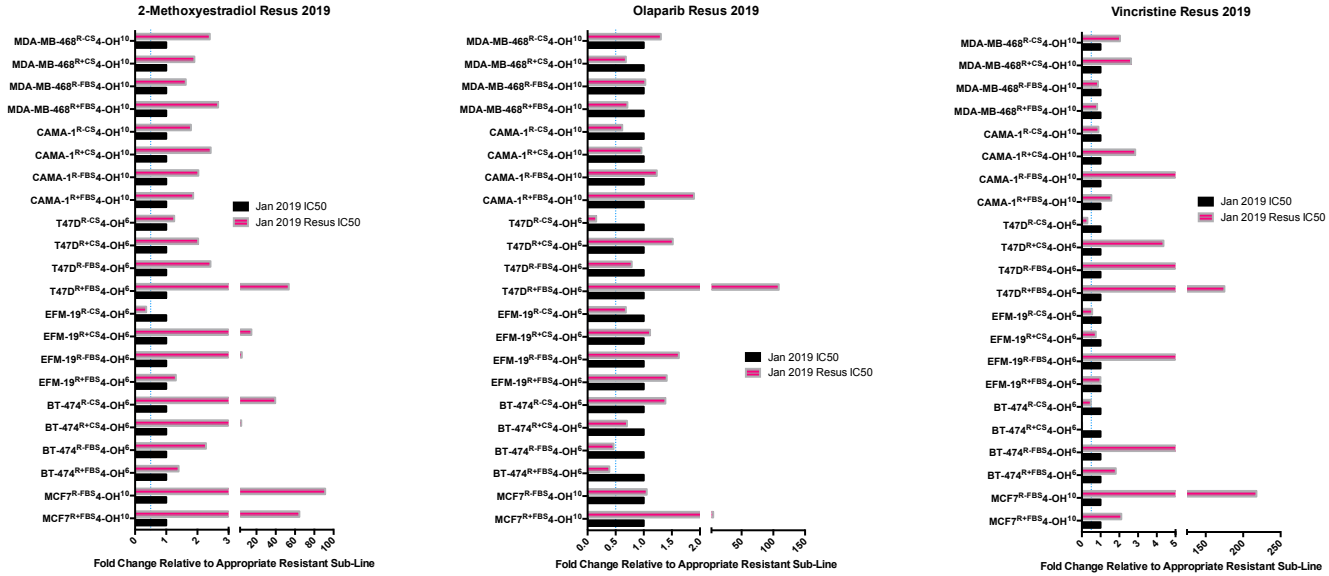


Figure 4.29: Fold changes calculated from experimentally obtained 2-methoxyoestradiol, olaparib and vincristine IC_{50} values for each of the tamoxifen-resistant cell lines. Red = resistant sub-line IC_{50} fold change from the resistant cell line that had previously been cryopreserved. Black =resistant cell line that has not previously been cryopreserved, this will always be equal to 1. Control IC_{50} values (those that were not previously cryopreserved, coloured in black) were obtained simultaneously to the drug-resistant sub-lines. Horizontal blue line marks when x=0.5, whilst horizontal red line marks where x=2. A value below 0.5 indicates sensitivity to the compound, whereas a value above 2 indicates resistance.

4.3: Discussion

4.3.1: Generation of resistant sub-lines

The first breast cancer cell lines to be investigated for intrinsic mechanisms of resistance to tamoxifen were created in 1981, when certain monoclonal populations of MCF7 were found to be unresponsive to growth inhibition from the drug (Nawata, Bronzert and Lippman, 1981). Since then, many breast cancer cell lines have been studied for acquired drug resistance by long-term exposure to tamoxifen (usually (Z)-4-OH-tamoxifen, like in this study) which has been documented to occur with varying protocols of tamoxifen treatment, concentrations and serum supplementation (Martin *et al.*, 2011; Nass and Kalinski, 2015). It would therefore not be surprising to find a number of different mechanisms of resistance to tamoxifen in an *in vitro* setting, just as would be the case for individual breast cancer patients. Here, a comparatively large number of tamoxifen-resistant cell lines have been developed simultaneously, and under the same selection protocol during this works, which allows for the future opportunity to study differences in the emergence of mechanisms of tamoxifen resistance between individual cell lines and under different growth conditions.

In this chapter, 22 (Z)-4-OH-tamoxifen resistant breast cancer sub-lines have been produced using the dose escalation method. It has been reported that the development of acquired drug-resistance in cancer cell lines can take anything from 3 to 18 months using this method, however, relatively little is published on the development of this process. It has also been reported that it is difficult to develop stably resistant cancer cell lines (McDermott *et al.*, 2014). We have shown here that resistance to tamoxifen can be obtained in around one year – this has been shown to be stable in the majority of cases with MTT data over three timepoints (Fig 4.1C), and after cryopreservation (Fig. 4.25). This is provided the cells remain constantly exposed to the drug, however. Resistance stability has not been assessed if the cell lines are released from drug at set intervals.

4.3.2: Response to Tamoxifen and Metabolites

Similarly to the concepts discussed in chapter 3, the idea of bias to the physiological production of certain metabolites (because of variation in CYP450 enzyme expression in the liver from patient to patient) having a notable association with cancer patient outcome has been discussed to varying degrees in the literature (Helland *et al.*, 2017). Polymorphisms to these enzymes, among a select few others, is a candidate mechanism for resistance to tamoxifen. Tamoxifen, as a pro-drug, is thought elicit the majority of anti-cancer effects though enzymatic conversion to 'active' metabolites (Helland *et al.*, 2017) – which is opposed to what was seen in this work, as the IC_{50} values for tamoxifen were similar to that of the other 'active' metabolites rather than something expected to have a 30-100 times lower affinity. As tamoxifen can be metabolised to an extent in breast tissue, CYP450 profiling of the breast cancer cell lines used in this chapter would be a logical next-step for this work – perhaps this would suggest a preference for metabolism towards n-desmethyltamoxifen or (Z)-4-OH-tamoxifen as these are the metabolites the tamoxifen IC_{50} values most closely matched.

The general consensus that is to be gained from searching through literature is that serum concentrations of endoxifen is key, closely followed by N-desmethyltamoxifen and (Z)-4-OH-tamoxifen for preferential response to tamoxifen treatment – due to them being extensively metabolised from tamoxifen by CYP3A4 and CYP2D6 (Ahmad *et al.*, 2010). Looking at responses of the (Z)-4-OH-tamoxifen resistant sub-lines to endoxifen (Fig. 4.12) and n-desmethyltamoxifen (Fig. 4.14), most cell lines do not appear to be cross-resistant to endoxifen. This suggests the potential for endoxifen to be used as a second-line anti-oestrogen therapy in the advent of resistance to tamoxifen. Similarities can be drawn between the resistance profiles of tamoxifen (Fig. 4.11) and (Z)-OH-tamoxifen (Fig. 4.10), suggesting that a mechanism of action is shared between these two compounds or that tamoxifen is metabolised to (Z)-4-OH-tamoxifen within the breast cancer cell lines. Further investigation would be needed to investigate this.

The data in this chapter pertaining to response of the (Z)-4-OH-tamoxifen resistant cells to tamoxifen and other clinically relevant primary metabolites, is based on resistance to this one particular metabolite. The vast majority of literature that documents *in vitro* studies into resistance mechanisms to tamoxifen is based on acquired resistance to this compound (Nass and Kalinski, 2015; Gao *et al.*, 2018). We saw in both chapters 3 and 4 that (Z)-4-OH-tamoxifen shows the lowest IC_{50} values of all of the metabolites tested here (fig 3.23 & 4.10), which is reason why this is used to model tamoxifen resistance in a variety of other studies. But, this may be wrong as it has always been assumed that the metabolites have the same effect on ERs. As we have seen in this chapter, resistance to one metabolite of tamoxifen does not infer resistance to the others investigated – this raises the question of how this would change if drug-resistance was generated to any of the other metabolites. This idea would be a good candidate for further investigation and future work.

4.3.3: Oestrogen receptor expression changes as a result of acquired resistance to tamoxifen

Even though oestrogen receptor expression is considered a marker for predicting likelihood of response to endocrine therapy, some patients that test positive for oestrogen receptor expression still result as unresponsive to tamoxifen (Murphy *et al.*, 2002). This may be due to a remiss in differentiating between oestrogen receptor isoforms in the clinic. Differences in ERα and ERβ expression have previously been proposed to be involved in tamoxifen sensitivity (Paech *et al.*, 1997). However, as the ER expression data in this study is only preliminary data, a good future study would be to sort cells into differentially highly expressing populations of ERα and ERβ expression by flow cytometry to investigate the effect this has on response to tamoxifen. Another potential future investigation would be the use of cellular fractionation techniques, coupled with western blotting, the elucidate the exact cellular location and proportions of which of

It has been reported that loss of ERα expression has been observed as a result of tamoxifen resistance in breast cancer cell lines, since the effects of tamoxifen are thought to primarily be mediated through this receptor (Rondon-Lagos *et al.*, 2016). Here we see that this can be seen in some of the cell lines, but that it is

specific to the individual cell line. Fig. 4.21 shows that compared to respective parental +FBS cell-lines, a reduction in expression was seen in the BT-474 and CAMA-1 cell lines, but an increase in expression was seen with MCF7, EFM-19, T47D and MDA-MB-468 cell lines. The location of ERs in the (Z)-4-OH-tamoxifen resistant sublines seems only to be affected by growth in oestrogen deprived conditions, this was not seen in the counterpart cell lines from chapter 3 (fig 4.15-20)– there is nothing currently in literature that documents this.

Murphy *et al.*, (2002) and Hopp *et al.*, (2004) discuss the observation of an increased amount of wild type ERβ in tamoxifen sensitive cell lines compared to tamoxifen resistant cell lines. The data presented in this study (Fig. 4.23) also shows a decrease in ERβ expression in a number of cell lines, but was not consistently influenced by media condition it is cultivated in. Clinical data states that patients that express high levels of ERβ have a significantly better overall survival after tamoxifen treatment than those that do not (Mann *et al.*, 2001). It Is thought that ERβ has a modulatory effect in breast tissue (Hall and McDonnel, 1999) – loss of this could also be an explanation to decreased sensitivity to tamoxifen, as ERα is shown to be upregulated in a number of the tamoxifen-resistance sub-lines in this study, this could dysregulate balance with ERβ in these cell lines. The location of ERβ only seems to be affected by oestrogen deprivation (+CS/-CS) in the majority of cell lines during the development of resistance (Fig. 4.15-20). There is currently nothing in the literature to support this finding.

Figure 4.23 looks at the ratio of whole cell: nuclear localisation of both receptor isoforms, we saw in this figure that both ERα and ERβ expression appears to be slightly more highly expressed in the cytoplasm compared to the nucleus, with the most notable trend with this seen in the CAMA-1^{r}4-OH. As this data is only preliminary, in terms of quantification, it can only be speculated what this could mean in terms of whether this is a potential mechanism of resistance to tamoxifen. As previously mentioned, subcellular fractionation techniques combined with western blotting would be a potential next step to aid in further elucidating the exact locations of these receptors and their isoforms. As for how localisation links to functionality of these receptors, chromatin immunoprecipitation could be performed to investigate the interaction of these

proteins with DNA, which may give further insight into the relevance of nuclear localisation, and gene expression (Gade and Kalvakolanu, 2012).

4.3.4: Response to other anti-cancer compounds

Here, the effect of 2-methoxyoestrodiol has been documented on the tamoxifen-resistant cell lines (Fig. 4.26). It should be noted that this compound is also a known tubulin binding agent, making it impossible to accurately differentiate between observed effects of the drug because of GPER1 stimulation and its tubulin-binding properties. However, the effect that 2-methoxyoestradiol exerts on the tamoxifen-resistant cell lines in this work can be compared to the cell response data from that displayed for vincristine (another tubulin-binding agent) (Fig. 4.28). These compounds, or a comparison between the two, has not been examined in the advent of tamoxifen-resistance in literature previously. The most notable difference between the cell line responses to these two drugs, is from the (Z)-4-OH-tamoxifen resistant MCF7, which are resistant to vincristine yet more sensitive to 2-methoxyoestroadiol, BT-474^{R+CS}4-OH and BT-474^{R-CS}4-OH shows the inverse of this. Suggesting that the compounds have completely different properties. But resistance is shared between a number of the other cell lines, such as that of EFM^{r-cs}4-OH^{6,} the +FBS/-FBS MDA-MB-468^{r} sub-lines. A more generalised resistance mechanism to may be responsible for observed cross resistance to either of these two compounds from tamoxifen. Such as an upregulation of drug efflux transporters that has been linked to drug-resistance in many tumour types (Wu *et al.*, 2013; Li *et al.*, 2015).

More similarities are shared between these two compounds when looking at fold changes observed before and after cryopreservation of the tamoxifen-resistant sub-lines in figure 4.29. A notable decrease in sensitivity to both of these compounds is seen following cryopreservation which may suggest changes to tubulin-arrangement and accessibility as a result of cryopreservation. This has not previously been reported in literature.

Much attention has been made in recent years to olaparib for the treatment of TNBC or ovarian cancer, with a focus on treating individuals with BRCA mutations (Lord and Ashworth, 2016). This induces synthetic lethality due to already existing faults in homologous combination repair. Olaparib was used in this study,

not only to look at the effect that tamoxifen-resistance has on the effectiveness of this drug, but to give an insight into effect changes that are potentially due to changes in DNA repair as a result of tamoxifen-resistance. Here we show that compared to parental cell lines that are grown in the same media condition, oestrogen deprivation causes a decrease in sensitivity to olaparib in tamoxifen-resistant breast cancer cell lines. Nothing has been reported in literature to further discussion on this matter, but if this finding suggests an alteration in DNA damage repair as a direct effect of tamoxifen resistance in oestrogen deprived conditions (which may mimic tamoxifen-resistance in post-menopausal women) an investigation into the use of DNA damaging agents in tamoxifen-resistance in these conditions would be a logical next step.

4.4: Conclusion and general summary

In this chapter we described the production and characterisation of a panel of 22 (Z)-4-OH-tamoxifen resistant breast cancer cell lines. Resistance to (Z)-4-OH-tamoxifen was evaluated at three separate stages of cell line development, ranging between 1 and 2 years after development initiation. The effect of cryopreservation was assessed on the cell lines, with most displaying similar levels of resistance post-resuscitation, confirming cell lines are not completely resensitised to (Z)-4-OH-tamoxifen after cryopreservation. We have investigated sensitivity to tamoxifen and a range of clinically relevant primary tamoxifen metabolites, compared them to their parental counterparts, and found that resistance to (Z)-4-OH-tamoxifen does not infer cross-resistance to other metabolites in all cases. But does show a trend of cross-resistance with unmetabolised tamoxifen, suggesting that all other metabolites may be potentially successful alternatives if patients show high serum levels of (Z)-4-OH-tamoxifen during tamoxifen treatment regimes in the clinic. The effect of oestrogen deprivation on these metabolites was seemingly only affected with regards to n-desmethyltamoxifen, which showed an interesting reversal in cellular response in our model of aromatase inhibition compared to those that have acquired resistance to tamoxifen. Further investigation is needed to elucidate a reason for this. Oestrogen receptor expression and location was also evaluated in these cell lines, with an observed nuclear localisation in oestrogen deprived conditions, increased in ER alpha expression in a number of cell lines and decrease in ER beta expression. However this was not observed in all cell lines – highlighting

heterogeneity that can be observed between cell lines in response to drug adaptation. The drug-resistant sub-lines were also evaluated for response to 2-methoxyoestradiol, olaparib and vincristine. Oestrogen deprivation affected response to olaparib, suggesting that abnormalities to DNA damage repair may be accentuated by oestrogen deprivation in the advent of tamoxifen resistance. The process of cryopreservation decreased sensitivity of the tamoxifen-resistant sub-lines to both vincristine and 2-methoxyoestradiol. These two compounds were assessed for similarities in cellular response as they are both known to be tubulin-binding agents – ubiquitous similarities in response to these two drugs was not observed suggesting that these two drugs have differing effects on tamoxifen-resistant sub-lines.

Chapter 5: Evaluation of Cross-Resistance to DNA Damaging Agents in Platinum Drug-Resistant Triple Negative Breast Cancer

The results in this chapter were a collaborative effort between the following individuals: Joanna. L. Bird[1], Helen. E. Grimsley[1], Genevieve Rogers[1], Thomas Jackon-Soutter[1], Hollie N.A. Brissenden[1], Amy J. Cooke[1], Amy J. Cox[1], Matthew D. Hogg[1], Rebecca A. Jones[1], Jade M.C. Stephens[1], Alba Subiri Verdugo[1], Gabrielle A. Wishart[1]

[1] School of Biosciences, University of Kent, Canterbury, United Kingdom

Breakdown of contribution to this work is as follows and is the result of data mostly generated by Joanna. L. Bird, and partly through supervision and training of the listed individuals by Joanna. L. Bird. This chapter was originally the result of a collaborative taught MSc project that was taken over and completed by Joanna. L. Bird. Routine culture of all of the cell lines in this chapter was maintained by Joanna. L. Bird. Other authors listed are taught MSc students, other than Helen Grimsley and Thomas-Jackson Souter who are postgraduate research students that assisted with some of the execution of practical work.

MTT data generated by: Joanna. L. Bird, Genevieve Rogers, Thomas Jackson-Soutter, Hollie N.A. Brissenden, Matthew D. Hogg, Rebecca A. Jones, Jade M.C. Stephens, Alba Subiri-Verdugo and Gabrielle A. Wishart

Western blots conducted by: Joanna. L. Bird, Helen. E. Grimsley, Amy J. Cooke and Amy J. Cox

5.1: Introduction

Breast cancers that express neither hormone receptors nor HER2 are usually categorised as triple-negative breast cancer (TNBC), although this is a heterogeneous group (Denkert *et al.*, 2017). TNBC accounts for 15% of breast cancer cases (Siegel, Miller and Jemal, 2015) and is currently treated using cytotoxic chemotherapy. Although many TNBCs are initially highly sensitive to therapy, recurrence and resistance formation are common, providing TNBC patients with the worst prognosis among breast cancer patients (Denkert *et al.*, 2017). Improved treatment options are therefore needed for those TNBC patients whose tumours have stopped to respond to the available treatment options.

Platinum (Pt)-based compounds are among the most commonly used anti-cancer agents (Kelland, 2007; Armstrong-Gordon *et al.*, 2018). Following the discovery of cisplatin in the 1960s (Rosenberg, Van Camp and Krigas, 1965), further Pt-based compounds have been synthesised and tested for anti-cancer activity resulting in the approval of cisplatin, carboplatin, and oxaliplatin for the treatment of for many cancer types (Kelland, 1993, 2007; Dilruba and Kalayda, 2016; Lambert and Sørensen, 2018). Cisplatin and carboplatin are commonly used as part of treatment regimens for TNBC (Gerratana *et al.*, 2016; Huang *et al.*, 2017; Foukakis, 2018; Poggio *et al.*, 2018; Zhang *et al.*, 2018). However, therapy outcomes are often unsatisfactory and acquired resistance formation after initial therapy response is common (Denkert *et al.*, 2017; Zhang *et al.*, 2018).

Oxaliplatin, the third Pt-based drug, which is widely approved, has only been occasionally tested in clinical trials for the treatment of TNBC (Hwang *et al.*, 2005; Liu *et al.*, 2015). Based on the analysis of drug-DNA adducts, oxaliplatin seems to differ in its mode of action from cisplatin and carboplatin, which appear to cause very similar effects (Ruggiero *et al.*, 2013; Perego and Robert, 2016). Moreover, cross-resistance profiles between oxaliplatin and cisplatin/carboplatin may be incomplete, and oxaliplatin may have potential as next-line therapeutic after failure of cisplatin or carboplatin and vice versa (Rixe *et al.*, 1996; Faivre *et al.*, 2002; Raez, Kobina and Santos, 2010; Mir *et al.*, 2012; Ruggiero *et al.*, 2013; Perego and Robert, 2016). However, there is a very limited number of studies that directly compare the three approved Pt-based drugs in the same system. The question whether acquired resistance to one Pt-based drug is associated

with cross-resistance to other Pt-based drugs has not been systematically investigated.

The pathways involved in cisplatin-induced cytotoxicity have been nicely explained previously by (Siddik, 2003), and how the steps between DNA adduct formation and the completion of cytotoxic processes is complex (Siddik, 2003). Such as preferential cisplatin-DNA adduct formation between certain nucleotides - ApG and GpG being the major form of crosslink, accounting for 85-90% of total lesions (Kelland, 1993). Aside from damage caused by adduct forming anti-cancer agents, our cells accumulate thousands of lesions every day from environmental and endogenous causatives. Thankfully, cells have multiple DNA repair mechanisms, such as: nucleotide excision repair (NER, which removes bulky DNA adducts), base excision repair (BER), mismatch repair (MMR) and interstrand cross-link repair (ICLR) – and that does not include repair pathways for backbone breakages like those involved in double-strand break (DSB) repair pathways (Kelland, 1993). To counteract DNA damage, like that inflicted by exposure to cisplatin, cells use DNA damage repair mechanisms and trans-lesion synthesis (Montecucco, Zanetta and Biamonti, 2015). Naturally, one reason for resistance to a drug like cisplatin (or any other of the Pt-based drugs) may be inferred by an upregulation of DNA repair rates, but this raises the question – are cell lines that are resistant to a drug that causes DNA damage, also resistant to other drugs that cause DNA damage?

Drug-adapted cancer cell lines are pre-clinical models that reflect clinically relevant resistance mechanisms (Engelman *et al.*, 2007; Nazarian *et al.*, 2010; Aziz, Shen and Maki, 2011; Poulikakos *et al.*, 2011; Michaelis, Rothweiler, Barth, Cinat, M Van Rikxoort, *et al.*, 2011; Domingo-Domenech *et al.*, 2012; Michaelis *et al.*, 2012; Joseph *et al.*, 2013; Korpal *et al.*, 2013; Crystal *et al.*, 2014; Niederst *et al.*, 2015; Jung *et al.*, 2016; Schneider *et al.*, 2017; Göllner *et al.*, 2017). Here, we introduce a novel set of Pt-based drug-adapted TNBC cell lines consisting of the TNBC cell lines SUM159PT, HCC1806, HCC38, and CAL51 and their sublines adapted to cisplatin, carboplatin, or oxaliplatin (see table 5.1). This novel cell line panel will be an important additional model system for the study of acquired resistance to Pt-based drugs in TNBC and for the comparison of acquired resistance formation against the three approved Pt-based agents.

Cell Line	Drug Adapted To	Concentration Maintained In
SUM159PT	-	-
SUM159PT^{r}CARBO^{4000}	Carboplatin	4000ng/ml
SUM159PT^{r}CDDP^{5000}	Cisplatin	1000ng/ml
SUM159PT^{r}OXALI^{5000}	Oxaliplatin	5000ng/ml
HCC38	-	-
HCC38^{r}CARBO^{3000}	Carboplatin	3000ng/ml
HCC38^{r}CDDP^{3000}	Cisplatin	3000ng/ml
HCC38^{r}OXALI^{5000}	Oxaliplatin	5000ng/ml
HCC1806	-	-
HCC1806^{r}CARBO^{2500}	Carboplatin	2500ng/ml
HCC1806^{r}CDDP^{1000}	Cisplatin	1000ng/ml
HCC1806^{r}OXALI^{2500}	Oxaliplatin	2500ng/ml
CAL51	-	-
CAL51^{r}CARBO^{5000}	Carboplatin	5000ng/ml
CAL51^{r}CDDP^{1000}	Cisplatin	1000ng/ml
CAL51^{r}OXALI^{5000}	Oxaliplatin	5000ng/ml

Table 5.1: List of the cell lines used and the concentrations of platinum drug the cell line is maintained in.

We have used a range of DNA-damaging agents for this study as preliminary data to gain insight into potential sensitivity or cross-resistance to other modes of DNA damage in triple negative breast cancer (TNBC) cell lines that have acquired resistance to Pt-drugs. The drugs selected for cross-resistance analysis in this study are Zeocin, Mitomycin C, Etoposide, and Bleomycin. We also look at potential changes in MEK/ERK and AKT signalling in the Pt-drug resistant sublines, along with sensitivity to MEK, AKT and ChK1 inhibitors.

5.2: Results

5.2.1: Images of the cell lines

Figures 5.1-5.4 show images taken of the cell lines HCC1806, SUM159PT, CAL51 and HCC38 – along with their oxaliplatin (OXALI), carboplatin (CARBO), and cisplatin (CDDP)-resistant sublines. Images of the cell lines were taken to confirm the viability of the cells cultured in the presence of drug, images were taken at random positions from culture flasks to ensure no bias was in place. The HCC1806 (Fig. 5.1) parental cell line showed no difference in morphology compared its platinum-resistant sublines, the cell line grows in a defined monolayer, no observed clumping or unusually high amounts of cellular debris were observed. The HCC1806 cell line morphology presents as almost fibroblast-like, with long reaching protrusions. The SUM159PT cell line appears epithelial-like (Fig 5.2), platinum-resistant (especially the carboplatin resistant sub-line) sublines appear to have a more spherical morphology (but still epithelial-like) at a low confluency compared to the parental cell line but form the same neat monolayers, with no apparent clumping.

CAL51 cell morphology also appears epithelial like (Fig 5.3), platinum resistant drugs appear to adopt a more spherical structure at lower confluences, like that of SUM159. The cisplatin-resistant subline showed considerable clumping and was the slowest growing in this cell line group (see fig 5.5).

Protrusions and subsequently elongated cells is also seen in the drug-resistant HCC38 cell line (Fig. 5.4), becoming most prominent in the cisplatin^{R} subline. The elongation of cells is specific to the drug-adapted sublines in this case. The HCC38 cell line is much flatter and more spread out than the other cell lines, which can be sign of quiescence, however the doubling time of the cell line would suggest otherwise (Fig 5.5) that is displayed in the next section. This cell line also has the slowest rate of growth.

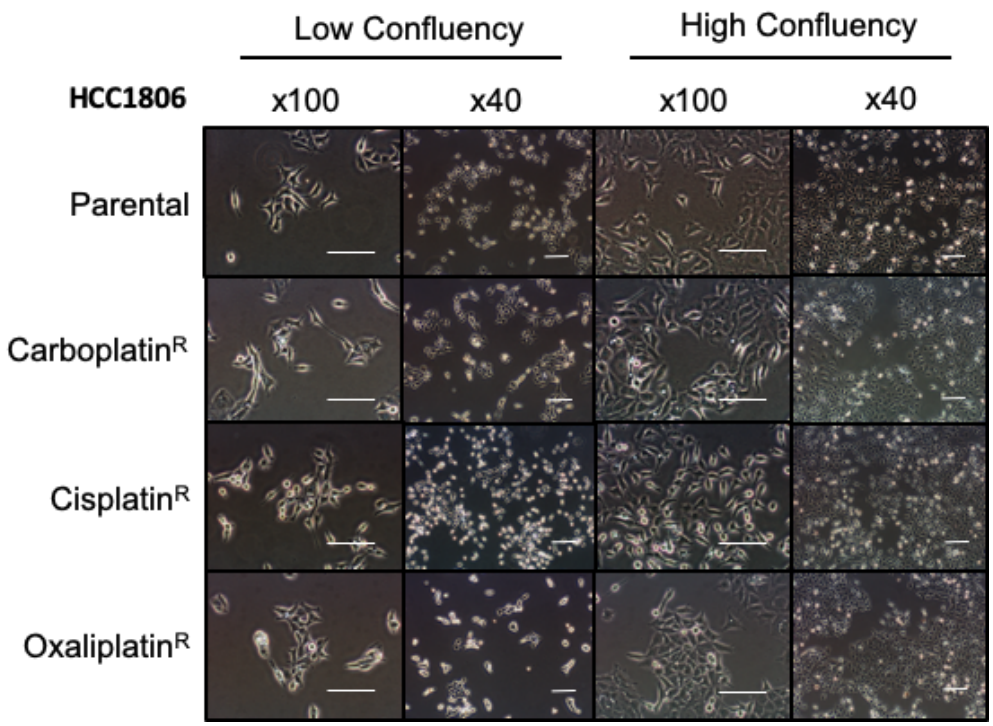


Figure 5.1: Images of HCC1806 cell line and derived platinum-drug resistant sub-lines. Images were taken at both a low and high confluency to show differences in cell morphology when given a greater amount of space to grow at a lower confluency, and when more tightly packed at a higher confluency. There are also images at a lower magnification (x40) and a higher one (x100). **Scale bars are representative of 50 microns.**

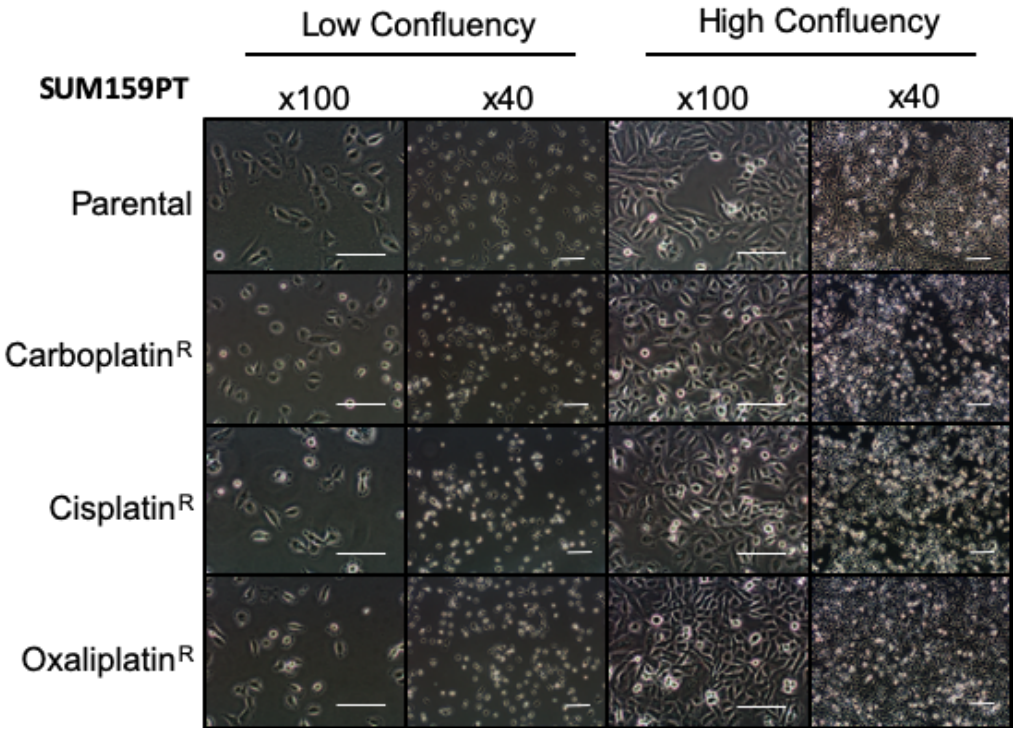


Figure 5.2: Images of SUM159PT cell line and derived platinum-drug resistant sub-lines. Images were taken at both a low and high confluency to show differences in cell morphology when given a greater amount of space to grow at a lower confluency, and when more tightly packed at a higher confluency. There are also images at a lower magnification (x40) and a higher one (x100). **Scale bars are representative of 50 microns.**

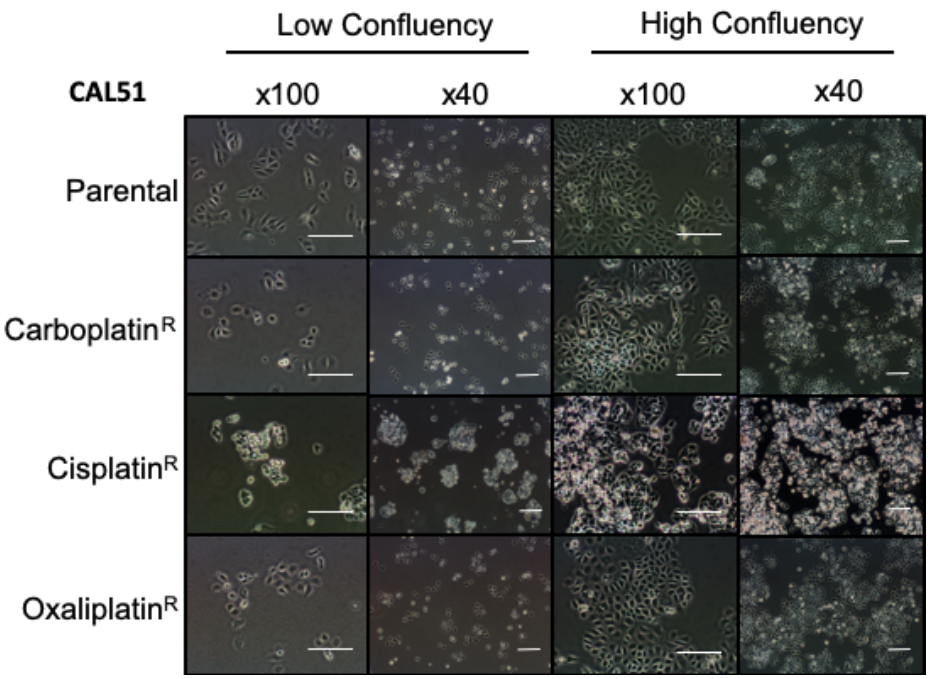


Figure 5.3: Images of CAL51 cell line and derived platinum-drug resistant sub-lines. Images were taken at both a low and high confluency to show differences in cell morphology when given a greater amount of space to grow at a lower confluency, and when more tightly packed at a higher confluency. There are also images at a lower magnification (x40) and a higher one (x100). **Scale bars are representative of 50 microns.**

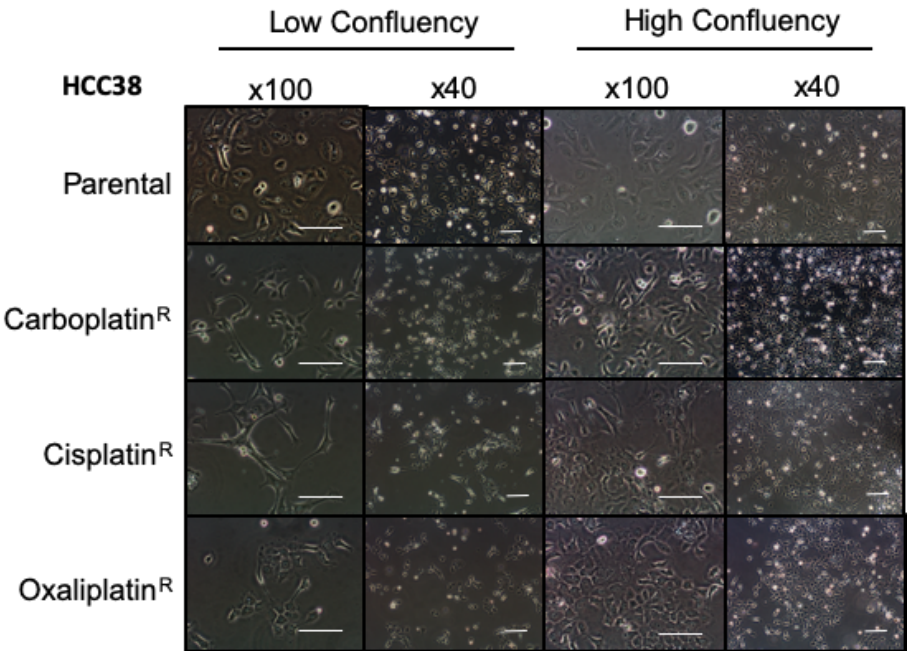
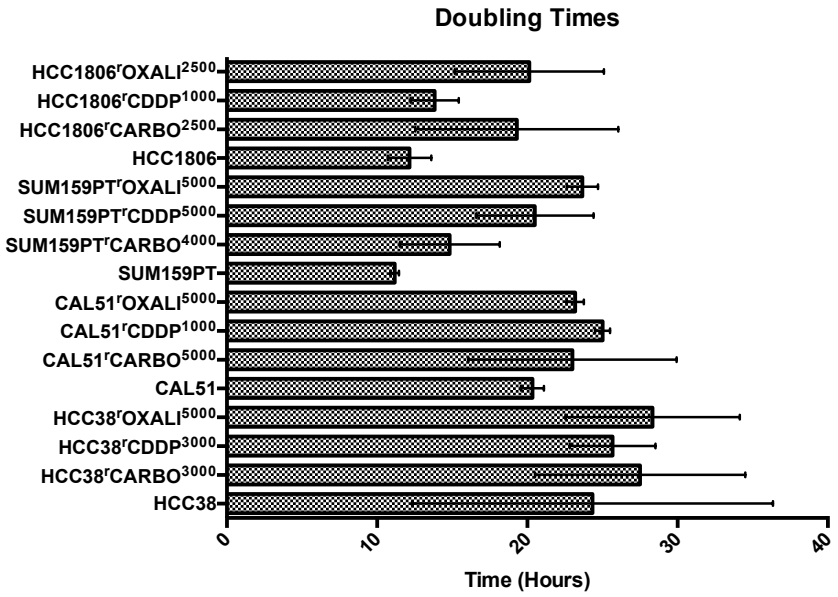


Figure 5.4: Images of HCC38 cell line and derived platinum-drug resistant sub-lines. Images were taken at both a low and high confluency to show differences in cell morphology when given a greater amount of space to grow at a lower confluency, and when more tightly packed at a higher confluency. There are also images at a lower magnification (x40) and a higher one (x10). **Scale bars are representative of 50 microns.**

5.2.2: Cell Growth Characterisation

The doubling times of the cell lines and respective platinum-drug resistant sub—lines was calculated as stated in section 2.2.5. Doubling times are representative of n=3 biological repeats. Doubling times for the drug-resistant sub-lines are on average higher than that of their parental cell lines. The HCC38 was the slowest growing group of cell lines with an average parental doubling time of 24.3 hours, the drug resistant doubling times



Cell Line	Doubling Time (Hours)			
	Parental	Carboplatin Resistant	Cisplatin Resistant	Oxaliplatin Resistant
HCC1806	12.2 (+/-1.4)	13.8 (+/-1.6)	20.1 (+/-5)	19.3 (+/-6.8)
SUM159PT	11.2 (+/-0.3)	20.5 (+/-4)	23.2 (+/-1)	14.8 (+/-3.3)
CAL51	20.3 (+/-0.8)	25 (+/-0.5)	23.2 (+/-0.6)	23 (+/-7)
HCC38	24.3 (+/-12)	25.7 (+/-2.9)	28.3 (+/-5.8)	27.5 (+/-7)

Figure 5.5: Doubling times of the 4 TNBC cell lines and their sub-lines as determined using the xCelligence system as previously described. Each data point is the average of three biological repeats. The doubling times of the cell lines ranged from 11.2-28.3hrs. Drug-resistant sub-lines were cultured in the presence of drug (see table 5.1 for more information on the drug concentrations for culture). Doubling times were calculated as per section 2.2.5.

5.2.3: Resistance status of the platinum drug resistant-cell lines

We analysed the sensitivity of all four sets of triple-negative breast cancer cell lines to carboplatin, cisplatin, and oxaliplatin. The parental cell lines (HCC38, SUM159PT, CAL51, HCC1806) displayed IC_{50} values in the range of clinically achievable drug concentrations. A review of maximum concentrations of anti-cancer drugs by Liston and Davis, (2017) states clinically achievable plasma concentrations of platinum based-drugs as follows: carboplatin IC_{50} values ranged from 1.4-3μM. Therapeutic carboplatin plasma concentrations were reported at a maximum of 135μM. Maximum therapeutic cisplatin plasma concentrations were reported at a maximum of 14.4μM. Cisplatin IC_{50} values were between 0.32 and 0.88μM. The oxaliplatin IC_{50} values displayed the widest distribution ranging from 0.43 to 2.78μM. Maximum therapeutic oxaliplatin plasma levels were reported to be 4.96μM. These values are represented as horizontal lines in figure 5.6.

FC values above 2 compared to respective parental cell lines were considered as resistant. All platinum drug-adapted sublines are cross-resistant to all other platinum-based compounds, aside from HCC38^{r}OXALI^{5000}, which does not display cross-resistance to cisplatin, and HCC38^{r}CARBO^{3000}, which does not display cross-resistance to oxaliplatin (Figure 5.6A). The cisplatin-resistant sublines show a higher degree of similarity to the carboplatin-resistant sublines than to the oxaliplatin-resistant sublines.

Resistance status was confirmed for all of the resistant cell lines used in this study, as they obtained fold change values greater than 2 when compared to their parental cell line.

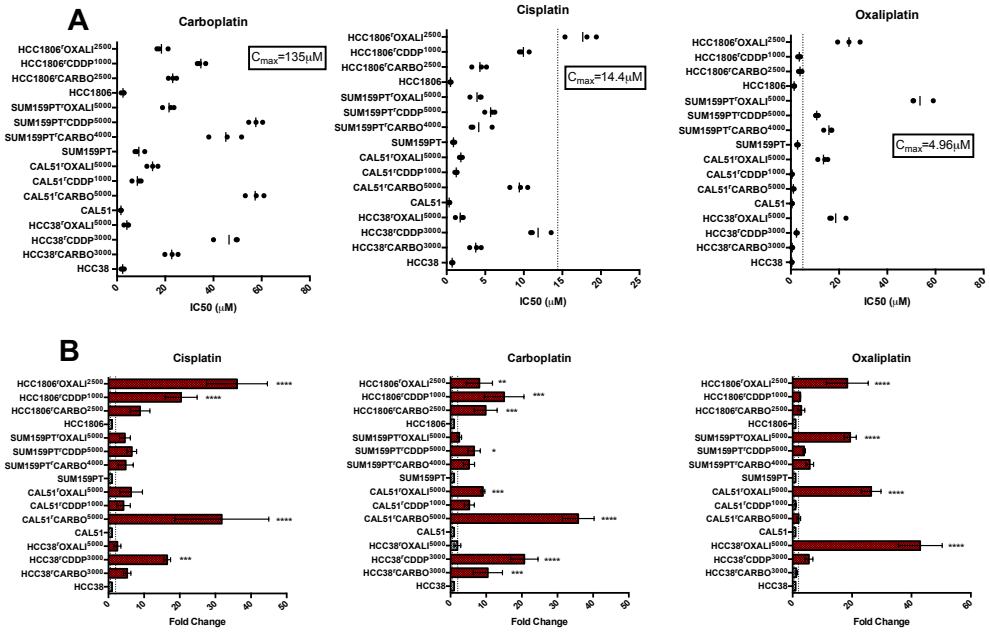


Figure 5.6. Drug sensitivity profiles of the TNBC cell lines and their drug resistant sublines to carboplatin, cisplatin and oxaliplatin respectively. **A)** IC50 concentrations as determined by MTT viability assay after 120hrs of incubation with the drug. Each dot represents a single biological repeat, which represents the average of one biological repeat. Average of n=3 biological repeats shown with a line **B)** sensitivity of the cell line relative to the respective parental line (fold change). All data is representative of n=3 biological repeats, each biological repeat is representative of n=3 technical repeats. Colour indicates resistance status: red = resistant (FC >2), blue = sensitive (FC <0.5). All error bars are representative of +/- SD of n=3 values. Statistical analysis was conducted using two-way ANOVA with tukeys correction. (**** - p<0.0001)(*** - p<0.005)(** - p<0.01)(* - p<0.05).

The IC_{50} data from figure 5.6 has been gathered into drug-resistance status specific groups, by average IC_{50} value. Fig 5.7A, below, plots the four average IC_{50} values for these groups, and fold changes relative to their parental cell lines. Plots pertaining to carboplatin and cisplatin IC_{50} values show similar trends in distribution of all data points and average of these. Sub-line groups that are resistant to carboplatin share similar carboplatin IC_{50} values to sub-lines that are resistant to cisplatin. Sub-line groups that are resistant to cisplatin share similar cisplatin IC_{50} values to sub-lines that are resistant to carboplatin. This trend is not seen with regards to the oxaliplatin-resistant group of cell lines – when tested against carboplatin and cisplatin. Figure 5.7B shows the average fold change of the drug-adapted cell lines relative to their parental cell line. Average oxaliplatin fold changes in the oxaliplatin resistant group was the only data point to show a significant difference to the other groups.

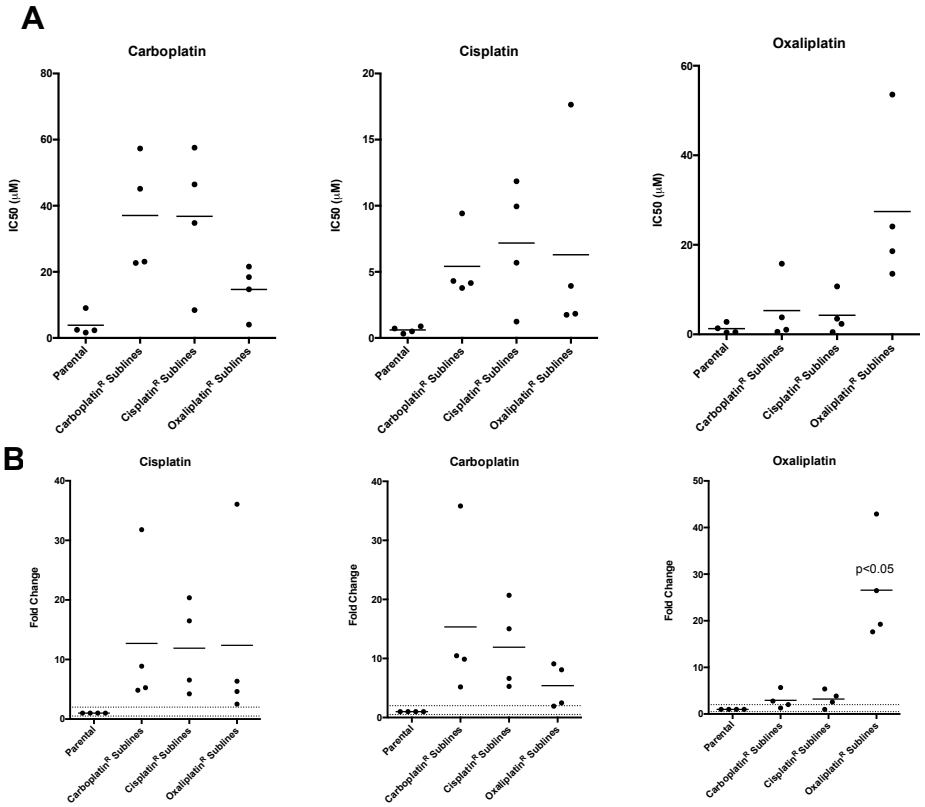


Figure 5.7. Platinum drug sensitivity profiles of the TNBC cell lines when grouped by drug resistance category. **(A)** IC50 concentrations as determined by MTT viability assay after 120hrs of incubation with the drug. Each dot represents the average fold change of three biological repeats - each dot is representative of the average of one cell line. Average of n=3 biological repeats shown with a line **(B)** Average fold changes in IC_{50} value of the cell lines when grouped by drug resistance category. Statistical analysis done by students t-test (* $p<0.05$). Horizontal lines indicate 0.5 and 2 on the Y axis – fold changes <0.5 indicate sensitivity, fold changes >2 indicate resistance.

5.2.4: Cross-resistance evaluation of other DNA damaging agents

We have used a range of DNA-damaging agents for this study as preliminary data to gain insight into potential sensitivity or cross-resistance to other modes of DNA damage in triple negative breast cancer (TNBC) cell lines that have acquired resistance to Pt-drugs. The drugs selected for cross-resistance analysis in this study are Zeocin, Mitomycin C, Etoposide, and Bleomycin.

To see whether platinum drug resistance is associated with a generally decreased sensitivity to DNA damage, the project cell lines were treated with the DNA-damaging agents zeocin, mitomycin C, etoposide, and bleomycin. Part of the bleomycin family, zeocin is most commonly known for its use as a eukaryotic selection antibiotic in molecular biology, but causes double-strand DNA breaks in mammalian cells (Chankova *et al.*, 2007). Mitomycin C, another compound first discovered as an antibiotic, causes the selective inhibition of DNA synthesis as a potent cross-linker of DNA (Tomasz, 1995). Etoposide forms ternary complexes with DNA and topoisomerase II which prevents the DNA from re-ligating during supercoiling, which causes DNA strand breaks (Pommier *et al.*, 2010). The exact mechanism by which bleomycin induces DNA damage is not clear, but it has been shown to be dependent on oxygen and metal ions *in vitro*. It is hypothesised that bleomycin chelates metal (in particular iron) ions, to produce a pseudoenzyme that facilitates the production of superoxide and hydroxide free radicals, which subsequently cleave DNA (Hecht, 2000).

Clinically achievable concentrations of these DNA damaging agents are 2.18μM for mitomycin C, 33.4μM for etoposide, and 706 μM for bleomycin (Liston and Davis, 2017). There is no clinical data available for zeocin as it is not traditionally used to treat patients. However, for the drugs that this data was available for, the observed effective concentrations in Fig 5.8 are in the range of achievable therapeutic plasma levels. Maximum serum concentrations are displayed on their respective graphs as C_{max} values.

Cell line sensitivity to these DNA damaging agents, as shown by the IC_{50} values in figure 5.8 appear to be clustered in cell-line specific groups, where cross-resistance to any one of the DNA damaging agents can be seen in of the multiple Pt-resistant sublines belonging to a cell line group. For example, all of the SUM159PT and HCC38 Pt-drug resistant sub-lines are resistant to zeocin,

where their parental counterparts are not (Fig 5.8B). A trend can be seen between the platinum-drug resistant sublines, and cross-resistance to the other DNA damaging agents, but this appears to be the case in a uniform manner for at least 2, if not all of the pt-resistant sublines.

Fold change data in figure 5.8B shows the HCC38 and SUM159PT set of drug-resistant sub-lines to be cross-resistant to zeocin when compared to than their respective parental lines, with the CAL51 set appearing more sensitive. The HCC1806 carboplatin and cisplatin sublines cell lines show no notable difference, but the oxaliplatin sublines show increased sensitivity. The SUM159PT subline shows the highest tolerance to this compound compared with all of the other TNBC cell lines (Fig 5.8A). As zeocin is known to cause double strand breaks, this may suggest trends in changes to the repair mechanisms for this mode of DNA damage in these individual cell lines as a direct result of resistance to platinum drugs, and therefore adaptation to growth in the presence of alylating agents like cisplatin.

Although some drug-resistant sub-lines are cross-resistant to mitomycin C, there does not appear to be a trend dependent on the platinum-drug that it is resistant to. All HCC1806 pt-resistant sublines are cross-resistant to mitomycin C. The oxaliplatin resistant subline of SUM159PT is resistant to mitomycin C, where no change is seen in the cisplatin resistant subline, and increased sensitivity FC<0.5 is seen in the carboplatin resistant subline. With the CAL51 subline, cross-resistance is confirmed in the carboplatin resistant subline, and sensitivity is seen in the cisplatin resistant subline – no change is seen in the oxaliplatin resistant subline. With the HCC38 sublines, cross resistance to mitomycin C in the cisplatin and carboplatin resistant sublines, but not in the oxaliplatin resistant subline.

No apparent trend between resistance to any one of the platinum based drugs can be seen for potential cross-resistance profiles to etoposide (Fig 5.8B). No change between the parental lines and the pt-resistant lines can be seen in FC values of the HCC1806 sublines. Only the cisplatin resistant subline for SUM159PT shows cross-resistance to etoposide. The CAL51 carboplatin and oxaliplatin resistant sublines show cross-resistance to etoposide, increases sensitivity is observed in the cisplatin resistant sublines. Cross resistance is

observed in the carboplatin and cisplatin resistant sublines of HCC38, and no difference is seen in the oxaliplatin subline.

The complete HCC38 set of sub-lines was seen to be cross-resistant to bleomycin, along with the CARBO^r and CDDP^r HCC1806 sub-lines. Cross-resistance is seen to all of the DNA damaging agents in the carboplatin and cisplatin resistant HCC38 sublines. No change was seen in response to any of the pt-resistant SUM159PT sublines. The only change seen in the CAL51 group of sublines, was an increased sensitivity of the cisplatin resistant subline to bleomycin.

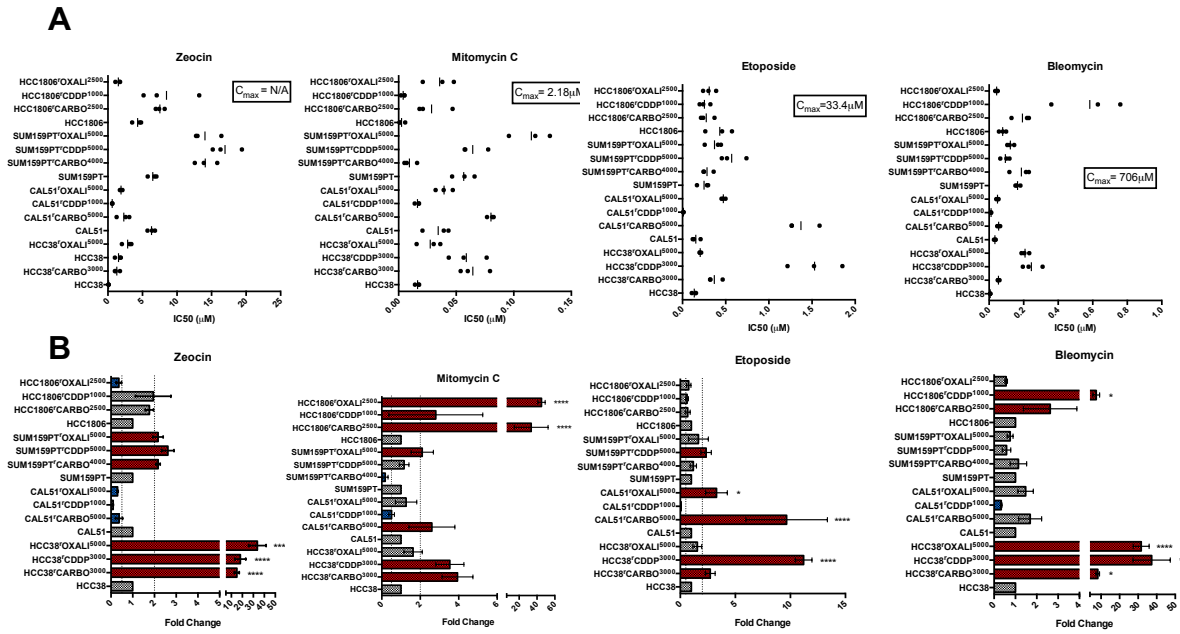


Figure 5.8. Drug sensitivity profiles of the TNBC cell lines and their drug resistant sublines to zeocin, mitomycin C, etoposide and bleomycin respectively. **A)** IC50 concentrations as determined by MTT viability assay after 120hrs of incubation with the drug. Each dot represents a single biological repeat, which represents the average of one biological repeat. Average of n=3 biological repeats shown with a line **B)** sensitivity of the cell line relative to the respective parental line (fold change). All data is representative of n=3 biological repeats, each biological repeat is representative of n=3 technical repeats. Colour indicates resistance status: red = resistant (FC >2), blue = sensitive (FC <0.5). If the bar is too small for blue colour to be visible, it has been indicated with a blue star. All error bars are representative of +/- SD of n=3 values. Statistical analysis was conducted using two-way ANOVA with tukeys correction. (**** - p<0.0001)(*** - p<0.005)(** - p<0.01)(* - p<0.05**).**

The same as how the drug-resistant groups were evaluated for trends in cross-resistance profiles between the platinum based drugs in section 5.2.3, the IC_{50} data from figure 5.8 has been gathered into drug-resistance status specific groups also, by average IC_{50} value. Fig 5.9A, below, plots the four average IC_{50} values for these groups, and fold changes relative to their parental cell lines. No significant difference is seen between any of the groups with regards to their IC_{50} values.

Figure 5.9B shows the average fold change of the drug-adapted cell lines relative to their parental cell line. Average oxaliplatin fold changes in the oxaliplatin resistant group was the only data point to show a significant difference to the other groups. All platinum drug resistant groups place above a fold change of 2 for zeocin, however no significant difference was found due to the wide spread of data points.

The average fold change values for the carboplatin and oxaliplatin resistant subline groups place higher than 2, indicating a potential trend in higher incidence of cross-resistance in these groups, however no significant difference was found due to the wide spread of data points (Fig 5.9B).

The average fold change value of the carboplatin and cisplatin resistant sublines was above 2 for etoposide indicating a potential trend in cross-resistance for these groups, but again, no significant difference was found between these groups due to the wide spread of data points (Fig 5.9B).

Similarly to the fold change values of zeocin, the average fold change of all pt-drug resistant groups to bleomycin was above 2, indicating a potential trend in cross-resistance for these groups, but no significant difference was found between these group due to the wide spread of data points (Fig 5.9B).

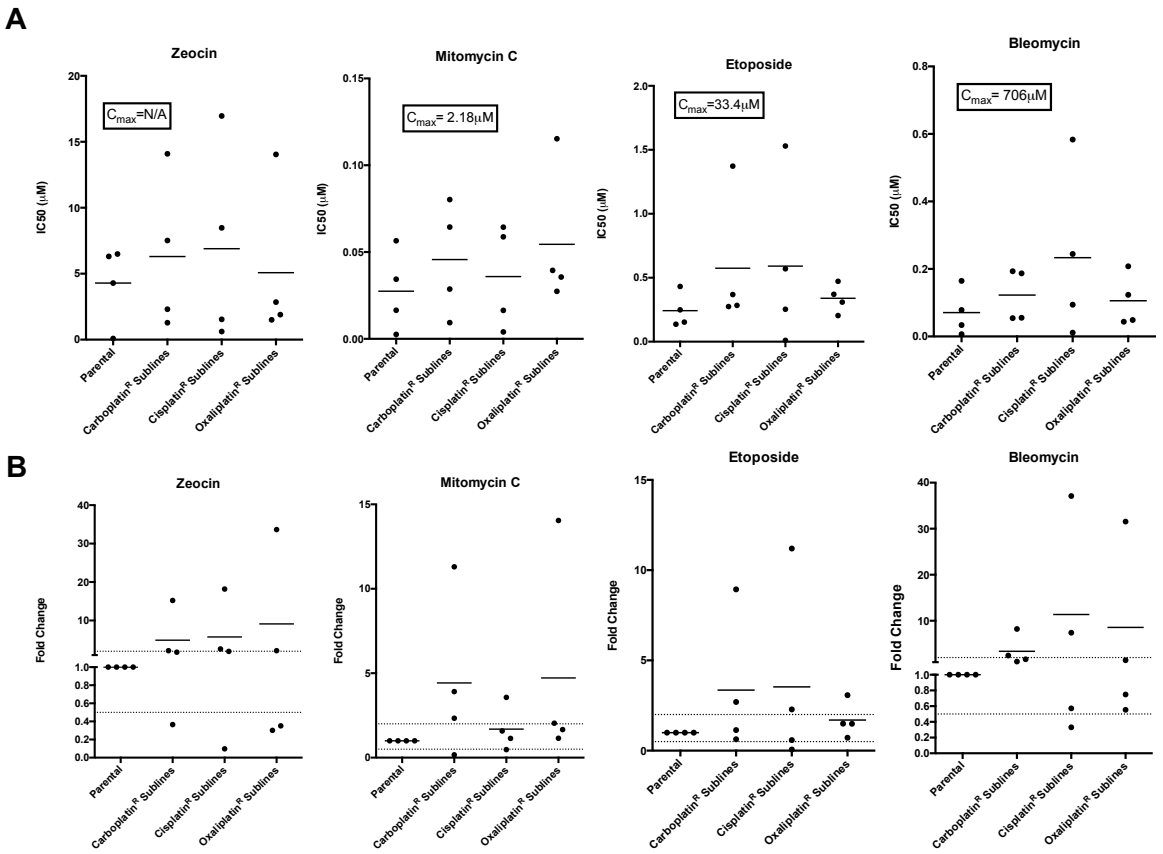


Figure 5.9. Drug sensitivity profiles of the TNBC cell lines to zeocin, mitomycin C, etoposide and bleomycin when grouped by drug resistance category. **(A)** IC50 concentrations as determined by MTT viability assay after 120hrs of incubation with the drug. Each dot represents the average fold change of three biological repeats - each dot is representative of the average of one cell line. Average of n=3 biological repeats shown with a line **(B)** Average fold changes in IC_{50} value of the cell lines when grouped by drug resistance category. Statistical analysis done by students t-test (* $p<0.05$). No Significance was found for any of the data points. Horizontal lines indicate 0.5 and 2 on the Y axis – fold changes <0.5 indicate sensitivity, fold changes >2 indicate resistance.

5.2.5: Western blot analysis of changes to intracellular signalling pathways

Next, the MEK/ERK and AKT intracellular signalling pathways were evaluated for changes in expression as a result of acquired resistance to carboplatin, cisplatin or oxaliplatin. Previous studies have shown that changes to MEK/ERK and AKT signalling plays a role in cisplatin resistance (Mitsuuchi *et al.*, 2000; Yeh *et al.*, 2002), therefore we qualitatively screened these targets, and others that are downstream of these to investigate any potential changes to relative cellular levels of these proteins via western blot, and sensitivity to inhibitors of these proteins *in vitro.*

The specific targets investigated were MEK, ERK, S6RP, AKT and GSK3beta. Antibodies for both phosphorylated and total forms were used. More information on the antibodies used can be found in section 2.2.10. The blots below are representative images of n=3 biological repeats (see appendix VIII and IX).

The individual blots shown in figure 5.10 have been arranged for ease of interpretation. ERK and S6RP are downstream of MEK, so have been arranged as such. GSK3 beta is downstream of AKT and therefore has been arranged as such also.

Cell Line	Main observation (that is consistent with n=3 repeats)
HCC1806	No consistent changes observed
SUM159PT	Upregulation of phosphorylated MEK in all drug resistant sub-lines relative to the parental cell line
CAL51	Downregulation of phosphorylated MEK in cisplatin resistant subline, upregulation of phosphorylated MEK in oxaliplatin resistant subline, no change in the carboplatin resistant subline. These changes are relative to the parental cell line.
HCC38	Upregulation of phosphorylated MEK and phosphorylated ERK in cisplatin-resistant sub-line, upregulation of phosphorylated S6RP in all drug-resistant sub-lines. Decreased amount of total AKT.

Table 5.2: Main observations that were consistently observed over all biological repeats of the data presented in figure 5.10

.

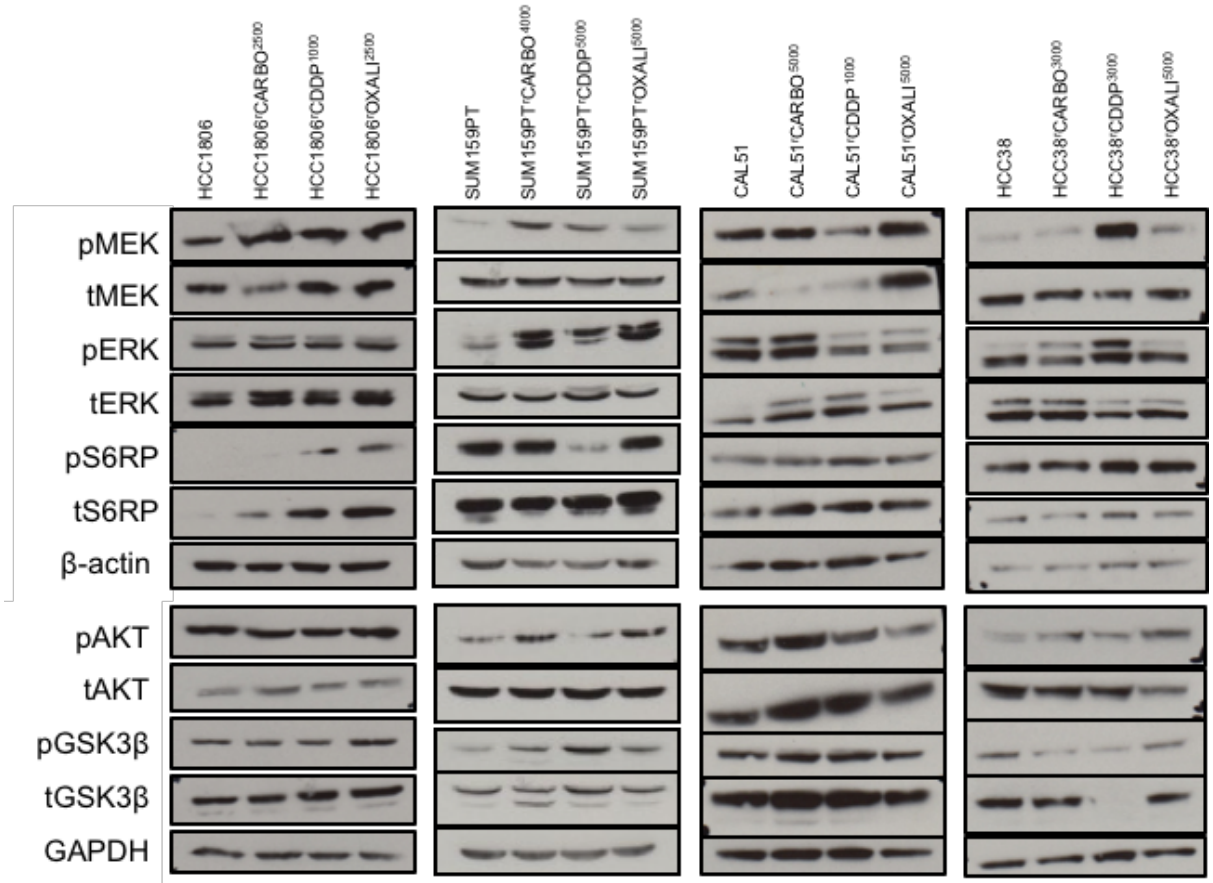


Figure 5.10. Western blot analysis of all four parental cell lines and their Pt-drug resistant sub-lines. Lysates were prepared from 70-80% confluent culture dishes of each cell line or subline. Cell lysates were analysed for expression of the indicated proteins. 'p' denotes a phosphorylated form and 't' denotes the total form of that protein. Each blot is representative the n=1 biological repeat. N=2 and n=3 can be found the supplementary material. All targets in this representative image of blots are all from the same cell lysates, on the same experimental run. Not all blots required the same exposure time, the most appropriate exposure has been selected for each.

5.2.6: Sensitivity to MEK, AKT and ChK1 Inhibition

Next, we used drugs targeted to MEK and AKT, along with a ChK1 inhibitor (known to play a role in breast cancer development and DNA damage response (Awasthi, Foiani and Kumar, 2016)); PD0325901 (MEK inhibitor), MK2206 (panAKT inhibitor) and MK8776 (Chk1 inhibitor).

Figure 5.11A showed the HCC38 sub-set of drug-resistant sublines to be sensitive to MEK inhibition, but resistant to AKT and ChK1 inhibition (relative to the parental counterpart; based on a fold change >2 or <0.5) – perhaps suggesting that the mechanism of resistance to platinum-drugs in this cell line is not only different to the other sub-sets presented here, but heavily reliant on MEK signalling – referring back to the western blot data from the previous section, an upregulation of phosphorylated MEK is seen notably in the cisplatin resistant subline (Fig 5.10), which coordinates with the increased sensitivity to pharmacological MEK inhibition observed. However, this same upregulation of phosphorylated MEK is not seen in the other drug-resistant HCC38 sublines, nor is any obvious difference seen in ERK expression – this may be explained by alterations to other targets downstream of MEK or ERK that have not been evaluated here. MEK inhibition has also been observed to overcome cisplatin resistance in squamous cell carcinoma cells lines (Kong *et al.*, 2015). On the other hand, all three of the Pt-drug resistant HCC1806 sublines, and the carboplatin and cisplatin adapted sublines of SUM159PT are resistant to MEK inhibition compared to the parental subline. There is no change to expression levels of MEK seen in the HCC1806, nor are there any changes seen in the downstream targets of MEK that were investigated. But, an upregulation is seen of phosphorylated MEK in the SUM159PT sublines which is contrary to what is seen in the HCC38 sublines.

The CAL51 oxaliplatin resistant subline shows sensitivity to MEK inhibition, but is not supported by any changes to MEK signalling in figure 5.10.

Fig 5.11A shows all HCC1806 and SUM159PT sublines to have comparably higher IC_{50} values to CAL51 and HCC38 sublines. Fig 5.11B shows none of the SUM159PT or CAL51 Pt-resistant sublines show any difference to AKT inhibition from the parental lines. The HCC38 Pt-resistant sublines are the only sublines shown to display a significantly decrease in sensitivity to AKT inhibition - the observation of an decreased amount of total AKT was observed in this cell line, but not in the cisplatin or carboplatin resistant sublines (Fig 5.10).

The parental SUM159PT cell line showed comparatively higher IC_{50} values to the other cell lines, suggesting that this cell line is less sensitive to ChK1 inhibition in general (Fig 5.11A). Both the HCC1806 and SUM159PT oxaliplatin resistant sublines showed sensitivity to ChK1 inhibition when compared to their parental cell lines. The CAL51 cisplatin subline also showed sensitivity to ChK1 inhibition compared to its parental subline. The HCC38 cisplatin and carboplatin resistant sublines showed a statistically significant increase in fold change value, and resistance to Chk1 inhibition.

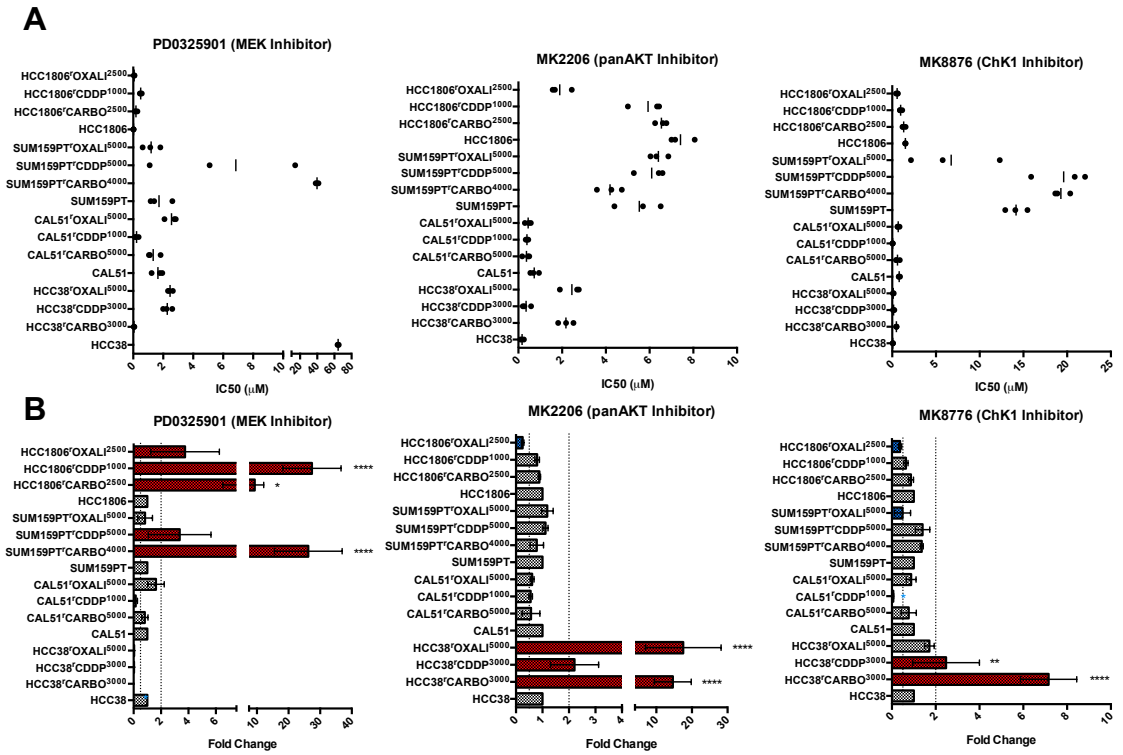


Figure 5.11. Drug sensitivity profiles of the TNBC cell lines and their drug resistant sublines to MK2206, MK8776 and PD0325901 respectively. **A)** IC50 concentrations as determined by MTT viability assay after 120hrs of incubation with the drug. Each dot represents a single biological repeat, which represents the average of one biological repeat. Average of n=3 biological repeats shown with a line **B)** sensitivity of the cell line relative to the respective parental line (fold change). All data is representative of n=3 biological repeats, each biological repeat is representative of n=3 technical repeats. Colour indicates resistance status: red = resistant (FC >2), blue = sensitive (FC <0.5). If the bar is too small for blue colour to be visible, it has been indicated with a blue star. All error bars are representative of +/- SD of n=3 values. Statistical analysis was conducted using two-way ANOVA with tukeys correction. (**** - p<0.0001)(*** - p<0.005)(** - p<0.01)(* - p<0.05**).**

Figure 5.12, below, shows the IC_{50} and fold change values of the three inhibitors used for this study and displayed in figure 5.11, above. Again, these have been grouped into drug-resistance specific categories. Figure 5.12A shows the IC_{50} values to be spread so variably between the cell lines that no significant difference can be observed between the individual inhibitors - resistance to either cisplatin, carboplatin or oxaliplatin does not appear to confer response to any one of these inhibitors in these cell lines. As clear patterns in resistance or sensitivity to certain inhibitors can be seen in figure 5.1, above, this suggests that response to MEK, AKT or ChK1 inhibition is cell line specific rather than drug-resistance group specific. Fig 5.12B shows the fold changes relative to the parental cell lines groups – here we are considering any variation from the range of 0.5-2 to show a notable difference in response compared to the parental cell lines. The average

fold changes for PD0325901 (MEK inhibitor) appear to be raised in the carboplatin and cisplatin resistant groups, but not the oxaliplatin resistant groups. – which fall within the 0.5-2 FC range, with the parental cell lines. However, this is likely due to the HCC38 cell lines This may suggest more of an involvement of MEK signalling activity in the carboplatin and cisplatin resistant sublines compared to the parental and oxaliplatin resistant sublines. Comparing this data to the western blot analysis from the previous section, a trend in increase of MEK phosphorylation was observed in the drug-resistant cell lines (Fig. 5.10) which may indicate an increased dependency on this pathway. No significant difference was found in any of these grouped analyses in figure 5.12, however.

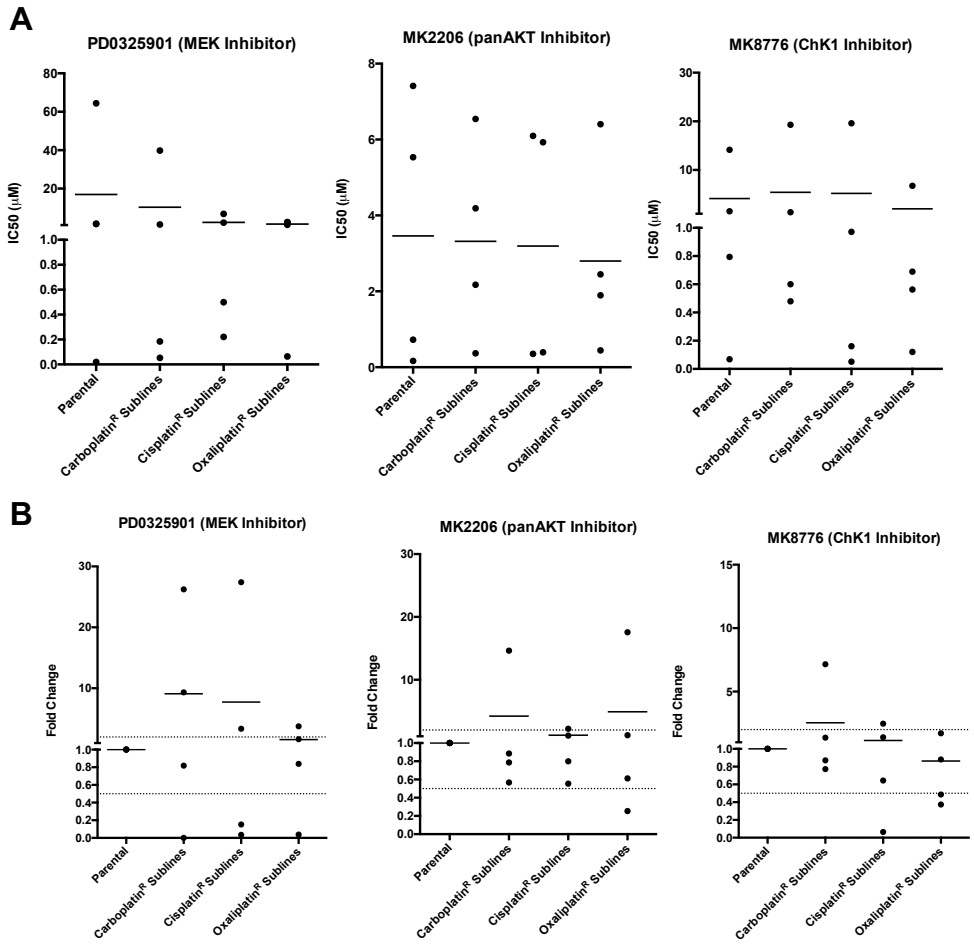


Figure 5.12. Drug sensitivity profiles of the TNBC cell lines to MEK, AKT and ChK1 inhibition when grouped by drug resistance category. **(A)** IC50 concentrations as determined by MTT viability assay after 120hrs of incubation with the drug. Each dot represents the average fold change of three biological repeats - each dot is representative of the average of one cell line. Average of n=3 biological repeats shown with a line **(B)** Average fold changes in IC_{50} value of the cell lines when grouped by drug resistance category. Statistical analysis done by students t-test (* $p<0.05$). No significant difference was found for any of the data points. Horizontal lines indicate 0.5 and 2 on the Y axis – fold changes <0.5 indicate sensitivity, fold changes >2 indicate resistance

5.3: Discussion

This study introduces a novel set of platinum drug-resistant TNBC cell lines including carboplatin-, cisplatin-, and oxaliplatin-adapted sublines of HCC38, SUM159PT, CAL51 and HCC1806. This novel cell line panel will be an important additional model system for the study of acquired resistance to Pt-based drugs in TNBC and for the comparison of acquired resistance formation against the three approved Pt-based agents. Cell lines derived from tumours comprise the most frequently utilised living systems to research tumour biology. Cancer cell lines, such as the ones used in this study, have been extensively used in screening studies involving the effectiveness of anti-cancer drugs (Yamori, 2003). This was work was conducted to not just evaluate the effect of cross-resistance to DNA-damaging agents in platinum-drug resistant cell lines, but to evaluate

TNBC cell line sensitivity to DNA damaging agents in general. This can be inferred by the response of the parental cell lines to each of the compounds utilised in this chapter.

5.3.1: Resistance status of the cell lines

Cross-resistance between platinum-based anti-cancer drugs has been observed in the clinic for more than 30 years (Gore *et al.*, 1989). Here we have confirmed *in vitro* that resistance to a specific platinum-based compound can also provide cross-resistance to other platinum based drugs in TNBC cell lines. It would be interesting to investigate whether this is also observed in cancer cell lines of differing tissue types – and is a pan-cancer trend.

A trend is seen throughout the panel of resistant sublines, that acquired resistance to one platinum-based compound shows cross-resistance to the other two platinum based compounds (see figure 5.6). We show that a relative sensitivity to carboplatin or cisplatin can be observed in oxaliplatin resistant cell lines. Oxaliplatin is a commonly used first-line therapy for malignancies such as non-small cell lung cancer (Raez, Kobina and Santos, 2010) that is not traditionally used as a first line therapy for the treatment of TNBC – here we evaluate the potential for its use as a first line therapy, and the potential use of carboplatin and cisplatin following oxaliplatin failure. Although here we saw a degree of cross-resistance to cisplatin and carboplatin, in the oxaliplatin resistant sub-lines investigated in this chapter, we saw that these drug-resistant sub-lines were far more resistant to oxaliplatin alone that to the other platinum based drugs. Where cell lines that had acquired resistance to carboplatin or cisplatin showed a great deal of cross-resistance to oxaliplatin.

Pt-based anti-cancer compounds work by forming platinum-DNA adducts, primarily intrastrand cross-link adducts, following uptake of the drug into the nucleus of the cell - these adducts are responsible for activating the cellular transduction pathways and processes that eventually lead to cell death (Wang and Lippard, 2005). Development of resistance to Pt-based compounds is complex and is not thought to be caused by any one mechanism; increased drug efflux, poor intracellular drug accumulation due to decreases in cell surface transporters or perhaps hyperactivity of DNA damage repair mechanisms may be

responsible (Galluzzi *et al.*, 2014; Sarin *et al.*, 2017; Rocha *et al.*, 2018). For future work on this novel panel of cell lines, and to further elucidate the mechanisms of resistance that will explain the data shown in this chapter – these factors should be investigated in the context of explaining the cross-resistance to other DNA damaging agents that we see in this chapter.

5.3.2: Cross resistance to other DNA-damaging agents

Each of the drugs used for sensitivity screening in this study were selected based on their differential modes of DNA damage. To summarise: Zeocin causes double strand breaks (Chankova *et al.*, 2007), Mitomycin C causes DNA cross-links (Tomasz, 1995), etoposide inhibits Topoisomerase II (preventing ssDNA breaks from reannealing) (Pommier *et al.*, 2010; Montecucco, Zanetta and Biamonti, 2015), and bleomycin has multiple modes of action but works primarily through double strand breakage (but also single strand breakage) due to superoxide and free radical formation in the presence of iron and oxygen (Hecht, 2000; Chen *et al.*, 2008). As we have not performed any quantitative studies on which particular DNA repair pathways have been activated in response to the DNA damaging drugs in this study, or compared their activity levels in the platinum drug resistant cell lines compared to the parental TNBC cell lines, we can only describe *in vitro* sensitivity to different DNA damaging agents in these cell lines and hypothesise which modes of DNA damage these cell lines may be more susceptible to.

Here we show that resistance to DNA damaging agents as a direct result of resistance to platinum-based drugs appears to be cell line specific, and not necessarily specific to the platinum drug that the sublines is resistant to. For example, Fig 5.8 shows all platinum drug resistant SUM159PT and HCC38 sublines to be cross-resistant to Zeocin, whereas all CAL51 platinum drug resistant sublines are sensitive to this compound. This uniformity in cross-resistance throughout all platinum drug resistant sublines is not seen for all of the DNA damaging drugs, however.

No significant relationship is found between resistance to any one platinum based drug, and cross-resistance to these other DNA damaging agents when grouped together in figure 5.9. Other methods would need to be combined with the data in this chapter to elucidate the extent, mechanism and locality of DNA damage caused by these individual agents. Incubation of these cell lines with an appropriate concentration of each of these agents, before further experimentation would be one methods for this – qPCR could be used to evaluate differences in DNA repair proteins to identify which DNA repair pathways are activated, super resolution immunostaining to evaluate locality of recruitment of DNA repair machinery for detection of DNA damage or techniques such as the comet assay

for detection of DNA breaks (Liao, McNutt and Zhu, 2009).

5.3.4: Evaluation of changes to intracellular signalling pathways

Previous studies suggest that changes to intracellular signalling cascades (that have been associated with cellular response to DNA damage, like that due to the formation of DNA adducts by cisplatin), such as the AKT and MEK pathways, has a strong association with the development of resistance to platinum compounds (Mitsuuchi *et al.*, 2000; Asselin, Mills and Tsang, 2001; Cheng *et al.*, 2002; Siddik, 2003).

The MEK/ERK and pathways are responsible for controlling a variety of intracellular processes (Shaul and Seger, 2007; Manning and Toker, 2017), but their involvement in platinum-drug resistance is not completely understood. The PI3K/AKT pathway is thought to be hyperactivated in ~10% of TNBC patients – hence why combination therapies with AKT inhibitors are becoming increasing popular in clinical trials (Vojtek *et al.*, 2019). Here we selected portions of those signalling cascades to investigate the impact that acquired resistance to platinum-based compounds may have on the expression of select components of these signalling pathways, and compare it to data that evaluates pharmacological inhibition of MEK and AKT. Overall, we saw no significant difference to inhibition of AKT, MEK or Chk1 when grouped by drug-resistance status in our four cell lines, and their respective platinum-drug resistant sublines. However, we did observe cross-resistance profiles that were separated by originating cell line. We observed the HCC1806 and SUM159PT panel of Pt-resistant sublines to be less sensitive to MEK inhibition, the CAL51 sublines were unaffected by any of the targets apart from the cisplatin resistant subline, that was sensitive to MEK and ChK1 inhibition, and the HCC38 sublines were all found to be sensitive to MEK inhibition, and resistant to AKT and ChK1 inhibition. This variability in response to inhibition of these targets in these cell lines again highlights heterogeneity in TNBC cell lines.

A study by Gohr *et al.*, (2017) looked at the effect of AKT inhibition of cisplatin resistant HCC38 and MDA-MB-231 cells. They deduced that an upregulation of AKT through epidermal growth factor (EGFR) and insulin-like growth factor-1 (IGF1R) was a causative factor for cisplatin resistance in their model, and combination inhibition of these two receptors and AKT was an effective strategy

to re-sensitise the cell lines to cisplatin. In our cell line models, we saw that the HCC38 set of platinum drug resistant sub-lines was the only cell line to show any difference from their parental cell lines – which supports the observation that AKT can play a role in platinum drug resistance, but not necessarily in all cases.

Combination studies of these inhibitors and their respective resistant drug would be the next step in this investigation for these cell lines.

Here we did not see any strong trends in either upregulation or downregulation of the majority of our chosen targets when in the context of resistance to platinum-based compounds – suggesting simply that these targets are not tightly regulated as a direct causative of resistance to platinum-based agents. However, the few observations that were consistently observed involved changes to phosphorylated MEK or phosphorylated ERK (see table 5.2, and appendix VIII and IX). As these observations were consistent only in phosphorylation levels of these components, this suggests that it may be the activation of certain intracellular signalling cascades that contributes to platinum drug resistance rather than the general over or under production of these total proteins compared to their parental counterparts. MEK signalling has been linked to cisplatin resistance, making this pathway a candidate for further investigation in these cell lines (Kong *et al.*, 2015).

5.3.5: Rationale for Selection of MEK, AKT and ChK1 Inhibitiors for This Study

In physiologically normal tissues, cellular signalling pathways are tightly regulated, but interconnected to form complex signalling networks. As such, they are an important consideration when it comes to investigating the dysregulation of growth that is seen in cancer. As hormone receptor negative breast cancer has notoriously limited treatment options, recent studies have identified intracellular signalling pathway inhibitors such as MEK and AKT inhibitors as promising candidates for monotherapies, and combination therapies in various cancer types including triple negative breast cancer (Naderi, Chia and Liu, 2011; Banerji *et al.*, 2018). As such, these inhibitors were selected for investigation with our panel of platinum resistant TNBC cell lines.

Furthermore, in recent years, a light has been shone on the potential of ChK1 inhibitors for the treatment of TNBC through clinical trials in combination with putative chemotherapeutic agents, and even as a monotherapy are proving to be viable treatment options for TNBC (Bryant, Rawlinson and Massey, 2014), hence its selection for use in this study also.

Combinations of these inhibitors are also being looked at in an ongoing fashion in pre-clinical studies and clinical trials, with interstrand crosslinking agents, such as the platinum-based agents used in this study (Armstrong-Gordon *et al.*, 2018; Wu *et al.*, 2019). Considering trends that were seen in a cell-line specific manner with the monotherapy inhibitor data in figure 5.11, in that some cell lines were either more resistant, or more sensitive to MEK, AKT or ChK1 inhibition when also resistant to each of the platinum based drugs used in this chapter – it would therefore be an interesting next step to look at combination therapies with these inhibitors, and also other emerging cell signalling inhibitors with the platinum drug resistant cell lines, when treated with the platinum drugs that they have been made resistant to.

5.4: Conclusions

This study introduces a novel set of platinum drug-resistant TNBC cell lines from HCC38, SUM159PT, CAL51, and HCC1806. We have shown that a great deal of cross resistance is shown between the platinum drugs We have shown that cisplatin and carboplatin may be viable second-line treatment options for patients with oxaliplatin non-responsive tumours in TNBC, even though oxaliplatin is not traditionally a treatment regimen employed for first line therapy in TNBC patients. Resistance to platinum drugs does not necessarily infer cross-resistance to DNA damaging agents of other mechanistic means, and in the instance of cross-resistance, is cell-line specific rather than drug-resistance status specific. We have also shown that platinum-drug resistant TNBC sub-lines are sensitive to intracellular signalling inhibition in a cell-line specific manner. We evaluated the cell lines for differences in MEK/ERK and AKT signalling, and found the only consistent differences between the parental and Pt-resistant sublines placed in the MEK signalling cascade, suggesting that the AKT pathway is not greatly associated with resistance in this panel of drug-resistant cell lines.

Chapter 6: General Discussion

6.1: General research aims of this work

In chapter 1, the complexity of oestrogen signalling, and how endocrine resistance emerges was discussed. It is clear from this that a number of factors can affect the emergence of acquired endocrine resistance (Musgrove and Sutherland, 2009; Rondon-Lagos *et al.*, 2016). Most publications investigate mechanisms of resistance in a single cell line setting, here we have systematically generated two panels of 6 ER+ breast cancer cell lines in tandem (resulting in a total of 46 sublines) one as a potential model for resistance to long-term systemic oestrogen deprivation (24 sublines), the other a model for acquired resistance to long-term tamoxifen exposure (22 sublines). These panels have been characterised for response to tamoxifen and other commonly used anti-cancer agents to treat breast cancer. Oestrogen receptor localisation and expression levels were evaluated for the purpose of evaluating the relative changes in expression of both ER alpha and beta. It is not clear from the majority of studies, on the broad topic of drug resistance in cancer, whether the emergence of resistance mechanisms is reproducible over many individual cell lines. Over the course of this thesis, drug response data has been presented for a large number of drug-adapted breast cancer cell lines, to evaluate the likelihood of heterogeneity between multiple breast cancer cell lines.

Although this thesis does not present any data to elude the mechanisms responsible for resistance to the drugs investigated, it does present preliminary data to suggest the directionality of future studies with panels of cell lines that have systematically been produced in tandem to model both aromatase inhibitor resistance and tamoxifen resistance. This work should be considered testament to the necessity to study drug resistance to cancer with large data sets or larger numbers of cell lines to account for observable heterogeneities in drug response and drug resistance in cancer.

6.2 Why MTT assays?

The MTT assay is one of the most versatile and popular techniques for measuring cell viability in a research setting. It does this, similarly to other viability assays such as MTS and Alamar Blue, by a measuring metabolic activity. Naturally, there is great debate in literature and between researchers as to what method is most accurate for the measure of cell viability. But, the advantage of the MTT assay is that it shows sensitivity to small changes in metabolic activity that can occur in response to cell stress caused by exposure to toxic agents, that may not necessarily directly cause cell death (Kumar, Nagarajan and Uchil, 2018). The rationale behind the MTT assay is that once cells lose viability, they lose the ability to convert MTT substrate to formazan, therefore producing an amount of formazan that is proportional to the amount of viable cells present. It can of course be argued that the MTT assay has drawbacks; such as its ability to be affected by factors like metabolic perturbations (Stepanenko and Dmitrenko, 2015). Generally speaking, the main points for comparison in chapters 3, 4 and 5 of this thesis (which investigate cellular response to anti-cancer drugs by means of MTT assay) are dependent on the comparisons of sublines that have undergone adaptation to growth in media conditions that are not orthodox for that cell line. Whether that be adaptation to growth in the absence of growth hormones, or adaptation to growth in the presence of an anti-cancer drug. This may have affected the metabolic activity of the adapted cell lines compared to those of the respective parental cell lines. However, all cell lines have been investigated in a controlled, comparable and systematic manner – by maintaining consistency in the protocol used for every data point produced by MTT assay in this thesis.

There are other viability assays that are also widely used for measures of cell viability, such as the exclusion trypan blue assay or the SRB assay. But this latter technique has its own drawback in that it differentiates viable cells and non-viable cells by means of measuring total protein, or in other words, what is still adhered to the bottom of a 96 well plate. Both of these assays have been compared in literature and are generally thought to be of comparable performance (Voigt, 2005). The MTT assay has been used throughout this thesis in order to maintain consistency between experiments - however, it would be interesting to assess the use of the SRB assay in parallel to the MTT assay with these cell lines.

6.3: Comparison and summary between cell lines in chapters 3 and 4

Two individual panels of ER+ breast cancer cell lines were adapted in this work to model endocrine resistance from two different viewpoints: acquired resistance to aromatase inhibitors and acquired resistance to tamoxifen – the two most commonly used therapies to treat ER+ breast cancer (Dowsett *et al.*, 2010). In this investigation, cell morphology was compared, in which little change was observed, aside from a clumping of cells when introduced to growth hormone deprived media conditions. Growth hormone deprivation of the charcoal stripped serum used in this study was confirmed by an observed difference in response between sublines that had been adapted and newly introduced to growth in this condition (see figure 3.7 and 3.8) – literature states that an observed quiescence of cell lines in this media containing charcoal stripped serum is a measure of this (Sikora *et al.*, 2016). Oestrogen receptors are known to form complexes with heat shock proteins in response to low levels of oestrogen (Lipovka and Konhilas, 2016). A qualitative evaluation of oestrogen alpha and beta localisation showed an increase in nuclear localisation of both oestrogen receptors in response to (Z)-4-OH-tamoxifen resistance status, and not necessarily due to oestrogen deprivation.

The metabolic processes associated with tamoxifen have been discussed at length within the results chapters. To summarise, data from chapter 3 showed us that not all metabolites of tamoxifen have the same potency. An interesting observation was that there is a shared relationship between cell line response to unmetabolised tamoxifen and (Z)-4-OH-tamoxifen, perhaps suggesting that the breast cancer cell lines show metabolic activity that has a preference for the production of (Z)-4-OH-tamoxifen, or that these two compounds share a mode of action that the other metabolites do not. It was also shown that response to n-desmethyltamoxifen is the only metabolite that is affected by oestrogen-deprivation. When bringing the data from chapter 4 into consideration with this, it is clear that resistance to (Z)-4-OH-tamoxifen does not confer cross-resistance to the other metabolites. In this regard, endoxifen was an interesting metabolite to consider as the fewest (Z)-4-OH-tamoxifen resistant sublines showed cross-resistance to this metabolite. For future work, it would be interesting to model the binding of each of these metabolites to oestrogen receptors, and which oestrogen receptor they may show preference for. Oestrogen receptors are known to strike

a balance between proliferative and anti-proliferative effects (Makinen, 2001; Mitra *et al.*, 2003) with alpha and beta respectively. One of the hallmarks of cancer is a dysregulation of growth (Hanahan and Weinberg, 2011) that can be brought about by imbalances in expression of these two controllers of cellular proliferation. The majority of literature states that an upregulation of ER alpha is observed in not only oestrogen deprivation, but also in resistance to tamoxifen (Chang, 2012; Darbre, 2014), which disrupts the balance that can be found in physiologically normal tissue, and disrupt further that which may already be disrupted in breast cancer cell lines. Here we show that changes in receptor expression, of both alpha and beta, occurs in a heterogeneous and cell line specific manner. Upregulation of ER alpha was observed in the largest proportion of both growth hormone deprived cell lines and tamoxifen resistant cell lines, but downregulation was also observed in some of the cell lines – this highlights the possibility of receptor expression changes to both extremes. ER beta expression was not seen to change drastically in the hormone deprivation adapted cell lines, but decreases were observed in the model of tamoxifen resistance. Levels of ER beta are not often considered when investigating resistance mechanisms to tamoxifen, so this would be an interesting point for further consideration.

In concentrations akin to that found in culture media, phenol red is thought to elicit an oestrogenic response. Phenol red itself is only thought to have 0.001% the binding affinity for oestrogen receptors to that of oestrogen (Berthois, Katzenellenbogen and Katzenellenbogen, 1986; Rajendran, Lopez and Parikh, 1987). This factor was included in this study to gain perspective on whether its presence in media that was intended to deprive cells of growth hormone, has enough of a stimulatory effect to negate the action of using charcoal stripped serum altogether. From the data gathered, this appears to be subjective to the cell line in question. Growth kinetics of the cell lines in +CS/-CS conditions (fig. 3.7) show comparable growth (or lack of growth in this case) in hormone deprived conditions that both do and do not contain phenol red. The CAMA-1 and MDA-MB-468 cell lines in +CS conditions show growth comparable to media conditions that contain FBS, and therefore growth hormones, when other cell lines do not show this trend. Oestrogen receptor expression levels have been shown to be cell line dependent, which must mean that the amount of oestrogen required for maximal oestrogenic stimulation of a cell line is also cell line dependent. Perhaps

in these cell lines, oestrogen requirements are lower, and therefore the oestrogenic stimulation that phenol red provides is enough to mimic the oestrogenic activity of FBS.

6.4: Heterogeneity of drug adapted cancer cell lines

The emergence of drug resistance in cancer cell lines has the possibility to be attributed to wide variety of mechanisms. Especially as commonly used systemic chemotherapies have a diversity of modes of action (Alfarouk *et al.*, 2015). Previous studies have shown that when clonal populations of the same cell line are exposed to an anti-cancer drug simultaneously for enough time to develop acquired resistance, different responses can be observed that contribute to resistance (Michaelis, Rothweiler, Barth, Cinat, M. Van Rikxoort, *et al.*, 2011). It is not unusual for studies that instigate the emergence of acquired drug resistance in cancer to include only one cell line. This does not allow for the observation of potential heterogeneity between cell lines, or between different populations of the same cell line. In this work, and for all chapters, multiple cell lines have been utilised to observe differential responses to anti-cancer drugs in the context of drug resistance for this very reason. In chapters 3, 4 and 5 of this thesis, it has been demonstrated that whether it is resistance to tamoxifen or platinum based-drugs in question, different cell lines present with differential responses to drug adaptation.

6.5: Future Work for chapters 3 and 4

There are a number of factors that have been discussed to attribute to resistance to endocrine therapy – these include mutations to ER receptors, changes to ER expression, changes to expression of other growth factor receptors and cross-talk with other signalling pathways (Massarweh *et al.*, 2008; Musgrove and Sutherland, 2009; Rondon-Lagos *et al.*, 2016; Mansouri *et al.*, 2018; Bhateja *et al.*, 2019). These are factors that can be investigated with these new panels of endocrine therapy resistant cell lines.

The results discussed in this thesis focus on the production of these cell lines, and a generalised look at cell growth, morphology, expression of only the wild-type ERs, and response to exposure to a variety of anti-cancer compounds. Given the complexity of oestrogen signalling that was discussed in chapter 1, there is a large number of factors that could potentially be altered to bring about

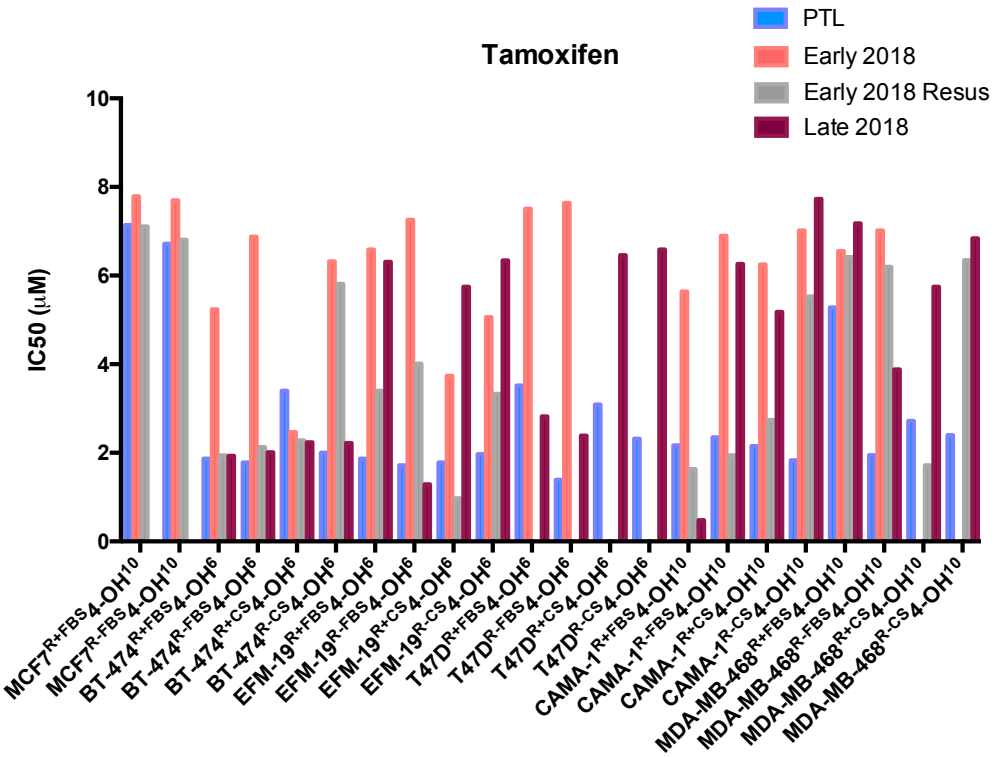
resistance to endocrine therapy. To look at the genomic changes to the drug-resistant cell lines, they could be whole genome sequenced and analysed for mutations compared to their respective originating cell lines and same-media parental sub-lines. Proteomics and metabolomics approaches also could elucidate changes to the signalling landscape of the cell lines. Aside from these more intricate approaches, the cell lines could be assessed for differing expression levels of the clinically relevant splice variants of the oestrogen receptors and GPER1, with the localisations of these individual variants also looked at. To delve into the functionality of the oestrogen receptor more, one possibility for future work could be co-localisation studies between ER alpha and beta, and chromatin immunoprecipitation to identify interactions of these receptors with DNA, to gain insight to what genes are directly interacted with by these receptors, and if possible, by what combinations of dimers of these receptors. We also saw in chapters 3 and 4, that when comparing when whole cell vs nuclear localisations of these receptors (Figures 3.21 And 4.23), the receptors appear to be generally ubiquitously expressed in the cell, in tamoxifen naïve cell lines, yet may show a preference for cytoplasmic localisation in drug adapted cell lines. Further experimentation would be needed to further elucidate if this plays a role in resistance. Super resolution microscopy could be one way of studying co-localisation of these receptors – until recently it has been difficult to study nanoscale interactions using microscopy, but the development of techniques such as PALM-STORM and spectral precision distance determination microscopy could make this possible (Henriques *et al.*, 2011; Cremer *et al.*, 2017). Now that we have observed the effect of phenol red and charcoal stripped medium alone have on these cell lines, it would be interesting to observe the effect of known quantities of oestrogens – for this we would take the adapted sublines from in -CS conditions and, begin to cultivate flasks of each with a gradient of known quantities of oestrogen. It would also be interesting to consider any differential effects that may be induced by the use of either oestrone, oestradiol or oestriol.

P-glycoprotein has been associated with resistance to a variety of anti-cancer compounds in cell lines (Cordon-Cardo *et al.*, 1989, 1990). Tamoxifen is known to interact with p-glycoprotein (Callaghan and Higgins, 1995), which raises the question of its involvement in the context of this study. Iusuf *et al.*, (2011)

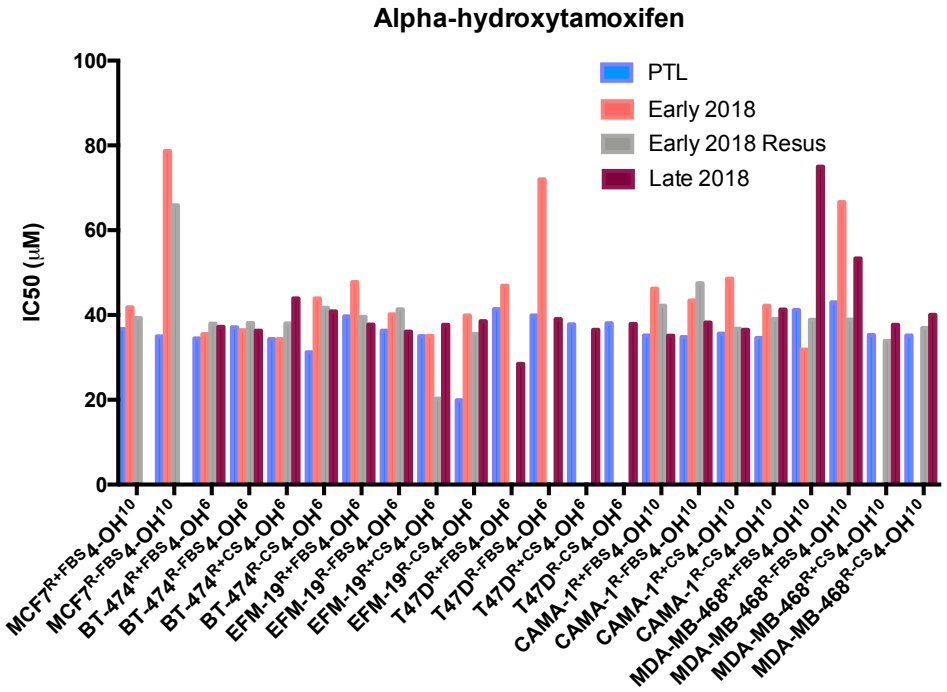
documents how the active metabolites of tamoxifen; endoxifen, n-desmethyltamoxifen and 4-OH-tamoxifen have differential potentials for transport by the ABCB1 transporter. This could be assessed in the panels of cell lines that model endocrine resistance in this work, to perhaps explain the differential effects we see from the individual metabolites of tamoxifen.

Furthermore, it has been discussed in previous chapters, how the data obtained and displayed in this thesis is that from 2D *in vitro* culture models. While this is a well-practiced and still trusted method in pre-clinical studies pertaining to anti-cancer drugs, the advantages in similarities in comparison to the extracellular environment that 3D cultures would provide would be an interesting next step with this research – specifically how a 3D culture environment for the cells would affect the trends shown in this thesis. Taking this logic a step further, another option to consider would be that of patient-derived xenograft models (PDX) with these cell lines, rather than patient derived tissues. This would create a more natural tumour environment allowing for these resistant cells to be studied in a more natural tumour environment, and observe the effect that this environment may have on its response to tamoxifen (Yoshida, 2020).

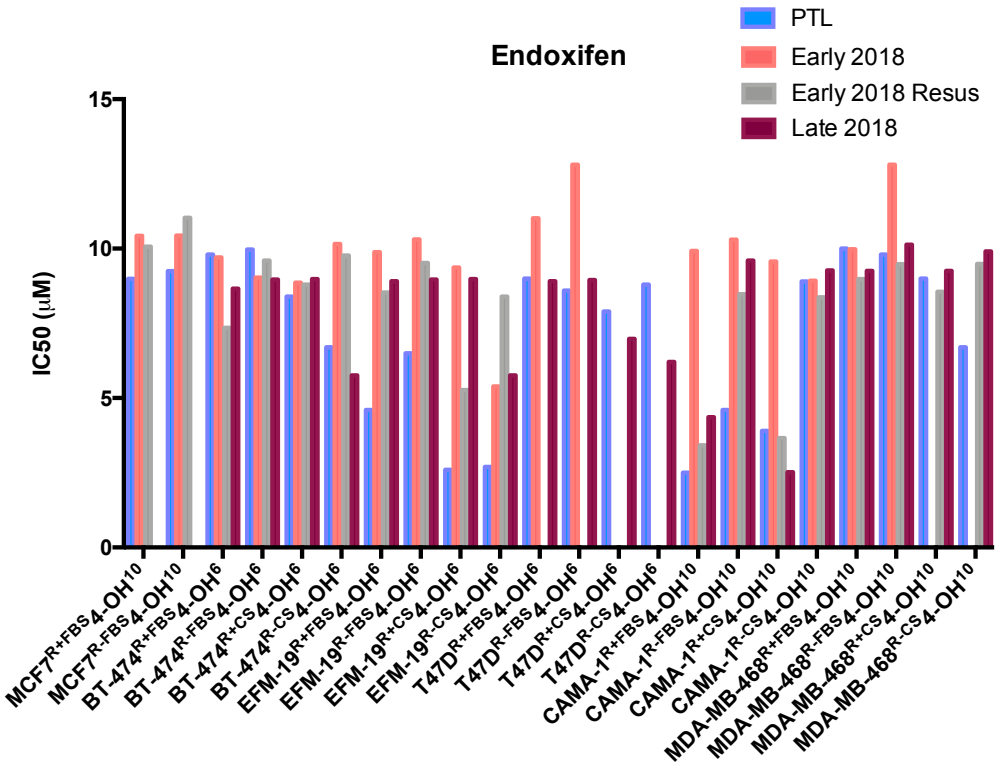
Appendix



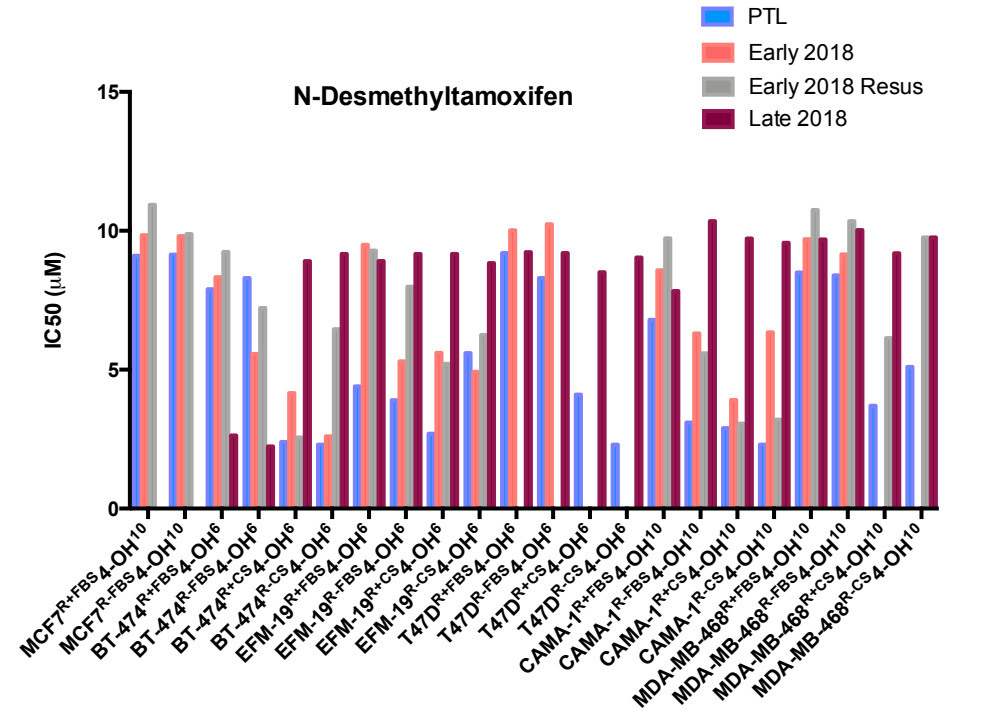
Appendix I: (Z)-4-OH-tamoxifen IC_{50} values of the (Z)-4-OH-tamoxifen resistant sub-lines during different stages of cell-line production compared to their respective parental sub-lines (PTL).



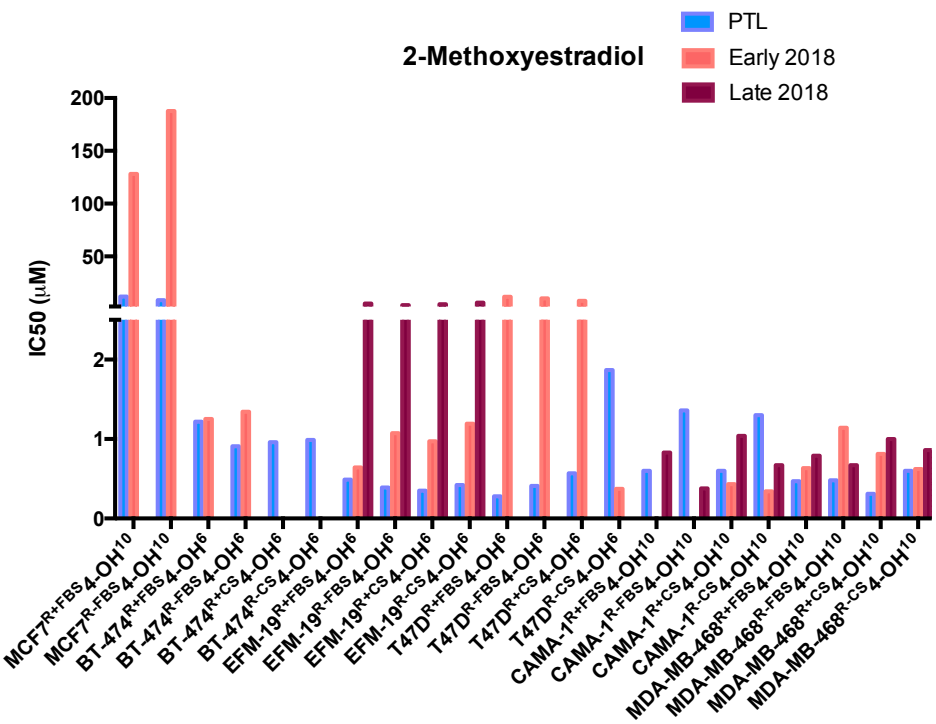
Appendix II: Alpha-hydroxytamoxifen IC_{50} values of the (Z)-4-OH-tamoxifen resistant sub-lines during different stages of cell-line production compared to their respective parental sub-lines (PTL).



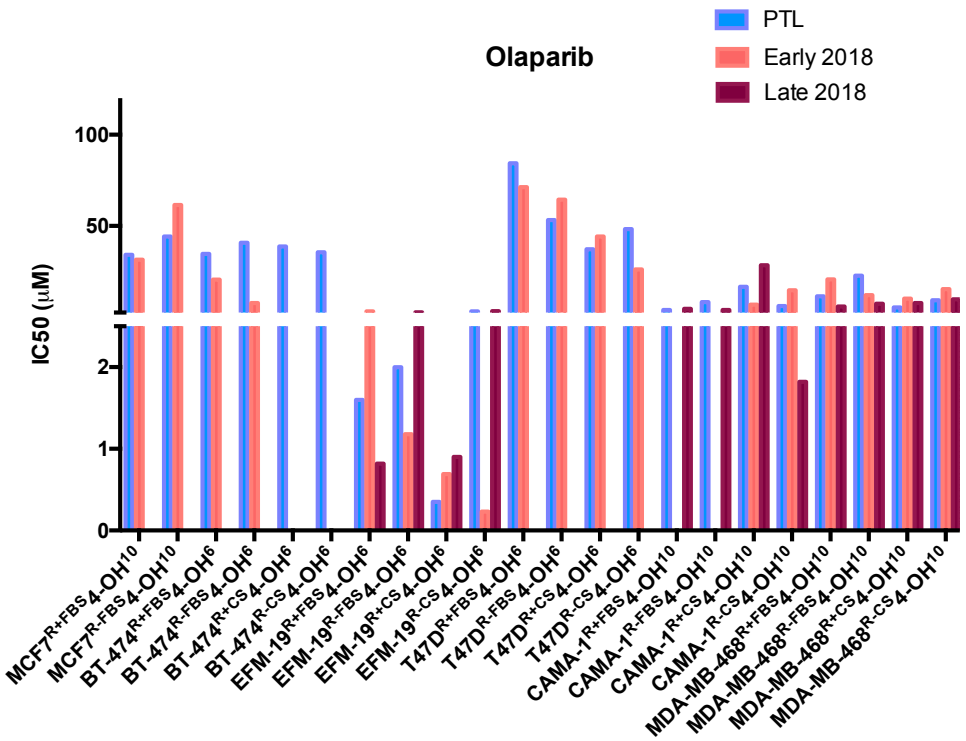
Appendix III: Endoxifen IC_{50} values of the endoxifen resistant sub-lines during different stages of cell-line production compared to their respective parental sub-lines (PTL).



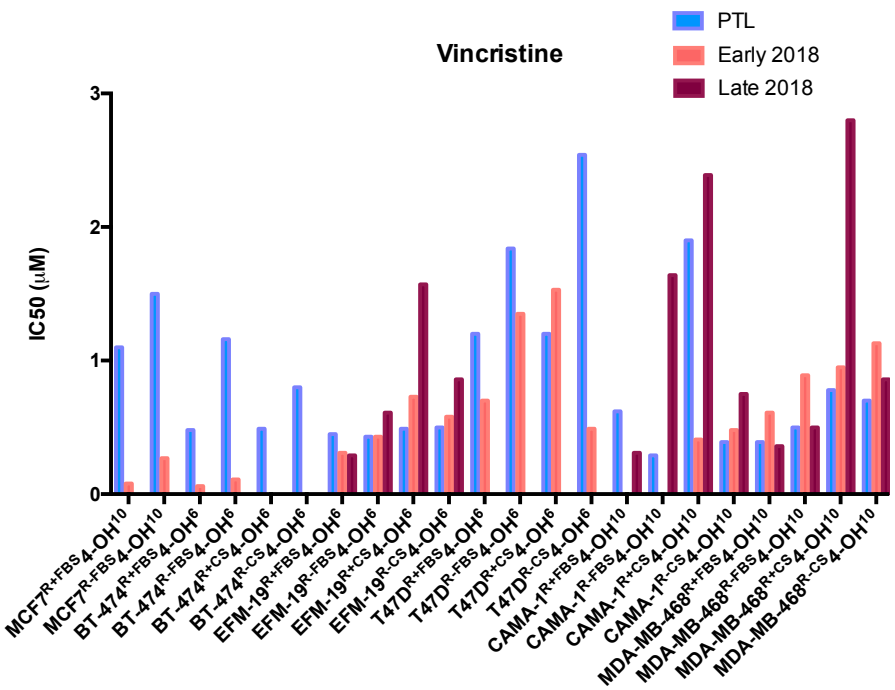
Appendix IV: Endoxifen IC_{50} values of the n-desmethyltamoxifen resistant sub-lines during different stages of cell-line production compared to their respective parental sub-lines (PTL).



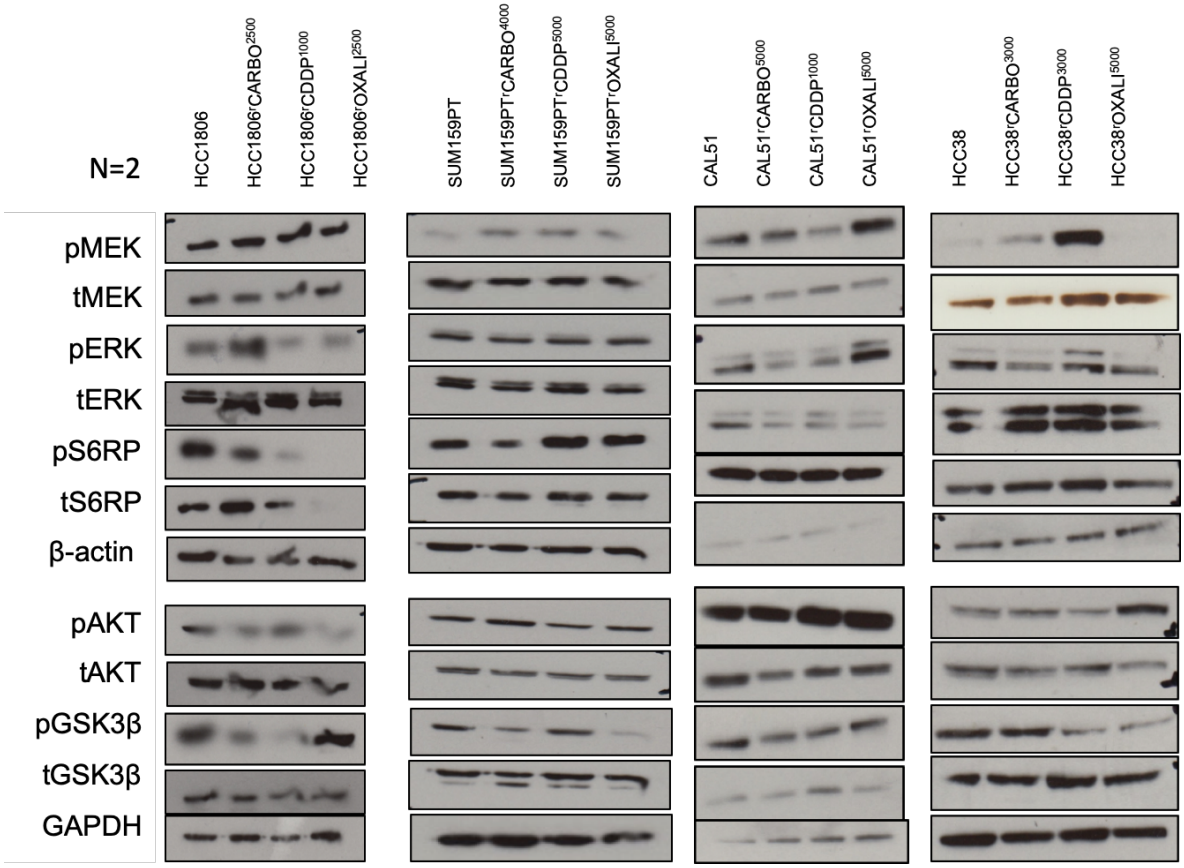
Appendix V: 2-methoxyoestradiol IC_{50} values of the n-desmethyltamoxifen resistant sub-lines during different stages of cell-line production compared to their respective parental sub-lines (PTL).



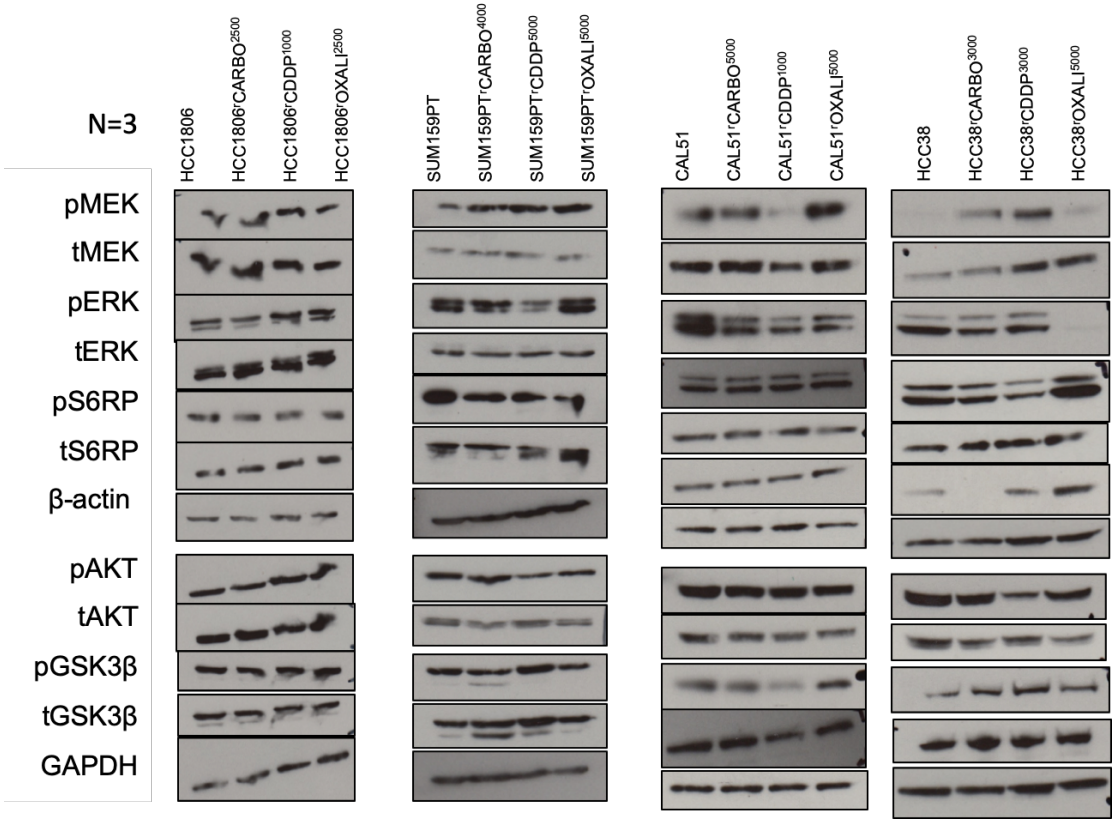
Appendix VI: Olaparib IC_{50} values of the n-desmethyltamoxifen resistant sub-lines during different stages of cell-line production compared to their respective parental sub-lines (PTL).



Appendix VII: Olaparib IC_{50} values of the n-desmethyltamoxifen resistant sub-lines during different stages of cell-line production compared to their respective parental sub-lines (PTL).



Appendix VIII. N=2 repeat of blots shown in figure 5.10. Western blot analysis of all four parental cell lines and their Pt-drug resistant sub-lines. Lysates were prepared from 70-80% confluent culture dishes of each cell line or subline. Cell lysates were analysed for expression of the indicated proteins. 'p' denotes a phosphorylated form and 't' denotes the total form of that protein. Each blot is representative the n=1 biological repeat. All targets in this representative image of blots are all from the same cell lysates, on the same experimental run. Not all blots required the same exposure time, the most appropriate exposure has been selected for each.



Appendix IX. N=3 repeat of blots shown in figure 5.10. Western blot analysis of all four parental cell lines and their Pt-drug resistant sub-lines. Lysates were prepared from 70-80% confluent culture dishes of each cell line or subline. Cell lysates were analysed for expression of the indicated proteins. 'p' denotes a phosphorylated form and 't' denotes the total form of that protein. Each blot is representative the n=1 biological repeat. All targets in this representative image of blots are all from the same cell lysates, on the same experimental run. Not all blots required the same exposure time, the most appropriate exposure has been selected for each.

References

Abbasi, S. *et al.* (2013) 'Association of estrogen receptor-α A908G (K303R) mutation with breast cancer risk.', *International journal of clinical and experimental medicine*, 6(1), pp. 39–49. Available at: http://www.ncbi.nlm.nih.gov/pubmed/23236557 (Accessed: 7 August 2019).

Abe, O. *et al.* (2011) 'Relevance of breast cancer hormone receptors and other factors to the efficacy of adjuvant tamoxifen: Patient-level meta-analysis of randomised trials', *The Lancet*. Elsevier, 378(9793), pp. 771–784. doi: 10.1016/S0140-6736(11)60993-8.

Ahmad, A. *et al.* (2010) 'Orally administered Endoxifen is a new therapeutic agent for breast cancer', *Breast Cancer Research and Treatment*, 122(2), pp. 579–584. doi: 10.1007/s10549-009-0704-7.

Alfarouk, K. O. *et al.* (2015) 'Resistance to cancer chemotherapy: Failure in drug response from ADME to P-gp', *Cancer Cell International*. BioMed Central, p. 71. doi: 10.1186/s12935-015-0221-1.

Ali, E. S., Mangold, C. and Peiris, A. N. (2017) 'Estriol: Emerging clinical benefits', *Menopause*, pp. 1081–1085. doi: 10.1097/GME.0000000000000855.

Alizart, M. *et al.* (2012) 'Molecular classification of breast carcinoma', *Diagnostic Histopathology*, 18(3), pp. 97–103. doi: 10.1016/j.mpdhp.2011.12.003.

De Amicis, F. *et al.* (2010) 'Androgen receptor overexpression induces tamoxifen resistance in human breast cancer cells', *Breast Cancer Research and Treatment*, 121(1), pp. 1–11. doi: 10.1007/s10549-009-0436-8.

Anestis, A. *et al.* (2019) 'Estrogen receptor beta increases sensitivity to enzalutamide in androgen receptor-positive triple-negative breast cancer', *Journal of Cancer Research and Clinical Oncology*, 145(5), pp. 1221–1233. doi: 10.1007/s00432-019-02872-9.

Anzick, S. L. *et al.* (1997) 'AIB1, a steroid receptor coactivator amplified in breast and ovarian cancer', *Science*, 277(5328), pp. 965–968. doi: 10.1126/science.277.5328.965.

Armstrong-Gordon, E. *et al.* (2018) 'Patterns of platinum drug use in an acute care setting: a retrospective study', *Journal of Cancer Research and Clinical Oncology*, 144(8), pp. 1561–1568. doi: 10.1007/s00432-018-2669-6.

Asselin, E., Mills, G. B. and Tsang, B. K. (2001) 'XIAP regulates Akt activity and caspase-3-dependent cleavage during cisplatin-induced apoptosis in human ovarian epithelial cancer cells', *Cancer Research*, 61(5), pp. 1862–1868. Available at: http://www.ncbi.nlm.nih.gov/pubmed/11280739 (Accessed: 12 November 2018).

Avramis, I. A., Kwock, R. and Avramis, V. I. (2001) 'Taxotere and vincristine inhibit the secretion of the angiogenesis-inducing vascular endothelial growth factor (VEGF) by wild-type and drug-resistant human leukemia T-cell lines', *Anticancer Research*, 21(4 A), pp. 2281–2286. Available at: http://www.ncbi.nlm.nih.gov/pubmed/11724283 (Accessed: 29 August 2019).

Awasthi, P., Foiani, M. and Kumar, A. (2016) 'Correction to ATM and ATR signaling at a glance [J. Cell Sci., 128, (2015) 4255-4262]', *Journal of Cell Science*, p. 1285. doi: 10.1242/jcs.188631.

Aziz, M. H., Shen, H. and Maki, C. G. (2011) 'Acquisition of p53 mutations in response to the non-genotoxic p53 activator Nutlin-3', *Oncogene*, 30(46), pp. 4678–4686. doi: 10.1038/onc.2011.185.

Banerji, U. *et al.* (2018) 'A phase i open-label study to identify a dosing regimen of the pan-akt inhibitor azd5363 for evaluation in solid tumors and in pik3ca-

mutated breast and gynecologic cancers', *Clinical Cancer Research*. American Association for Cancer Research Inc., 24(9), pp. 2050–2059. doi: 10.1158/1078-0432.CCR-17-2260.
Bansal, R. and Acharya, P. C. (2014) 'Man-made cytotoxic steroids: Exemplary agents for cancer therapy', *Chemical Reviews*, pp. 6986–7005. doi: 10.1021/cr4002935.
Berthois, Y., Katzenellenbogen, J. A. and Katzenellenbogen, B. S. (1986) 'Phenol red in tissue culture media is a weak estrogen: Implications concerning the study of estrogen-responsive cells in culture', *Proceedings of the National Academy of Sciences of the United States of America*, 83(8), pp. 2496–2500. doi: 10.1073/pnas.83.8.2496.
Bhateja, P. *et al.* (2019) 'The Hedgehog Signaling Pathway: A Viable Target in Breast Cancer?', *Cancers*, 11(8), p. 1126. doi: 10.3390/cancers11081126.
Biedler, J. L. and Riehm, H. (1970) 'Cellular Resistance to Actinomycin D in Chinese Hamster Cells in Vitro: Cross-Resistance, Radioautographic, and Cytogenetic Studies', *Cancer Research*, 30(4).
Björnström, L. and Sjöberg, M. (2005) 'Mechanisms of Estrogen Receptor Signaling: Convergence of Genomic and Nongenomic Actions on Target Genes', *Molecular Endocrinology*. Narnia, 19(4), pp. 833–842. doi: 10.1210/me.2004-0486.
Bourdeau, V. *et al.* (2004) 'Genome-Wide Identification of High-Affinity Estrogen Response Elements in Human and Mouse', *Molecular Endocrinology*, 18(6), pp. 1411–1427. doi: 10.1210/me.2003-0441.
Brisken, C. and Ataca, D. (2015) 'Endocrine hormones and local signals during the development of the mouse mammary gland', *Wiley Interdisciplinary Reviews: Developmental Biology*, pp. 181–195. doi: 10.1002/wdev.172.
Broselid, S. *et al.* (2014) 'G protein-coupled receptor 30 (GPR30) forms a plasma membrane complex with membrane-associated guanylate kinases (MAGUKs) and protein kinase a-anchoring protein 5 (AKAP5) that constitutively inhibits cAMP production', *Journal of Biological Chemistry*. American Society for Biochemistry and Molecular Biology, 289(32), pp. 22117–22127. doi: 10.1074/jbc.M114.566893.
Bryant, C., Rawlinson, R. and Massey, A. J. (2014) 'Chk1 Inhibition as a novel therapeutic strategy for treating triple-negative breast and ovarian cancers', *BMC Cancer*. BioMed Central Ltd., 14(1), p. 570. doi: 10.1186/1471-2407-14-570.
Callaghan, R. and Higgins, C. F. (1995) 'Interaction of tamoxifen with the multidrug resistance P-glycoprotein', *British Journal of Cancer*. Nature Publishing Group, 71(2), pp. 294–299. doi: 10.1038/bjc.1995.59.
Carroll, J. S. *et al.* (2005) 'Chromosome-wide mapping of estrogen receptor binding reveals long-range regulation requiring the forkhead protein FoxA1', *Cell*, 122(1), pp. 33–43. doi: 10.1016/j.cell.2005.05.008.
Carroll, J. S. *et al.* (2006) 'Genome-wide analysis of estrogen receptor binding sites', *Nature Genetics*, 38(11), pp. 1289–1297. doi: 10.1038/ng1901.
Carroll, J. S. (2016) 'Eje prize 2016: Mechanisms of oestrogen receptor (ER) gene regulation in breast cancer', *European Journal of Endocrinology*. Bioscientifica Ltd., pp. R41–R49. doi: 10.1530/EJE-16-0124.
Chan, C. M. . *et al.* (2002) 'Molecular changes associated with the acquisition of oestrogen hypersensitivity in MCF-7 breast cancer cells on long-term oestrogen deprivation', *Journal of Steroid Biochemistry and Molecular Biology*. Pergamon, 81(4–5), pp. 333–341. doi: 10.1016/S0960-0760(02)00074-2.
Chang, M. (2012) 'Tamoxifen resistance in breast cancer', *Biomolecules and*

Therapeutics. Korean Society of Applied Pharmacology, pp. 256–267. doi: 10.4062/biomolther.2012.20.3.256.
Chankova, S. G. *et al.* (2007) 'Induction of DNA double-strand breaks by zeocin in Chlamydomonas reinhardtii and the role of increased DNA double-strand breaks rejoining in the formation of an adaptive response', *Radiation and Environmental Biophysics*, 46(4), pp. 409–416. doi: 10.1007/s00411-007-0123-2.
Chen, J. *et al.* (2008) 'Mechanistic studies on bleomycin-mediated DNA damage: Multiple binding modes can result in double-stranded DNA cleavage', *Nucleic Acids Research*. Oxford University Press, 36(11), pp. 3781–3790. doi: 10.1093/nar/gkn302.
Cheng, G. *et al.* (2005) 'A Role for the Androgen Receptor in Follicular Atresia of Estrogen Receptor Beta Knockout Mouse Ovary1', *Biology of Reproduction*, 66(1), pp. 77–84. doi: 10.1095/biolreprod66.1.77.
Cheng, J. Q. *et al.* (2002) 'Role of X-linked inhibitor of apoptosis protein in chemoresistance in ovarian cancer: Possible involvement of the phosphoinositide-3 kinase/Akt pathway', *Drug Resistance Updates*, pp. 131–146. doi: 10.1016/S1368-7646(02)00003-1.
Cochrane, D. R. *et al.* (2014) 'Role of the androgen receptor in breast cancer and preclinical analysis of enzalutamide', *Breast Cancer Research*, 16(1), p. R7. doi: 10.1186/bcr3599.
Coelingh Bennink, H. J. T. *et al.* (2017) 'The use of high-dose estrogens for the treatment of breast cancer', *Maturitas*. Elsevier, pp. 11–23. doi: 10.1016/j.maturitas.2016.10.010.
Conde, M. C. M. *et al.* (2016) 'Does cryopreservation affect the biological properties of stem cells from dental tissues? A systematic review', *Brazilian Dental Journal*, 27(6), pp. 633–640. doi: 10.1590/0103-6440201600980.
Cordon-Cardo, C. *et al.* (1989) 'Multidrug-resistance gene (P-glycoprotein) is expressed by endothelial cells at blood-brain barrier sites', *Proceedings of the National Academy of Sciences of the United States of America*. National Academy of Sciences, 86(2), pp. 695–698. doi: 10.1073/pnas.86.2.695.
Cordon-Cardo, C. *et al.* (1990) 'Expression of the multidrug resistance gene product (P-Glycoprotein) in human normal and tumor tissues', *Journal of Histochemistry and Cytochemistry*. SAGE PublicationsSage CA: Los Angeles, CA, 38(9), pp. 1277–1287. doi: 10.1177/38.9.1974900.
Costa, R. L. B., Han, H. S. and Gradishar, W. J. (2018) 'Targeting the PI3K/AKT/mTOR pathway in triple-negative breast cancer: a review', *Breast Cancer Research and Treatment*. Springer US, pp. 397–406. doi: 10.1007/s10549-018-4697-y.
Coutts, A. S. and Murphy, L. C. (1998) 'Elevated mitogen-activated protein kinase activity in estrogen- nonresponsive human breast cancer cells', *Cancer Research*. American Association for Cancer Research, 58(18), pp. 4071–4074. Available at: http://www.ncbi.nlm.nih.gov/pubmed/9751612 (Accessed: 13 September 2019).
Cremer, C. *et al.* (2017) 'Super-resolution microscopy approaches to nuclear nanostructure imaging', *Methods*, 123, pp. 11–32. doi: 10.1016/j.ymeth.2017.03.019.
Cronin-Fenton, D. P., Damkier, P. and Lash, T. L. (2014) 'Metabolism and transport of tamoxifen in relation to its effectiveness: New perspectives on an ongoing controversy', *Future Oncology*, pp. 107–122. doi: 10.2217/fon.13.168.
Crystal, A. S. *et al.* (2014) 'Patient-derived models of acquired resistance can identify effective drug combinations for cancer', *Science*, 346(6216), pp. 1480–

1486. doi: 10.1126/science.1254721.
D'Amato, R. J. *et al.* (1994) '2-Methoxyestradiol, an endogenous mammalian metabolite, inhibits tubulin polymerization by interacting at the colchicine site', *Proceedings of the National Academy of Sciences of the United States of America*. National Academy of Sciences, 91(9), pp. 3964–3968. doi: 10.1073/pnas.91.9.3964.
Dagogo-Jack, I. and Shaw, A. T. (2018) 'Tumour heterogeneity and resistance to cancer therapies', *Nature Reviews Clinical Oncology*. Nature Publishing Group, pp. 81–94. doi: 10.1038/nrclinonc.2017.166.
Darbre, P. D. (2014) 'Hypersensitivity and growth adaptation of oestrogen-deprived MCF-7 human breast cancer cells.', *Anticancer research*. International Institute of Anticancer Research, 34(1), pp. 99–105. Available at: http://www.ncbi.nlm.nih.gov/pubmed/24403449 (Accessed: 31 August 2019).
Dekker, J. *et al.* (2002) 'Capturing chromosome conformation', *Science*, 295(5558), pp. 1306–1311. doi: 10.1126/science.1067799.
Denkert, C. *et al.* (2017) 'Molecular alterations in triple-negative breast cancer—the road to new treatment strategies', *The Lancet*. Elsevier, pp. 2430–2442. doi: 10.1016/S0140-6736(16)32454-0.
Dilruba, S. and Kalayda, G. V. (2016) 'Platinum-based drugs: past, present and future', *Cancer Chemotherapy and Pharmacology*. Springer Berlin Heidelberg, pp. 1103–1124. doi: 10.1007/s00280-016-2976-z.
Domingo-Domenech, J. *et al.* (2012) 'Suppression of Acquired Docetaxel Resistance in Prostate Cancer through Depletion of Notch- and Hedgehog-Dependent Tumor-Initiating Cells', *Cancer Cell*, 22(3), pp. 373–388. doi: 10.1016/j.ccr.2012.07.016.
Dowsett, M. *et al.* (2010) 'Meta-analysis of breast cancer outcomes in adjuvant trials of aromatase inhibitors versus tamoxifen', *Journal of Clinical Oncology*, 28(3), pp. 509–518. doi: 10.1200/JCO.2009.23.1274.
Dowsett, M. and Howell, A. (2002) 'Breast cancer: Aromatase inhibitors take on tamoxifen', *Nature Medicine*. Nature Publishing Group, pp. 1341–1344. doi: 10.1038/nm1202-1341.
Droog, M. *et al.* (2013) 'Tamoxifen resistance: From bench to bedside', *European Journal of Pharmacology*, pp. 47–57. doi: 10.1016/j.ejphar.2012.11.071.
Dumontet, C. and Jordan, M. A. (2010) 'Microtubule-binding agents: A dynamic field of cancer therapeutics', *Nature Reviews Drug Discovery*. Nature Publishing Group, pp. 790–803. doi: 10.1038/nrd3253.
Eeckhoute, J. *et al.* (2007) 'Positive cross-regulatory loop ties GATA-3 to estrogen receptor α expression in breast cancer', *Cancer Research*, 67(13), pp. 6477–6483. doi: 10.1158/0008-5472.CAN-07-0746.
Engelman, J. A. *et al.* (2007) 'MET amplification leads to gefitinib resistance in lung cancer by activating ERBB3 signaling', *Science*, 316(5827), pp. 1039–1043. doi: 10.1126/science.1141478.
Enmark, E. *et al.* (1997) 'Human estrogen receptor β-gene structure, chromosomal localization, and expression pattern', *Journal of Clinical Endocrinology and Metabolism*. Narnia, 82(12), pp. 4258–4265. doi: 10.1210/jcem.82.12.4470.
Escuin, D., Kline, E. R. and Giannakakou, P. (2005) 'Both microtubule-stabilizing and microtubule-destabilizing drugs inhibit hypoxia-inducible factor-1α accumulation and activity by disrupting microtubule function', *Cancer Research*, 65(19), pp. 9021–9028. doi: 10.1158/0008-5472.CAN-04-4095.
Faivre, S. *et al.* (2002) 'Phase I-II and pharmacokinetic study of gemcitabine

combined with oxaliplatin in patients with advanced non-small-cell lung cancer and ovarian carcinoma.', *Annals of oncology : official journal of the European Society for Medical Oncology*, 13(9), pp. 1479–89. Available at: http://www.ncbi.nlm.nih.gov/pubmed/12196375 (Accessed: 16 November 2018).
Filardo, E. J. *et al.* (2000) 'Estrogen-induced activation of Erk-1 and Erk-2 requires the G protein-coupled receptor homolog, GPR30, and occurs via trans-activation of the epidermal growth factor receptor through release of HB-EGF', *Molecular Endocrinology*. Narnia, 14(10), pp. 1649–1660. doi: 10.1210/mend.14.10.0532.
Filardo, E. J. (2002) 'Epidermal growth factor receptor (EGFR) transactivation by estrogen via the G-protein-coupled receptor, GPR30: A novel signaling pathway with potential significance for breast cancer', *Journal of Steroid Biochemistry and Molecular Biology*. Pergamon, 80(2), pp. 231–238. doi: 10.1016/S0960-0760(01)00190-X.
Filardo, E. J. and Thomas, P. (2012) 'Minireview: G protein-coupled estrogen receptor-1, GPER-1: Its mechanism of action and role in female reproductive cancer, renal and vascular physiology', *Endocrinology*. The Endocrine Society, pp. 2953–2962. doi: 10.1210/en.2012-1061.
Foukakis, T. (2018) 'Carboplatin in the neoadjuvant treatment of triple-negative breast cancer — Ready for prime time?', *Annals of Oncology*, pp. 2278–2280. doi: 10.1093/annonc/mdy494.
Franken, N. A. P. *et al.* (2006) 'Clonogenic assay of cells in vitro', *Nature Protocols*. Nature Publishing Group, 1(5), pp. 2315–2319. doi: 10.1038/nprot.2006.339.
Freedman, R. A. and Partridge, A. H. (2013) 'Management of breast cancer in very young women', *The Breast*, 22, pp. S176–S179. doi: 10.1016/j.breast.2013.07.034.
Fullwood, M. J. *et al.* (2009) 'An oestrogen-receptor-α-bound human chromatin interactome', *Nature*, 462(7269), pp. 58–64. doi: 10.1038/nature08497.
Fuqua, S. A. W. *et al.* (2000) 'A Hypersensitive Estrogen Receptor-α Mutation in Premalignant breast Lesions1', *Cancer Research*, 60(15), pp. 4026–4029. Available at: http://www.ncbi.nlm.nih.gov/pubmed/10945602 (Accessed: 7 August 2019).
Gade, P. and Kalvakolanu, D. V (no date) 'Chromatin Immunoprecipitation Assay as a Tool for Analyzing Transcription Factor Activity'. doi: 10.1007/978-1-61779-376-9_6.
Galluzzi, L. *et al.* (2014) 'Systems biology of cisplatin resistance: Past, present and future', *Cell Death and Disease*. doi: 10.1038/cddis.2013.428.
Gao, A. *et al.* (2018) 'LEM4 confers tamoxifen resistance to breast cancer cells by activating cyclin D-CDK4/6-Rb and ERα pathway', *Nature Communications*. Nature Publishing Group, 9(1), p. 4180. doi: 10.1038/s41467-018-06309-8.
Gerratana, L. *et al.* (2016) 'Do platinum salts fit all triple negative breast cancers?', *Cancer Treatment Reviews*, pp. 34–41. doi: 10.1016/j.ctrv.2016.06.004.
Girgert, R., Emons, G. and Gründker, C. (2012) 'Inactivation of GPR30 reduces growth of triple-negative breast cancer cells: Possible application in targeted therapy', *Breast Cancer Research and Treatment*, 134(1), pp. 199–205. doi: 10.1007/s10549-012-1968-x.
Girgert, R., Emons, G. and Gründker, C. (2019) 'Estrogen signaling in ERα-negative breast cancer: ERβ and GPER', *Frontiers in Endocrinology*, p. 781. doi: 10.3389/fendo.2018.00781.

Glover, J. F., Irwin, J. T. and Darbre, P. D. (1988) 'Interaction of Phenol Red with Estrogenic and Antiestrogenic Action on Growth of Human Breast Cancer Cells ZR-75-1 and T-47-D', *Cancer Research*, 48(13), pp. 3693–3697. Available at: http://cancerres.aacrjournals.org/content/48/13/3693.full-text.pdf (Accessed: 2 July 2019).
Gohr, K. *et al.* (2017) 'Inhibition of PI3K/Akt/mTOR overcomes cisplatin resistance in the triple negative breast cancer cell line HCC38', *BMC Cancer*. BioMed Central, 17(1), p. 711. doi: 10.1186/s12885-017-3695-5.
Göllner, S. *et al.* (2017) 'Loss of the histone methyltransferase EZH2 induces resistance to multiple drugs in acute myeloid leukemia', *Nature Medicine*, 23(1), pp. 69–78. doi: 10.1038/nm.4247.
Gore, M. E. *et al.* (1989) 'Cisplatin/carboplatin cross-resistance in ovarian cancer', *British Journal of Cancer*. Nature Publishing Group, 60(5), pp. 767–769. doi: 10.1038/bjc.1989.356.
Gruvberger-Saal, S. K. *et al.* (2007) 'Estrogen receptor β expression is associated with tamoxifen response in ERα-negative breast carcinoma', *Clinical Cancer Research*, 13(7), pp. 1987–1994. doi: 10.1158/1078-0432.CCR-06-1823.
Halachmi, S. *et al.* (1994) 'Estrogen receptor-associated proteins: Possible mediators of hormone-induced transcription', *Science*, 264(5164), pp. 1455–1458. doi: 10.1126/science.8197458.
Hall, J. M. and McDonnel, D. P. (1999) 'The estrogen receptor β-isoform (ERβ) of the human estrogen receptor modulates ERα transcriptional activity and is a key regulator of the cellular response to estrogens and antiestrogens', *Endocrinology*. Narnia, 140(12), pp. 5566–5578. doi: 10.1210/endo.140.12.7179.
Hanahan, D. and Weinberg, R. A. (2011) 'Hallmarks of cancer: The next generation', *Cell*, pp. 646–674.
Harbeck, N. and Gnant, M. (2016) 'Breast cancer Breast cancer : epidemiology', *The Lancet*. Elsevier, 6736(16), pp. 1134–1150. doi: 10.1016/S0140-6736(16)31891-8.
Hecht, S. M. (2000) 'Bleomycin: New perspectives on the mechanism of action', *Journal of Natural Products*, pp. 158–168. doi: 10.1021/np990549f.
Helland, T. *et al.* (2017) 'Serum concentrations of active tamoxifen metabolites predict long-term survival in adjuvantly treated breast cancer patients', *Breast Cancer Research*, 19(1), p. 125. doi: 10.1186/s13058-017-0916-4.
Henriques, R. *et al.* (2011) 'PALM and STORM: Unlocking live-cell super-resolution', *Biopolymers*, 95(5), pp. 322–331. doi: 10.1002/bip.21586.
Hess, J. (2004) 'AP-1 subunits: quarrel and harmony among siblings', *Journal of Cell Science*, 117(25), pp. 5965–5973. doi: 10.1242/jcs.01589.
Holohan, C. *et al.* (2013) 'Cancer drug resistance: An evolving paradigm', *Nature Reviews Cancer*. Nature Publishing Group, pp. 714–726. doi: 10.1038/nrc3599.
Honma, N. *et al.* (2008) 'Clinical importance of estrogen receptor-β evaluation in breast cancer patients treated with adjuvant tamoxifen therapy', *Journal of Clinical Oncology*, 26(22), pp. 3727–3734. doi: 10.1200/JCO.2007.14.2968.
Hopp, T. A. *et al.* (2004) 'Low levels of estrogen receptor β protein predict resistance to tamoxifen therapy in breast cancer', *Clinical Cancer Research*. American Association for Cancer Research, 10(22), pp. 7490–7499. doi: 10.1158/1078-0432.CCR-04-1114.
Huan, J. *et al.* (2014) 'Insights into significant pathways and gene interaction networks underlying breast cancer cell line MCF-7 treated with 17β-Estradiol

(E2)', *Gene*, 533(1), pp. 346–355. doi: 10.1016/j.gene.2013.08.027.
Huang, L. *et al.* (2017) 'Cisplatin versus carboplatin in combination with paclitaxel as neoadjuvant regimen for triple negative breast cancer', *OncoTargets and Therapy*, 10, pp. 5739–5744. doi: 10.2147/OTT.S145934.
Hwang, J. *et al.* (2005) 'The time-dependent serial gene response to zeocin treatment involves caspase-dependent apoptosis in HeLa cells', *Microbiology and Immunology*. Taylor & Francis, 49(4), pp. 331–342. doi: 10.1111/j.1348-0421.2005.tb03737.x.
Iusuf, D. *et al.* (2011) 'P-glycoprotein (ABCB1) transports the primary active tamoxifen metabolites endoxifen and 4-hydroxytamoxifen and restricts their brain penetration', *Journal of Pharmacology and Experimental Therapeutics*, 337(3), pp. 710–717. doi: 10.1124/jpet.110.178301.
Jager, N. G. L. *et al.* (2014) 'Tamoxifen dose and serum concentrations of tamoxifen and six of its metabolites in routine clinical outpatient care', *Breast Cancer Research and Treatment*. Springer US, 143(3), pp. 477–483. doi: 10.1007/s10549-013-2826-1.
Jeng, M. H. *et al.* (1998) 'Estrogen receptor expression and function in long-term estrogen-deprived human breast cancer cells', *Endocrinology*. Narnia, 139(10), pp. 4164–4174. doi: 10.1210/endo.139.10.6229.
Jensen, E. V. and DeSombre, E. R. (1973) 'Estrogen-receptor interaction', *Science*, pp. 126–134. doi: 10.1126/science.182.4108.126.
Jeselsohn, R. *et al.* (2014) 'Emergence of constitutively active estrogen receptor-α mutations in pretreated advanced estrogen receptor-positive breast cancer', *Clinical Cancer Research*, 20(7), pp. 1757–1767. doi: 10.1158/1078-0432.CCR-13-2332.
Jordan, V. C. (2003) 'Tamoxifen: A most unlikely pioneering medicine', *Nature Reviews Drug Discovery*, pp. 205–213. doi: 10.1038/nrd1031.
Jordan, V. C. (2015) 'The new biology of estrogen-induced apoptosis applied to treat and prevent breast cancer', *Endocrine-Related Cancer*, pp. R1–R31. doi: 10.1530/ERC-14-0448.
Joseph, C. *et al.* (2018) 'Breast cancer intratumour heterogeneity: current status and clinical implications', *Histopathology*. John Wiley & Sons, Ltd (10.1111), pp. 717–731. doi: 10.1111/his.13642.
Joseph, J. D. *et al.* (2013) 'A clinically relevant androgen receptor mutation confers resistance to second-generation antiandrogens enzalutamide and ARN-509', *Cancer Discovery*, 3(9), pp. 1020–1029. doi: 10.1158/2159-8290.CD-13-0226.
Jung, J. *et al.* (2016) 'TP53 mutations emerge with HDM2 inhibitor SAR405838 treatment in de-differentiated liposarcoma', *Nature Communications*, 7. doi: 10.1038/ncomms12609.
Kamel, D. *et al.* (2018) 'PARP Inhibitor Drugs in the Treatment of Breast, Ovarian, Prostate and Pancreatic Cancers: An Update of Clinical Trials', *Current Drug Targets*, 19(1), pp. 21–37. doi: 10.2174/1389450118666170711151518.
Kao, J. *et al.* (2009) 'Molecular profiling of breast cancer cell lines defines relevant tumor models and provides a resource for cancer gene discovery', *PLoS ONE*. Public Library of Science, 4(7), p. e6146. doi: 10.1371/journal.pone.0006146.
Kapałczyńska, M. *et al.* (2018) '2D and 3D cell cultures – a comparison of different types of cancer cell cultures', *Archives of Medical Science*. Termedia Publishing House Ltd., 14(4), pp. 910–919. doi: 10.5114/aoms.2016.63743.
Kastrati, I. *et al.* (2019) 'Insights into how phosphorylation of estrogen receptor

at serine 305 modulates tamoxifen activity in breast cancer', *Molecular and Cellular Endocrinology*. Elsevier Ireland Ltd, pp. 97–101. doi: 10.1016/j.mce.2019.01.014.
Kelland, L. (2007) 'The resurgence of platinum-based cancer chemotherapy', *Nature Reviews Cancer*, pp. 573–584. doi: 10.1038/nrc2167.
Kelland, L. R. (1993) 'New platinum antitumor complexes.', *Critical reviews in oncology/hematology*, 15(3), pp. 191–219. Available at: http://www.ncbi.nlm.nih.gov/pubmed/8142057 (Accessed: 12 November 2018).
Kisanga, E. R. *et al.* (2004a) 'Tamoxifen and Metabolite Concentrations in Serum and Breast Cancer Tissue during Three Dose Regimens in a Randomized Preoperative Trial', *Clinical Cancer Research*. American Association for Cancer Research, 10(7), pp. 2336–2343. doi: 10.1158/1078-0432.CCR-03-0538.
Kisanga, E. R. *et al.* (2004b) 'Tamoxifen and Metabolite Concentrations in Serum and Breast Cancer Tissue during Three Dose Regimens in a Randomized Preoperative Trial', *Clinical Cancer Research*. American Association for Cancer Research, 10(7), pp. 2336–2343. doi: 10.1158/1078-0432.CCR-03-0538.
Klinge, C. M. (2001) 'Estrogen receptor interaction with estrogen response elements', *Nucleic Acids Research*, 29(14), pp. 2905–2919. doi: 10.1093/nar/29.14.2905.
Kong, L. R. *et al.* (2015) 'MEK inhibition overcomes cisplatin resistance conferred by SOS/MAPK pathway activation in squamous cell carcinoma', *Molecular Cancer Therapeutics*. American Association for Cancer Research, 14(7), pp. 1750–1760. doi: 10.1158/1535-7163.MCT-15-0062.
Korach, Kenneth S *et al.* (2003) 'Update on animal models developed for analyses of estrogen receptor biological activity.', *The Journal of steroid biochemistry and molecular biology*, 86(3–5), pp. 387–91. Available at: http://www.ncbi.nlm.nih.gov/pubmed/14623535 (Accessed: 25 July 2019).
Korach, Kenneth S. *et al.* (2003) 'Update on animal models developed for analyses of estrogen receptor biological activity', in *Journal of Steroid Biochemistry and Molecular Biology*, pp. 387–391. doi: 10.1016/S0960-0760(03)00348-0.
Korpal, M. *et al.* (2013) 'An F876l mutation in androgen receptor confers genetic and phenotypic resistance to MDV3100 (Enzalutamide)', *Cancer Discovery*, 3(9), pp. 1030–1043. doi: 10.1158/2159-8290.CD-13-0142.
Kotchetkov, R. *et al.* (2005) 'Increased malignant behavior in neuroblastoma cells with acquired multi-drug resistance does not depend on P-gp expression', *International Journal of Oncology*. Spandidos Publications, 27(4), pp. 1029–1037. doi: 10.3892/ijo.27.4.1029.
Kuiper, G. G. *et al.* (2002) 'Cloning of a novel receptor expressed in rat prostate and ovary.', *Proceedings of the National Academy of Sciences*. National Academy of Sciences, 93(12), pp. 5925–5930. doi: 10.1073/pnas.93.12.5925.
Kuiper, G. G. J. M. *et al.* (1996) 'Cloning of a novel estrogen receptor expressed in rat prostate and ovary', *Proceedings of the National Academy of Sciences of the United States of America*, 93(12), pp. 5925–5930. doi: 10.1073/pnas.93.12.5925.
Kumar, P., Nagarajan, A. and Uchil, P. D. (2018) 'Analysis of cell viability by the MTT assay', *Cold Spring Harbor Protocols*, 2018(6), pp. 469–471. doi: 10.1101/pdb.prot095505.
Lambert, I. H. and Sørensen, B. H. (2018) 'Facilitating the cellular accumulation of Pt-based chemotherapeutic drugs', *International Journal of Molecular*

Sciences. Multidisciplinary Digital Publishing Institute, p. 2249. doi: 10.3390/ijms19082249.
Law, E. K. *et al.* (2016) 'The DNA cytosine deaminase APOBEC3B promotes tamoxifen resistance in ER-positive breast cancer', *Science Advances*. American Association for the Advancement of Science, 2(10), p. e1601737. doi: 10.1126/sciadv.1601737.
Leung, Y.-K. *et al.* (2006) 'Estrogen receptor (ER)-beta isoforms: A key to understanding ER-beta signaling', *Proceedings of the National Academy of Sciences*. National Academy of Sciences, 103(35), pp. 13162–13167. doi: 10.1073/pnas.0605676103.
Levin, E. R. (2009) 'Plasma membrane estrogen receptors', *Trends in Endocrinology and Metabolism*, pp. 477–482. doi: 10.1016/j.tem.2009.06.009.
Li, S. *et al.* (2015) 'Mouse ATP-Binding Cassette (ABC) Transporters Conferring Multi-Drug Resistance', *Anti-Cancer Agents in Medicinal Chemistry*, 15(4), pp. 423–432. doi: 10.2174/1871520615666150129212723.
Liao, W., McNutt, M. A. and Zhu, W. G. (2009) 'The comet assay: A sensitive method for detecting DNA damage in individual cells', *Methods*. Academic Press, pp. 46–53. doi: 10.1016/j.ymeth.2009.02.016.
Lin, C. Y. *et al.* (2007) 'Inhibitory effects of estrogen receptor beta on specific hormone-responsive gene expression and association with disease outcome in primary breast cancer', *Breast Cancer Research*. BioMed Central, 9(2), p. R25. doi: 10.1186/bcr1667.
Lindner, V. *et al.* (1998) 'Increased expression of estrogen receptor-β mRNA in male blood vessels after vascular injury', *Circulation Research*, 83(2), pp. 224–229. doi: 10.1161/01.RES.83.2.224.
Lipovka, Y. and Konhilas, J. P. (2016) 'The complex nature of oestrogen signalling in breast cancer: enemy or ally?', *Bioscience Reports*, 36(3), pp. e00352–e00352. doi: 10.1042/BSR20160017.
Liston, D. R. and Davis, M. (2017) 'Clinically Relevant Concentrations of Anticancer Drugs: A guide for Nonclinical Studies', *Clinical Cancer Research*, 23(14), pp. OF1-9. doi: 10.1158/1078-0432.CCR-16-3083.
Litwiniuk, M. M. *et al.* (2008) 'Expression of estrogen receptor beta in the breast carcinoma of BRCA1 mutation carriers', *BMC Cancer*. BioMed Central, 8(1), p. 100. doi: 10.1186/1471-2407-8-100.
Liu, J. *et al.* (2015) 'Clinical efficacy of administering oxaliplatin combined with S-1 in the treatment of advanced triple-negative breast cancer', *Experimental and Therapeutic Medicine*, 10(1), pp. 379–385. doi: 10.3892/etm.2015.2489.
Liu, X. *et al.* (2013) 'U-Shape Suppressive Effect of Phenol Red on the Epileptiform Burst Activity via Activation of Estrogen Receptors in Primary Hippocampal Culture', *PLoS ONE*. Edited by A. H. Kihara. Public Library of Science, 8(4), p. e60189. doi: 10.1371/journal.pone.0060189.
Liu, Y. *et al.* (2019) 'Multi-omic measurements of heterogeneity in HeLa cells across laboratories', *Nature Biotechnology*. Nature Publishing Group, 37(3), pp. 314–322. doi: 10.1038/s41587-019-0037-y.
Lord, C. J. and Ashworth, A. (2016) 'BRCAness revisited', *Nature Reviews Cancer*, 16(2), pp. 110–120. doi: 10.1038/nrc.2015.21.
Lösel, R. and Wehling, M. (2003) 'Nongenomic actions of steroid hormones', *Nature Reviews Molecular Cell Biology*. Nature Publishing Group, pp. 46–56. doi: 10.1038/nrm1009.
Lubahn, D. B. *et al.* (1993) 'Alteration of reproductive function but not prenatal sexual development after insertional disruption of the mouse estrogen receptor gene', *Proceedings of the National Academy of Sciences of the United States of*

America, 90(23), pp. 11162–11166. doi: 10.1073/pnas.90.23.11162.
Madlensky, L. *et al.* (2011) 'Tamoxifen metabolite concentrations, CYP2D6 genotype, and breast cancer outcomes', *Clinical Pharmacology and Therapeutics*. NIH Public Access, 89(5), pp. 718–725. doi: 10.1038/clpt.2011.32.
Magnani, L. *et al.* (2011) 'PBX1 genomic pioneer function drives ERα signaling underlying progression in breast cancer', *PLoS Genetics*. Edited by B. E. Clurman, 7(11), p. e1002368. doi: 10.1371/journal.pgen.1002368.
Makinen, S. (2001) 'Localization of oestrogen receptors alpha and beta in human testis', *Molecular Human Reproduction*, 7(6), pp. 497–503. doi: 10.1093/molehr/7.6.497.
Malvezzi, M. *et al.* (2016) 'European cancer mortality predictions for the year 2016 with focus on leukaemias', *Annals of Oncology*. Narnia, 27(4), pp. 725–731. doi: 10.1093/annonc/mdw022.
Mann, S. *et al.* (2001) 'Estrogen receptor beta expression in invasive breast cancer', *Human Pathology*. W.B. Saunders, 32(1), pp. 113–118. doi: 10.1053/hupa.2001.21506.
Manning, B. D. and Toker, A. (2017) 'AKT/PKB Signaling: Navigating the Network', *Cell*, pp. 381–405. doi: 10.1016/j.cell.2017.04.001.
Mansouri, S. *et al.* (2018) 'A Review on The Role of VEGF in Tamoxifen Resistance', *Anti-Cancer Agents in Medicinal Chemistry*, 18(14), pp. 2006–2009. doi: 10.2174/1871520618666180911142259.
Martin, L. A. *et al.* (2011) 'An in vitro model showing adaptation to long-term oestrogen deprivation highlights the clinical potential for targeting kinase pathways in combination with aromatase inhibition', in *Steroids*. Elsevier, pp. 772–776. doi: 10.1016/j.steroids.2011.02.035.
Massarweh, S. *et al.* (2008) 'Tamoxifen resistance in breast tumors is driven by growth factor receptor signaling with repression of classic estrogen receptor genomic function', *Cancer Research*, 68(3), pp. 826–833. doi: 10.1158/0008-5472.CAN-07-2707.
Matevossian, A. and Resh, M. D. (2015) 'Hedgehog Acyltransferase as a target in estrogen receptor positive, HER2 amplified, and tamoxifen resistant breast cancer cells', *Molecular Cancer*, 14(1), p. 72. doi: 10.1186/s12943-015-0345-x.
Matthews, J. and Gustafsson, J. A. (2003) 'Estrogen signaling: a subtle balance between ER alpha and ER beta.', *Molecular interventions*, pp. 281–292. doi: 10.1124/mi.3.5.281.
McDermott, M. *et al.* (2014) 'In vitro development of chemotherapy and targeted therapy drug-resistant cancer cell lines: A practical guide with case studies', *Frontiers in Oncology*. Frontiers, 4 MAR, p. 40. doi: 10.3389/fonc.2014.00040.
Meitzen, J. *et al.* (2013) 'Palmitoylation of estrogen receptors is essential for neuronal membrane signaling', *Endocrinology*, 154(11), pp. 4293–4304. doi: 10.1210/en.2013-1172.
Menasce, L. P. *et al.* (1993) 'Localization of the estrogen receptor locus (esr) to chromosome 6q25.1 by fish and a simple post-fish banding technique', *Genomics*. Academic Press, 17(1), pp. 263–265. doi: 10.1006/geno.1993.1320.
Merenbakh-Lamin, K. *et al.* (2013) 'D538G mutation in estrogen receptor-α: A novel mechanism for acquired endocrine resistance in breast cancer', *Cancer Research*, 73(23), pp. 6856–6864. doi: 10.1158/0008-5472.CAN-13-1197.
Mermelstein, P. G. (2009) 'Membrane-localised oestrogen receptor α and β influence neuronal activity through activation of metabotropic glutamate receptors', in *Journal of Neuroendocrinology*, pp. 257–262. doi: 10.1111/j.1365-2826.2009.01838.x.

Michaelis, M., Rothweiler, F., Barth, S., Cinat, J., Van Rikxoort, M, *et al.* (2011) 'Adaptation of cancer cells from different entities to the MDM2 inhibitor nutlin-3 results in the emergence of p53-mutated multi-drug-resistant cancer cells', *Cell Death and Disease*, 2(12). doi: 10.1038/cddis.2011.129.
Michaelis, M., Rothweiler, F., Barth, S., Cinat, J., Van Rikxoort, M., *et al.* (2011) 'Adaptation of cancer cells from different entities to the MDM2 inhibitor nutlin-3 results in the emergence of p53-mutated multi-drug-resistant cancer cells', *Cell Death and Disease*, 2(12), pp. e243–e243. doi: 10.1038/cddis.2011.129.
Michaelis, M. *et al.* (2012) 'Human neuroblastoma cells with acquired resistance to the p53 activator RITA retain functional p53 and sensitivity to other p53 activating agents', *Cell Death and Disease*, 3(4), p. 294. doi: 10.1038/cddis.2012.35.
Michaelis, M., Wass, M. and Cinatl, J. (2016) 'The Resistant Cancer Cell Line (RCCL) collection', *European Journal of Cancer*. Elsevier, 61, p. S120. doi: 10.1016/s0959-8049(16)61426-0.
Mir, O. *et al.* (2012) 'Pemetrexed, oxaliplatin and bevacizumab as first-line treatment in patients with stage IV non-small cell lung cancer', *Lung Cancer*. Elsevier, 77(1), pp. 104–109. doi: 10.1016/j.lungcan.2012.01.014.
Mitra, R. *et al.* (2011) 'CYP3A4 mediates growth of estrogen receptor-positive breast cancer cells in part by inducing nuclear translocation of phospho-Stat3 through biosynthesis of (±)-14,15-epoxyeicosatrienoic acid (EET)', *Journal of Biological Chemistry*. JBC Papers in Press, 286(20), pp. 17543–17559. doi: 10.1074/jbc.M110.198515.
Mitra, S. W. *et al.* (2003) 'Immunolocalization of estrogen receptor β in the mouse brain: Comparison with estrogen receptor α', *Endocrinology*, 144(5), pp. 2055–2067. doi: 10.1210/en.2002-221069.
Mitsuuchi, Y. *et al.* (2000) 'The phosphatidylinositol 3-kinase/AKT signal transduction pathway plays a critical role in the expression of p21(WAF1/CIP1/SDI1) induced by cisplatin and paclitaxel', *Cancer Research*, 60(19), pp. 5390–5394. Available at: http://www.ncbi.nlm.nih.gov/pubmed/11034077 (Accessed: 12 November 2018).
Molina, L. *et al.* (2017) 'GPER-1/GPR30 a novel estrogen receptor sited in the cell membrane: therapeutic coupling to breast cancer', *Expert Opinion on Therapeutic Targets*, pp. 755–766. doi: 10.1080/14728222.2017.1350264.
Montecucco, A., Zanetta, F. and Biamonti, G. (2015) 'Molecular mechanisms of etoposide.', *EXCLI journal*. Leibniz Research Centre for Working Environment and Human Factors, 14, pp. 95–108. doi: 10.17179/excli2015-561.
Moore, J. *et al.* (1998) 'Cloning and characterization of human estrogen receptor beta isoforms', *Biochem Biophys Res Commun*, 247(1), pp. 75–8. doi: 10.1006/bbrc.1998.8738.
Mosselman, S., Polman, J. and Dijkema, R. (1996) 'ERβ: Identification and characterization of a novel human estrogen receptor', *FEBS Letters*, 392(1), pp. 49–53. doi: 10.1016/0014-5793(96)00782-X.
Murphy, L. C. *et al.* (2002) 'Relationship of coregulator and oestrogen receptor isoform expression to de novo tamoxifen resistance in human breast cancer', *British Journal of Cancer*. Nature Publishing Group, 87(12), pp. 1411–1416. doi: 10.1038/sj.bjc.6600654.
Musgrove, E. A. and Sutherland, R. L. (2009) 'Biological determinants of endocrine resistance in breast cancer', *Nature Reviews Cancer*, pp. 631–643. doi: 10.1038/nrc2713.
Naderi, A., Chia, K. M. and Liu, J. (2011) 'Synergy between inhibitors of

androgen receptor and MEK has therapeutic implications in estrogen receptor-negative breast cancer', *Breast Cancer Research*. BioMed Central, 13(2), pp. 1–16. doi: 10.1186/bcr2858.
Nakhjavani, M., Stewart, D. J. and Shirazi, F. H. (2017) 'Effect of steroid and serum starvation on a human breast cancer adenocarcinoma cell line.', *Journal of experimental therapeutics & oncology*, 12(1), pp. 25–34. Available at: http://www.ncbi.nlm.nih.gov/pubmed/28472561 (Accessed: 2 July 2019).
Nass, N. and Kalinski, T. (2015) 'Tamoxifen resistance: From cell culture experiments towards novel biomarkers', *Pathology Research and Practice*. Urban & Fischer, pp. 189–197. doi: 10.1016/j.prp.2015.01.004.
Nawata, H., Bronzert, D. and Lippman, M. E. (1981) 'Isolation and characterization of a tamoxifen-resistant cell line derived from MCF-7 human breast cancer cells', *Journal of Biological Chemistry*, 256(10), pp. 5016–5021. Available at: http://www.jbc.org/ (Accessed: 9 September 2019).
Nazarian, R. *et al.* (2010) 'Melanomas acquire resistance to B-RAF(V600E) inhibition by RTK or N-RAS upregulation', *Nature*, 468(7326), pp. 973–977. doi: 10.1038/nature09626.
Nejlund, S. *et al.* (2016) 'Cryopreservation of Circulating Tumor Cells for Enumeration and Characterization', in *Biopreservation and Biobanking*, pp. 330–337. doi: 10.1089/bio.2015.0074.
Niederst, M. J. *et al.* (2015) 'RB loss in resistant EGFR mutant lung adenocarcinomas that transform to small-cell lung cancer', *Nature Communications*, 6. doi: 10.1038/ncomms7377.
Niu, J. *et al.* (2015) 'Incidence and clinical significance of ESR1 mutations in heavily pretreated metastatic breast cancer patients', *OncoTargets and Therapy*, 8, pp. 3323–3328. doi: 10.2147/OTT.S92443.
O'Lone, R. *et al.* (2004) 'Genomic Targets of Nuclear Estrogen Receptors', *Molecular Endocrinology*, 18(8), pp. 1859–1875. doi: 10.1210/me.2003-0044.
O ate, S. A. *et al.* (2006) 'Sequence and Characterization of a Coactivator for the Steroid Hormone Receptor Superfamily', *Science*, 270(5240), pp. 1354–1357. doi: 10.1126/science.270.5240.1354.
Paech, K. *et al.* (1997) 'Differential ligand activation of estrogen receptors ERα and ERrβ at AP1 sites', *Science*. American Association for the Advancement of Science, 277(5331), pp. 1508–1510. doi: 10.1126/science.277.5331.1508.
Panda, M. and Biswal, B. K. (2019) 'Cell signaling and cancer: a mechanistic insight into drug resistance', *Molecular Biology Reports*. doi: 10.1007/s11033-019-04958-6.
Park, K. J. *et al.* (2016) 'Role of vincristine in the inhibition of angiogenesis in glioblastoma', *Neurological Research*. Taylor & Francis, 38(10), pp. 871–879. doi: 10.1080/01616412.2016.1211231.
Park, S. *et al.* (2010) 'Expression of androgen receptors in primary breast cancer', *Annals of Oncology*, 21(3), pp. 488–492. doi: 10.1093/annonc/mdp510.
Pasqualato, A. *et al.* (2012) 'Quantitative shape analysis of chemoresistant colon cancer cells: Correlation between morphotype and phenotype', *Experimental Cell Research*, 318(7), pp. 835–846. doi: 10.1016/j.yexcr.2012.01.022.
Pearce, S. T. and Jordan, V. C. (2004) 'The biological role of estrogen receptors α and β in cancer', *Critical Reviews in Oncology/Hematology*, pp. 3–22. doi: 10.1016/j.critrevonc.2003.09.003.
Pedram, A., Razandi, M. and Levin, E. R. (2006) 'Nature of Functional Estrogen Receptors at the Plasma Membrane', *Molecular Endocrinology*. Narnia, 20(9), pp. 1996–2009. doi: 10.1210/me.2005-0525.

Penot, G. *et al.* (2005) 'The human estrogen receptor-α isoform hERα46 antagonizes the proliferative influence of hERα66 in MCF7 breast cancer cells', *Endocrinology*, 146(12), pp. 5474–5484. doi: 10.1210/en.2005-0866.
Perego, P. and Robert, J. (2016) 'Oxaliplatin in the era of personalized medicine: From mechanistic studies to clinical efficacy Cytotoxic Reviews Godefridus J. Peters and Eric Raymond', *Cancer Chemotherapy and Pharmacology*, pp. 5–18. doi: 10.1007/s00280-015-2901-x.
Perez, R. *et al.* (2012) 'Antagonists of growth hormone-releasing hormone suppress in vivo tumor growth and gene expression in triple negative breast cancers', *Oncotarget*, 3(9), pp. 988–997. doi: 10.18632/oncotarget.634.
Peters, A. A. *et al.* (2009) 'Androgen receptor inhibits estrogen receptor-α activity and is prognostic in breast cancer', *Cancer Research*. American Association for Cancer Research, 69(15), pp. 6131–6140. doi: 10.1158/0008-5472.CAN-09-0452.
Poggio, F. *et al.* (2018) 'Platinum-based neoadjuvant chemotherapy in triple-negative breast cancer: A systematic review and meta-analysis', *Annals of Oncology*, pp. 1497–1508. doi: 10.1093/annonc/mdy127.
Pommier, Y. *et al.* (2010) 'DNA topoisomerases and their poisoning by anticancer and antibacterial drugs', *Chemistry and Biology*. Cell Press, pp. 421–433. doi: 10.1016/j.chembiol.2010.04.012.
Poulard, C. *et al.* (2019) 'Oestrogen Non-Genomic Signalling is Activated in Tamoxifen-Resistant Breast Cancer', *International Journal of Molecular Sciences*, 20(11), p. 2773. doi: 10.3390/ijms20112773.
Poulikakos, P. I. *et al.* (2011) 'RAF inhibitor resistance is mediated by dimerization of aberrantly spliced BRAF(V600E)', *Nature*, 480(7377), pp. 387–390. doi: 10.1038/nature10662.
Pritchard, K. I. (2008) 'Combining endocrine agents with chemotherapy: Which patients and what sequence?', in *Cancer*. John Wiley & Sons, Ltd, pp. 718–722. doi: 10.1002/cncr.23189.
Raez, L. E., Kobina, S. and Santos, E. S. (2010) 'Oxaliplatin in first-line therapy for advanced non-small-cell lung cancer', *Clinical Lung Cancer*. Elsevier, pp. 18–24. doi: 10.3816/CLC.2010.n.003.
Rajendran, K. G., Lopez, T. and Parikh, I. (1987) 'Estrogenic effect of phenol red in MCF-7 cells is achieved through activation of estrogen receptor by interacting with a site distinct from the steroid binding site', *Biochemical and Biophysical Research Communications*, 142(3), pp. 724–731. doi: 10.1016/0006-291X(87)91474-4.
Rakha, E. A., El-Sayed, M. E., Green, A. R., Lee, Andrew H.S., *et al.* (2007) 'Prognostic markers in triple-negative breast cancer', *Cancer*, 109(1), pp. 25–32. doi: 10.1002/cncr.22381.
Rakha, E. A., El-Sayed, M. E., Green, A. R., Lee, Andrew H. S., *et al.* (2007) 'Prognostic markers in triple-negative breast cancer', *Cancer*, 109(1), pp. 25–32. doi: 10.1002/cncr.22381.
Reinbolt, R. E. *et al.* (2015) 'Endocrine therapy in breast cancer: The neoadjuvant, adjuvant, and metastatic approach', *Seminars in Oncology Nursing*. W.B. Saunders, 31(2), pp. 146–155. doi: 10.1016/j.soncn.2015.02.002.
Revankar, Chetana M *et al.* (2005) 'A transmembrane intracellular estrogen receptor mediates rapid cell signaling', *Science*. American Association for the Advancement of Science, 307(5715), pp. 1625–1630. doi: 10.1126/science.1106943.
Revankar, Chetana M. *et al.* (2005) 'A transmembrane intracellular estrogen receptor mediates rapid cell signaling', *Science*. American Association for the

Advancement of Science, 307(5715), pp. 1625–1630. doi: 10.1126/science.1106943.
Ribnikar, D. *et al.* (2015) 'Breast Cancer Under Age 40: a Different Approach', *Current Treatment Options in Oncology*, p. 16. doi: 10.1007/s11864-015-0334-8.
Rixe, O. *et al.* (1996) 'Oxaliplatin, tetraplatin, cisplatin, and carboplatin: Spectrum of activity in drug-resistant cell lines and in the cell lines of the National Cancer Institute's Anticancer Drug Screen panel', *Biochemical Pharmacology*. Elsevier, 52(12), pp. 1855–1865. doi: 10.1016/S0006-2952(97)81490-6.
Robert, M. *et al.* (2017) 'Expert Opinion on Investigational Drugs Olaparib for the treatment of breast cancer', *Expert Opinion on Investigational Drugs*, 26(6), pp. 751–759. doi: 10.1080/13543784.2017.1318847.
Robinson, J. L. L. *et al.* (2012) 'Erratum: Androgen receptor driven transcription in molecular apocrine breast cancer is mediated by FoxA1 (The EMBO Journal (2012) 31 (1617) DOI:10.1038/emboj.2012.59)', *EMBO Journal*. John Wiley & Sons, Ltd, p. 1617. doi: 10.1038/emboj.2012.59.
Robinson, S. P. *et al.* (1991) 'Metabolites, pharmacodynamics, and pharmacokinetics of tamoxifen in rats and mice compared to the breast cancer patient', *Drug Metabolism and Disposition*, 19(1), pp. 36–43.
Rocha, C. R. R. *et al.* (2018) 'DNA repair pathways and cisplatin resistance: An intimate relationship', *Clinics*. Hospital das Clinicas da Faculdade de Medicina da Universidade de Sao Paulo, p. e478s. doi: 10.6061/clinics/2018/e478s.
Rondon-Lagos, M. *et al.* (2016) 'Tamoxifen Resistance: Emerging Molecular Targets.', *International journal of molecular sciences*, 17(8), pp. 1–31. doi: 10.3390/ijms17081357.
Rosenberg, B., Van Camp, L. and Krigas, T. (1965) 'Inhibition of cell division in Escherichia coli by electrolysis products from a platinum electrode [17]', *Nature*, pp. 698–699. doi: 10.1038/205698a0.
Ruggiero, A. *et al.* (2013) 'Platinum compounds in children with cancer: Toxicity and clinical management', *Anti-Cancer Drugs*. Anti-Cancer Drugs, pp. 1007–1019. doi: 10.1097/CAD.0b013e3283650bda.
Sabaila, A., Fauconnier, A. and Huchon, C. (2015) 'Chimiothérapie intrapéritonéale pressurisée en aérosol (CIPPA): Une nouvelle voie d'administration dans les carcinoses péritonéales d'origine ovarienne', *Gynecologie Obstetrique et Fertilite*. John Wiley & Sons, Ltd, 43(1), pp. 66–67. doi: 10.1002/ijc.29210.
Saji, S. *et al.* (2000) 'Estrogen receptors α and β in the rodent mammary gland', *Proceedings of the National Academy of Sciences of the United States of America*. National Academy of Sciences, 97(1), pp. 337–342. doi: 10.1073/pnas.97.1.337.
Salgia, R. and Kulkarni, P. (2018) 'The Genetic/Non-genetic Duality of Drug "Resistance" in Cancer', *Trends in Cancer*. Cell Press, pp. 110–118. doi: 10.1016/j.trecan.2018.01.001.
Samartzis, E. P. *et al.* (2014) 'The G protein-coupled estrogen receptor (GPER) is expressed in two different subcellular localizations reflecting distinct tumor properties in breast cancer', *PLoS ONE*. Edited by A. Ahmad, 9(1), p. e83296. doi: 10.1371/journal.pone.0083296.
Sampson, J. N. *et al.* (2017) 'Association of estrogen metabolism with breast cancer risk in different cohorts of postmenopausal women', *Cancer Research*, 77(4), pp. 918–925. doi: 10.1158/0008-5472.CAN-16-1717.
Sarin, N. *et al.* (2017) 'Cisplatin resistance in non-small cell lung cancer cells is

associated with an abrogation of cisplatin-induced G2/M cell cycle arrest', *PLOS ONE*. Edited by A. Ahmad. Public Library of Science, 12(7), p. e0181081. doi: 10.1371/journal.pone.0181081.
Schneider, C. *et al.* (2017) 'SAMHD1 is a biomarker for cytarabine response and a therapeutic target in acute myeloid leukemia', *Nature Medicine*. Nature Publishing Group, 23(2), pp. 250–255. doi: 10.1038/nm.4255.
Schumacher, H. M., Westphal, M. and Heine-Dobbernack, E. (2015) 'Cryopreservation of plant cell lines', *Methods in Molecular Biology*, 1257, pp. 423–429. doi: 10.1007/978-1-4939-2193-5_21.
Shaul, Y. D. and Seger, R. (2007) 'The MEK/ERK cascade: From signaling specificity to diverse functions', *Biochimica et Biophysica Acta - Molecular Cell Research*. Elsevier, pp. 1213–1226. doi: 10.1016/j.bbamcr.2006.10.005.
Shim, G.-J. *et al.* (2003) 'Disruption of the estrogen receptor gene in mice causes myeloproliferative disease resembling chronic myeloid leukemia with lymphoid blast crisis', *Proceedings of the National Academy of Sciences*, 100(11), pp. 6694–6699. doi: 10.1073/pnas.0731830100.
Shoker, B. S. *et al.* (1999) 'Oestrogen receptor expression in the normal and pre-cancerous breast', *Journal of Pathology*, 188(3), pp. 237–244. doi: 10.1002/(SICI)1096-9896(199907)188:3<237::AID-PATH343>3.0.CO;2-8.
Siddik, Z. H. (2003) 'Cisplatin: Mode of cytotoxic action and molecular basis of resistance', *Oncogene*. Nature Publishing Group, pp. 7265–7279. doi: 10.1038/sj.onc.1206933.
Siegel, R. L., Miller, K. D. and Jemal, A. (2015) 'CA : A Cancer Journal for Clinicians 4863) Early View 4863 / earlyview), Article first published online : 5 JAN 2015', *CA: A Cancer Journal for Clinicians*, 65(1), pp. 5–29. doi: 10.3322/caac.21254.
Sikora, M. J. *et al.* (2016) 'Endocrine response phenotypes are altered by charcoal-stripped serum variability', *Endocrinology*, 157(10), pp. 3760–3766. doi: 10.1210/en.2016-1297.
Skliris, G. P. *et al.* (2006) 'Expression of oestrogen receptor-β in oestrogen receptor-α negative human breast tumours', *British Journal of Cancer*. Nature Publishing Group, 95(5), pp. 616–626. doi: 10.1038/sj.bjc.6603295.
Steding, C. E. (2016) 'Creating chemotherapeutic-resistant breast cancer cell lines: Advances and future perspectives', *Future Oncology*. Future Medicine Ltd London, UK, pp. 1517–1527. doi: 10.2217/fon-2016-0059.
Stepanenko, A. A. and Dmitrenko, V. V. (2015) 'Pitfalls of the MTT assay: Direct and off-target effects of inhibitors can result in over/underestimation of cell viability', *Gene*, 574(2), pp. 193–203. doi: 10.1016/j.gene.2015.08.009.
Stocco, C. (2012) 'Tissue physiology and pathology of aromatase', *Steroids*. Elsevier, pp. 27–35. doi: 10.1016/j.steroids.2011.10.013.
Ström, A. *et al.* (2004) 'Estrogen receptor β inhibits 17β-estradiol-stimulated proliferation of the breast cancer cell line T47D', *Proceedings of the National Academy of Sciences of the United States of America*, 101(6), pp. 1566–1571. doi: 10.1073/pnas.0308319100.
Sun, X. and Kaufman, P. D. (2018) 'Ki-67: more than a proliferation marker', *Chromosoma*. NIH Public Access, pp. 175–186. doi: 10.1007/s00412-018-0659-8.
Tan, H., Zhong, Y. and Pan, Z. (2009) 'Autocrine regulation of cell proliferation by estrogen receptor-alpha in estrogen receptor-alpha-positive breast cancer cell lines', *BMC Cancer*. BioMed Central, 9(1), p. 31. doi: 10.1186/1471-2407-9-31.
Tan, S. K. *et al.* (2011) 'AP-2γ 3 regulates oestrogen receptor-mediated long-

range chromatin interaction and gene transcription', *EMBO Journal*, 30(13), pp. 2569–2581. doi: 10.1038/emboj.2011.151.
Tao, H., Mei, J. and Tang, X. (2019) 'The anticancer effects of 2-methoxyestradiol on human huh7 cells in vitro and in vivo', *Biochemical and Biophysical Research Communications*. Academic Press, 512(3), pp. 635–640. doi: 10.1016/j.bbrc.2019.02.068.
Teunissen, S. F. *et al.* (2011) 'Investigational study of tamoxifen phase I metabolites using chromatographic and spectroscopic analytical techniques', *Journal of Pharmaceutical and Biomedical Analysis*, 55(3), pp. 518–526. doi: 10.1016/j.jpba.2011.02.009.
Teymourzadeh, A. *et al.* (2017) 'ER-α36 Interactions With Cytosolic Molecular Network in Acquired Tamoxifen Resistance', *Clinical Breast Cancer*. Elsevier, pp. 403–407. doi: 10.1016/j.clbc.2017.03.013.
Thekkumkara, T., Snyder, R. and Karamyan, V. T. (2016) 'Competitive binding assay for the g-protein-coupled receptor 30 (GPR30) or G-protein-coupled estrogen receptor (GPER)', in *Methods in Molecular Biology*, pp. 11–17. doi: 10.1007/978-1-4939-3127-9_2.
Thomas, M. P. and Potter, B. V. L. (2013) 'The structural biology of oestrogen metabolism', *Journal of Steroid Biochemistry and Molecular Biology*, pp. 27–49. doi: 10.1016/j.jsbmb.2012.12.014.
Tica, A. A. *et al.* (2011) 'G protein-coupled estrogen receptor 1-mediated effects in the rat myometrium', *American Journal of Physiology - Cell Physiology*. American Physiological Society Bethesda, MD, 301(5), pp. C1262–C1269. doi: 10.1152/ajpcell.00501.2010.
Tomasz, M. (1995) 'Mitomycin C: small, fast and deadly (but very selective)', *Chemistry and Biology*, pp. 575–579. doi: 10.1016/1074-5521(95)90120-5.
Tora, L. *et al.* (1989) 'The human estrogen receptor has two independent nonacidic transcriptional activation functions', *Cell*, 59(3), pp. 477–487. doi: 10.1016/0092-8674(89)90031-7.
Toy, W. *et al.* (2013) 'ESR1 ligand-binding domain mutations in hormone-resistant breast cancer', *Nature Genetics*, 45(12), pp. 1439–1445. doi: 10.1038/ng.2822.
Välimaa, H. *et al.* (2004) 'Estrogen receptor-β is the predominant estrogen receptor subtype in human oral epithelium and salivary glands', *Journal of Endocrinology*, 180(1), pp. 55–62. doi: 10.1677/joe.0.1800055.
Vanacker, J. M. *et al.* (1999) 'Transcriptional targets shared by estrogen receptor-related receptors (ERRs) and estrogen receptor (ER) α, but not by ERβ', *EMBO Journal*, 18(15), pp. 4270–4279. doi: 10.1093/emboj/18.15.4270.
Voigt, W. (2005) 'Sulforhodamine B Assay and Chemosensitivity BT - Chemosensitivity: Volume 1 In Vitro Assays', in *Chemosensitivity*. New Jersey: Humana Press, pp. 39–48. doi: 10.1385/1-59259-869-2:039.
Vojtek, M. *et al.* (2019) 'Anticancer activity of palladium-based complexes against triple-negative breast cancer', *Drug Discovery Today*. Elsevier Current Trends, pp. 1044–1058. doi: 10.1016/j.drudis.2019.02.012.
Vrtačnik, P. *et al.* (2014) 'The many faces of estrogen signaling', *Biochemia Medica*, pp. 329–342. doi: 10.11613/BM.2014.035.
Wang, D. and Lippard, S. J. (2005) 'Cellular processing of platinum anticancer drugs', *Nature Reviews Drug Discovery*. Nature Publishing Group, pp. 307–320. doi: 10.1038/nrd1691.
Wang, Q. *et al.* (2018) 'Tamoxifen enhances stemness and promotes metastasis of ERα36 + breast cancer by upregulating ALDH1A1 in cancer cells', *Cell Research*. Nature Publishing Group, 28(3), pp. 336–358. doi:

10.1038/cr.2018.15.
Wang, S. *et al.* (2018) 'Genome-wide investigation of genes regulated by ERα in breast cancer cells', *Molecules*. MDPI AG, 23(10). doi: 10.3390/molecules23102543.
Wang, Z. Y. *et al.* (2006) 'A variant of estrogen receptor-α, hER-α36: Transduction of estrogen- and antiestrogen-dependent membrane-initiated mitogenic signaling', *Proceedings of the National Academy of Sciences of the United States of America*, 103(24), pp. 9063–9068. doi: 10.1073/pnas.0603339103.
Weihua, Z. *et al.* (2000) 'Estrogen receptor (ER) β, a modulator of ERα in the uterus', *Proceedings of the National Academy of Sciences of the United States of America*, 97(11), pp. 5936–5941. doi: 10.1073/pnas.97.11.5936.
Weihua, Z. *et al.* (2002) 'A role for estrogen receptor in the regulation of growth of the ventral prostate', *Proceedings of the National Academy of Sciences*, 98(11), pp. 6330–6335. doi: 10.1073/pnas.111150898.
Welshons, W. V. *et al.* (1988) 'Estrogenic activity of phenol red', *Molecular and Cellular Endocrinology*. Elsevier, 57(3), pp. 169–178. doi: 10.1016/0303-7207(88)90072-X.
Westfalewicz, B., Dietrich, M. A. and Ciereszko, A. (2015) 'Impact of cryopreservation on bull (Bos taurus) semen proteome', *Journal of Animal Science*, 93(11), pp. 5240–5253. doi: 10.2527/jas.2015-9237.
Williams, S. P. and McDermott, U. (2017) 'The Pursuit of Therapeutic Biomarkers with High-Throughput Cancer Cell Drug Screens', *Cell Chemical Biology*, pp. 1066–1074. doi: 10.1016/j.chembiol.2017.06.011.
Williams, T. M. and Lisanti, M. P. (2004) 'The caveolin proteins', *Genome Biology*. BioMed Central, p. 214. doi: 10.1186/gb-2004-5-3-214.
Wu, C. P. *et al.* (2013) 'Overexpression of ATP-binding cassette transporter ABCG2 as a potential mechanism of acquired resistance to vemurafenib in BRAF(V600E) mutant cancer cells', *Biochemical Pharmacology*, 85(3), pp. 325–334. doi: 10.1016/j.bcp.2012.11.003.
Wu, X. *et al.* (2011) 'Estrogen receptor-beta sensitizes breast cancer cells to the anti-estrogenic actions of endoxifen', *Breast Cancer Research*, 13(2), p. R27. doi: 10.1186/bcr2844.
Wu, Y. *et al.* (2018) 'Tamoxifen resistance in breast cancer is regulated by the EZH2–ERa–GREB1 transcriptional axis', *Cancer Research*. American Association for Cancer Research, 78(3), pp. 671–684. doi: 10.1158/0008-5472.CAN-17-1327.
Wu, Y. H. *et al.* (2019) 'Akt inhibitor SC66 promotes cell sensitivity to cisplatin in chemoresistant ovarian cancer cells through inhibition of COL11A1 expression', *Cell Death and Disease*. Nature Publishing Group, 10(4), pp. 1–16. doi: 10.1038/s41419-019-1555-8.
Yamori, T. (2003) 'Panel of human cancer cell lines provides valuable database for drug discovery and bioinformatics', in *Cancer Chemotherapy and Pharmacology, Supplement*, pp. 74–79. doi: 10.1007/s00280-003-0649-1.
Yang, J. *et al.* (2008) 'The F-domain of estrogen receptor-alpha inhibits ligand induced receptor dimerization', *Molecular and Cellular Endocrinology*, 295(1–2), pp. 94–100. doi: 10.1016/j.mce.2008.08.001.
Yang, X. *et al.* (2001) 'Synergistic activation of functional estrogen receptor (ER)-alpha by DNA methyltransferase and histone deacetylase inhibition in human ER-alpha-negative breast cancer cells.', *Cancer research*, 61(19), pp. 7025–9. Available at: http://www.ncbi.nlm.nih.gov/pubmed/11585728 (Accessed: 7 August 2019).

Yang, X. *et al.* (2013) ‘Estradiol increases ER-negative breast cancer metastasis in an experimental model’, *Clinical and Experimental Metastasis*, 30(6), pp. 711–721. doi: 10.1007/s10585-012-9559-0.
Yeh, P. Y. *et al.* (2002) ‘Increase of the resistance of human cervical carcinoma cells to cisplatin by inhibition of the MEK to ERK signaling pathway partly via enhancement of anticancer drug-induced NF kappa B activation.’, *Biochemical pharmacology*, 63(8), pp. 1423–30. Available at: http://www.ncbi.nlm.nih.gov/pubmed/11996883 (Accessed: 12 November 2018).
Yi, P. *et al.* (2014) ‘The Effects of Estrogen-Responsive Element- and Ligand-Induced Structural Changes on the Recruitment of Cofactors and Transcriptional Responses by ERα and ERβ’, *Molecular Endocrinology*, 16(4), pp. 674–693. doi: 10.1210/mend.16.4.0810.
Yin, F.-F. *et al.* (2019) ‘Intra-tumor heterogeneity for endometrial cancer and its clinical significance’, *Chinese Medical Journal*, 132(13), pp. 1550–1562. doi: 10.1097/cm9.0000000000000286.
Yoshida, G. J. (2020) ‘Applications of patient-derived tumor xenograft models and tumor organoids’, *Journal of Hematology and Oncology*. BioMed Central Ltd., pp. 1–16. doi: 10.1186/s13045-019-0829-z.
Zhang, J. *et al.* (2018) ‘Biomarker assessment of the CBCSG006 trial: A randomized phase III trial of cisplatin plus gemcitabine compared with paclitaxel plus gemcitabine as first-line therapy for patients with metastatic triple-negative Breast cancer’, *Annals of Oncology*. Oxford University Press, 29(8), pp. 1741–1747. doi: 10.1093/annonc/mdy209.
Zhao, C. *et al.* (2007) ‘Estrogen receptor β2 negatively regulates the transactivation of estrogen receptor α in human breast cancer cells’, *Cancer Research*, 67(8), pp. 3955–3962. doi: 10.1158/0008-5472.CAN-06-3505.
Zhao, Y. W. *et al.* (2005) ‘Identification, cloning, and expression of human estrogen receptor-α36, a novel variant of human estrogen receptor-α66’, *Biochemical and Biophysical Research Communications*, 336(4), pp. 1023–1027. doi: 10.1016/j.bbrc.2005.08.226.
Zheng, Z. Y. *et al.* (2008) ‘Anti-estrogenic mechanism of unliganded progesterone receptor isoform B in breast cancer cells’, *Breast Cancer Research and Treatment*. Springer US, 110(1), pp. 111–125. doi: 10.1007/s10549-007-9711-8.